UNIVERSITY OF LIVERPOOL

Competition of Staphylococci as probe for Novel Antibiotics

Hanaa Ghabban

Thesis submitted in accordance with the requirements of the University of Liverpool for the degree of Doctor in Philosophy

April 2019

Competition of Staphylococci as probe for Novel Antibiotics

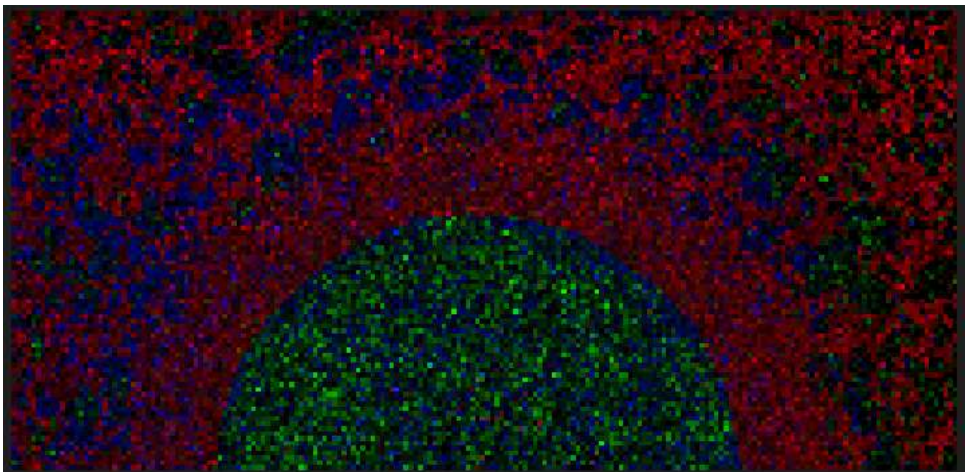

Hanaa Ghabban

Thesis submitted in accordance with the requirements of the Universityof Liverpool for the degree of Doctor in Philosophy

April 2019

Acknowledgement

"Thanks to the Almighty God for His infinite blessings and mercies upon my life".

I express my sincere gratitude to my supervisor Dr Mal Horsburgh who has been a constant source of ideas, guidance, and motivation from beginning to end. It was a great honour to work under his supervision. I would like also to thank my secondary supervisor Dr Jo Fothergill for her useful advice. I would like to extend my thanks to Dr Jo Moran for her help and valuable suggestions in bioinformatics analysis, Dr Sam Haldenby for his help with RNA data analysis, Dr Xizhang Zhao and Dr Jamal Alorabi for their generous advice and assistance. My thanks also go to the lab manager Paul Loughnane for his help in the lab and cooperation.

Specifically, I acknowledge the Ministry of Education and Tabuk University, Saudi Arabia for offering the fund for the study.

I am grateful for all my friends and colleagues for helping hand and sharing a great moment with me and made this research journey enjoyable: Hind Alrajeh, Hanshuo lu, Batool Almarzouq, Wazeera Abdullah, Charlotte chong, Abhipsa Sahu, Hashim Felemban and Hassan Abul.

My appreciation also extends to all my family members, my beloved father who no longer with us but I couldn't have done this without his whishes and encouragement, my mum for her prayers and emotional support in my life, for my two lovely sisters who are always there when I need them. Special thanks to my brother Mohammad who supported and helped me a lot throughout my years of study.

Last but not least, I would like to express my warmest regards to all my lovely friends for listening to me and being by my side through this entire process; Hibah Ameen, Dikhnah Alshehri, Fawzyah Albalawi, Fato Alrefai, Ahood Almaswadi and Hanan Alatawi.

Abstract

Staphylococci are frequent members of the human skin microbiome. It was previously determined that *Staphylococcus aureus* meets widespread antagonism from coagulase-negative staphylococci. Furthermore, cumulative antagonisms by species in the niche correlate with the absence of *S. aureus* nasal colonisation, supporting collective antagonism trait expression as a barrier. However, genetics factors and adaptive pathways of bacterial interactions remain uncharacterised.

Using a two species system, strongly antagonistic inhibitor-producing *S. epidermidis* B155 was co-cultured with *S. aureus* SH1000 to identify determinants of competition and resistance using an experimental evolution approach. In the presence of *S. epidermidis* B155, *S. aureus* evolved a high relative fitness due to inhibitor resistance after several days of *S. epidermidis* co-culture. Unexpectedly, rather than known two-component system TCS loci associated with antimicrobial resistance, Illumina platform genome resequencing of *S. aureus* identified single nucleotide polymorphisms (SNPs) in both sensor kinase (*desK*) and response regulator (*desR*) genes that comprise the poorly described DesKR homologous TCS. The DesKR-like TCS system is located in an operon with two genes encoding an ABC transporter with homology to ABC polyketide efflux transporters. Genetic analysis identified that allelic replacement of *desK* or in-frame deletion of the *SAOUHSC_01312* ABC efflux transporter gene decreased survival of *S. aureus* in competition with *S. epidermidis*, supporting the transporter as a resistance module. The *desK* gene mutant revealed reduced growth rate at both low (25°C) and high (42°C) temperatures compared with its parent strain. Gene inactivation of the *desKR* locus reduced pigment production with both *desK* and *SAOUHSC_01312* mutants expressing less staphyloxanthin.

PacBio genome sequencing of *S. epidermidis* B155 and antiSMASH identified a 55 kb plasmid with a unique polyketide/nonribosomal peptide synthetase (NRPS) gene cluster likely encoding the inhibitor of *S. aureus* growth. This cluster shares considerable sequence homology with a gene cluster encoding a polyketide/NRPS of *Streptococcus* mutans. Due to the production of this unique antimicrobial, further skin-isolated bacteria were screened for those that inhibit *S. aureus* SH1000 WT strain but not a *desR* SNP variant, thereby identifying *Bacillus flexus* B003. PacBio genome sequencing and antiSMASH identified genome-encoded polyketide synthase and linear azol(in)e-containing peptides (LAP) genes that might have the same mode of action as *S. epidermidis* B155 or DesKR resistance mechanism.

RNAseq was performed to probe the regulon of the *S. aureus* DesKR-like TCS using WT to compare with the *desR* SNP variant, plus *desK* allelic replacement and *SAOUHSC_01312* mutants. From this analysis, it was identified that the five genes *SAOUHSC_01311-01312-desKR* operon and *SAOUHSC_01315* were very highly expressed in the *desR* SNP variant and these five genes are likely to comprise the DesKR-like regulon. Moreover, these data support the central role of this TCS in *S. aureus* resistance to the *S. epidermidis* B155 and *B. flexus* B003 antimicrobials. In contrast, transcriptome analysis of *desK* and transporter *SAOUHSC_01312* mutant strains revealed hundreds of genes were differentially expressed in pathways associated with metabolism, virulence and regulations.

The DesKR-like regulon has undefined roles that could be linked to membrane homeostasis and these findings provide significant insights into pathways that impact bacterial growth, resistance and microbial interaction. Ultimately, the TCS and its functions identified here might represent a future target for novel therapeutics targeting *S. aureus.*

Table of Contents

List of Tables

List of Figures

List of Abbreviation

agr	Accessory gene regulator
AIP	Autoinducer peptide
AMP	Antimicrobial peptides
BHI	Brain Heart Infusion
BLAST	Basic Local Alignment Search Tool
BraRS	Bacitracin resistance associated Sensor/Regulator
CAMPs	Cationic antimicrobial peptides
cDNA	Complementary DNA
CoNS	Coagulase-negative staphylococci
DE	Differentially expressed
ESP	Endoserine peptidase
et al.	*Et alia* (and others)
FDR	False Discovery Rate
Fig.	Figure
FPKM	FPKM Fragments mapped per kilobase per million reads mapped
GC	Guanine-cytosine content
GO	Gene Ontology
GraRS	Glycopeptides resistance associated-regulator and sensor
Indels	Insertions or deletions of a number of nucleotides in a DNA sequence
KEGG	Kyoto Encyclopedia of Genes and Genomes
LB	Luria Bertani Broth
MGEs	Mobile genetics elements
NRBS	Nonribosomal peptide synthetases
OD	Optical density
PacBio	Pacific Biosciences
PBS	Phosphate buffered saline
PCA	Principal Component Analysis
PCR	Polymerase chain reaction
PKs	Polyketide synthases
PSM	phenol soluble modulin
qPCR	Quantitative polymerase chain reaction
RIN	RNA integrity number

Sar	Staphylococcal accessory regulator
SNP	Single nucleotide polymorphism
TCSs	Two component systems
UV	Ultraviolet
WT	Wild type

Units and measurements

bp	Base pair
CFU	Colony forming units
cm	Centimetres
g	Gram
h	Hour
Kb	kilobase
kDa	Kilodalton
M	Molar
mg	Milligram
min	Minute
ml	Millilitres
mM	Millimolar
mm	Millimetres
ng	Nanogram
nm	Nanometre
^{o}C	Degree Celsius
rcf	Relative centrifugal force
rpm	Revolutions per minute
sec (s)	Second
v/v	Volume per volume
w/v	weight per volume
µg	Microgram
µl	Micro litre
µM	Micro molar

Chapter1: General Introduction

1.1 Roles of human skin

Human skin is a physical barrier between the body and the environment thereby providing: maintenance of body temperature; protection against pathogenic microorganisms; preventing harm of toxic substances; and the escape of moisture (Iwase *et al.*, 2010). The skin structure contains sweat glands (eccrine and apocrine), hair follicles and sebaceous glands. The eccrine sweat glands secrete water and electrolytes that contribute to regulation of skin temperature and have a role in the acidification of the skin via lactate release (pH ~ 4.5-5.9). The apocrine sweat glands secrete odourless substances proposed to contain pheromones. Moreover, the sebaceous glands that are connected to hair follicles secrete sebum that contains wax esters and squalene, triglycerides and smaller amounts of cholesterol/cholesterol esters (Stefaniak and Harvey, 2006; Pappas, 2009). There are also combinations of ~28% free fatty acid and antimicrobial peptide (Stefaniak and Harvey, 2006; Pappas, 2009). In contrast, the epidermal keratinocytes secrete lipids that are a discrete mixture of almost equal proportions of free fatty acids, ceramides and cholesterol (Pappas, 2009). A significant enhancement in ceramides, cholesterol and fatty acids synthesis has been shown to be associated with disruption of the skin barrier. This finding was supported by inhibition of the synthesis pathways resulting in delayed recovery of the barrier function (Elias and Feingold, 1992). Free fatty acids, including sapienic acid, palmitoleic acid, linoleic acid and oleic acid (Grice and Segre, 2011) are important for preserving an acidic skin mantle (Grice *et al.*, 2008). Furthermore, they been identified as important innate defences inhibiting the growth of potential pathogens while favouring symbiotic commensals (Grice *et al.*, 2008; Ryu *et al.*, 2014). Skin bacteria that were found to be more sensitive to elevated fatty acids include, *Micrococcus sp.*, *S. pyogenes, S. aureus* and *S. epidermidis* (Drake *et al.,* 2008). Several studies have concluded that particular skin surface fatty acids can be more effective antimicrobials than others. For example, sapienic acid was shown to effectively inhibit *S. aureus* growth compared to other free fatty acids (Drake *et al.*, 2008).

Although constantly exposed to a wide range of microorganisms there is plentiful evidence indicating a key contribution of human antimicrobial peptides (AMPs) to both control colonisation and limit infection of the skin (Otto, 2010). Most skin AMPs are cationic and keratinocytes produce three types of β-defensins (hBD-1, hBD-2 and hBD-3) (Hancock and Sahl, 2006). HBD-1 is constitutively expressed in human skin without prior stimulation (Nurjadi *et al.,* 2012). Both hBD-2 and hBD-3 are found at low levels in healthy skin while they are highly expressed in response to inflammation or bacterial stimuli (Zanger *et al.*, 2010). Cathelicidins are found mostly in mammals, and humans express only LL-37 that is synthesised by epithelial cells and secreted by infiltrating immune cells, such as neutrophils that transport LL-37 to the wounded or infected skin (Reinholz *et al.*, 2012). Additionally, keratinocytes produce RNase7 which has bactericidal or bacteriostatic activity toward a variety of bacteria, including *S. aureus* (Peschel, 2002). In healthy skin, RNase 7 is expressed at high levels. When expressed at lower concentrations, it is linked with increased risk for new onset of *S. aureus* skin infection (Zanger *et al.*, 2009; Zanger *et al.*, 2011). RNase7 can bind to the bacterial membrane that becomes more permeable by action of clustered lysine residues, which leads to pore formation and disruption of cell membrane integrity (Huang *et al.*, 2007). The central roles in skin defence of the panoply of skin antimicrobials is supported by the finding that *S. aureus* colonisation is increased in skin lesions caused by atopic dermatitis, owing to reductions in the levels of cathelicidin and β-defensins and altered levels of antimicrobial fatty acids, ceramides and sphingosines (Braff *et al.*, 2005; Ryu *et al.*, 2014).

1.2 Skin microbiome

Nearly all skin niches are occupied by symbiotic microorganisms that provide protection against invasion by more harmful or pathogenic organisms (Grice and Segre, 2011). The skin microbiota is dynamic and exhibits diversity between individuals and types of bacterial species that colonise specific sites on skin depending on the local skin environment, including keratinocyte cell surface adhesion proteins, moisture levels and pH that can influence the skin microbial flora (Williams and Gallo, 2015). For instance, the axillary vault, groin and toe

web are partially occluded with a higher humidity and temperature that encourage the growth of bacterial genera that thrive under the moist conditions, such as corynebacteria, staphylococci and Gram-negative bacilli (Roth and James, 1988). Host and external factors such as gender, age, hygiene products and antibiotic usage can also affect microbial colonisation at specific skin regions (Grice and Segre, 2011).

Microorganisms that are normally found on humans can be classified into three groups: the residents that permanently inhabit the skin; temporary resident microbes that can maintain growth rates sufficient to remain in the skin niche for a short period of time; and transients that are intermittent skin colonisers and are either non-replicating or their growth rates are too low to sustain their presence in the niche (Holland and Bojar, 2002).

The microbial composition of skin was determined by a combination of culturing methods and using 16S rRNA gene sequencing techniques (Cogen *et al.*, 2008; Grice *et al.*, 2008). Coagulase-negative staphylococci (CoNS) are the dominant facultative anaerobes on the skin by culturing techniques (Cogen *et al.*, 2008) while propionibacteria are the dominant anaerobe by culturing methods and 16S rRNA gene sequencing (Cogen *et al.*, 2008; Costello *et al.*, 2009). The use of 16S rRNA gene-based methods further confirmed the presence of *Propionibacterium* spp., *Corynebacterium* spp. and *Staphylococcus* spp. as the major genera that exist on human skin (Dekio *et al.*, 2005; Grice *et al.*, 2008; Grice *et al.*, 2009). Genomic approaches to characterise skin bacteria have revealed a much greater diversity of species than that found by culture-based methods (Gao *et al.*, 2007). Among the most common skin colonisers identified, include *Micrococcus spp., Brevibacterium spp.* and the skin fungus *Malassezia spp.* (Cogen *et al.*, 2008).

1.3 The Staphylococci

Staphylococcus is a genus of the Gram-positive family *Staphylococcaceae* in the Firmicutes phylum. Several of the species are widespread in nature, although they are mainly found living on the skin, skin glands, and mucous membranes of mammals and birds (Nagase *et al.*, 2002; Costello *et al.*, 2009; Otto, 2009) and

extensive studies have focused on this resident skin flora because of its ubiquitous colonisation of human skin (Cogen *et al.*, 2008). The *Staphylococcus* genus contains over 40 species and a subset of them can cause serious infections in humans, most commonly *S. aureus*. This species has evolved the ability to survive in many environmental conditions, which leads to it being frequently described as versatile (Lowy, 1998). *S. epidermidis* is the most prevalent staphylococcal species that inhabits human skin and it comprises more than 90% of the aerobic resident flora at some sites. Although previously considered innocuous, over the past 20 years *S. epidermidis* has evolved efficient survival strategies and increased antimicrobial resistance to emerge as a causative agent of nosocomial infections (Cogen *et al.*, 2008). Other coagulase-negative staphylococci (CoNS) frequently colonise the skin including *S. hominis* and *S. capitis* and less frequent colonisers include *S. warneri, S. pettenkoferi, S. lugdunensis* and *S. haemolytic*us (Otto, 2010).

Consistently, compared with *S. aureus*, CoNS have fewer virulence factors responsible for aggression (Kloos and Schleifer, 1975) and develop a relationship with their host, only opportunistically switching from commensal to pathogen after damage to natural barriers such as the skin (Otto, 2008). Approximately 20-30% of healthy humans are persistently colonised by coagulase-positive *S. aureus* in the nose and perineum leading to it being commonly isolated from the skin of these carriers. Despite these locales in colonised individuals who shed the bacteria onto their skin, *S. aureus* is not considered part of the microbiota that persistently colonises skin (Tannock, 1994).

S. aureus encodes multiple virulence determinants to cause clinical diseases that range from minor and self-limited skin infections to more penetrating pathology. Cutaneous *S. aureus* infections are very frequent in humans and include subcutaneous abscesses, folliculitis, impetigo, furuncles and less frequently through the production of exfoliative toxins, staphylococcal scalded skin syndrome (Brown *et al.*, 2003; Iwatsuki *et al.*, 2006; Cogen *et al.*, 2008). While *S. epidermidis* is currently considered an important pathogen in catheter-related bloodstream infections, it frequently causes prosthetic valve endocarditis,

replacement joint infections and other biomedical device-associated infections (Kahl *et al.*, 2016).

Resistance to antibiotics became a major concern related to *S. aureus* due to the prevalence of methicillin resistant (MRSA) between countries (Fair and Tor, 2014). All MRSA strains contain the mobile genetic element SCC*mec*, which encodes the *mecA* gene, thus conferring resistance to methicillin and all β-lactam antibiotics (Lyon *et al.*, 1984). The use of vancomycin was instigated as the only effective antibiotic against MRSA and its use selected the first vancomycin-intermediate *S. aureus* strains (VISA) (Fair and Tor, 2014). These strains absorb the vancomycin due to their thickened cell wall that enables enough synthesis of new peptidoglycan for survival (Cui *et al.*, 2003). Ultimately, emergence of vancomycin intermediate-resistant *S. aureus* (VRSA) encoding for the resistance to glycopeptides (*vanA* operon) in *S. aureus* strains arose from a conjugal transfer with a vancomycin-resistant *E. faecalis* (Alibayov *et al.,* 2014).

1.5 *Staphylococcus* survival

Staphylococci have evolved multiple molecular factors to escape killing by human host defence peptides, adhesion to the skin and compete with other microbes for successful colonisation. Adhesion to host tissue is achieved using an array of surface proteins, with a wide range of binding capabilities, surface teichoic acid and secreted enzymes (Otto, 2010; Li *et al.*, 2014). Colonisation occurs when the top epithelial layer is traversed and a high affinity adherence between host extracellular matrix proteins and bacterial cell-surface virulence factors known as microbial surface components recognising adhesive matrix molecules (MCSCRAMMS) (Patti *et al.*, 1994). Many members of the MSCRAMM family have been characterised, which include staphylococcal protein A (SpA), clumping factors (ClfA and ClfB), fibronectin binding proteins (FnbpA and FnbpB) and collagen binding protein (Cna) (Foster and Höök, 1998); these all have ability to inhibit phagocytic engulfment (Foster, 2005). There are up to 20 MSCRAMMs that have been identified in *S. aureus* while *S. epidermidis* encodes 12 MSCRAMMs (Coates *et al.*, 2014; Foster *et al.,* 2014). This group of adhesins are not fully

understood in other staphylococci. It was reported that the *S. saprophyticus* genome includes three genes (serine-aspartate repeat-containing protein (*sdrI*), uroadherance factor B (*uafB*) and multifunctional protein (*aas*) (Hell *et al.*, 1998; Sakınç *et al.*, 2009; King *et al.*, 2011). Generally, *S. epidermidis* produces fewer virulence determinants and most of these are related to biofilm synthesis (Fey and Olson, 2010). On the host, staphylococcal SpA binds the Von Willebrand factor and immunoglobulin G, ClfA and ClfB both bind fibrinogen, FnbpA and FnbpB bind fibronectin and fibrinogen. These host ligands are glycoproteins found in the extracellular matrix and blood plasma, and play a role in thrombogenesis. The binding of these MSCRAMMS to host proteins produces an agglutination phenotype, aids bacterial attachment to damaged tissue, and contributes to pathogenesis (Joh *et al.*, 1999).

Staphylococcus species, and most prominently *S. aureus*, have the ability to survive within different types of host-derived cells, even neutrophils, through inhibition of phagosome lysosome fusion, neutralisation of phagosome contents by staphyloxanthin, resistance to lysozyme and subsequent escape into the cell cytoplasm (Foster, 2005; Clauditz *et al.*, 2006). Invasive bacterial infection occurs when *S. aureus* shifts from attachment to an invasive phase by breaching the skin barrier and entering the host. This must be accompanied by the expression of enzymes, including lipases, proteases, nucleases and hyaluronidases (Lowy, 1998).

Beside the host invasion factors, *S. aureus* employs a myriad of toxins that promote virulence. The major virulence determinants include hemolysins (alpha toxin, beta toxin, delta toxin and gamma hemolysin) and Panton-Valentine Leukocidin (PVL). Secretion of these toxins aid the organism to face host immune defenses (Otto, 2013). Cell wall-anchored teichoic acids (WTA), fatty acid modifying enzyme (FAME), catalase and staphyloxanthin are factors that inactivate host bactericidal components. Staphyloxanthin is a membrane bound carotenoid pigment that gives *S. aureus* its characteristic yellow colour. Functionally, it acts as a biological antioxidant by scavenging and detoxifying environmental reactive oxidative species (ROS) such as H_2O_2, O_2^- and ClO^-,

including those produced by human neutrophils (Clauditz *et al.*, 2006). Catalase is a secreted enzyme that breaks down host produced H_2O_2 into H_2O and O_2 (Grüner *et al.*, 2007). FAME is a secreted protein found on the skin and in abscesses, which catalyses the esterification of long-chain free fatty acids to alcohol and cholesterol that inactivates the bactericidal activity of lipids (Chamberlain and Imanoel, 1996). WTA and FAME both target antimicrobial fatty acids found on skin. Kohler *et al.* have shown that WTA prevents the binding of antimicrobial free fatty acids at the bacterial cell surface to allow bacteria to colonise skin (Kohler *et al.*, 2009).

Biofilm formation is a key mechanism for evading host defenses and decreases the effect of antimicrobials (Sánchez *et al.*, 2013). Strains that are able to form robust biofilms were more frequently observed to have a multi-drug resistance phenotype (Sánchez *et al.*, 2013). In their natural environment, bacteria have the ability to form single species biofilms or more commonly, coexisting in multispecies communities and form mixed biofilms on different solid surfaces or food products (Wang *et al.*, 2013). There is increased frequency of the *icaADBC* operon in clinical *S. epidermidis* strains, the gene products of which synthesise polysaccharide intercellular adhesion (PIA) as the main adhesive component in biofilm (Gerke *et al.*, 1998) and was found to affect the osmotic stress tolerance in staphylococci (McKenney *et al.*, 1998). Biofilm is commonly produced by *S. aureus* and other staphylococci (Heilmann *et al.*, 1996). Poly-γ-glutamic acid (PGA) is the bacterial exopolymer produced by certain coagulase-negative staphylococci, *S. caprae*, *S. warneri*, *S. hominis* and *S. capitis* and *capBCAD* locus is responsible for PGA production (Kocianova *et al.*, 2005; Joo and Otto, 2015). Both PIA and PGA protect the bacterial cell from cationic and anionic human AMPs, such as HBD3, LL-37 and dermcidin (Joo and Otto, 2015). Clinical *S. epidermidis* infections are commonly associated with biofilm and depend on factors such as PIA to cause robust colonisation of medical devices. Biofilm formation may have limited advantages for commensal growth, since Rogers *et al.* showed *ica*-negative *S. epidermidis* strains were able to outcompete *ica* positive strains for growth in a human skin model (Rogers *et al.*, 2008). *S. epidermidis* and *S. aureus* are the best studied biofilm producing species in the genus and they use similar

molecular factors for biofilm formation, although there are differences in other CoNS that are not entirely understood relative to colonisation (Otto, 2008).

Microbes that are known to colonise the same niches in the human body usually compete with each other. For example, several species exclude *S. aureus* colonisation in the nasal cavity, including *S. epidermidis, S. haemolyticus*, *S. hominis, Finegoldia magna*, *Micrococcus* sp. and *Corynebacterium accolens* (Iwase *et al.*, 2010; Wos-Oxley *et al.*, 2010; Libberton *et al.*, 2014). In the presence of glycerol, a natural product on the skin, *Propionibacterium acnes* was reported to be able to reduce *S. aureus* viability *in vivo* and *in vitro* via production of propionic acid (Shu *et al.*, 2013). *P. acnes* was also able to reduce wound size in a mouse skin abscess model when added prior to *S. aureus* infection (Shu *et al.*, 2013). *Lactobacillus fermentum* was shown to interfere with *S. aureus* colonisation and prevented *S. aureus* infections in an animal model. It was also identified that a collagen-binding protein secreted by *L. fermentum* is likely responsible for this result (Gan *et al.,* 2002). Bacteriophages may participate in the multiple species competition on the skin and they were shown to increase the survival stress of staphylococcal colonisers (Aswani *et al.,* 2011). Moreover, most staphylococci are able to produce phenol-soluble modulins (PSMs) and in particular *S. epidermidis* and *S. aureus* (Li *et al.*, 2014). PSM peptides can act as virulence determinant in a community-associated MRSA (CA-MRSA) skin infection model (Liu, 2009). *S. epidermidis* PSM-δ and PSM-γ peptides selectively cause a reduction of survival of *S. aureus, S. pyogenes* and *E. coli* but not *S. epidermidis* (Cogen *et al.*, 2010). Additionally, these PSMs are able to induce lipid vesicle leakage and exert antimicrobial activity against *S. aureus* (Cogen *et al.*, 2010). *S. epidermidis* can convert glycerol to succinic acid and this leads to inhibition of the growth of *P. acnes* and reduce *P. acnes* lesions in mouse models (Wang *et al.*, 2014). Staphylococci also produce different types of antimicrobials that are active against different skin commensals. Competition will be discussed further later in (section 1.5.2).

1.5 *Staphylococcus* competition

1.5.1 Types of interspecific competitive interactions

Much attention has been given to interspecies competitive strategies and revealed how bacterial species employ several mechanisms for coexisting with or dominating other competitors for the same pool of resources (Hibbing *et al.*, 2010). There are different types of interspecific interactions that could be driving a negative association between multiple species with staphylococci, particularly *S. aureus* in the same community. Interactions include competition for limited resources, competition by producing antibiotics, disruption of signaling, competition for receptors or by induction of host defense (Fig 1.1).

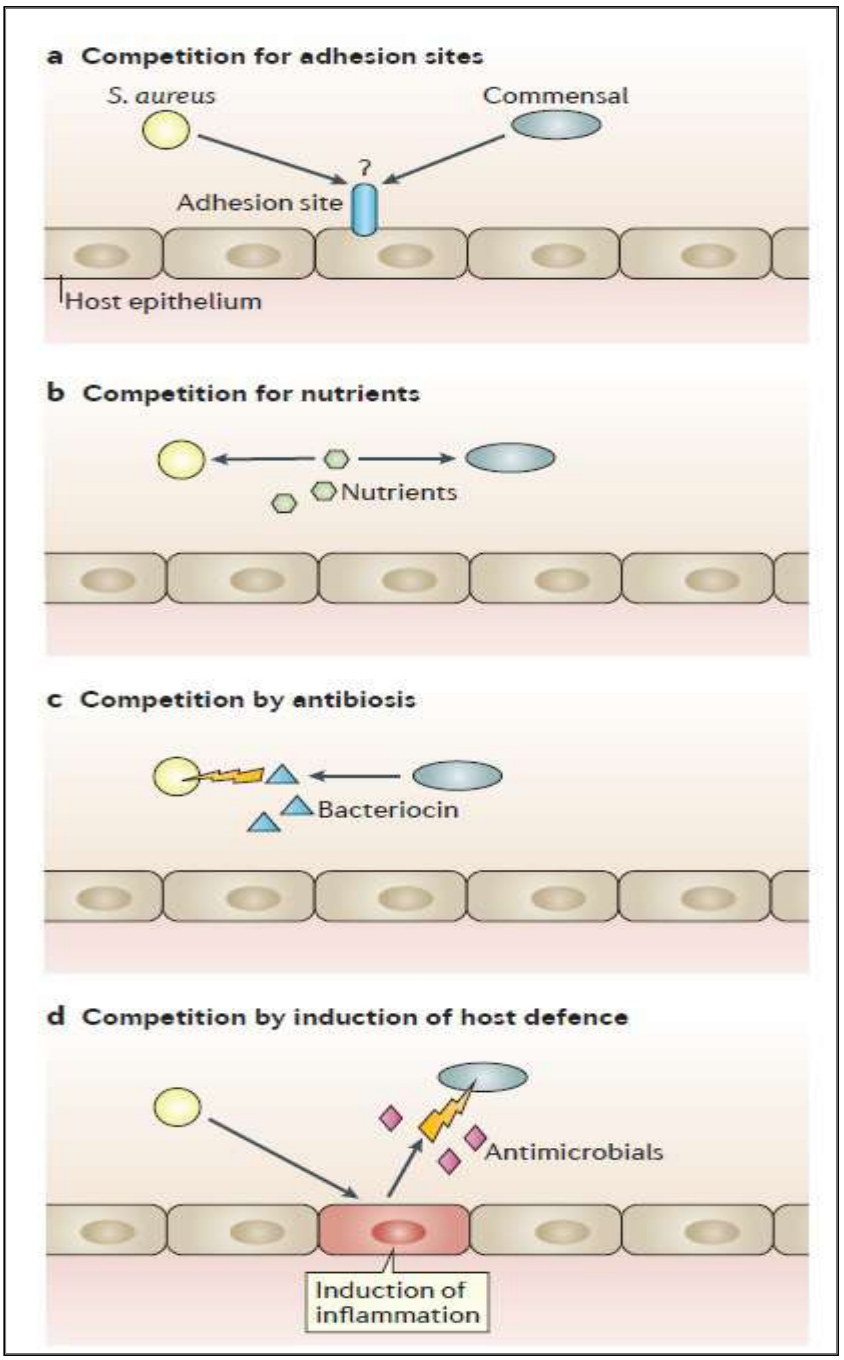

Figure 1.1 Competition mechanisms between *S. aureus* and nasal bacteria. Bacterial competition: (A) for limited host receptors (B) for limited nutrients (C) By production of antimicrobial (D) by induction of host defences that kill commensal bacteria but not affect *S. aureus.* Adapted from (Krismer *et al.*, 2017).

1.5.1.1 Resource competition

Competition for resources occurs when members of two separate species have limited resources in the same niche. Microbial competition for nutritional resources is a focal point because there is an association between the concentration of limiting nutrients and the growth of bacteria (Hibbing *et al.*, 2010). Research revealed that *S. aureus* grows better compared with CoNS, which have a slower growth rate in synthetic nasal medium (SNM) that comprises the same concentration of molecules present in nasal secretions, including sodium chloride, a low concentration of potassium, amino acids and sugar. From this data it was proposed that the nose is not a favoured colonisation site for CoNS and was considered a transient habitat. (Krismer *et al.*, 2014). Moreover, *S. aureus* can secrete GlpQ phosphodiesterase that is able to digest the glycerophosphocholine (GroPC) head group of phosphatidylcholine, which is released from eukaryotic cells. This activity makes *S. aureus* unique among *Staphylococcus* species and it helps provide glycerol-3-phosphate (Gro-3P) as a carbon and phosphate source enabling *S. aureus* growth in nutrient-limited conditions in the presence of host GroPC (Jorge *et al.*, 2017). Microbes secrete small iron-sequestering molecules called siderophores as a key microbial mechanism for acquisition of iron (Wandersman and Delepelaire, 2004). The importance of iron was confirmed by several examples of siderophore-mediated interspecies interactions in different environments. The competitive scavenging of iron resources has been shown between *S. aureus* and *P. aeruginosa* (Harrison *et al.*, 2008).

1.5.1.2 Antagonistic interactions

Toxin-mediated interference competition is caused by the production of a compound by one organism that reduces the relative fitness of another organism in the community (Morin, 1999). The toxic compounds are usually generated by non-ribosomal peptide synthetases (NRPS) or they are ribosomally synthesised with post-translational modifications (RiPPs), and collectively termed bacteriocins (Krismer *et al.*, 2017). Nasal *Staphylococcus* species were found to secrete antimicrobials at high frequency (86%) and they are active toward other nasal isolates (Janek *et al.*, 2016). Several types of interactions between bacteria have been described in mixed species biofilms. A study of six intergeneric

heterotrophic bacteria, which included Gram-positive and Gram-negative species, showed either neutral interactions or cooperation with respect to biomass formation in mixed organisms biofilm (Simões *et al.*, 2007). Tait & Sutherland (2002) examined antagonistic interactions between bacteriocin-producing enteric bacteria and showed that each strain was able to form its own microcolonies within mixed biofilms (Tait and Sutherland, 2002). Antagonism between *Streptococcus pneumoniae* and *S. aureus* can be mediated through the production of hydrogen peroxide by *S. pneumoniae in vitro* (Regev-Yochay *et al.*, 2006; Bessesen *et al.*, 2015). However, *S. aureus* survival in a rat nasal colonisation model was not affected by H_2O_2-producing *S. pneumoniae* (Margolis, 2009).

1.5.1.3 Antagonism of signaling

Disruption of quorum sensing is a mechanism allowing commensal bacteria to reduce their competitor's fitness (Dong *et al.*, 2002; Fleming *et al.*, 2006). Inhibition of quorum sensing was identified between *Staphylococcus* spp. particularly between *S. epidermidis* and *S. aureus* (Otto, 2009). *S. epidermidis* AIP signal class I was shown to inhibit all *S. aureus agr* classes (I, II and III) except type IV, while only *S. aureus* type IV could inhibit *S. epidermidis agr* type I (Otto *et al.*, 2001). In *S. aureus*, signal peptides of one class such as AIP II can inhibit sensing of the other AIP signal classes, which suggests the inhibition of quorum sensing within species (Ji *et al.,* 1997). Subsequently, it was also shown that the interference between different *agr* types reduced virulence in an insect model (Fleming *et al.*, 2006).

A recent study revealed that S*. caprae* secretes an AIP that strongly inhibits all classes of *S. aureus* quorum sensing and it was proposed that the inhibitory AIP may give *S. caprae* competitive advantage during interaction with *S. aureus* in the cutaneous environment (Paharik *et al.*, 2017). This finding was confirmed by performing competition experiments between *S. caprae* and MRSA that revealed a greater reduction in MRSA burden using murine models of both skin colonisation and intradermal infection (Paharik *et al.*, 2017). The human skin commensal *Corynebacterium striatum* was also found to repress the function of

quorum-sensing in *S. aureus*. In a murine subcutaneous abscess model, *S. aureus* abundance was reduced during co-infection with *C. striatum* (Ramsey *et al.*, 2016).

1.5.1.4 Competition for receptors

Bacteria compete for a limited number of host receptors (Liu, 2009). Studies have indicated that *S. aureus* adhesins, including wall teichoic acid, IsdA and ClfB promote *S. aureus* nasal colonisation (Mulcahy *et al.*, 2012; Baur *et al.*, 2014). Many of these adhesin proteins have homologs in other staphylococcal species including *S. epidermidis*, and it is known that some of these homologs can bind to the same receptors (Coates *et al.*, 2014). Identified homologous microbial adhesins that bind to the same host receptors include autolysin/adhesin Aae from *S. epidermidis* that is a homolog of Aaa expressed by *S. aureus* (Heilmann *et al.*, 2005), but the study did not characterise *S. aureus* attachment to host cells. *S. aureus* adhesins for collagen type I, fibronectin and fibrinogen are expressed also by *S. pyogenes* (Edwards *et al.*, 2004; Brouwer *et al.*, 2016). It is possible that these bacteria could displace or inhibit *S. aureus* colonisation in similar way that was shown with lactobacilli that inhibit *S. pyogenes* adherence to host epithelial cells (Saroj *et al.*, 2016). *S. epidermidis* secretes an endoserine peptidase (Esp) that inhibits nasal *S. aureus* colonisation by degradation of *S. aureus* surface proteins and host receptors that are important for the interaction of the bacterial pathogen with the host cell (Sugimoto *et al.*, 2013).

1.5.1.5 Induction of host defence

Several studies have identified that *S. aureus* colonisation can lead to enhanced inflammation in the nasal epithelium, possibly due to the activation Toll-like receptor 2 (TLR2) as a result of secreted of pro-inflammatory molecules, such as lipoproteins (Krismer *et al.*, 2017). Increased expression of PSM peptides by certain *S. aureus* strains can stimulate lipoprotein release from the *S. aureus* cytoplasmic membrane (Hanzelmann *et al.*, 2016). Increased production of anti-microbial peptides and proteins by the host usually results from inflammation. However, *S. aureus* tends to be less affected by higher concentrations of host antimicrobials compared with commensal bacteria. Hence, it is possible that *S.*

aureus is able to induce inflammation to eliminate human commensals that consequently face difficulty to survive in the nasal fluid (Krismer *et al.*, 2017).

S. epidermidis also stimulates antimicrobial peptide expression from keratinocytes and therefore augments skin defence towards pathogenic bacteria (Lai *et al.*, 2010). Moreover, resistance of CoNS and *S. aureus* to high concentrations of CAMPs is due to their ability to modify the teichoic acids and phospholipids with D-alanine and L-lysine, respectively, which leads to reduction of the affinity of the cell envelope for CAMPs (Peschel and Sahl, 2006). Contrastingly, other nasal bacteria are more sensitive to cationic antimicrobial peptides (CAMPs) than staphylococci, such as *P. acnes* (Lee *et al.*, 2008). Moreover, whilst many nasal commensal bacteria are susceptible to lysozyme, most human-associated CoNS and *S. aureus* are resistant because they modify *N*-acetylmuramic acid residues of peptidoglycan, with additional acetyl groups or WTA polymers that inhibit lysozyme digestion (Herbert *et al.*, 2007). The exact mechanisms behind the high resistance of staphylococci to lysozyme are unknown but several studies proposed that both modifications sterically block efficient lysozyme binding to the peptidoglycan sugar backbone (Krismer *et al.*, 2017).

1.5.2 Staphylococcal bacteriocins and their mode of action

Antimicrobial proteins and peptides that are produced by commensal skin microbes are a key mechanism against other bacteria that might seek to colonise the skin surface. Bacteriocins secreted by many varieties of bacteria have a role in antagonistic interactions between the producing strains and other closely related bacteria and their inhibitory activity gives the producer a competitive advantage in the environment (Guder *et al.*, 2000). Colicins were the first antimicrobial peptide compounds identified as secreted by *E. coli* (Riley and Wertz, 2002). Now, bacteriocins have been found in all major bacterial lineages and the lactic acid bacteria (LAB) are the most abundant producers of bacteriocins, being widely used for centuries as species to ferment foods (Riley and Wertz, 2002).

Bacteriocins are a class of ribosomally-synthesised antimicrobial peptides and those produced by Gram-positive bacteria have common features such as protease resistance, heat stability, and faster migration through an SDS-PAA gel than predicted on the basis of their sizes (Sharma *et al.,* 2016). They are classified into four groups: Class I (lantibiotics) are small peptides (<5 kDa), containing modified amino acids such as didehydroamino and thioether; Class II are small peptides (<10 kDa), containing no modified amino acids and are heat stable bacteriocins; Class III are large, heat-labile proteins and Class IV includes complex bacteriocins that contain important lipids or carbohydrate moieties in addition to protein (Klaenhammer, 1993; Margolles *et al.*, 2006; Bastos *et al.*, 2009).

Species of the *Staphylococcus* genus are frequently producers of bacteriocin, which are collectively termed staphylococcins (Gagliano and Hinsdill, 1970; Bastos *et al.*, 2009). Most staphylococcins are type A lantibiotics and well-studied representatives are epidermin, Pep5, epicidin 280, epilancin K7 and nukacin (Fig. 1.2). Their structures are flexible, elongated amphipathic screw-shaped cationic peptides (Nagao *et al.*, 2006) and the characteristic feature of this class are unique amino acid residues from post-translational modifications that lead to intramolecular thioether bridges (Bastos *et al.*, 2009).

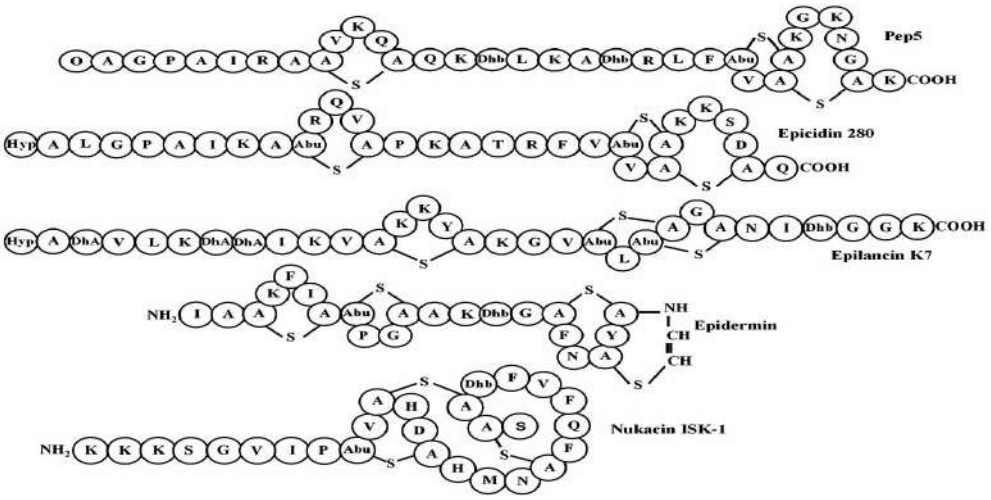

Figure 1.2 Structure of selected lantibiotics produced by staphylococci. Pep5, epidermin, epicidin 280, and epilancin K7 were identified in *S. epidermidis* while nukacin ISK-1 was identified in *S. warneri*. Adapted from (Bastos *et al.*, 2009).

Epidermin is a well characterised bacteriocin and is isolated most commonly from *S. epidermidis* strains (Bastos *et al.*, 2009). Epidermin has 22 residues (Fig. 1.2) and 11 genes were identified to encode proteins for biosynthesis of this bacteriocin. These genes were located on plasmid Tü32 in *S. epidermidis* Tü3298 including *epiA,* which is the structural gene and the associated operon *epiBCDQPGEFHT* (Bastos *et al.*, 2009; Ceotto *et al.*, 2009; Götz *et al.*, 2014). Epidermin synthesis is controlled by Agr that was shown to control functional EpiP expression that interferes with proteolytic processing during epidermin maturation (Kies *et al.*, 2003). Epidermin exhibits a bactericidal activity against *S. aureus* (Fontana *et al.*, 2006). A study by Ungermann *et al* suggested that epidermin might be effective as a therapeutic agent to treat acne in humans (Ungermann *et al.,* 1991). Similar to nisin activity, epidermin interacts with lipid I, II, III and IV resulting in the inhibition of not only murein but also wall teichoic acid (WTA) biosynthesis (Müller *et al.*, 2012; Götz *et al.*, 2014). Binding of nisin to lipid II can cause pore formation of the bacterial cell membrane while interaction of epidermin with membrane lipids causes cell death without pore formation (Hasper *et al.*, 2006; Götz *et al.*, 2014).

Gallidermin is composed of 22 amino acid and belongs to class I (lantibiotics) and it was identified in *S. gallinarum* (KELLNER *et al.*, 1988). Gallidermin acts

similarly to epidermin and nisin and it possesses the same putative lipid II binding motif (Saising *et al.*, 2012). Studies reported that the capacity for pore formation by gallidermin depends on the thickness of membrane. The interaction of gallidermin with lipids I and II instead of pore formation contributes to bacterial killing (Bonelli *et al.*, 2006; Saising *et al.*, 2012). Activity was demonstrated against propionibacteria therefore it was proposed to have potential as a therapeutic in acne disease (KELLNER *et al.*, 1988). The importance of gallidermin was also shown to be effective prevention of biofilm formation by *S. aureus* and *S. epidermidis* (Saising *et al.*, 2012).

Pep5 is 34-amino-acid tricyclic peptide identified in *S. epidermidis* (Kaletta *et al.*, 1989; Meyer *et al.*, 1995). Genes for biosynthesis of Pep5 were organised in an operon *pepTIAPBC*, located to the pED50 plasmid (Kaletta *et al.*, 1989; Meyer *et al.*, 1995). Pep5 acts by forming pores in the cytoplasmic membrane of Gram-positive bacteria (Kordel *et al.*, 1988). Pep5 weakens cell walls causing the release of membrane-associated autolytic enzymes from their inhibitors, including teichoic acid and teichuronic acid (Bierbaum and Sahl, 1991; McAuliffe *et al.*, 2001). Combining cell wall weakening and increased osmotic pressure resulting from pore formation ultimately causes cell lysis (McAuliffe *et al.*, 2001).

Epicidin 280 was identified first in *S. epidermidis* BN 280 and it has high similarity of around 75 % with Pep5 (Ceotto *et al.*, 2009). The biosynthetic genes were located in plasmid pCH01 (Bastos *et al.*, 2009). Epicidin 280 is another type A lantibiotic that exerts its function by pore formation in the bacterial membrane. Pore formation by type A lantibiotics has been studied widely and it was reported that all of them contain a central flexible hinge region that is important for their activity (Heidrich *et al.*, 1998). Moreover, the lower toxicity of epicidin 280 in comparison with Pep5 occurs because of a shorter flexible region in the latter protein (Heidrich *et al.*, 1998).

Nukacin ISK-1 lantibiotic was identified to be secreted by *S. warneri* ISK-1 and comprises 27 amino acids, including a dehydrobutyrine, a 3-methyllanthionine, and two lanthionine residues (Fig. 1.2) (Kimura *et al.*, 1998). Nukacin ISK-1 was

encoded by an operon located to plasmid pPI-1, including its structural gene *nukA* (Ceotto *et al.*, 2009). Nukacin ISK-1 activity completely arrested the growth of *B. subtilis* JCM 1465 without lytic activity or pore formation (Asaduzzaman *et al.*, 2009). Contrastingly, a further study discovered this lantibiotic has potent bactericidal activity against *S. simulans* and *M. luteus* by binding to lipid II and altering the integrity of the cell membrane due to dissipation of membrane potential and formation of small-sized or specific potassium ion-conducting pores, which leads to cell death (Roy *et al.*, 2014). Subsequently, it was suggested that Nukacin ISK-1 mode of action depends on physical properties of the target species, such as membrane thickness and membrane lipid composition (Roy *et al.*, 2014). Recently, Nukacin IVK45 produced by *S*. *epidermidis* strain IVK45 was identified. The operon was similar to that encoding nukacin ISK-1 of *S*. *warneri* ISK-1, together with a different location and orientation of the precursor peptide gene *nukA* (Janek *et al.*, 2016). Nukacin IVK45 showed bacteriostatic activity against Gram-positive bacteria (Janek *et al.*, 2016) with biosynthesis increased under iron limiting condition and hydrogen peroxide-induced oxidative stress, which could reflect conditions experienced by bacteria colonising the nasal cavity (Janek *et al.*, 2016).

Zipperer et al (2016) recently identified a novel antimicrobial peptide, lugdunin, secreted by nasal isolate *S. lugdunensis* IVK28 (Zipperer *et al.*, 2016). Lugdunin is composed of non-ribosomally synthesised peptides encoded by the *lugABCD* operon. Lugdunin displayed bactericidal activity toward several Gram-positive bacteria, including methicillin-resistant and vancomycin-resistant *S. aureus* and *Enterococcus* isolates (Zipperer *et al.*, 2016). Lugdunin was shown to effectively reduce the number of viable cells of *S. aureus* in a mouse skin infection model and it was proposed that the absence of *S. aureus* in the nose was associated with the presence of *S. lugdunensis* secreting lugdunin (Zipperer *et al.*, 2016). The mechanism of action of lugdunin is still unknown however the authors suggested that it might inhibit protein, DNA and/or peptidoglycan synthesis in *S. aureus.*

Aureocin A53 is a class II bacteriocin (unmodified, heat-stable peptides) secreted by *S. aureus* A53 and was located to a 10.4-kb plasmid named pRJ9 (Giambiagi-

Marval *et al.*, 1990). Aureocin A53 has strong activity against multidrug-resistant nosocomial staphylococcal strains such as the multidrug-resistant *S. aureus* (MRSA) clone endemic in most Brazilian hospitals and in other different countries, various CoNS strains and *S. agalactiae* isolated from bovine mastitis. The bacteriocin is also active against *L. monocytogenes*, an important food-borne pathogen (dos Santos Nascimento *et al.*, 2012).

The bacteriocin C55 also belongs to class II bacteriocins and is produced by exfoliative toxin B (ETB)-positive *S. aureus* (Navaratna *et al.,* 1998). The bacteriocin immunity factors and ETB are encoded on the plasmid pETB (Kawada-Matsuo *et al.*, 2016). ETB comprises three distinct peptides C55α, C55β, and C55γ where both C55α and C55β act synergistically being more active towards *Micrococcus luteus* and *S. aureus,* but not *S. epidermidis* (Navaratna *et al.,* 1998). Co-cultivation of C55-positive and negative strains showed that C55 production reduced the levels of non-expressing isolates after 8 h (Kawada-Matsuo *et al.*, 2016).

Hominicin is a type A lantibiotic identified in *S*. *hominis* MBBL 2–9. The structure of hominicin contains the uncommon amino acids characteristic of the type A lantibiotics but without thioether bridges integral to the lanthionine ring structure (Kim *et al.*, 2010). Hominicin exerts antimicrobial activity against vancomycin-intermediate *S*. *aureus* (VISA) and methicillin-resistant *S*. *aureus* (MRSA) (Kim *et al.*, 2010). Hominicin was shown to have a high thermal stability up to 121°C for 15 min and remains active under both basic and acidic conditions (Kim *et al.*, 2010). More recently, Nakatsuji et al. demonstrated that *S. hominis* strains isolated from skin can provide protection from *S. aureus* colonisation in atopic dermatitis patients via production of antimicrobial (Nakatsuji *et al.*, 2017).

Bacteria that are producers of any type of lantibiotics must express protection mechanisms to prevent toxicity of the bacteriocin. Self-immunity is provided by dedicated ABC transporters (LanFEG) or via specific proteins (LanI) (Bastos *et al.*, 2009). For example, immunity of *S. warneri* ISK-1 strain against nukacin ISK relies on the cooperative action of the membrane bound immunity protein NukH

and the NukFEG transporter (Aso *et al.*, 2004). This nukacin ISK-1 immunity system was shown to confer active immunity to lacticin but not to nisin (Bastos *et al.*, 2009). Pep5 was proposed to require a simple mechanism of protection by PepI immunity peptide. PepI accumulates at the membrane-cell wall interface and may bind to Pep5 target molecule thus protecting the producer strain from the bacteriocin. (Hoffmann *et al.*, 2004). Similarly in the case of nisin-producing *L. lactis*, the membrane-bound lipoprotein NisI interact with nisin to reduce its local concentration (Stein *et al.*, 2003; Takala and Saris, 2006). Recent study has revealed that staphylococci skin isolates producing inhibitory activity of the same species or have similar pulsotype had the same immune to each other, suggested that they may produce the same bacteriocins or probably they are the same strain (O'Sullivan, 2018).

1.5.3 Methods for investigating antagonistic activity

16S rRNA gene sequencing is frequently used to study competitive exclusion among microbial consortia by determining the correlations between presence and absence of bacterial species (Frank *et al.*, 2010; Wos-Oxley *et al.*, 2010). However, intraspecific trait variations, for instance the ability to produce antimicrobial peptides may greatly inhibit coexistence studies at species level (Libberton *et al.,* 2014). Since 16S rRNA sequencing cannot differentiate between discrete strains of the same species, intraspecific trait variation is more difficult to test at the population level (Moran *et al.*, 2016).

There are several techniques used to detect antimicrobial activity in *vitro* and most are based on individual assays to determine diffusion of inhibitors through solid or semi-solid culture media that affect the growth of a sensitive indicator microorganism (Velho-Pereira and Kamat, 2011). Agar disk-diffusion inhibition is a well-known method and it is performed by inoculation the microbial strain of interest on agar plates. Next, filter paper discs (about 6 mm in diameter), containing a desired concentration of antimicrobial are placed on the agar surface. After incubation period, the compound diffuses into the agar and inhibits growth of the test strain. Based on diameters of inhibition of growth zones the activity can be estimated (Balouiri *et al.*, 2016). This method is used to simply test

a wide range of antibiotics and study different phenotypic effects of antimicrobials between two or more strains or wild-type and mutants. The latter was performed with a catalase mutant strain of *S. aureus* that was shown to be more sensitive to *S. pneumoniae* producing H_2O_2 compared with the wild-type strain, supporting the contribution of catalase in niche competition (Park *et al.*, 2008) (Fig 1.3). Spot-on-lawn is the simplest assay that has been used to study antagonism. Briefly, spotting a test strain in the centre of an agar plate, followed after incubation with overlay of the indicator strain in soft agar (Schillinger and Lücke, 1989). Alternatively, a cross streak method was used by Lertcanawanichakul et al. (2011) to rapidly screen for antagonistic interactions among microorganisms. This assay was performed by drawing a single streak of the strain of interest down the middle of an agar plate. After a sufficient incubation period, estimated based on the microorganisms used, the indictor microbial strain is then seeded with a single perpendicular streak across the test strain. The antimicrobial interface is observed after further incubation to quantify the inhibition zone size (Lertcanawanichakul and Sawangnop, 2011). Studies have highlighted that greater inhibition of indicator bacteria are obtained using the cross streak method compared with an alternative agar well diffusion assay based on inoculation of agar punches with the test strain (Lertcanawanichakul and Sawangnop, 2011). However, it is quite difficult to obtain quantitative data from these assays due to the margins of inhibition zone often being indistinct (Williston *et al.*, 1947).

An alternative approach is to determine the MIC values for crude extracted antimicrobial, using a standard dilution method. The exact concentration of antimicrobial agent can only be estimated in the agar (agar dilution) or broth medium (macrodilution or microdilution) (Balouiri *et al.*, 2016). Semi-quantitative methods were described by Moran et al. (2016) using a modified deferred inhibition assay. The method detects negative and positive growth interactions, where the presence of one species can inhibit or promote the competitor strain. This method was used to generate quantitative (inhibition degree) and qualitative data (clarity of the zone) and these data were used to identify correlations between inhibition of individual species and cumulative

inhibition to determine correlates of association between trait variation and competitive exclusion in the anterior nares (Libberton *et al.*, 2014; Moran *et al.*, 2016).

Genomics combined with bioinformatic studies of many bacteria discovered that some bacteria encode gene clusters for important or novel secondary metabolites with known or predicted antimicrobial activity (Scherlach and Hertweck, 2009). Actinomycetes are a rich source for the production of antibiotics; complete genome sequencing of *Streptomyces parvulus* revealed 109 gene clusters contributing to the biosynthesis of known or unique bioactive compounds (Hu *et al.,* 2019). Studies speculate that many bacteria could possess cryptic genes that encode new bioactive molecules that could be secreted during interspecific interactions that have not yet appeared in standard laboratory cultivation (Bertrand *et al.*, 2014; Marmann *et al.*, 2014). Microbial interactions could select for antimicrobial production through activation of such cryptic genes.

Mass spectrometry (MS) tools have been developed recently with the aim of understanding metabolism of entire cells or populations and is termed metabolomics. Uses include determing the effects of therapeutic agents (Esquenazi *et al.*, 2009). Imaging MALDI (Matrix Assisted Laser Desorption Ionization) has concomitantly been used for imaging biological samples and it can analyse a high molecular mass > 100 kDa down to small molecules with a molecular mass of < 1 kDa (Schwamborn and Caprioli, 2010). The method has been applied to detect differences in production of metabolites when two or more microorganisms are grown in the presence or absence of each other (Gonzalez *et al.*, 2011; Barger *et al.*, 2012; Traxler *et al.*, 2013). In several studies it has enabled the identification of antimicrobial agents produced by a competitor (Barger *et al.*, 2012). For example, Gonzalez et al applied the emerging approach of imaging mass spectrometry (IMS) to the study of the interaction between two well-characterised Gram-positive bacterial species, *B. subtilis* and *S. aureus.* IMS data showed an increased amount of surfactin produced by *B. subtilis* during interface with *S. aureus;* plipastatin was also able to restrict the growth of *S. aureus* (Fig. 1.4) (Gonzalez *et al.,* 2011).

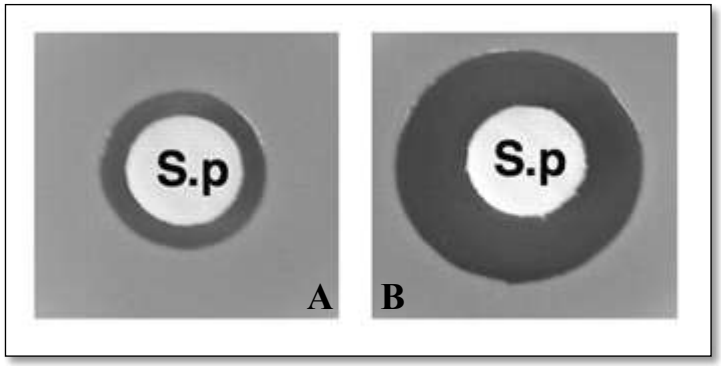

Figure 1.3 Agar disk-diffusion method. Disks with *S. pneumoniae* producing H_2O_2 caused partially inhibited growth of the *S. aureus* WT (A) and this inhibition effect increase in catalase mutant strain (B). Image adapted from (Park *et al.*, 2008).

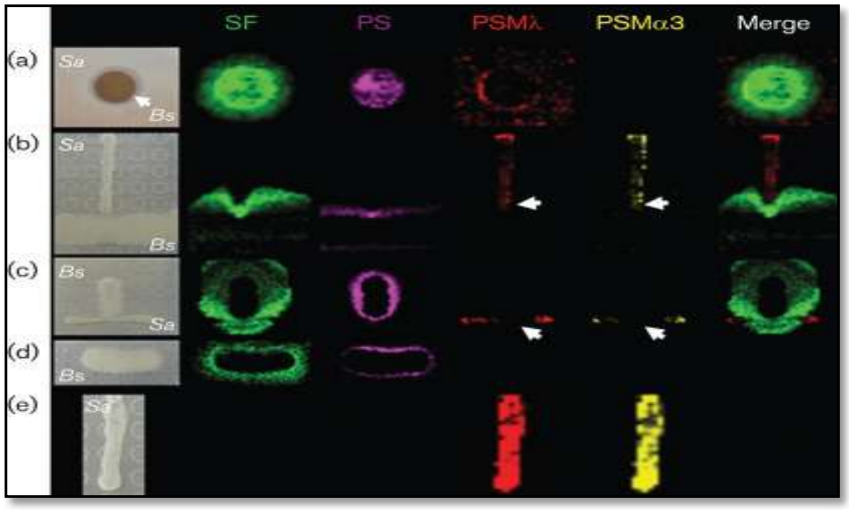

Figure 1.4 IMS of the interaction between *S. aureus* (Sa) and *B. subtilis* (Bs). (a) Zone of inhibition; (B) and (C) T-shape experiment for both species (D) *B. subtilis* alone; (E) *S. aureus* alone. Ion distributions are represented by colour: surfactin (SF; green), plipastatin (PS; magenta), PSMλ (red) and PSMα3 (yellow). Arrows indicate areas of toxin suppression. Image adapted from (Gonzalez *et al.*, 2011).

1.6 *S. aureus* regulatory systems

Mechanisms of bacterial signalling via two component regulatory systems (TCSs) are found in bacteria and functionally enable the cell to sense, respond and adapt to changes and stresses in the environment. The archetype TCS structure includes a membrane histidine kinase (HK), which acts as a signal sensor/transducer through phosphorylation of its cognate response regulator (RR) that acts as a transcription activator or repressor (Grebe and Stock, 1999). Genome studies of *S. aureus* identified that there are 16 core genome TCS with many different functions being described (Table 1.1). Studies have shown TCS can interact with each other and also regulate target genes in an independent manner from each other (Novick and Jiang, 2003; Cheung *et al.*, 2004; Novick and Geisinger, 2008). The different types of DNA binding domains of the response regulators of *S. aureus* NCTC 8325 are shown with most belonging to the OmpR type (Fig. 1.5). An additional TCS was found encoded on the mobile element, staphylococcal cassette chromosome *mec* present in MRSA isolates, where it regulates induction of methicillin resistance (Hiron *et al.*, 2011). With few of these TCS remaining to be characterised, a shared role of at least five is antimicrobial peptide (AMP) resistance including BraRS, GraRS and VraRS (Gardete *et al.*, 2006; Meehl *et al.*, 2007; Hiron *et al.*, 2011). Additionally, overlapping roles of WalKR, ArlRS and LytRS that sense changes in bacterial cell wall and membrane integrity collectively control peptidoglycan biosynthesis (Brunskill and Bayles, 1996; Fournier and Hooper, 2000; Dubrac *et al.*, 2007). AgrCA is a very well-studied quorum sensing TCS that regulates virulence gene regulation (Novick *et al.*, 1995; Novick and Geisinger, 2008). SaeSR and SrrAB are also responsible for the global regulation of virulence genes in *S. aureus* and responses to anaerobiosis by the latter (Novick and Jiang, 2003; Pragman *et al.*, 2004). AirSR was recently identified to have a role in modulation of the nitrate respiratory pathway under anaerobic conditions (Sun *et al.*, 2011). HssRS is a regulatory system that have homeostatic function for haem-iron (Torres *et al.*, 2007) while KdpED has a conserved role in potassium homeostasis described in many bacteria (Freeman *et al.*, 2013). To date, the DesKR TCS is only partly characterised. Kim et al. (2016) proposed this TCS in *S. aureus* might function similarly to the *B. subtilis* DesKR but provided only weak data that there were functional similarities (Kim *et al.,*

2016). In *B. subtilis*, DesKR TCS regulates gene expression in response to low temperatures with the major activity being upregulation of a lipid desaturase to control membrane fluidity changes (Aguilar *et al.*, 2001). The functions of PhoPR in *S. aureus* have not been unambiguously assigned but its homolog in *B. subtilis* controls the transcriptional response to phosphate limitation (Botella *et al.*, 2014). Studies of TCS across other staphylococci are much more limited. Homologues of some of these TCS described above are present in *S. epidermidis* and are proposed to have similar roles (Wu *et al.*, 2012; Xu *et al.*, 2017). More recently, comparative genomic analysis revealed that skewed distribution of GraSR and BraSR TCS across different staphylococcal species suggesting a gene duplication/acquisition event that was mostly confined, but not exclusively, to species colonising humans and mammals (Coates-Brown *et al.*, 2018).

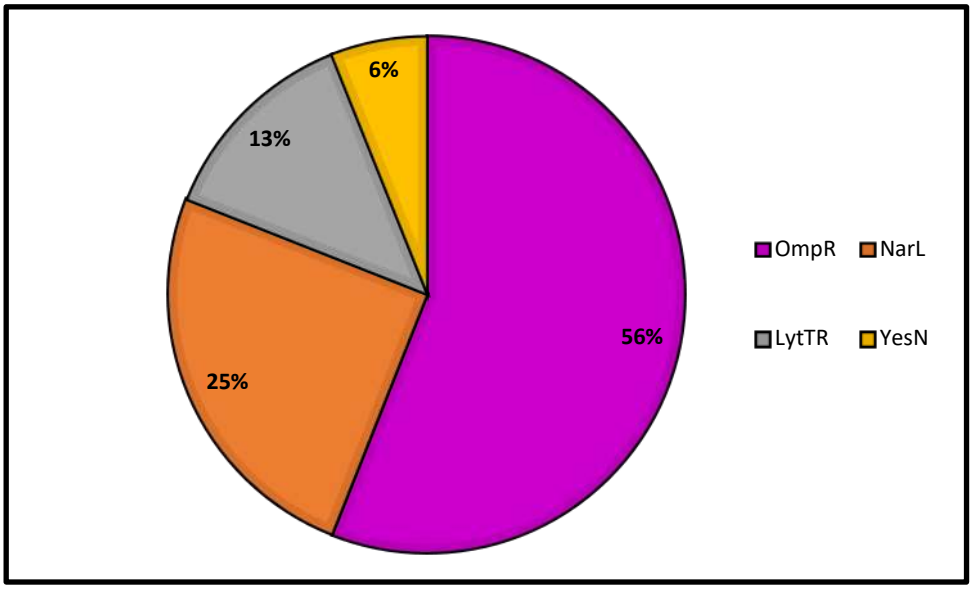

Figure 1.5 The proportion of each type of DNA-binding domains for the 16 response regulators from *S. aureus* NCTC 8325. OmpR: WalR, BceR, HssR, GraR, KdpE, PhoR, SrrA, ArlR and SaeR. NarL: Nrec, VraR, DesR and AirA. LytTR: AgrA and LytR. YesN: Unassigned regulator. The information was obtained from P2CS database (Barakat *et al.*, 2010).

Table 1.1. Two component systems identified in *S. aureus* NCTC 8325. Summary of the 16 putative TCSs identified in *S. aureus* and their assigned roles to date. The table includes the histidine kinase (HK) and response regulator (RR) with their accession number, their function and key references. These TCS were identified based on the KEGG pathways database (Kanehisa *et al.,* 2013) and AureoWiki (Fuchs *et al.,* 2018).

TCS	Gene name (NCTC 8325) HK/RR	Function	References
AgrCA	SAOUHSC_02264/ SAOUHSC_02265	Quorum sensing and virulence genes regulation	(Novick *et al.*, 1993; Novick *et al.*, 1995)
SaeRS	SAOUHSC_00714/ SAOUHSC_00715	Virulence genes regulation and oxidative stress response	(Novick and Jiang, 2003)
SrrAB	SAOUHSC_01585/ SAOUHSC_01586	Virulence genes regulation	(Pragman *et al.*, 2004)
WalKR/YycFG	SAOUHSC_00021/ SAOUHSC_00020	Cell wall turnover, autolysis and biofilm formation	(Dubrac *et al.*, 2007)
ArlRS	SAOUHSC_01419/ SAOUHSC_01420	Autolysis regulation and biofilm formation	(Fournier and Hooper, 2000)
LytRS	SAOUHSC_00230/ SAOUHSC_00231	Autolysis regulation and biofilm formation	(Brunskill and Bayles, 1996)
BraRS/NsaRS	SAOUHSC_02955/ SAOUHSC_02956	AMP resistance	(Hiron *et al.*, 2011)
GraRS/ApsRS	SAOUHSC_00665/ SAOUHSC_00666	AMP resistance	(Falord *et al.*, 2012)
VraRS	SAOUHSC_02098/ SAOUHSC_02099	Cell wall biosynthesis, AMP and antibiotic resistance	(Pietiäinen *et al.*, 2009)
HssRS	SAOUHSC_02643/ SAOUHSC_02644	Heme sensing	(Torres *et al.*, 2007)
NreBC	SAOUHSC_02676/ SAOUHSC_02677	Nitrate respiration, anaerobic growth	(Schlag *et al.*, 2008)
KdpED	SAOUHSC_02314/ SAOUHSC_02315	Potassium transport	(Freeman *et al.*, 2013)
AirSR	SAOUHSC_01980/ SAOUHSC_01981	Nitrate respiration	(Sun *et al.*, 2011)
PhoPR (putative)	SAOUHSC_01799/ SAOUHSC_01800	Unknown function	---------
DesKR (putative)	SAOUHSC_01313/ SAOUHSC_01314	Unknown function	(Kim *et al.*, 2016)
Undescribed TCS	SAOUHSC_00185/ SAOUHSC_00184	Unknown function	---------

1.6.1 TCS, and quorum sensing and transcriptional regulator involved in virulence factor production

1. The two component system *agr* (accessory gene regulator)

The accessory gene regulator (*agr*) is the most extensively characterised global regulatory TCS of *S*. *aureus.* Many virulence determinants associated with infections caused by staphylococci, such as surface-associated adhesins, autolysins toxins and hemolysin are regulated by quorum sensing through *agr*-dependent TCS activity (Novick and Jiang, 2003; Chan *et al.*, 2004). The *agr* system comprises of two adjacent but divergent transcriptional units (RNAII and RNAIII) under the control of the P2 and P3 promoters, respectively (Morfeldt *et al.*, 1995; Thoendel and Horswill, 2010)(Fig. 1.6). RNAII consists of the four genes of the quorum-sensing module *agrBDCA*. AgrC and AgrA are the two-component signal transduction system, AgrB is an export enzyme and AgrD the propeptide which is processed by AgrB into a thiolactone peptide (autoinducing peptide, AIP) (Novick *et al.*, 1993; Novick and Geisinger, 2008). There are four different structural types of AIP produced by *S. aureus* (Novick, 2006). In mid-exponential growth phase, the auto-activating circuit is initiated, when high concentrations of AgrD peptide are produced intracellularly, processed by AgrB, and secreted from the cell in the form of AIP. Increased AIP concentration in the extracellular environment activates the AgrC sensor via autophosphorylation on the membrane surface. The phosphate is transferred to the response regulator AgrA that can now bind to the intergenic region of *agr* P2 promoter and the adjacent P3 promoter. Consequently, AgrA produces upregulation of transcript *agrBDCA* and RNAIII (Fig. 1.6) (Novick *et al.*, 1993; Qiu *et al.*, 2005; Novick and Geisinger, 2008). RNAIII serves as the main effector molecule of the *agr* operon (Morfeldt *et al.*, 1995). Beside its regulatory functions, it encodes delta-haemolysin (Janzon and Arvidson, 1990). Several studies conducted to investigate the role of RNAIII as an effector molecule in the *agr* system identified that mutation of RNAIII leads to reduced expression of low molecular weight toxins and the exoenzymes, such as Geh lipase and Ecp protease (Xiong *et al.*, 2002). RNAIII functions to activate expression of extracellular proteins, including hemolysins, while it represses others such as coagulase, adhesins and protein A (Goerke *et al.*, 2000).

Expression of the *agr* system can impact many significant aspects of the lifecycle, including biofilm phenotypes and impact upon surface attachment, biofilm dispersion, and the chronic nature of biofilm-associated infections (Chan *et al.*, 2004). The important role of the *agr* system was demonstrated in many infection models. Mutation of *agr* reduced the capacity of *S. aureus* to cause abscesses compared with its parent strain when assessed in different murine and rabbit models for skin abscess, endocarditis and osteomyelitis (Abdelnour *et al.*, 1993; Cheung *et al.*, 1994; Gillaspy *et al.*, 1995; Cheung *et al.*, 2011).

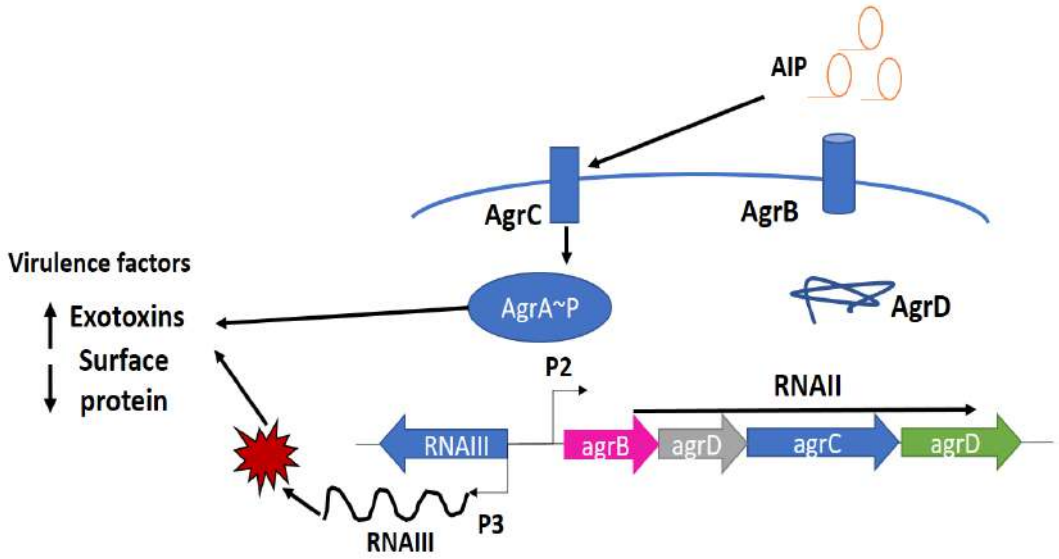

Figure 1.6 The *S. aureus* accessory gene regulator. A quorum sensing locus encoded in *S. aureus* consists of RNAII and RNAIII that are transcribed by two divergent promoters, P2 and P3, respectively. A cyclic thiolactone AIP induces a surface signal through the AgrC, a histidine protein kinase which then autophosphorylates upon binding the AIP to activate the response regulator AgrA via phosphotransfer. AgrA binds to the P2 and P3 promoters resulting in positive feedback of AIP production to activate transcription of RNAIII, the regulatory effector of the *agr* system. RNAIII upregulates expression of exotoxins and downregulates cell surface and secreted proteins. Modified from (Novick and Geisinger, 2008; Rutherford and Bassler, 2012).

2. Accessory sigma factor B (σ^B)

In many bacteria, the alternative sigma factors of RNA polymerase are essential for cell adaptation to different environmental stress (Nair *et al.*, 2003). Only four sigma factors are encoded in the *S. aureus* genome. SigA is the housekeeping σ factor and it directs transcription of the bulk of cellular RNA with three alternative σ factors σ^B, σ^H and σ^S (Tao *et al.*, 2010). The gene *sigB* is located within an operon of *S. aureus* with the regulatory genes *rsbUVW* that alter σB availability for transcription (Wu *et al.*, 1996). The activity of σ^B reaches a peak in the late exponential phase of growth and then reduces during stationary phase (Bischoff *et al.*, 2001). Transcription of more than 250 genes are controlled as part of the σ^B regulon, including proteins involved in signalling pathways, metabolism and cell wall synthesis (Bischoff *et al.*, 2004). Among virulence-associated genes, the transcription of several exoproteins and toxins are repressed while adhesins genes appear to be upregulated (Bischoff *et al.*, 2004). Beside its role in controlling the expression of virulence factors of *S. aureus*, σ^B environmentally regulates genes that confer resistance to antibiotics, heat and oxidative stressors (Tuchscherr *et al.*, 2015). Deora *et al.,* reported that the transcription of the global regulator SarA in *S. aureus* is at least partially controlled by σ^B (Deora *et al.*, 1997). Consequently regulation has an opposite effect to Agr with reduced production of several exotoxins such as , α-hemolysin and coagulase (Bischoff *et al.*, 2004). Additionally, σ^B is the major transcriptional regulator of staphyloxanthin biosynthesis producing the characteristic golden pigment of *S. aureus* that has essential roles in oxidative stress resistance (Kullik *et al.*, 1998).

3. SarA family

The *sarA* locus comprises of three overlapping transcripts, with common 3′ ends. The transcripts, *sarP1* (0.58 kb), *sarP3* (0.84 kb) and *sarP2* (1.15 kb) are controlled from three promoters (P1, P3 and P2, respectively)(Bayer *et al.*, 1996; Manna and Cheung, 2001). These three transcripts encode the 14.5-kDa SarA protein (Bayer *et al.*, 1996). It has been clearly indicated the transcriptional regulation from the three *sarA* promoters is complex. SarA acts to positively regulate its own expression in particular at P1. However, P2 appears to be silent

and P3 is σ^B-dependent. (Deora *et al.*, 1997). SarA activates the *agr* operon by binding to its P2 and P3 promoter regions, which increases RNAII and RNAIII levels, thus altering virulence expression via the *agr*-dependent pathway (Morfeldt *et al.*, 1996; Cheung *et al.*, 1997). Activation of *agr* can alter the transcription of *sarA* while a family of SarA-like proteins described below create a complex regulatory network allowing the cell to respond to different environmental stresses. The close inter-regulatory relationship between *agr*, *S*arA and SarA-like homologs is shown in (Fig. 1.7) also revealing its complexity (Ballal *et al.*, 2009).

Previous studies showed that SarA promotes the transcriptional expression of several target genes such as hemolysins *fnBPA* and *fnBPB*, leukotoxins (*LukED*, *LukSF*), superantigen TSST-1 and enterotoxins (Wolz *et al.*, 2000; Andrey *et al.*, 2010). By contrast, *SarA* negatively regulates other target genes including *sspA* (staphylococcal serine protease), *cna* and *spa* (Blevins *et al.*, 1999; Dunman *et al.*, 2001). SarA can stimulate biofilm formation of *S. aureus* by upregulating expression of biofilm-associated protein (Cheung *et al.*, 2008). SarA expression in *vivo* has an essential role in pathogenesis and a double mutant of *agr-sar* in a rabbit model of endocarditis had diminished virulence compared with an *agr* mutant (Cheung *et al.*, 1994).

Based on sequence alignment, multiple SarA homologs are encoded in the genome of *S. aureus*. The genes include *sarR, sarS, sarT, sarU, sarV, sarX, sarY, sarZ, mgrA* and *rot* (Cheung *et al.*, 2004; Rogasch *et al.*, 2006). SarR shares ~51% homology with SarA. SarR negatively regulates the three promoters of *sarA* by direct binding to repress SarA expression particularly in the late exponential and stationary growth (Manna and Cheung, 2001). Moreover, SarR binds to the *agr* P2 promoter to repress it (Reyes *et al.*, 2011). SarR contributes to regulation of virulence genes including, the metalloprotease aureolysin and SspA (V8 serine protease) (Gustafsson and Oscarsson, 2008). A further SarA-like member is SarS, (or SarH1) that binds to the *ssp* (serine protease) and *agr* P3 promoters (Manna and Cheung, 2001). SarS is likely repressed by SarA and *agr*. Gel shift assays showed that SarS binds to the *spa* promoter region while the exact influence of

SarS on virulence gene expression depends upon both *sarA* and *agr* (Tegmark *et al.*, 2000; Cheung *et al.*, 2001).

SarT negatively regulates the transcription *hla* while *sarT* itself is repressed by *agr* and SarA. It seems that SarA has a role in regulation of the transcription of *hla* through SarT (Schmidt *et al.*, 2001). Furthermore, SarT activation can lead to expression of SarS (Cheung *et al.*, 2004) and subsequently suppressed activation of *spa* and *hla* (Tegmark *et al.*, 2000). SarU acts as an activator of the *agr* locus (Manna and Cheung, 2003) and is involved in the expression of most of the virulence determinants controlled as part of the *agr* regulon (Manna *et al.*, 2004; Cheung *et al.*, 2008).

MgrA (Multiple gene regulator A) is another SarA homolog that regulates autolysis via mechanisms independent of other global regulators (Ingavale *et al.*, 2005). A transcriptional study of *S. aureus* Newman by microarray identified 355 genes controlled by MgrA in all function categories. The down-regulation of surface proteins and upregulation of exoproteins by MgrA shows a similarity with the *agr* response (Ingavale *et al.*, 2005; Luong *et al.*, 2006). MgrA mutation decreases the expression of *hla, agr* and RNAIII while upregulation of *sarS* and *spa* occurs (Ingavale *et al.*, 2005). The transcription of *sarA* was unchanged by *mgrA* mutation, which indicates that MgrA regulates both *hla* and *spa* genes independently of SarA (Ingavale *et al.*, 2005).

Rot (repressor of toxins) is a SarA-like family protein that has global regulatory effects on expression, as determined by microarray analysis. Rot increases the expression of SarS and protein A while it represses the transcription of α and β-hemolysin, urease, lipase and proteases, (Said-Salim *et al.*, 2003). Rot-related changes in target gene expression appear to be opposite that of Agr for example *spa*, *sspB* and *sspC* were up-regulated by Rot but down-regulated by *agr* (Said-Salim *et al.*, 2003). Furthermore, it was found that the RNAIII can prevent the translation of Rot by binding to the *rot* transcript (Geisinger *et al.*, 2006).

Others SarA members are SarZ and SarV (Cheung *et al.*, 2004). Under standard in *vitro* growth conditions, both SarA and MgrA appear to repress *sarV* since transcription is greatly enhanced in *sarA* and *mgrA* mutant strains (Cheung *et al.*, 2004). Inactivation of *sarV* produced a high level of resistance to detergent-induced lysis in comparison with wild type while the opposite effect occurred in both *mgrA* and *sarA* mutants (Manna *et al.*, 2004). Overexpression of *sarV* reduced autolysis to support that SarV controls genes associated with *S. aureus* autolysis (Cheung *et al.*, 2004).

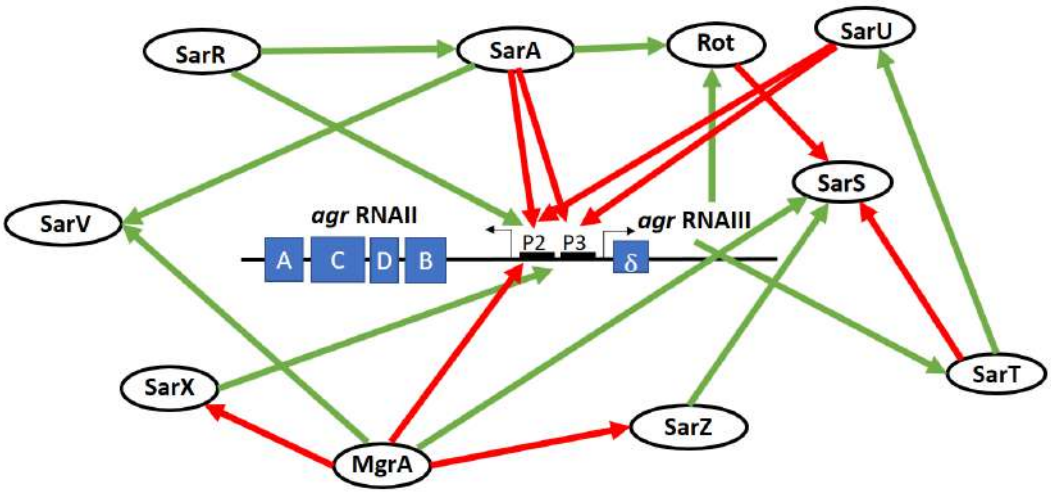

Figure 1.7 Regulation networks between SarA-family DNA-binding proteins and the *agr* locus. Each Sar-like protein has an effect on one or more of these regulatory systems, thereby generating a complex network of control on target genes. Red arrows represent activation while green arrows represent repression. Modified from (Pragman and Schlievert, 2004; Ballal *et al.*, 2009).

1.6.2 TCS regulating cell wall metabolism, autolysis and cell death

1. WalKR

WalKR encodes the only essential TCS of *S. aureus* and was first identified and characterised in *B. subtilis*. The WalKR locus is conserved among Gram-positive bacteria, including *S. aureus* and *S. pneumoniae* (Dubrac and Msadek, 2004). In *B. subtilis,* the *walKR* genes are expressed during log phase but not upon entry into stationary growth, indicating there is activation of this regulatory system, and that it is important during active replication (Fabret and Hoch, 1998). WalKR modulates autolytic activity of *S. aureus* via regulated expression of two major autolysin activities, AtlA and AtlM (Dubrac *et al.*, 2007). WalKR alters the expression of 13 genes proposed to contribute to degradation and metabolism of cell wall and increase Triton X-100 and lysostaphin resistance when lower levels of WalKR are artificially produced in the bacterial cell (Dubrac *et al.*, 2007; Delaune *et al.*, 2011). By contrast, lower levels of WalKR significantly decrease the biosynthesis of peptidoglycan, its turnover and changes to the cell wall, such as increases in peptidoglycan crosslinking and glycan chain length (Dubrac *et al.*, 2007). Howden et al. reported the WalKR locus is associated with vancomycin resistance (Howden *et al.*, 2011) that was confirmed by reduction of *S. aureus* susceptibility to vancomycin (Shoji *et al.*, 2011).

2. ArlRS

The ArlRS TCS is involved in regulation of autolysis and cell wall together with numerous virulence genes. Inactivation of *arlS* showed increased adherence of cells to polystyrene, decreased extracellular protease activity and increased cell autolysis (Fournier and Hooper, 2000). Furthermore, an *arlSR* mutant led to decreased transcription of *sarA,* while the level of RNAII and RNAIII transcripts increased (Fournier *et al.*, 2001).

3. LytSR

The LytRS TCS has a central role in autolysis (Brunskill and Bayles, 1996). This TCS positively regulates the transcription of *lrgA* and *lrgB* genes that are found directly downstream of the *lytSR* locus. These *lrgAB* genes were proposed to have

roles in autolysis and murein hydrolase activity (Brunskill and Bayles, 1996). Mutation of the *lrgA* and *lrgB* genes increased extracellular murein hydrolase activity compared with the parent strain and the double mutant exhibited high levels of resistance to penicillin-induced lysis (Groicher *et al.*, 2000). LytSR also contributes to develop *S. aureus* biofilm (Sharma-Kuinkel *et al.*, 2009).

1.6.3 TCS associated with AMPs response and cell wall damage

1. VraSR

The first study of VraSR reported upregulation of *vraSR* transcription in vancomycin intermediate resistant *S. aureus* (VISA) strains Mu50 and Mu3 in comparison with vancomycin-susceptible *S. aureus* (VSSA) (Kuroda *et al.*, 2000). VraS is the sensor HK, while VraR is its response regulator RR (Fig. 1.8). The VraSR proteins are homologues of the YvqEC system of *B. subtilis* (Kobayashi *et al.*, 2001). Exposure of *S. aureus* to many antibiotics that have major effects on biosynthesis of cell wall peptidoglycan can induce the VraSR system, whereby a *vraSR* mutant displayed susceptibility to D-cycloserine, β-lactams, glycopeptides, bacitracin and cationic antimicrobial peptides (CAMPs) (Kuroda *et al.*, 2000; Levinger *et al.*, 2012; Su *et al.*, 2015). Furthermore, a transcriptional study of vancomycin treatment that compared *S. aureus* N315 and an isogenic *vraSR* allelic replacement mutant revealed 139 genes induced after challenge and 46 not expressed in a *vraSR* mutant (Kuroda *et al.*, 2003). Many of these identified genes have roles in the biosynthesis of peptidoglycan, such as methicillin-resistance-related protein (*fmtA*), monofunctional glycosyltransferase (*sgtB*), pencillin-binding protein 2 (*pbp2*), teicoplanin-resistance-related proteins (*tcaA*/*tcaB*) and UDP-N-acetylglucosamine 1-carboxylvinyl transferase 2 murein monomer precursor synthesis (*murZ*) (Kuroda *et al.*, 2003). Stimulation of VraSR signalling might upregulate expression of cell-wall biosynthesis enzymes to increase both the bacterial cell wall thickness and its resistance to cell wall-related antibiotics (Haag and Bagnoli, 2015).

2. GraSR

The glycopeptide-resistance-associated GraXRS of *S. aureus* (antimicrobial peptide sensor ApsRS of *S. epidermidis*) is one of several important TCS (VraSR,

GraXRS and BraRS) that coordinate the staphylococcal responses to CAMP (Fig. 1.8) (Falord *et al.*, 2011). The *graSR* genes are located upstream of ABC transporter genes *vraF*G that collectively have increased expression in VISA strains of *S. aureus* demonstrating their association with resistance to vancomycin (Kuroda *et al.*, 2000). *S. aureus* convers resistance to CAMPs by increasing positive cell surface charge through D-alanylation of wall teichoic acid (WTA) and lysinylation of phosphatidylglycerol within the bacterial cell membrane (Herbert *et al.*, 2007; Li *et al.*, 2007). These modifications are facilitated by enzymes encoded by the *dltABCD* and *mprF* operons, respectively and GraR directly regulates these two operons (Meehl *et al.*, 2007). GraSR does not regulate its own expression (Falord *et al.*, 2011), however, it influences the expression of 248 genes, some of them are related to colonisation factors, exotoxin-encoding genes, virulence determents and also the *ica* operon (Haag and Bagnoli, 2015). The genes *sarS, mgrA* and *rot* were shown to be positively regulated by GraRS, therefore GraRS might indirectly regulate virulence genes in staphylococci (Haag and Bagnoli, 2015). In *S. aureus,* the GraRS response was induced by a more restricted set of AMPs compared with *S. epidermidis.* One of the explanations proposed for this variation is a structural difference in the AMP binding region on the highly negatively charged loop of the GraS sensor protein (Li *et al.*, 2007).

3. BraRS

The BraRS (bacitracin resistance-associated) TCS, also called NsaSR (nisin susceptibility associated) was identified as one of three TCS (with GraSR and VraSR) contributing to the *S. aureus* response to nisin and bacitracin antimicrobials (Hiron *et al.*, 2011; Kawada-Matsuo *et al.*, 2011). BraSR shares some common characteristics with GraSR and may have arisen by gene duplication being only present in limited staphylococci (Coates-Brown et al., 2018). Both TCS belong to the intramembrane sensor kinase family and are important for resistance to nisin and control the synthesis of VraFG and VraDE encoding ABC transporters (Hiron *et al.*, 2011). There are *braS* binding sites upstream of the *braD* and *braE* genes that encode an ABC transporter (Fig. 1.8) that has a role in resistance (Hiron *et al.*, 2011). Activation of *vraDE* and *braDE*

operon transcription by BraRS can occur at low concentrations of antibiotic. The activation of *vraDE* aids the cell as a detoxification module, especially for bacitracin resistance (Kawada-Matsuo *et al.*, 2013). Studies showed that induction of these two operons in different mutants in the presence of nisin or bacitracin depend on BraRS but not on GraSR or VraSR (Hiron *et al.*, 2011; Kolar *et al.*, 2011). An isogenic *braS* mutant altered the expression of 245 genes including genes have roles in drug resistance, amino acid metabolism, transportation, virulence, cell envelope synthesis and transcriptional regulation (Kolar *et al.*, 2011). However, inactivation of the TCS genes does not indicate the regulon genes directly regulated by BraSR, merely those with altered expression when functionality is lost.

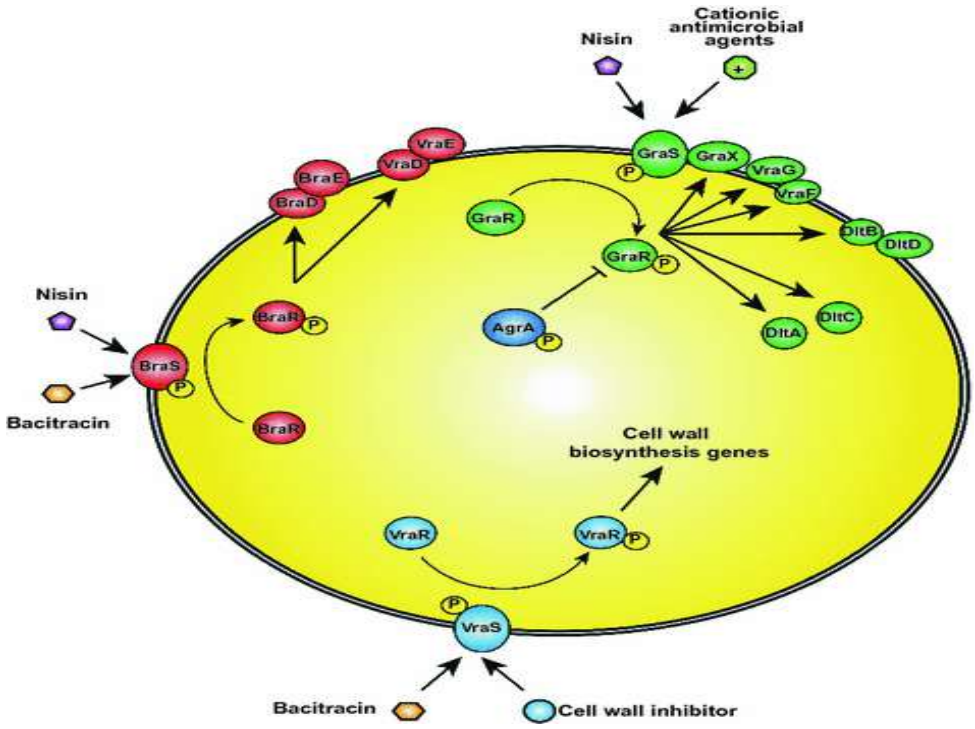

Figure 1.8 ***S. aureus*** **TCS responses to antimicrobial agents**. VraS responds to the action of cell wall active antibiotics that affect cell wall biosynthesis. Following activation, VraS phosphorylates its response regulator VraR and triggers altered expression of cell wall biosynthesis genes. GraSR TCS is activated in response to cationic AMPs and regulates the adjacent genes encoding the VraFG efflux pump that has a role in the signalling cascade by sensing the presence of CAMPs and signalling through GraS to activate GraR-dependent transcription. GraSR also regulates D-alanylation of teichoic acids that contributes to resistance of *S. aureus* to cationic AMPs. BraRS activates the transcription of genes encoding ABC transporters, *BraDE* and *VraDE.* BraDE participates in bacitracin sensing and signalling via BraSR, while VraDE serves as a detoxification module and it confers resistance to nisin and bacitracin when produced on its own. Adapted from (Haag and Bagnoli, 2015).

Thesis aims

The variety of molecular mechanisms used by *Staphylococcus* species to compete with each other in the same niche are not fully understood. The central hypothesis for the study is that staphylococci can evolve both general and specific mechanisms to interact with each other as major skin competitors. The aims of this study were therefore to extend our understanding of the evolution of these continually interacting species of *Staphylococcus,* with particular focus on *S. aureus* and *S. epidermidis* that cohabit the anterior nares.

Specifically, the research aims were:

(1) Studying the impact of interspecific interactions on the fitness of *S. aureus* and *S. epidermidis* by screening for interference competition with respect to antimicrobial production and resistance using experimental evolution.

(2) Characterising genetic changes resulting from selection during competition using genome resequencing with investigation of plasmids harbouring genes encoding antimicrobials.

(3) Construction of isogenic single SNP variants from sequence variants identified during resequencing to identify the role of individual sequence changes in competition and resistance to other niche stresses. In addition, comparison would be made between the transcriptomes of evolved or single SNP variants and wild type to identify the major effects of mutation on global gene expression.

Chapter 2: Materials and Methods

2.1 Bacterial strains, plasmids and growth conditions

Bacterial strains and plasmids used in the study are listed in Table 2.1. Strain stocks were maintained by adding 700 µl of an overnight culture to 300 µl of 50% (v/v) glycerol (Fisher chemical) with storage at -80°C. *Staphylococcus* species and *S. aureus* mutants were typically grown in brain heart infusion (BHI) (LAB M, Quest Park, Lancashire, UK) at 37°C with shaking at 250 rpm. *E. coli* strains were cultured overnight in Luria-Bertani (LB) medium (LAB M, Quest Park, Lancashire, UK) at 37°C with shaking at 250 rpm.

For standard growth, strains were grown overnight aerobically in appropriate media at 37°C with shaking at 250 rpm. Optical density (OD_{600}) was recorded by using a 1 cm path length spectrophotometer.

Table 2.1 Bacterial strains and plasmids used in this study. Antibiotics (Sigma) are as follows: ampicillin (Amp), 100 µg ml^{-1}; erythromycin (Ery), 10 µg ml^{-1} and tetracycline (Tet), 5 µg $ml.^{-1}$

Species	Strain ID	Relevant characteristics	References
S. aureus	SH1000	Wild-type strain, *rsbU* repaired strain of *S. aureus* 8325-4	(Horsburgh *et al.*, 2002)
S. aureus	Newman	Wild type strain	(Duthie and Lorenz, 1952)
S. aureus	SF8300	Clinical isolate (USA300)	(Montgomery *et al.*, 2009)
S. aureus	B032	Nasal isolate	(Libberton *et al.*, 2014)
S. aureus	RN4220	Intermediate cloning host restriction negative, methylation-positive	(Novick, 1991)
S. aureus	SH1000 *desK*	Allelic replacement mutant (*desK*::tet)	(Al-Dayel, 2015)
S. aureus	SH1000 *SA01312*	In-frame deletion mutant *SA01312*	(Harrington, 2017)
S. aureus	SH1000 SHG01	Evolved strain with SNP in *desR* (01314) gene isolated from day 12	This study
S. aureus	SH1000 SHG02	Evolved strain with SNP in *desK* (01313) gene isolated from day 15	This study
S. epidermidis	B115	Nasal isolate	(Libberton *et al.*, 2014)
S. epidermidis	B155	Nasal isolate	(Libberton *et al.*, 2014)
S. epidermidis	J008	Skin isolate	(Kelly, 2013)
S. epidermidis	J014	Skin isolate	(Kelly, 2013)
S. epidermidis	B004	Nasal isolate	(Libberton *et al.*, 2014)

S. epidermidis	B015	Nasal isolate	(Libberton *et al.*, 2014)
S. epidermidis	B021	Nasal isolate	(Libberton *et al.*, 2014)
S. epidermidis	B025	Nasal isolate	(Libberton *et al.*, 2014)
S. epidermidis	B030	Nasal isolate	(Libberton *et al.*, 2014)
S. epidermidis	B033	Nasal isolate	(Libberton *et al.*, 2014)
S. epidermidis	B035	Nasal isolate	(Libberton *et al.*, 2014)
S. epidermidis	B040	Nasal isolate	(Libberton *et al.*, 2014)
S. epidermidis	B043	Nasal isolate	(Libberton *et al.*, 2014)
S. epidermidis	B048	Nasal isolate	(Libberton *et al.*, 2014)
S. epidermidis	B056	Nasal isolate	(Libberton *et al.*, 2014)
S. epidermidis	B057	Nasal isolate	(Libberton *et al.*, 2014)
S. epidermidis	B074	Nasal isolate	(Libberton *et al.*, 2014)
S. epidermidis	B082	Nasal isolate	(Libberton *et al.*, 2014)
S. epidermidis	B084	Nasal isolate	(Libberton *et al.*, 2014)
S. epidermidis	B092	Nasal isolate	(Libberton *et al.*, 2014)
S. epidermidis	B095	Nasal isolate	(Libberton *et al.*, 2014)
S. epidermidis	B101	Nasal isolate	(Libberton *et al.*, 2014)
S. epidermidis	B105	Nasal isolate	(Libberton *et al.*, 2014)
S. epidermidis	B124	Nasal isolate	(Libberton *et al.*, 2014)
S. epidermidis	B129	Nasal isolate	(Libberton *et al.*, 2014)
S. epidermidis	B131	Nasal isolate	(Libberton *et al.*, 2014)
S. epidermidis	B138	Nasal isolate	(Libberton *et al.*, 2014)
S. epidermidis	B142	Nasal isolate	(Libberton *et al.*, 2014)
S. epidermidis	B158	Nasal isolate	(Libberton *et al.*, 2014)
S. epidermidis	B164	Nasal isolate	(Libberton *et al.*, 2014)
S. epidermidis	B170	Nasal isolate	(Libberton *et al.*, 2014)
S. epidermidis	B176	Nasal isolate	(Libberton *et al.*, 2014)
S. epidermidis	B180	Nasal isolate	(Libberton *et al.*, 2014)
S. epidermidis	B185	Nasal isolate	(Libberton *et al.*, 2014)
S. epidermidis	B180	Nasal isolate	(Libberton *et al.*, 2014)
S. epidermidis	B185	Nasal isolate	(Libberton *et al.*, 2014)
S. epidermidis	B188	Nasal isolate	(Libberton *et al.*, 2014)
S. epidermidis	B193	Nasal isolate	(Libberton *et al.*, 2014)
S. epidermidis	B197	Nasal isolate	(Libberton *et al.*, 2014)
S. epidermidis	B203	Nasal isolate	(Libberton *et al.*, 2014)
S. epidermidis	B208	Nasal isolate	(Libberton *et al.*, 2014)
S. epidermidis	B224	Nasal isolate	(Libberton *et al.*, 2014)
S. epidermidis	B230	Nasal isolate	(Libberton *et al.*, 2014)
S. epidermidis	B232	Nasal isolate	(Libberton *et al.*, 2014)
S. epidermidis	B240	Nasal isolate	(Libberton *et al.*, 2014)
S. hominis	B002	Nasal isolate	(Libberton *et al.*, 2014)
S. hominis	B026	Nasal isolate	(Libberton *et al.*, 2014)
S. hominis	B150	Nasal isolate	(Libberton *et al.*, 2014)
S. hominis	B175	Nasal isolate	(Libberton *et al.*, 2014)
S. hominis	B217	Nasal isolate	(Libberton *et al.*, 2014)
S. hominis	B227	Nasal isolate	(Libberton *et al.*, 2014)
S. capitis	B010	Nasal isolate	(Libberton *et al.*, 2014)
S. capitis	B022	Nasal isolate	(Libberton *et al.*, 2014)
S. capitis	B041	Nasal isolate	(Libberton *et al.*, 2014)
S. capitis	B077	Nasal isolate	(Libberton *et al.*, 2014)
S. capitis	B098	Nasal isolate	(Libberton *et al.*, 2014)
S. capitis	B122	Nasal isolate	(Libberton *et al.*, 2014)

S. capitis	B160	Nasal isolate	(Libberton *et al.*, 2014)
S. capitis	B273	Nasal isolate	(Libberton *et al.*, 2014)
S. warneri	B016	Nasal isolate	(Libberton *et al.*, 2014)
S. warneri	B020	Nasal isolate	(Libberton *et al.*, 2014)
S. warneri	B047	Nasal isolate	(Libberton *et al.*, 2014)
S. warneri	B102	Nasal isolate	(Libberton *et al.*, 2014)
S. warneri	B187	Nasal isolate	(Libberton *et al.*, 2014)
S. warneri	B235	Nasal isolate	(Libberton *et al.*, 2014)
Bacillus flexus	B003	Skin isolate	This study
Bacillus flexus	DSM 1667	Soil isolate	DSMZ-German collection of microorganisms and Cell Cultures
Bacillus flexus	DSM 1316		DSMZ-German collection of microorganisms and Cell Cultures
Bacillus flexus	DSM 1320		DSMZ-German collection of microorganisms and Cell Cultures
E. coli	Top10	Cloning host	(Hanahan *et al.,* 1991)
E. coli	pMutin4	Suicide vector for allelic replacements *lacZ*. Amp, *E. coli*; Ery *S. aureus.*	(Vagner *et al.*, 1998)

2.2 Deferred growth inhibition assay

A 25 µl (approximately 10^8 cells) volume of an overnight bacterial culture (inhibitor strains) was spotted onto the middle of 15 ml of brain heart infusion (BHI) agar plate (LAB M, Quest Park, Lancashire, UK) prior to incubation for 18 h at 37°C. Ten-fold diluted overnight culture approximately 4 x 10^6 CFU ml^{-1} (OD_{600} 0.3 ± 0.05) of competitor strains were sprayed over the plates using plastic perfume vaporiser bottles, then plates were re-incubated for a further 18 h at 37°C (Libberton *et al.*, 2015; Moran *et al.*, 2016). The assessment of growth inhibition was based on the diameter of the inhibition zone and a qualitative scoring system based on degree of growth prevention, from 1 corresponding with no detectable growth reduction to 4 corresponding to no growth (completely clear zone).

2.3 Overlay agar assay

A further growth inhibition method was performed for antimicrobial detection was modified from (Polak-Berecka *et al.*, 2009). Overnight culture (25 µl) of inhibitory strains were spotted on the central of plates containing 10 ml of BHI

agar then were incubated overnight at 37°C. The plates were overlaid with 10 ml top agar (0.7% w/v agar) containing approximately 1×10^6 CFU ml^{-1} of indicator strains. Plates were rocked gently to ensure the top agar solution evenly covered the whole surface. The inhibitory zone was evaluated after 24 hrs of incubation at 37°C.

2.4 Comparison of competitive interactions in planktonic and agar plate growth

2.4.1 Species interactions in planktonic growth with experimental evolution

All strains were cultured in 10 ml BHI broth and incubated overnight at 37°C with 200 rpm shaking prior to competition experiments. A 250 ml flask containing 50 ml BHI media was inoculated with overnight cultures of *S. aureus* SH1000 and *S. epidermidis* B155 (inhibitor producing) and mixed together at 1:1 ratio at an optical density OD_{600} = 0.1. Separate overnight cultures of each strain were cultured separately as controls. All flasks were incubated overnight at 37°C with shaking at 250 rpm. Viable counts were used to quantify the outcome of competition and colonies of the two bacteria were differentiated by the presence/absence of pigmentation. The planktonic community was transferred to a new flask every day for 15 days (serial passage). As a comparison *S. epidermidis* B115 (inhibitor non-producing) was co-cultured with *S. aureus* SH1000 and the same procedure was performed.

2.4.2 Species interactions on agar with experimental evolution

For sessile growth competition, all strains were cultured on (BHI) agar plates (LAB M, Quest Park, Lancashire, UK) at 37°C overnight prior to competition experiments. Two species were scraped off separate agar plates and suspended in 10 ml of phosphate buffered saline (PBS) (Sigma-Aldrich) and vortexed to mix thoroughly. The bacterial suspensions were diluted to OD_{600} = 0.1 and the two organisms were then co-cultured together at ratio 1:1. The co-culture mixtures were vortexed and 50 µl (approximately 2.5×10^6 cells) was spotted onto 25 ml BHI agar plates. Single species were used as a control and all the plates were

incubated at 37°C for 24 h. Next, the entire colonies were resuspended in 10 ml PBS and communities were transferred to new agar plates every day for 8 d. Viable counts were used to calculate each species and the two bacteria were differentiated by their morphology and pigmentation.

2.5 DNA purification techniques

2.5.1 Genomic DNA extraction

DNA was extracted from a 2 ml sample of a 10 ml overnight culture using the DNeasy Blood and Tissue Kit (Qiagen) following the manufacturer's instructions for Gram-positive organisms. The cells were centrifuged at 7500 rpm and resuspended in 180 µl enzymatic lysis buffer with 2 µl lysostaphin (5mg ml^{-1}) (Sigma-Aldrich) and 5 µl mutanolysin (5 kU ml^{-1}) (Sigma-Aldrich). After mixing, the cells were incubated for 1 h at 37°C. A 25 µl aliquot of proteinase K and 200 µl of buffer Al were added to the samples with 18 µl of RNase A solution (Invitrogen). All samples were incubated at 56°C for 1 h prior 200 µl of 100% (v/v) ethanol being added to the mixtures. Subsequently, all samples were washed twice by adding 500 µl (AW1 buffer) and (AW2 buffer), respectively. Finally, DNA was eluted with 100 µl of pre-warmed dH_2O.

2.5.2 Plasmid extraction from bacteria

Plasmid DNA was purified from *E. coli* strains prior to transformation of competent cells or to preform restriction analysis. *E. coli* strains were grown in LB broth with addition of 0.1 mg ml^{-1} ampicillin (Melford Biolaboratories Ltd., Ipswich, UK) and incubated at 37°C with shaking at 200 rpm for overnight. Next, a 5 ml overnight culture was centrifuged at 14000 rpm for 10 min and the supernatant discarded. Plasmid extraction was performed with the Isolate II Plasmid Mini Kit (Bioline). Briefly, the pellet was resuspended in 250 µl resuspension buffer P1 (containing RNase A) and mixed by inverting then incubated for 5 min at room temperature. Next, 250 µl of lysis buffer P2 was added to the mixture and inverted 6-8 times before adding 350 µl neutralization buffer P3 and mixing prior to centrifugation at 11,000 x g for 10 min. The clarified supernatant phase was transferred to a spin column and centrifuged at 11,000 x g for 1 min. Subsequently, 500 µl of wash buffer PW1 was added directly onto the

membrane column and centrifuged at 11,000 x g for 1 min. A second wash with 600 µl of buffer PW2 was applied to the column and centrifuged again at 11,000 x g for 1 min. The flow through was discarded and the silica membrane dried by centrifuging the spin column at 11,000 x g for 2 min. Finally, the plasmid DNA was collected into a sterile 1.5 ml tube by adding 50 µl ddH2O onto the spin column and centrifuging at 11,000 x g for 1 min. DNA was stored at -20°C until use.

2.5.3 Verifying DNA quality and quantity

The purity of DNA was determined using a Nanodrop spectrophotometer (Thermoscientific) to confirm that samples were not contaminated with significant amounts of protein or RNA. A260/A280 and A260/A230 ratios ≥ 1.8 were generally accepted as sufficiently pure for DNA in downstream experimentation. DNA quality was assessed by gel electrophoresis. Gels were prepared by melting a mixture of 1x TAE buffer and 1% (w/v) agarose (Bioline). Next, gel mixture stain was added at 2µl/100ml of Midori green (Nippon Genetics) and mixed gently before pouring into a gel tray. Hyperladder I (Bioline) was used as the DNA size marker and gel electrophoresis was run at 120 V for 30 min, unless otherwise stated. The gels were visualised under a UV transilluminator at a wavelength of 302 nm and images were recorded using GeneSnap software (Syngene). High molecular weight genomic DNA was confirmed as an intact band. The quantity of DNA was determined further using a Qubit (Invitrogen) according to manufacturer's instructions.

2.6 Oligonucleotide primers

Oligonucleotide primers for amplification of each gene of interest are outlined in Table 2.2. Primers were designed based on the following criteria; each primer consists of 18 to 26 bases. All selected primers had a GC content of approximately 50%. The annealing temperature (Tm) of all primers was between 55^{o}C and 65^{o}C. All primers were obtained from Eurofins Genomics, Germany and they were dissolved in Milli-Q water as 10 µM working solutions, then stored at - 20^{o}C.

Table 2.2 Oligonucleotide primers designed for PCR amplification in this study. The sequence of restriction enzyme (RE) sites are underlined.

Gene ID	Application	Sequence (5' to 3')	RE
16S rRNA-PA	16s rRNA amplification	AGAGTT TGA TCCTGGCTCAG	
16SrRNA- PH	16s rRNA amplification	AAGGAGGTGATCCAG CCGC	
DesR-FW	*desR* amplification	ACGACAGGCAATGGTTCAAT	
DesR-RV	*desR* amplification	TCCAGCCTTTTTCATTTGCCT	
Desk-FW	*desK* amplification	AGTGCTTTTGCCGTTCCATT	
Desk-RV	*desK* amplification	TGAGTCGACTGCTAAAGTTCCA	
DesR (F)	*desR* SNP gene amplification	ACTGAATTCACGCGTGAAGCGATAAATAATGT	*Eco*RI
DesR (R)	*desR* SNP gene amplification	ACTGGATCCTGGGTATCTTTGTAGGCTTTATCGT	*Bam*HI
tarM_FW	*tarM* amplification	ACGACTGGTACATATATTGCCTACA	
tarM_RV	*tarM* amplification	TCGCTTCGTTGGTACCATTCT	
rpmF_FW	*rpmF* amplification	GACAAGTTGATCCAAGGCTTCA	
rpmF_RV	*rpmF* amplification	ACTTCAGCAGGTTCTAGCGA	
mnmA_FW	*mnmA* amplification	AGGATCGCCATCTCCACCTA	
mnmA_RV	*mnmA* amplification	TGTCGTTGGTATGTCAGGCG	
cymR_FW	*cymR* amplification	ACTGCGTCTTTAGCTTTATCCA	
cymR_RV	*cymR* amplification	TTTTGGGCGCATTCTCGATG	
sbcC_FW	*sbcC* amplification	TGGCTGAAATTGTCAGTGGT	
sbcC_RV	*sbcC* amplification	TCATCGCGTTTGCTTTATTCATCT	
rpsB_FW	*rpsB* amplification	TGACGATGTTATCTTGGCGGT	
rpsB_RV	*rpsB* amplification	TAGCATCGTCGTTTGCTGGG	
salA_FW	*salA* amplification	CCGTTGCCTTAGCTCGTGAA	
salA_RV	*salA* amplification	CTGCTGTAGGATGAGGTGTCG	
scrA_FW	*scrA* amplification	TGGGTCTGGTACAGGGGAA	
scrA_RV	*scrA* amplification	CCACCAATTGCACCACCAAA	
hisF_FW	*hisF* amplification	GCGTCACGCTTGTTTATCCC	
hisF_RV	*hisF* amplification	CATAGCCGTTGTTTCGACCG	

2.7 Polymerase Chain reaction PCR amplification

BioMix^{TM} Red polymerase (Bioline Reagents Ltd, London, UK) was used in all PCR reactions. Components of a standard 50 µl reaction, made up with sterile deionised water, were as follows: 25 µl BioMix Red (Bioline), supplemented with 2.5 U ACCUZYME DNA Polymerase (Bioline) according to manufacturer's instructions, 1.5 µl primers (100 pmol μl^{-1}), 1.5 µl template DNA (~2.5 ng) and Up to 50 µl ddH_2O.

PCR reactions were carried out using a Mastercycler (Eppendorf). Standard settings used were: 30 cycles; initial denatureturation: 94°C for 15 s, denaturation: 94°C for 15 s, annealing: 55°C for 15 s, extension: 72°C for 1 min per kb of DNA amplified, final extension: 72°C for 2 min.

2.8 Purification of PCR products

Isolate II PCR and Gel kit (Bioline, A Meridian Life Science, UK) was used to purify PCR products according to the manufacturer's instructions. Briefly, binding buffer was added to PCR product at a ratio of 2 volumes to 1 and mixed by vortexing. The mixture was transferred to a spin column and centrifuged at 11,000 x g for 30 s. Following that, wash buffer was added to the spin column and centrifuged at 11,000 x g for 30 s, discarding the flow through and then centrifuged at 11,000 x g for 1 min to remove any residual ethanol. Finally, the column was transferred to a microfuge tube, 30 µl sterile ddH_2O added, incubated at room temperature for 1 min and centrifuged at 11,000 x g for 1 min to elute the DNA.

2.9 DNA sequencing

2.9.1 DNA library preparation and Whole-genome Sequencing

DNA sequencing libraries for WT and evolved samples of *S. aureus* SH1000 and *S. epidermidis* B155 selected from different days of experiments were prepared using Illumina TRUSEQ small insert libraries (Paired-end sequencing (2x250 bp)) with PCR-free 350 bp insert sizes according to the manufacturer's instructions. All samples were sequenced using the Illumina MiSeq platform at

the Centre for Genomic Research (CGR), University of Liverpool.

2.9.2 PacBio sequencing libraries

PacBio sequencing libraries were prepared and sequenced on the PacBio RS II platform using the sixth generation of polymerase and the fourth generation of chemistry (P6/C4) by the Centre for Genomic Research (CGR), University of Liverpool.

2.9.3 *Bacillus* species identification

16S ribosomal gene sequencing was used to identify a *Bacillus* isolate. Genomic DNA was extracted as described above (method 2.5.1). The 16S rRNA gene was amplified using pA and pH primers (Table 2.2) with BioMix Red polymerase (Bioline) supplemented with 2.5 U ACCUZYME DNA Polymerase (Bioline) according to manufacturer's instructions. PCR cycling conditions were used as follow: initial denaturation at 95°C for 5 min, followed by 30 cycles [95°C for 1 min, 55°C for 1 min, 72°C for 1.5 min] and a final extension at 72°C for 7 min.

Amplified PCR products were checked for purity by electrophoretic separation as described in section (2.5.3). Agarose gels were visualised using a UV transilluminator set with a long wavelength, 365 nm (UV-P, USA), to minimise damage. DNA was extracted using the manufacturer's protocol for the Isolate II PCR and Gel kit (Bioline, A Meridian Life Science, UK) as described in section (2.7). Subsequently, DNA was sequenced by GATC-Biotech (Konstanz, Germany) using the Sanger method. The 16S DNA sequences were analysed with the Sequence Match program on the RDP database (http://rdp.cme.msu.edu/) (Michigan State University) to identify the closest matching sequences over the entire length and considering the lowest e- value.

2.10 SNP analysis

The Centre for Genome Research (CGR), University of Liverpool processed short reads output to remove adapter sequences and poor quality reads. The FastQC tool was used to investigate the quality of raw sequence reads (Patel and Jain, 2012). Burrows-Wheeler aligner (BWA) (version 0.5.9-r16) was used to align the sequencing reads to the reference genome sequence (Li and Durbin, 2009). GeneBank accession of *S. aureus* SH1000 reference genome (NC_007795.1) was downloaded from the NCBI website (http://www.ncbi.nlm.nih.gov/). A reference genome was generated for the *S. epidermidis* B155 strain using snpEff (version 4.0). Alignments were converted from sequence alignment map (SAM) format to sorted, indexed binary alignment map (BAM) files which were converted to bcf (binary variant call files) using Samtools (Version 0.1.18-r580) (Li *et al.*, 2009). These files were used for SNP calling using mpileup package. The output file from mpileup was then used to generate Variant Call Format (VCF) using bcftool and the genomic variants were annotated using the SnpEff package (version 3.4e) based on their genomic locations, such as intronic, untranslated regions, upstream, downstream, and intergenic regions. The output also reveals coding effects such as synonymous or non-synonymous amino acid replacement (Cingolani *et al.*, 2012). The workflow used in this study is shown in Fig. 2.1. A Perl script was used to compare SNPs found in the parent strains and evolved strains (unique_SNPs.pl).

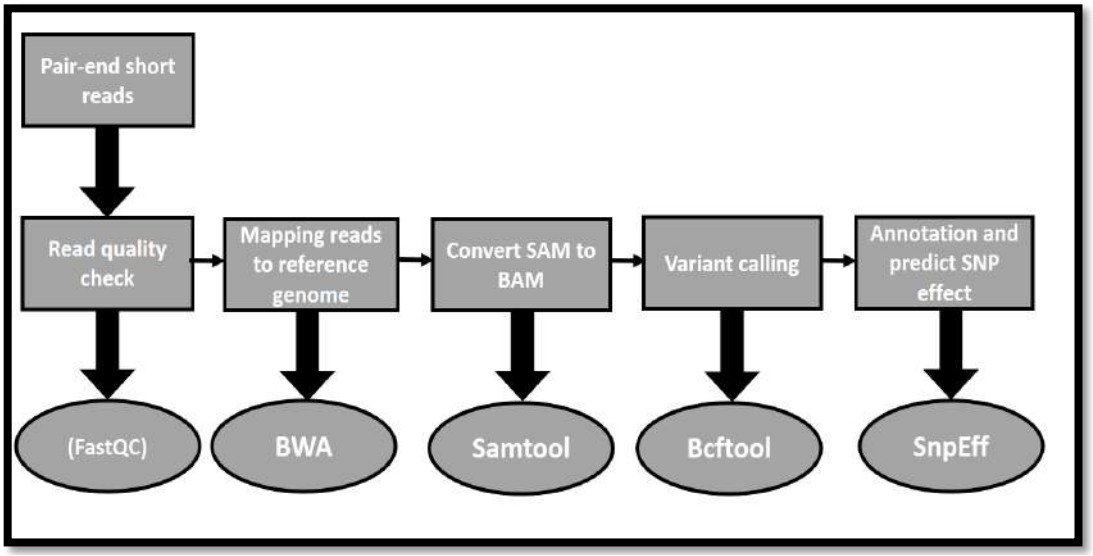

Figure 2.1 SNPs calling pipeline workflow

2.11 Genome assembly

Genomic DNA of *S. epidermidis* B155 and *Bacillus flexus* B003 were sequenced using the PacBio platform, as described above. The genomes were assembled using the PacBio distributed assembler hierarchical genome assembly process (HGAP) to correct errors in raw reads, while the longest reads were assembled using Celera assembler followed by using Quiver for genome polishing.

2.12 Genome annotation

Annotation of all genomes was preformed using PROKKA (version 1.5.2). PROKKA is a command line tool, which annotates a bacterial genome very quickly on a desktop computer in ~10 min (Seemann, 2014). The relevant features on the genome are predicted using the external tools: Prodigal for coding DNA sequences (Hyatt *et al.*, 2010); RNAmmer for predicting rRNAs (Lagesen *et al.*, 2007); Aragorn for identifying tRNA genes (Laslett and Canback, 2004); SignalP for predicting the location and presence of signal peptides (Petersen *et al.*, 2011); and Infernal for non-coding RNA annotation (Kolbe and Eddy, 2011). A genome in concatenated fasta format was used as input for the PROKKA program.

2.13 Constructing allelic replacement SNP variant of *desR* gene

2.13.1 Restriction enzyme digests

Restriction enzymes *Eco*RI/*Bam*HI were obtained from New England Biolabs Inc., Singapore. The *desR* SNP variant gene was amplified using primers DesR (F) and DesR (R) (Table 2.2) and then digested with *Eco*RI/*Bam*HI at the same time as separately digesting pMutin4 plasmid with the same enzymes. The reaction was set up in 50 µl including 2-8 units of restriction enzyme per 1 µg of DNA, 5 µl of appropriate 10x restriction buffer and ddH_2O was added up to volume. DNA digestion was performed for 1 h at 37^{o}C. For confirmation of the digestion, gel separation of desired DNA portions was performed. For this 5x loading buffer was mixed followed with separation by electrophoresis on 1% (w/v) agarose for 30 min at 120 V. DNA was extracted from agarose as described in section (2.8) and stored at –20 ^{o}C until its use.

2.13.2 DNA ligation

Digested insert DNA was used for ligation into the corresponding restriction enzyme digested plasmid. The ligation reaction was set up in a 20 µl volume as follows: insert DNA and plasmid DNA were quantified to establish the volumes required for fragment to vector ratios of 3:1, 1 µl of T4 DNA ligase (New England Biolabs Inc., Singapore), 2 µl of 10x buffer and ddH2O was added to a total of 20 µl. The mixture was incubated overnight at 4°C before use.

2.13.3 Preparation of chemically competent *E. coli* Top10

To produce competent cells for transformation, *E. coli* Top10 was streaked onto an LB plate and incubated overnight at 37°C. Several colonies were cultured in 20 ml SOB broth [0.5% (w/v) yeast extract (Sigma-Aldrich, St. Louis, USA), 2% (w/v) tryptone (Lab M Limited, Lancashire, UK), 0.0584% (w/v) NaCl (Sigma-Aldrich, St. Louis, USA), 0.0186% potassium chloride (KCl) (VWR Chemicals, Belgium), 0.24% (w/v) $MgSO_4$ (Fisher Scientific, Leicestershire, UK)] and incubated at 37°C with 250 rpm shaking until the OD_{600} nm reached 0.4 – 0.5. The culture was then centrifuged for 10 min at 4,000 rpm and the pellet re-suspended in 20 ml 0.1 M $CaCl_2$ (Melford Biolaboratories Ltd., Ipswich, UK). Cells were incubated on ice for 30 min, then centrifuged for 10 min at 4,000 rpm. Finally, the pellet was re-suspended in 1 ml 0.1 M $CaCl_2$ and incubated on ice for 5 min, then separated into 200 µl aliquots.

2.13.4 *E. coli* TOP10 transformation

For transformation, 10 µl of ligation product was added to 200 µl competent cells, and 1 µl (100 ng/µl) pMUTIN4 served as a control. The cells and DNA were incubated on ice for 30 min then subjected to heat shock at 42°C for 45 s. The samples were returned to wet ice for 3 min. Next, 800 µl SOC broth [SOB, 20% glucose] (Sigma-Aldrich) was added to the cells and incubated for 1 h at 37°C with 200 rpm shaking. Subsequently, 50-100-200 µl of each sample were spread onto LB agar (Miller) containing ampicillin (0.1 mg ml^{-1}) (Melford Biolaboratories Ltd., Ipswich, UK) plates and incubated overnight at 37°C. Successful transformation of *E. coli* was confirmed after selecting several colonies to culture separately in 10 ml LB broth with ampicillin (0.1 mg ml^{-1}) for 16 h at 37°C, with 200 rpm

shaking. The recombinant plasmids were extracted using the ISOLATE II Plasmid Mini Kit (Bioline) as described in (2.5.2). Plasmids then were digested with the appropriate restriction enzyme followed by gel electrophoresis at 120 V for 30 min using a 1 kb ladder (Bioline Reagents Ltd., London, UK), on a 1% (w/v) agarose gel (Bioline Reagents Ltd., London, UK) to confirm the presence of the correctly-sized insert. Clones were stored with 15% (v/v) glycerol at - 80°C until use.

2.13.5 DNA Precipitation

Precipitation was performed to increase the plasmid DNA concentration to a suitable amount for electroporation (~ 30 µg). Typically, 1 volume of plasmid DNA was mixed with 1 volume of isopropanol (Fisher Scientific) and 0.1 volume of 3 M sodium acetate, pH 5.2 (VWR Chemicals). The sample was incubated at room temperature for 1 min and centrifuged for 20 min at 13,000 rpm. Afterward, the pellet was washed with 300 µl ice-cold 100% (v/v) ethanol then centrifuged for 10 min at 13,000 rpm. The ethanol was removed and the pellet was air-dried for 10 min. The DNA was eluted in 20 µl ddH2O and stored at -20°C.

2.13.6 Preparation of electrocompetent *S. aureus* RN4220

The strain *S. aureus* RN4220 was used as an intermediate cloning host. To produce electrocompetent cells, *S. aureus* RN4220 was grown in 10 ml B2 broth [2.5% (w/v) yeast extract, 0.1% (w/v) K_2HPO_4, 2.5% (w/v) NaCl, 1% (w/v) casein acid hydrolysate, 0.5% (w/v) glucose, pH 7.5] (Sigma-Aldrich) and incubated overnight, at 37°C with 200 rpm shaking. Next, 4 ml of overnight culture (ODO_{600}) was used to inoculate 100 ml B2 broth (pre-warmed at 37°C) in a 500 ml conical flask. The culture was incubated at 37°C for 2 h with 200 rpm shaking until OD_{600} reached 0.8. After incubation, the culture was centrifuged for 10 min at 4,000 rpm after it was divided into two 50 ml aliquots in separate falcon tubes. The supernatant was removed and the pellet was resuspended in 15 ml ddH_2O prior centrifuged again, followed by two washes with 10 ml then 2 ml of 10% (v/v) glycerol (Fisher Scientific), respectively. The culture was incubated at room temperature for 15 min and then aliquoted in 200 µl amounts. Then cells were resuspended in 0.75 ml of 10% (v/v) glycerol. The cells were pelleted

10,000 rpm for 2 min, and each pellet re-suspended in 70 µl 10% (v/v) glycerol. The electrocompetent cells were directly stored at -80°C until use.

2.13.7 Transformation of *S. aureus* by electroporation

For electroporation, 2 µl of precipitated plasmid DNA and 70 µl electrocompetent *S. aureus* RN4220 cell were added in a sterile 0.1 cm electroporation cuvettes (Techtum Lab AB) and a cuvette without DNA served as a control. The cuvettes were incubated at room temperature for 15 min then placed on ice. The cells were pulsed using an electroporator (Gene Pulser™, Bio-Rad) at 2.3 kV, 25 µF and resistance 100 Ω. The cuvettes were immediately replaced on ice for 3 min and 1 ml of B2 broth (pre-warmed at 37°C) was added. Cells were transferred to a 15 ml falcon tube and incubated at 37°C with 200 rpm shaking for 2 h for recovery before plating 200 µl onto B2 agar plates [B2 broth, 1.5% (w/v) agar] (VWR Chemicals) containing erythromycin (0.03 mg ml^{-1}) (Duchefa Biochemie) and incubated at 37°C for 48 h. For verification of successful transformation with cloned plasmid DNA into *S. aureus* RN4220, colonies were streaked on B2 agar plates with lincomycin (0.025 mg ml^{-1}) (Sigma-Aldrich).

2.13.8 Phage transduction into *S. aureus* SH1000

Prior to phage transduction, a lysate was produced of the *S. aureus* SH1000 strain bearing the SNP *desR* gene variant. The donor strain (transformed *S. aureus* RN4220) was cultured overnight in 20 ml Brain Heart Infusion (BHI) Broth (Lab M) containing erythromycin (0.03 mg ml^{-1}) and incubated overnight at 37°C with 200 rpm shaking. Following this, 1 ml of overnight culture was transferred to 25 ml BHI broth with erythromycin (0.03 mg ml^{-1}) and incubated at 37°C with 250 pm shaking until OD_{600} reached to 0.5 – 0.8. Next, 3 ml of the cells were centrifuged at 4,000 rpm for 5 min and the pellet suspended in 5 ml BHI broth, then transferred to a detergent-free, sterile 100 ml glass flask. 5 ml phage buffer [0.6055% (w/v) Tris-HCl (pH 7.8) (Fisher Scientific), 0.59% (w/v) NaCl (Sigma-Aldrich), 0.012% (w/v) $MgSO_4$ (Fisher Scientific), 0.0445% (w/v) $CaCl_2$ (Melford Biolaboratories Ltd., Ipswich, UK), 0.1% (w/v) Gelatin (BDH Chemicals)] was added to the flask, alongside 30 µl stock ϕ11 lysate. The flask was then incubated at room temperature for 10 min, followed by incubation for 4 h at 30°C with 50

rpm shaking. The lysate was kept stationary at room temperature overnight until it was clear. The lysate was filter sterilised (0.22 µm MILLEX®GP) and stored at 4°C.

To determine the success of the lysate as a transducing lysate, *S. aureus* SH1000 was cultured to log phase in BHI broth. Dilutions of the phage lysate were prepared in phage buffer to 10^{-7} then 100 µl of phage dilution was added to 400 µl of SH1000. 50 µl of 1 M $CaCl_2$ was added and tubes were incubated at room temperature for 10 min. After incubation, phage top agar [0.3% (w/v) yeast extract (Sigma-Aldrich), 0.59% (w/v) NaCl (Sigma-Aldrich), 0.3% (w/v) casein acid hydrolysate (Sigma-Aldrich), 0.5% (w/v) Agar] was cooled to 50°C and 5 ml added to the cultures. The cultures were poured onto phage bottom agar plates [0.3% (w/v) yeast extract (Sigma-Aldrich), 0.59% (w/v) NaCl (Sigma-Aldrich) 0.3% (w/v) casein acid hydrolysate (Sigma-Aldrich), 1.5% (w/v) Agar] and incubated overnight at 37°C. The number of plaques were counted to confirm there was an average of 10^7 – 10^{10} plaque forming units (pfu) ml^{-1} which indicated the lysate was likely to produce a successful transduction.

For transduction of *S. aureus* SH1000 (recipient strain), cells were cultured in 20 ml LK broth [1% (w/v) tryptone, 0.5% (w/v) yeast extract (Sigma-Aldrich), 0.7% (w/v) KCl (VWR Chemicals, Belgium)] and incubated overnight at 37°C with 200 rpm shaking. Following incubation, the culture was then centrifuged at 4,000 rpm for 10 min and the pellet re-suspended in 1 ml LK broth. A 500 µl of the recipient cell suspension was added to 1 ml LK with 10 mM $CaCl_2$ plus 500 µl of ϕ11 lysate then incubated stationary at 37^{O}C for 25 min followed by 15 min with shaking at 250 rpm. Following this, 1 ml ice-cold 0.02 M sodium citrate (VWR Chemicals) was added to the mixture and incubated on ice for 5 min. Cells were then centrifuged at 4,000 rpm for 10 min at 4°C and the pellets resuspended in 1 ml ice cold 0.02 M sodium citrate and incubated on ice for 1.5-2 h. Next, 200 µl aliquots were spread on LK Citrate agar plates (LK broth, 0.68% (v/v) 0.5 M sodium citrate (VWR Chemicals), 1.5% (w/v) agar) and the plates were incubated at 37°C for 1.5 h. Cells were then overlaid with 5 ml phage top agar with erythromycin (0.03 mg ml^{-1}), and incubated again for 48 h at 37°C.

2.13.9 Screening for successful recombination

Two colonies were selected from each transduction plate and then cultured on BHI agar plates (BHI Broth, 1.5% (w/v) agar) with erythromycin (0.3 mg ml^{-1}) and incubated overnight at 37°C. A single colony from each plate was used to inoculate 10 ml BHI broth and cultured overnight at 37°C with 200 rpm shaking. Next, 100 µl of culture was added to 10 ml BHI broth and incubated overnight at 37°C with 200 rpm shaking. Another 100 µl was taken from the overnight cultures and diluted to 10^{-6} in Phosphate Buffered Saline (PBS) (Sigma-Aldrich). Next, 100 µl of the 10^{-6} dilution was spread on BHI agar with X-Gal (0.04 mg ml^{-1}) (Melford Biolaboratories) plates and incubated overnight at 37°C. After incubation, the plates were kept at room temperature for 48 h. The plasmid free colonies (non-blue pigmented) were selected and spotted onto BHI agar plates; with and one without erythromycin (0.03 mg ml^{-1}), and incubated overnight at 37°C. This selection process was repeated every day until colonies were identified that could not grow in the presence of erythromycin, indicating recombination had occurred and the plasmid DNA was absent.

2.14 Growth at different temperatures

S. aureus SH1000 strains: wild type, *desK::tet* mutant and *SAOUHSC_01312* mutant were cultured in 10 ml BHI broth and incubated overnight at 37°C with 250 rpm shaking. The overnight cultures were diluted to an OD_{600} of 0.05 OD in 50 ml BHI broth, in 250 ml sterile conical flasks. The cultures were then incubated at three different temperatures; 25°C, 37°C and 42°C with 125 rpm shaking, and OD_{600} readings were measured hourly for a 7 h period. The exponential growth phase doubling time was calculated using the equation: $\frac{\boldsymbol{Duration\ of\ growth} \times \boldsymbol{log}(2)}{\boldsymbol{log}\ (\boldsymbol{Final\ OD}) - \boldsymbol{log}\ (\boldsymbol{Initial\ OD})}$ and the mean doubling time for each strain determined. The experiment was repeated three times.

2.15 Pigmentation analysis

The *S. aureus* SH1000 strains; wild type, *desK*::tet mutant and *SAOUHSC_01312* mutant were cultured overnight in 10 ml BHI broth and incubated aerobically at 37°C with 200 rpm shaking. Cells were centrifuged for 10 min at 4000 rpm and the supernatant discarded. Cell pellets were re-suspended in 1 ml 100 % (v/v) methanol (Fisher Scientific, Leicestershire, UK) and vortexed vigorously. Samples were then incubated for 15 min at 37°C with 50 rpm shaking prior centrifugation at 4000 rpm for 5 min. For each sample, four 250 µl aliquots of each supernatant were added to a 96-well polystyrene microtitre plates, and the carotenoid absorbance spectrum read from 350 nm to 550 nm was measured using the Omega plate reader (BMG Labtech, Germany). The mean value was then calculated for each strain.

2.16 RNA sequencing

2.16.1 Notes

All work with RNA was done using RNase free plasticware and RNase free filter tips. Benches and pipettes were cleaned with RNaseZap (Ambion). 0.1 % (v/v) diethypyrocarbonate was added to any water used and incubated at 37°C overnight, prior to sterilisation by autoclaving (DEPC treated water).

2.16.2 Cells preparation for RNA extraction

Bacterial cells were grown exponentially to an OD_{600} of 0.5 then were harvested by pelleting for 5 min at 4,000 RCF at 4 °C. Pellets were resuspended in 2 volumes of RNAlater (Qiagen) and incubated overnight at 4°C.

2.16.3 RNA extraction

Cells were pelleted at 6,000 RCF for 5 min at 4 °C, and resuspended in 42 µl of 1 mg ml^{-1} lysostaphin (Sigma-Aldrich), 33 µl of 5 KU ml^{-1} mutanolysin (Sigma-Aldrich) and 1 µl of 100x TE buffer. This mixture was incubated at 37°C for 30 min with mixing every 5 min. Subsequently, 25 µl of Proteinase K (Qiagen) was added to the samples and incubated for a further 30 min at 37°C. Total RNA was

extracted using the RNeasy kit (Qiagen), with slight alterations to the manufacturer's protocol. Briefly, the method was as follows: 350 µl buffer RLT containing 10 % (v/v) β-mercaptoethanol was added to the lysed cells and mixed before the addition of of 250 ml of 100 % (v/v) ethanol. This suspension was centrifuged through the RNeasy column for 15 s at 10,000 rpm. Samples were then washed twice with 700 µl buffer RW1 for 15 s at 14,000rpm. Next, the column was then washed three times with 500 µl buffer RPE for 15 s at 14,000 rpm and centrifuged again in a clean collection tube for 1 min with the column lid off. The column was then air dried for 5 min. RNA was eluted twice with 30 µl RNAase free water (pre-warmed to 70 °C). 0.5 µl of RNasin (Promega) was added according to the manufacturer's instructions. A 2 µl aliquot of the sample was used for total RNA quantification using Qubit RNA assay kit (Invitrogen), according to manufacturer's protocol.

Turbo DNase (Ambion) was used according to the manufacturer's instructions to treart samples with > 3 µg total RNA. DNase was removed using RNeasy MinElute clean up (Qiagen) according to the manufacturer's instructions, with the addition of 10 % (v/v) β-mercaptoethanol to the buffer RLT and elution was in 20 µl water. An aliquot of 4 µl was taken for quality control analysis, whilst the rest was frozen at -80 °C.

2.16.4 RNA quality control

Quality control analysis was determined using: a Qubit (Invitrogen) for quantification; a 2100 Bioanalyser (Agilent technologies) to assess degradation levels; and a Nanodrop (Thermoscientific) to assess protein or solvent contamination of bacterial RNA. Samples with a paired control and test condition sample with the following parameters were suitable for sequencing: Qubit read indicating 3 µg RNA; Bioanalyser RIN ≥ 7.0, Bioanalyser trace indicating good integrity; Nanodrop 260/280 and 260/230 ≥ 1.8.

2.16.5 RNA library preparation and sequencing

Library preparations were performed by the Centre for Genome Research, University of Liverpool, UK. Total RNA samples were rRNA depleted using the

Ribo Zero magnetic kit for Gram positive bacteria (Epicentre); this was repeated for samples with poor initial rRNA removal. Libraries were then prepared using strand specific ScriptSeq kits (epicentre). Samples were sequenced using paired end sequencing on the HiSeq platform (Illumina).

2.16.6 RNA sequencing data analysis

RNA data analysis was performed by Centre for Genome Research, University of Liverpool, UK. Briefly, reads were mapped to the reference genome using Tophat version 2.1.0 (Langmead and Salzberg, 2012). Gene expressions were calculated from the alignment files using htseq-count (Anders *et al.*, 2015). The raw count data were also converted into FPKM (Fragments per Kilobase per Million reads) values. The count numbers per gene were used during the subsequent differential expression analysis. The main processes of the analysis include data variation assessment, data modelling, model fitting, testing and DE (Differentially Expressed) gene detection. All the DGE (Differential Gene Expression) analyses were performed in R (version 3.3.3) environment using the DESeq2 package (Love *et al.*, 2014). The count data was used to obtain the logFC values for the required comparison. The estimated log2 Fold Changes (logFC) were also tested in DESeq2 using a Likelihood-Ratios (LR) test (Wilks, 1938). P-values associated with logFC were adjusted for multiple testing using the False Discovery Rate (FDR) approach (Benjamini and Hochberg, 1995). Significantly differentially expressed genes were defined as those with FDR-adjusted P-value < 5%.

Gene Ontology (GO) (Ashburner *et al.*, 2000) and KEGG (Kyoto Encyclopedia of Genes and Genomes) pathways (Kanehisa *et al.*, 2013) analysis were performed to determine the function of differentially expressed genes.

2.17 qPCR

2.17.1 Primer design

Primers were designed using primer-BLAST (Ye *et al.*, 2012) with the following parameters: a length between 15 and 25 bp; predicated to have only one product; a Tm of 60 ± 2 °C; low level of single base repeats; and a GC clamp towards the 3' end.

Primer efficiency was confirmed to be within 90-100% using a dilution curve with gDNA as described previously (Nolan *et al.*, 2006). Efficiency testing was done the same conditions as for qPCR reactions (described below). The reactions mix in a total volume of 20 µl was set up with 0.5 µM of each primer, 10 µl SensiFAST and a dilution range of gDNA between $1x10^0$ - $1x10^4$, with a starting concentrations of 10 million copies. Negative controls without template were also implemented. Efficiency values generated by the qPCR machine software, and an average of at least three resulting efficiency values was taken.

2.17.2 cDNA generation

The tetro cDNA synthesis kit (Bioline) was used for cDNA synthesis according to the manufacturer's instructions using random hexamer primers and approximately 2 µg RNA per reaction. Only RNA samples determined to have high integrity (described above) were used for these reactions.

2.17.3 qPCR conditions

All qPCR reactions were set up using SensiFAST SYBR HiMROX kit (Bioline) with the ABI StepOnePlus (Life Technologies) machine. The reaction mix contained 10 µl SensiFAST, 0.5 µM of each primer, 80 µg cDNA and DEPC-treated water up to a total reaction size of 20 µl. The run cycle was 95°C for 5 min, then 40 cycles of 95°C for 10 s, 62°C for 30 s. Data analysis was preformed using the ABI StepOnePlus software. At least two technical replicates and three biological replicates were used to determine fold change in gene expression between samples.

2.18 Statistical Analysis

Statistical tests for deferred growth inhibition assay data were analysed using the student's *t*-test or one-way analysis of variance (ANOVA), and further comparisons between strains performed using the *Tukey post hoc* test, with $P < 0.05$ considered significant. Temperature response growth curve data were analysed using Tukey test to compare multiple groups. All statistical tests were conducted using the GraphPad Prism 7 software (GraphPad Software, La Jolla, CA, USA).

Chapter 3: Exploring the ecological role of antimicrobial activity on intragenic interactions and evolution of staphylococci

3.1 Introduction

Microbial competition on human skin and mucosal surfaces determines the composition of our normal flora that contributes to human health and maintains homeostasis of the immune system (Gonzalez *et al.*, 2011; Christensen *et al.*, 2016). Competition between species of bacteria can be indirect when individuals compete for the same resources such as space and nutrients (Hibbing *et al.*, 2010) or it can be direct via chemically antagonistic interactions between competing species, which is known as interference competition (Morin, 1999; Hibbing *et al.*, 2010). Certain microorganisms have evolved an ability to utilise various toxic compounds that confer antimicrobial activity as competitive tools (Hibbing *et al.*, 2010; von Bronk *et al.*, 2017) such as secondary metabolites, including broad-spectrum antibiotics, which have inhibitory effects even at low concentrations (Jack *et al.*, 1995; Demain and Fang, 2000), bacteriocins with a narrow killing spectrum (Jack *et al.*, 1995; Majeed *et al.*, 2011), iron-scavenging siderophores and other damaging molecules (Hibbing *et al.*, 2010). The secretion of bacterial toxins enables bacteria to: i) inhibit or kill other strains, and produces significant advantage in preventing competing strains from niche invasion (Wiener, 1996); ii) act supportively to aid invasion of new niches (Wiener, 1996; Kommineni *et al.*, 2015); or iii) kill coexisting strains (Gordon and Riley, 1999; Majeed *et al.*, 2011). For many decades, study of the production of bacterial toxins and its regulation has been important as several of these toxins are clinical antibiotics (Slattery *et al.*, 2001; Lewis, 2013).

Antibiotics are the best known secondary metabolites and have been commercially exploited (Abbas *et al.*, 2014). Each year, around 500 antibiotics are in use with 80% of clinical antibiotics being originally isolated from soil microbes (Dischinger *et al.*, 2009; Falkinham *et al.,* 2009). Traditionally, *Bacillus* species isolated from soil are the most important source of antibiotics production and the genus is a dominant producer (Abdulkadir and Waliyu., 2012)

Streptomyces and certain fungi have been routinely used to produce the antibiotics on an industrial scale (de Lima Procópio *et al.,* 2012)

Environmental acquisition of plasmids carrying genes associated with antibiotic production commonly occurs by transformation of one organism after release or mating with another (Woappi *et al.*, 2013; Abbas *et al.*, 2014). The acquisition of such plasmids can allow the coexistence of antibiotic-producer species with antibiotic-resistant strains via new bioactive products synthesis allowing competition with their continuously evolving and now antibiotic resistant counterparts (Woappi *et al.*; Abbas *et al.*, 2014). Because of the identification and spread of resistance bacteria, there is greater need for alternative new and more effective antibiotics. (Abbas *et al.*, 2014; Allen *et al.*, 2014). In addition to the essential role of the production of antibiotics in interference competition in microbial community, certain antibiotics are known to influence the producer organism's quorum sensing systems, possibly indicating a contribution in cell signaling between bacteria (Davies, 2006; Yim *et al.*, 2006) while at sub inhibitory concentrations they can change bacterial gene expression (Tyc *et al.*, 2014).

Various ecological and evolutionary aspects of bacteriocin production have been determined (Gardner *et al.*, 2004; Gillor *et al.*, 2008). In a model for parasitic infections, it was observed that the production of bacteriocin can be a spiteful trait. This spiteful behavior within a population can be seen if the bacteriocin producer is at an intermediate frequency compared with those that are bacteriocin-sensitive within the interacting population (Gardner *et al.*, 2004). When the producer frequency is too low, the susceptible strains would be sharing some of the resources due to the reduction of population densities. However, increased frequency of the producer would lead to decreased fitness of competing susceptible strains. The spiteful behaviour at intermediate frequencies also was predicted to contribute in the reduction of parasite virulence (Gardner *et al.*, 2004). Producer bacteria can often absorb bacteriocin in which cells are not affected by the toxin because of the presence of an immunity protein encoded with the production gene in the same genetic cluster (Michel-Briand and Baysse, 2002; Riley and Wertz, 2002). There are various mechanisms

described by which bacteriocins target intracellular processes in the bacterial cell (Yeaman and Yount, 2003). Commonly, the positive charge of bacteriocin molecules and the negative charge of bacterial cell membrane produce an electrostatic interaction between them leading to an inhibition mechanism and consequently gaining access to the cellular targets of the bacterial cell (Yeaman and Yount, 2003; Malanovic and Lohner, 2016). Changing properties of the bacterial cell surface can lead to resistance to bacteriocins (Ernst and Peschel, 2011). It might be difficult for a susceptible species to evolve resistance to such inhibitors as it typically requires a novel gene or there may be a large fitness cost associated with resistance, which is common with antibiotic resistance (MacLean *et al.*, 2010). Studies have demonstrated resistance development to bacteriocins, including lysostaphin, nisin, lacticin 3147, and pediocin- like bacteriocins (Rasch and Knöchel, 1998; Kusuma *et al.*, 2007; Draper *et al.*, 2009).

Antimicrobial secretion-based competitive interactions between microorganisms appear to be most effective between species of the same genus or closely related species, which likely results from them often coexisting in the same ecological niche (Brown *et al.*, 2013). Many studies support the importance of a variety of molecules, including bacteriocins and antibiotics in antagonistic relationships between staphylococci. Bacteriocins were proposed to contribute to the negative association between *S. aureus* and *S. epidermidis* (Frank *et al.*, 2010; Libberton *et al.*, 2014; Libberton *et al.*, 2015). In addition to the production of lantibiotics by staphylococci (chapter 1), exclusion mechanisms between *S. aureus* and *S. epidermidis* in nasal communities revealed that *S. epidermidis* strains possess an endoserine peptidase (ESP) capable of inhibiting formation of *S. aureus* biofilm *in vitro*. A further mechanism operates to inhibit *S. aureus* colonisation via *S. epidermidis* stimulating keratinocyte production of hBD2 and hBD3 (Iwase *et al.*, 2010; Coates *et al.*, 2014). Phenol-soluble modulin peptides (PSMs) are produced by staphylococcal species, including pathogenic *S. aureus* and *S. epidermidis* and likely other staphylococcal species (Li *et al.*, 2014). PSM-δ and PSM-γ both have antimicrobial activity similar to cathelicidins and defensins, which disrupt microbial membranes to kill the organism (Cogen *et al.*, 2010). PSMδ and PSMγ produced by *S. epidermidis* act as an antimicrobial against *S.*

aureus and play a key role in the activation of Toll-like receptor 2 (TLR2) on keratinocytes. TLR2 activation leads to production of CAMPs including RNase 7, hBD2 and hBD. Consequently the immune responses are further amplified, which acts to diminish colonisation of *S. aureus* (Lai *et al.,* 2010). δ-toxin produced by *S. aureus* lacks antimicrobial activity although it has physicochemical properties similar to PSM-γ of *S. epidermidis* (Dhople and Nagaraj, 2005). Perhaps studies are lacking into the antimicrobial activity of *S. aureus* against other species. Nonetheless, the existence of interspecies competition between *S. epidermidis* and *S. aureus*, means more details are needed to further explore and to understand staphylococcal molecular interactions.

In the laboratory, understanding the factors that affect relationship between species is based on studying isolated single species. However, species live and evolve within complex and variable multispecies communities where they interact with each other (Celiker and Gore, 2012). Culture-independent studies fail therefore to address the importance of interactions between species within a community in driving their structure. Thus, competitive culture models enable us to determine competition dynamics, including the function and contribution of secondary metabolism and also help our understating of the host-microbe interaction (Stubbendieck and Straight, 2016). One limitation of this approach of culture studies is that they typically use a small number of isolates and species competing with each other in liquid or on agar media (Little *et al.*, 2008).

3.2 Aims

Since the staphylococci are frequent members of the complex communities of microbes living on and within human skin, they must compete with each other for different resources such as nutrients and living space. *S. aureus* and *S. epidermidis* are proposed to be significant in their interactions with humans and many studies have confirmed these two species employ competitive exclusion mechanisms, such as lantibiotic bacteriocin production. *Staphylococcus* species have developed multiple resistance mechanisms to combat these substances. Among these, the well-studied two-component systems GraRS, BraRS and VraSR independently sense environmental antimicrobials and direct collective cell surface changes that contribute to resistance from certain lantibiotics.

The main aim of this chapter was to screen multiple coagulase-negative staphylococci (CoNS) for their ability to inhibit the growth of different *S. aureus* strains using the deferred growth inhibition assay, which provides high throughput screening. This approach would give an idea about the extent and diversity of potential interactions in the niche. In these experiments, all possible pairwise species combinations would be examined. In addition, investigation of the growth dynamics of competition between staphylococcal species would be studied, focusing upon *S. aureus* and *S. epidermidis* as two of most important species within human skin and nasal microbiomes. Moreover, there would be study of the potential of these species to modulate the action of antimicrobials as consequences of competition over time by co-culturing toxin producing *S. epidermidis* and susceptible *S. aureus* under two growth conditions of batch culture and agar plates. The hypothesis was proposed that resistance to antimicrobials can be accrued as a result of competition to produce a wider perspective of possible contributing genetic determinants.

3.3 Results

3.3.1 A diversity of coagulase-negative staphylococci (CoNS) have antimicrobial activity against *S. aureus*

To visualise and quantify interference competition phenotypes between *Staphylococcus* species, the ability of a suite of 62 coagulase-negative *Staphylococcus* (CoNS) strains including: *S. epidermidis*, *S. hominis* and *S. capitis* and *S. warneri*, to secrete inhibitors that measurably restrict *S. aureus* growth was tested by using a deferred growth inhibition assay. Four *S. aureus* strains (SH1000, Newman, SF8300 (USA300) and B032) were used as the assay indicators. Of these, SH1000, Newman and USA300 are well-characterised *S. aureus* strains. While *S. aureus* B032 and the CoNS staphylococci test isolates were available from a previous study of the nasal microbiome in the research group (Libberton *et al.,* 2014). It should be emphasized here the strains were selected randomly and were not important to represent human skin microbiota since it was primarily a screen for interactions.

Within the deferred inhibition assay, growth of a producer strain at a central location on an agar plate overnight should lead to secretion of antimicrobials into the agar. This secretion is measurable by the subsequent spraying over of a test *S. aureus* strain. After an overnight incubation to enable indicator growth and inhibition, any areas of interference were recorded. Zones of inhibition resulting from the deferred inhibition assay were quantified by measuring the diameter of its zone which was expected to vary according to multiple different factors, such as expression level of the compound(s) produced and properties responsible for the antimicrobial activity. The appearance of the zone was also classified qualitatively.

Growth inhibition was qualitatively scored for clarity, ranging from 4, being completely clear with no growth in zone (red colour), to 1, representing no inhibition (blue colour) (Fig. 3.1). The zone of inhibition was quantified for effectiveness of each antimicrobial strain. Red colour represents the largest diameter from 9 mm to up to 1cm while blue colour indicates no inhibition zone (Fig. 3.2). From these assays, 33 out of 62 CoNS isolates showed varying degrees

of inhibitory activity against all four or some of the four *S. aureus* indicators while 29 CoNS isolates did not show any inhibitory activity against any of the indicator *S. aureus*. Among the inhibitory strains, 8 of them showed a very pronounced activity based on their clarity scores, 6 *S. epidermidis* strains (J008, BJ014, B004, B155, B180 and B224) and 2 *S. capitis* strains (B160 and 237) (Fig. 3.1). Strain BJ014 produced a large inhibition zone of growth with *S. aureus* Newman, USA300 and B032 with average diameters of 12, 16 and 14 mm) respectively, compared with other isolates (Fig. 3.2). Whereas, B180 and B224 produced a small inhibitory zone (2 mm) against all tested strains (Fig. 3.2) but with clarity of score 4 (Fig. 3.1). Strain *S. epidermidis* B155 produced inhibitory zone (4 mm) toward all *S. aureus* tested strains (Fig. 3.2) also with with clarity of score 4. Most commonly, inhibitory strains produced a zone with diameter on average 5 - 8 mm (orange colour) while 9 strains displayed a larger range of zone diameter (9 to > 10 mm) represented with red colour (Fig. 3.2).

The inhibitor toxin producing bacteria showed variance with different tested *S. aureus* where some of them inhibited one strain but were not active against others. For example, *S. warneri* B020 was negatively affected growth of *S. aureus* B032 (clarity score =3) but was not able to inhibit other strains. Meanwhile, *S. epidermidis* B043 and B021 had some inhibitory effect with clarity score of 2 against USA300 but were not active toward other indicator strains (Fig. 3.1). *S. hominis* was only represented by 6 strains yet all except S. *hominis* B277 and B217 showed a very low inhibition ability against *S. aureus* B032 with clarity score of 2; while strains B150 and B175 had a low inhibition of SH1000 and Newman (clarity score =2) (Fig. 3.1). None of the 6 *S. hominis* strains had any effect on the growth of USA300 strain (Fig. 3.1). *S. warneri* B020 and B235 observed a good activity (clarity score= 3) against *S. aureus* B032 strain (Fig. 3.1) with inhibition zone size 6 and 10 mm, respectively (Fig. 3.2). *S. aureus* Newman was inhibited by *S. warneri* strains B187 and B235 with scores of 3 (Fig. 3.1).

From the collection of species assayed, CoNS staphylococci were identified that inhibit growth of *S. aureus* via the production of antimicrobial substances. This phenotype among staphylococci was frequent. However, those bacteria that

possess antimicrobial properties did not necessarily exert their activity on all species or isolates tested. Thus, 21/43 *S. epidermidis*, 4/6 *S. hominis*, 5/8 *S. capitis* and 3/6 *S. warneri* isolates exhibited activity towards *S. aureus* in the assay. *S. hominis* was the least effective species at killing *S. aureus* based on the clarity score, with the isolates tested being ranked at the minimum level of inhibition. *S. epidermidis* was most effective proportionately as an inhibitory CoNS species based on a score of 4 for clarity and therefore complete killing of *S. aureus*, at least under the conditions studied. Despite the observation, few isolates of *S. epidermidis* displayed this pronounced killing activity, as evidenced by clear zones with no indicator growth against all four *S. aureus*. The presence of a clarity score of 4 was also associated with activity against all of the isolates tested.

To take the study forward, *S. epidermidis* B155 inhibitory strain (clarity score=4) and *S. epidermidis* B115 non-inhibitory strain (clarity score=0) were chosen as representatives for further experiments. Of note, no *S. aureus* strains tested from the lab collection were observed to show any antibacterial activity against CoNS staphylococci.

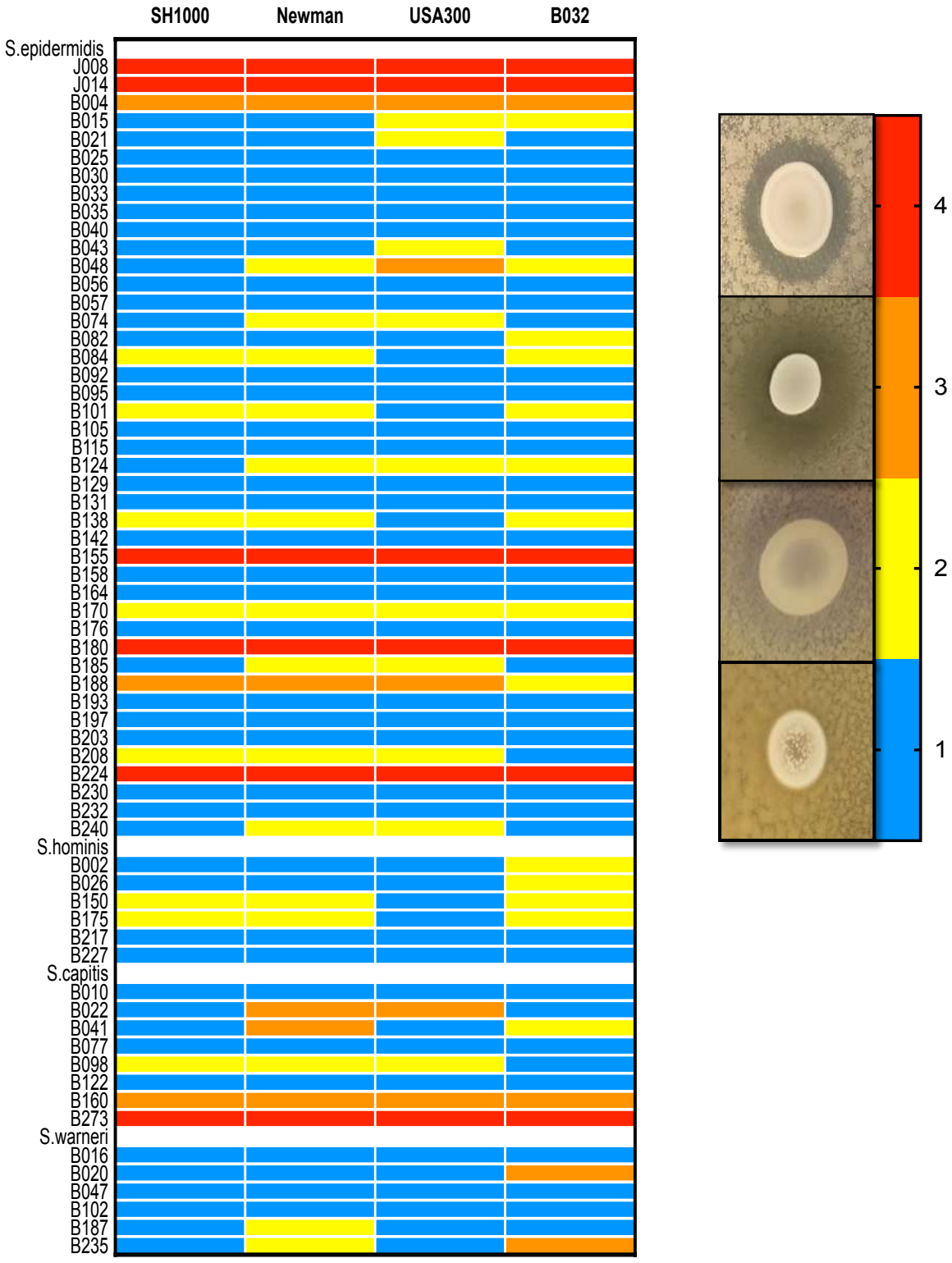

Figure 3.1 Qualitative visual score of antimicrobial activity of 62 coagulase-negative staphylococci (CoNS) against *S. aureus*. The inhibition corresponds with overlaid colours indicating the assigned score of clarity. Scale from blue (no inhibition, score of 1), yellow (reduced growth, score of 2), orange (cloudy growth score of 3) and red (pronounced inhibition and complete killing, score of 4). These data are derived from 6 biological replicates.

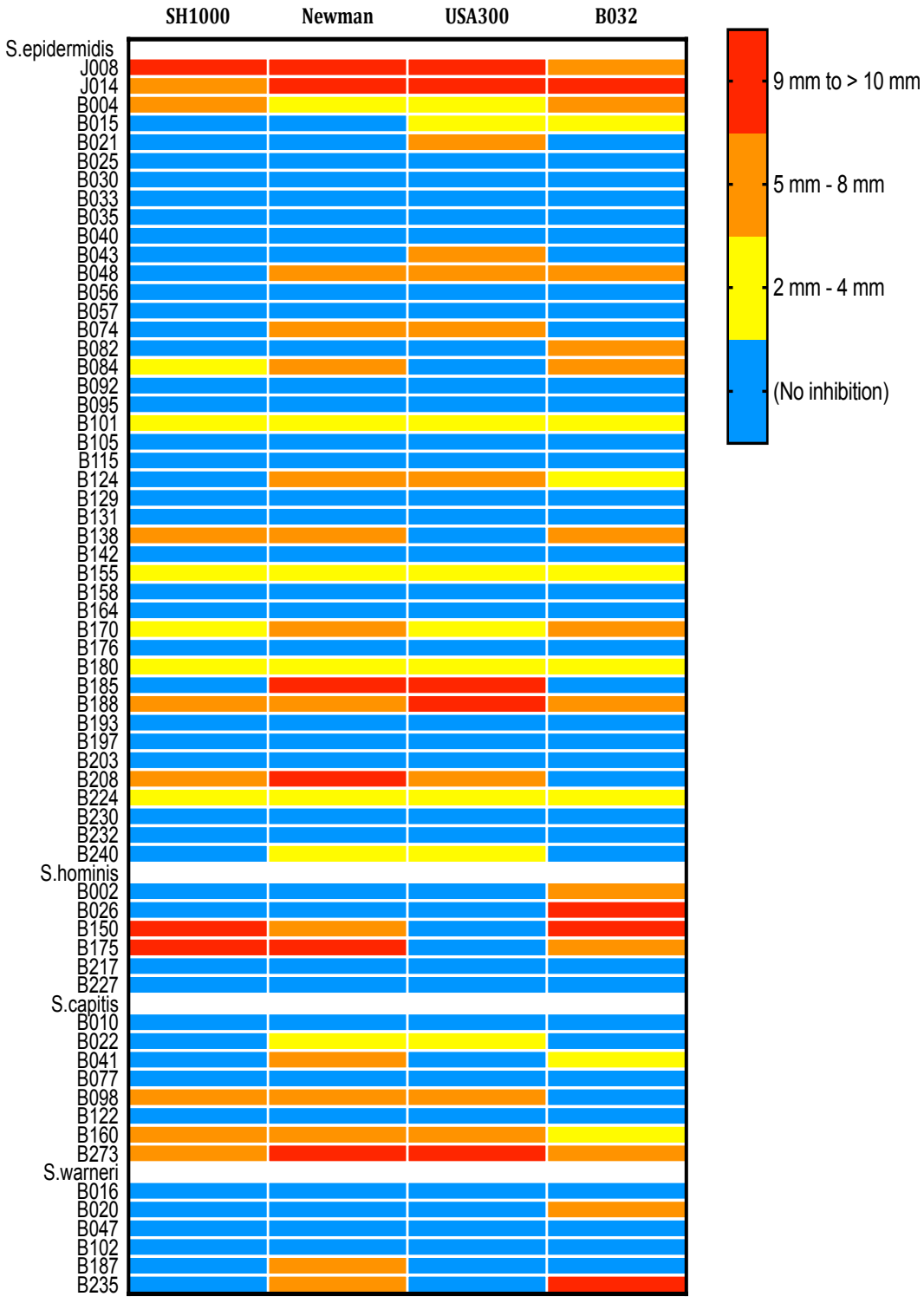

Figure 3.2 Quantitative growth inhibition from antimicrobial activity of 62 coagulase negative staphylococci (CoNS) against *S. aureus*. The inhibition area overlaid with colours indicating the relative size of the growth inhibition zone. Scale from blue (no inhibition zone), yellow (2-4 mm), orange (5-8 mm) and red (9 to up to10 mm). These data are the mean of 6 biological replicates.

3.3.3 Growth characteristics of competition between staphylococci

3.3.3.1 Determination of doubling time

Growth curves were performed for selected *Staphylococcus* species to determine their doubling times, prior to competition experiments. An initial OD_{600} = 0.05 was used for inoculation and the growth duration was 7 h at 37°C with the measurement of optical density every hour. *S. aureus* SH1000 was used as a competition control to compare it with the *S. epidermidis* strains. The exponential doubling times of *S. epidermidis* B155 and B115 although greater were not significantly different from *S. aureus* SH1000 (Dennett's test, *P*=0.079 and *P*=0.090 respectively) (Table 3.1).

Table 3.1 Doubling times of *S. aureus, S. epidermidis* B155 and *S. epidermidis* B115. The doubling times calculated in hours represent the mean values from 3 technical replicates. *S. aureus* SH1000 doubling time was used as control to compare it with *S. epidermidis* both B155 and B115. There was no significant difference between any of the *S. epidermidis* strains tested and the *S. aureus* strain SH1000 used in this study.

Species/Strains	Doubling Time (h)	T Value	P Value
***S. aureus* SH1000**	0.88	NA	NA
***S. epidermidis* B155**	1.01	-0.1254	0.079
***S. epidermidis* B115**	0.93	-0.0424	0.090

3.3.3.2 Interaction of *S. epidermidis* (inhibitor/non inhibitor-producing strains) with *S. aureus* in planktonic batch culture

Previous observation from a study in the laboratory conducted by Libberton *et al.*, 2015 showed that toxin-producing *S. epidermidis* could invade a sensitive *S. aureus* strain from rare frequency (ratio) at (0.001). Here, we evaluated the growth dynamic of *S. aureus* laboratory strain SH1000 in co-culture with inhibitor-producing *S. epidermidis* B155 where both species have similar growth rates to assess if the species would evolve potential adaptations over the competition period of time. The experiments were performed using planktonic batch cultures in shaking flasks. The growth yields of *S. aureus* SH1000 and the inhibitor-producing *S. epidermidis* B155 were determined in both mono- and co-culture. Both species of bacteria were co-cultured in liquid medium at 1:1 ratio and incubated for 24 h. Each subsequent day the community was transferred to fresh growth media and repeat cultured for 15 days. The numbers of bacteria were counted every day as colony forming units (CFU) and species were distinguished based on colony pigmentation and morphology.

From comparison of co-cultures, there was a different dynamic between species over time, in contrast to each species grown as mono-culture where a steady population yield was determined. *S. aureus* appeared to grow to greater yield in the BHI medium than *S. epidermidis* B155 (Fig. 3.3). However, when the species were co-culture a different pattern was clearly observed. Over the first two days, greater numbers of *S. epidermidis* B155 cells than SH1000 were observed, based on the viable counts (CFU) suggesting that the role of its antimicrobial action against *S. aureus* was a contribution (Fig. 3.3) given the success of this toxin-producing isolate on BHI agar. Then, the *S. epidermidis* B155 population decreased about 1.7-fold compared with day 2, while *S. aureus* SH1000 yield increased around 3-fold. On the fourth day of co-culture, the two species showed equivalent cell numbers before S. *epidermidis* B155 yield increased to dominate again and was consistently greater on subsequent days, including days 5-7, while *S. aureus* SH1000 cell yield declined steadily. *S. aureus* SH1000 produced a higher growth yield, reaching around 9 x 10^8 CFU ml^{-1} of population cells on day eight. By day 12 the *S. aureus* SH1000 population increased before remaining relatively

constant until day 15 when it reached 2.5 x 10^9 CFU ml^{-1}. In contrast, over this latter time period gradually the yield of *S. epidermidis* B155 declined from day 12 to day 15 (Fig. 3.3). From the growth yields, it was hypothesised that *S. aureus* SH1000 acquired some genetic change to cope with toxin producing *S. epidermidis* B155 that enabled it to effectively compete and outgrow it.

For comparison, growth of *S. aureus* SH1000 and the non-inhibitory strain *S. epidermidis* B115 was determined using the same culture conditions and following the same procedure described above. A different growth pattern was observed (Fig. 3.4). When the two bacteria were inoculated individually, over 15 days *S. aureus* SH1000 grew to cell densities slightly higher than *S. epidermidis* B115, although each had similar cell numbers on the first and seventh day of about 3.7 x 10^9 and 4.3 x 10^9 CFU ml^{-1}, respectively. In co-culture, *S. aureus* SH1000 was the dominant species throughout the experiment suggesting that SH1000 had greater fitness in these conditions (Fig. 3.4).

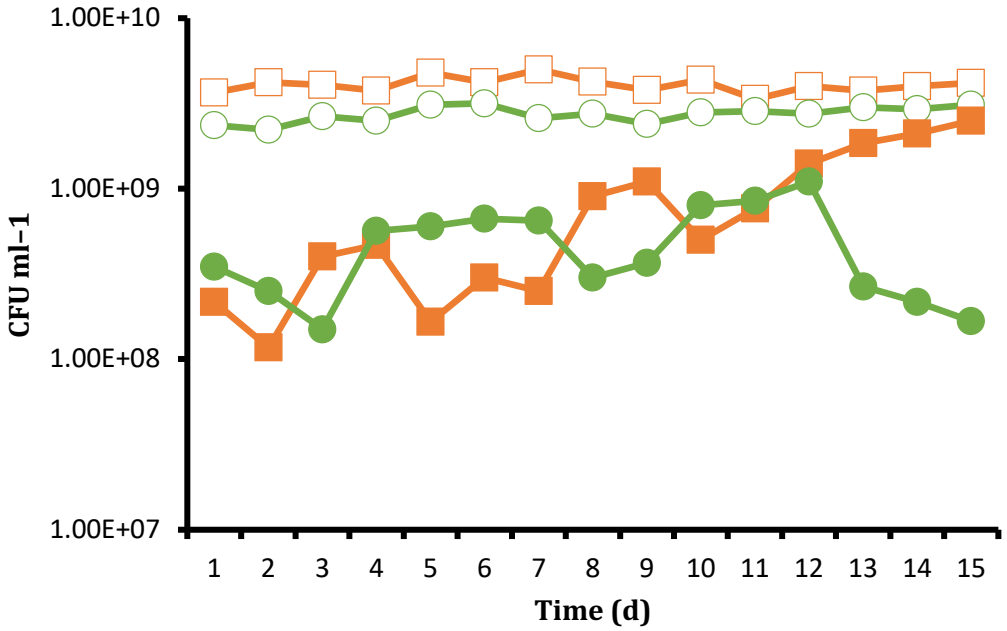

Figure 3.3 Competition dynamic between *S. aureus* SH1000 and inhibitor-producing *S. epidermidis* B155. Bacterial growth in mono- and mixed culture in BHI with shaking. Cells were sampled and transferred daily (24 h) to fresh media. Growth was determined by viable counts. *S. aureus* mono-culture (empty orange square), *S. aureus* from coculture (solid orange square), *S. epidermidis* single culture (empty green circle) and *S. epidermidis* from coculture (solid green circle). Experiments were performed in triplicate with one representative graph shown.

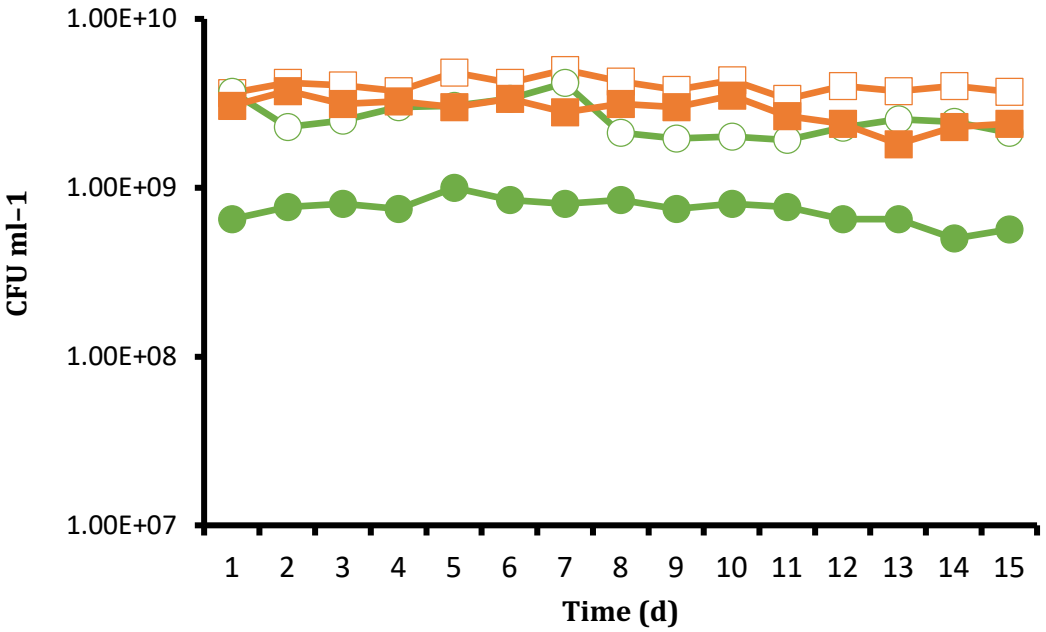

Figure 3.4 Competition dynamic between *S. aureus* SH1000 and inhibitor non-producing *S. epidermidis* B115. Bacterial growth in mono- and mixed culture in BHI with shaking. Cells were sampled and transferred daily (24 h) to fresh media. Growth was determined by viable counts. *S. aureus* mono-culture (empty orange square), *S. aureus* from coculture (solid orange square), *S. epidermidis* single culture (empty green circle) and *S. epidermidis* from coculture (solid green circle). Experiments were performed in triplicate with one representative graph shown.

3.3.2.3. Interaction of inhibitor producing and non-producing *S. epidermidis* with *S. aureus* on agar surface

From the previous experiment it was established that there was a potential role for secreted antimicrobial to modulate competition between *S. aureus* and *S. epidermidis*. To further assess these two species under competitive conditions, growth of the selected isolates was further evaluated by coculture using agar. This experimental design would enable the physical proximity of species upon competition outcomes to comparatively evaluate with the former planktonic growth experiment. *S. aureus and S. epidermidis* were mixed at ratio 1:1 in PBS and 50 µl (2.5×10^6 cells of each) was spotted onto the middle of a BHI agar plate. Every 24 h, the entire colony was scraped off and resuspended in 10 ml of PBS before 50 µl of cell suspension was plated onto fresh BHI agar; the experiment was carried out for eight days.

In coculture, *S. epidermidis* B155 had greater cell yield than *S. aureus* SH1000 after the first and second day suggesting that *S. epidermidis* B155 exerted effective antimicrobial activity on *S. aureus* SH1000 growth. This followed the same characteristic behaviour of their interaction in liquid culture for the first two days (Fig. 3.5). From day 3, *S. aureus* SH1000 and *S. epidermidis* B155 yields fluctuated. Over this time, the yield of *S. aureus* SH1000 increased around 4-fold compared with day 2 while *S. epidermidis* B155 numbers were steady (Fig. 3.5). Upon day 4, the number of viable cells of SH1000 decreased 3-fold from 7.5×10^8 to 2.65×10^8 CFU ml^{-1} and *S. epidermidis* B155 decreased less than 2-fold to 5×10^8 CFU ml^{-1} indicating little relative difference (Fig. 3.5). The *S. aureus* yield increased 5-fold on day six and seven compared with day five. However, the population of *S. epidermidis* B155 showed a drop in cell numbers to 1.5×10^8 on day 8 (Fig. 3.5). Overall the pattern of growth yield indicates under these conditions of competitive growth on an agar surface there were very similar dynamics to the competition in liquid medium over time.

Co-cultivation of *S. aureus* SH1000 and non-inhibitory *S. epidermidis* B115 was similarly tested. *S. aureus* SH1000 was the dominant species in coculture and the population remained relatively stable during eight days (Fig. 3.6). However, *S.*

epidermidis B115 had lower growth yield and it experienced ten-fold fluctuations over time; the maximum number of viable cells was determined on day one with 4.65×10^8 CFU ml^{-1} and the minimum numbers were on the last day with 5×10^7 CFU ml^{-1} (Fig. 3.6). Clearly, *S. epidermidis* B115 was affected by its competitor but remained present throughout the experimental period. When *S. epidermidis* B115 was grown in monoculture its growth yield was comparable to that of *S. aureus* (Fig. 3.6). Collectively, these results demonstrate that *S. aureus* SH1000 was more competitive than the tested *S. epidermidis* toxin non-producing strain.

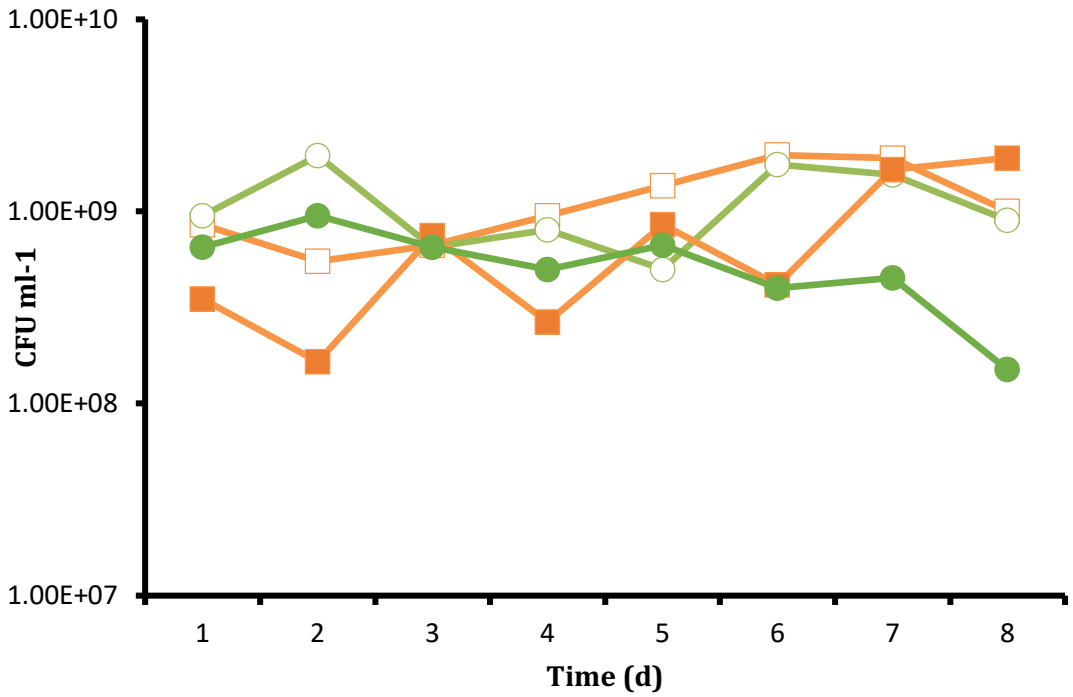

Figure 3.5 Competition dynamic between *S. aureus* SH1000 and inhibitor-producing *S. epidermidis* B155. Bacterial growth in mono- and coculture on BHI agar. Cells were recovered, sampled and transferred daily (24 h) to fresh media. Growth was determined by viable counts. *S. aureus* monoculture (empty orange square), *S. aureus* from coculture (solid orange square), *S. epidermidis* monoculture (empty green circle) and *S. epidermidis* from coculture (solid green circle). Experiments were performed in triplicate with one representative graph shown

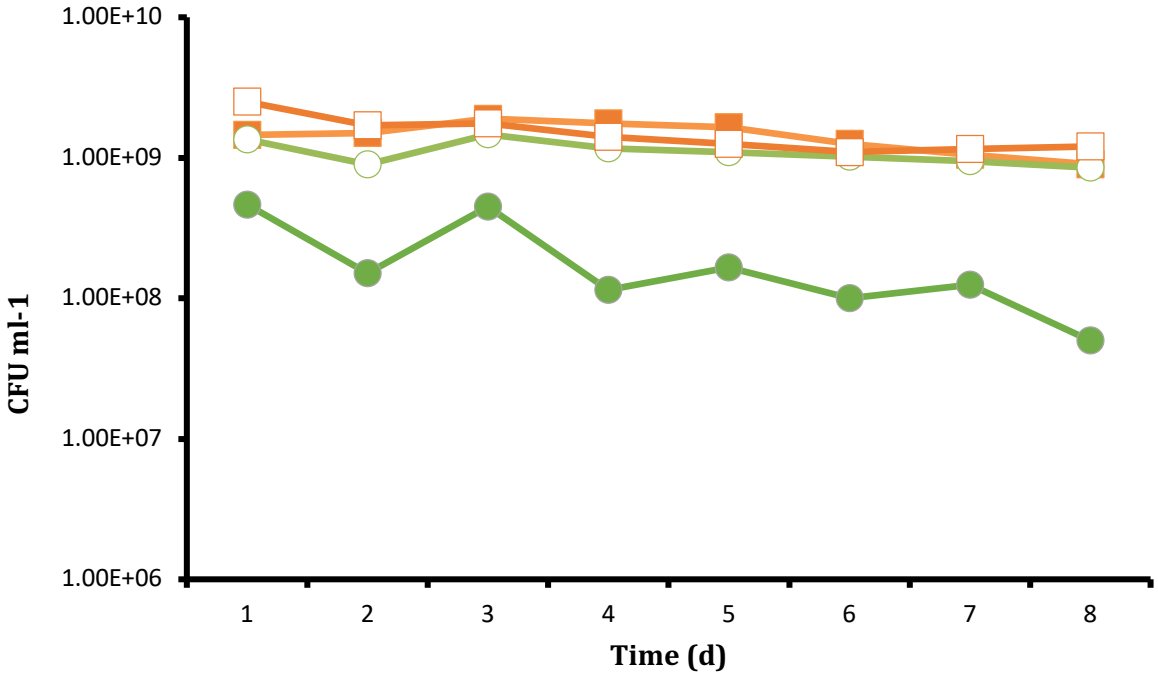

Figure 3.6 Competition dynamic between *S. aureus* SH1000 and inhibitor non-producing *S. epidermidis* B115. Bacterial growth in mono and coculture on BHI agar. Cells were recovered, sampled and transferred daily (24 h) to fresh media. Growth was determined by viable counts. *S. aureus* monoculture (empty orange square), *S. aureus* from coculture (solid orange square), *S. epidermidis* monoculture (empty green circle) and *S. epidermidis* from coculture (solid green circle). Experiments were performed in triplicate with one representative graph shown.

3.3.4 *S. aureus* SH1000 evolved a resistance phenotype to antimicrobial produced by *S. epidermidis* B155

Based on the observations from competition experiments with both planktonic and growth on agar plate, *S. aureus* SH1000 clones from the end of the experiment were tested using the deferred inhibition spray assay to determine whether they had adapted with a fixed genetic phenotype due to competition with *S. epidermidis* B155. Around 50 *S. aureus* SH1000 clones were selected from different days (day 1, 12 and 15) and competed with ancestor and *S. epidermidis* B155 clones from the end of the experiment using a deferred growth inhibition assay. Clones were tested from both of the previous competition experiments. Growth inhibition measurements were recorded based on clarity score and zone size in millimeters (Libberton *et al.,* 2014).

From the assay, it was evident that *S. aureus* SH1000 from day 1 was sensitive to *S. epidermidis* B155 secreted antimicrobial of both the ancestor and the *S. epidermidis* clone from day 1 as the same as *S. aureus* SH1000 parent strain (Fig. 3.7A,B). This was confirmed by the presence of an inhibition zone surrounding the *S. epidermidis* B155 ancestor strain with diameters of 4.3 ± 0.46 mm (Fig. 3.8A) and 4.17 ± 0.40 mm with B155 clone from day 1 (Fig. 3.8B). *S. aureus* wild type showed inhibition zone of 4.2 ± 0.43 with *S. epidermidis* B155 ancestor strain (Fig. 3.8A) and with *S. epidermidis* B155 clone day1 4.16 ± 0.40 (Fig. 3.8B). Therefore, there was no significant difference detected between the diameters of inhibition zones of SH1000 parent and clones from competition day1 with *S. epidermidis* B155 ancestor (t-test, P=0.9) with clone (t-test, $P > 0.9$).

S. aureus SH1000 clones from day 12 and day 15 had evolved resistance to the inhibitor produced by both ancestral and clone *S. epidermidis* B155 (Fig. 3.7C, D, E, F). Resistance was evident by the absence of an inhibition zone around both the ancestor *S. epidermidis* B155 or its clones picked from day 12 and day 15. Statistical analysis supported there was a significant different between the S. *aureus* SH1000 from the beginning and the end of the competition experiment (t-test, $P < 0.05$) (Fig. 3.8A) and (Fig. 3.8B).

The deferred inhibition assay was also used to investigate whether *S. aureus* displays a similar resistance pattern during competition using solid agar as that identified during competition in planktonic growth. Tested *S. aureus* clones from day 1 in the experiment showed growth inhibition when was competed with *S. epidermidis* B155 parent strain and a clone isolated from day 1 (Fig. 3.9A&B) with zone of inhibition (4.16 ± 0.40 mm) and (4.17 ± 0.20 mm), respectively (Fig. 3.10A&B). Comparing to wild type, no statistically significant difference was identified in growth inhibition early in the competition (with *S. epidermidis* B155 parent strain t-test, P=0.7 and *S. epidermidis* B155 clone isolated from day 1 P=0.5). By contrast, an obvious change of inhibition was seen with the *S. aureus* clone isolated from day 8 where no inhibition zone was evident for the *S. aureus* clone competed with *S. epidermidis* B155, either the parent or the clone isolated from day 8 (Fig. 3.9C&D); there was a statistically significant difference compared with *S. aureus* wild type (t-test, $P < 0.05$) (3.10A&B). This supported that increased resistance to *S. epidermidis* B155 secreted antimicrobial occurred because of fixed genetic changes.

Next, the evolution of *S. epidermidis* B155 phenotype during competition with *S. aureus* SH1000 during the experiments was investigated. *S. aureus* SH1000 ancestor strain was sprayed over selected B155 clones from different days. Clearly, *S. epidermidis* B155 clones produced inhibition area against *S. aureus* SH1000 ancestor that was indistinguishable from the ancestral *S. epidermidis* B155. The mean inhibition zone diameter of *S. epidermidis* B155 clones from day 1, 12 and 15 was not statistically different from the ancestor strain (t-test, P=0.50, P=0.8, P=0.41) respectively (Fig. 3.11). Since there was no definite change in *S. epidermidis* B155 antimicrobial phenotype during the experiment it was hypothesised that *S. epidermidis* B155 was not likely to co-evolve with *S. aureus* with respect to this phenotype, but this could only be confirmed by examining genotype.

The competition data presented here provide confirmatory evidence that *S. aureus* evolved fixed genetic changes that enabled it to compete and survive *S. epidermidis* antagonism. Based on the clones tested it was hypothesised that that

the resistance emerged from day 12 in the planktonic growth and day 7 in the case of growth on agar. It could not be determined when the resistance evolution occurred and whether it was present in the original inoculum, though it might be that clones evolved during days prior to their observed emergence. Since there was no significant difference with *S. epidermidis* clones from the competition when tested for inhibition of *S. aureus* ancestral strain, this may indicate that *S. epidermidis* was not selected for increased fitness via enhanced antimicrobial expression during competition with *S. aureus* over the time length of the assay . All proposed fixed genetic changes from experimental evolution will be confirmed further by genome resequencing.

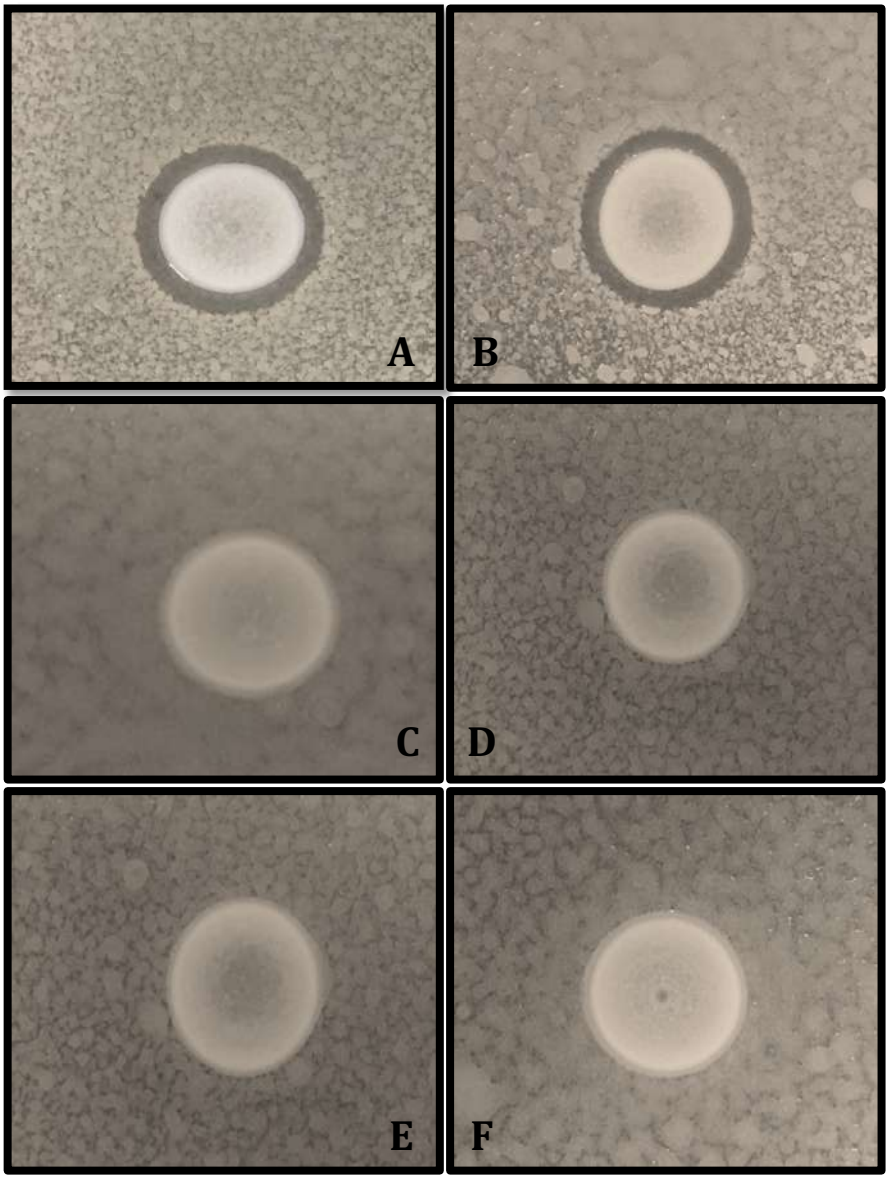

Figure 3.7 *S. aureus* SH1000 developed resistance to *S. epidermidis* B155 inhibitory toxin during competition in liquid culture. Deferred inhibition assay was performed by spotting overnight culture of *S. epidermidis* 155 (central spot) WT or clones isolated on different days of competition. BHI plates were incubated at 37°C before being sprayed with *S. aureus* SH1000 and incubated overnight. (A) Ancestor *S. epidermidis* 155 competed with a clone of *S. aureus* SH1000 day 1. (B) Day 1 clones of *S. epidermidis* 155 with clone *S. aureus* SH1000 day1. (C) Ancestor *S. epidermidis*155 with evolved *S. aureus* SH1000 day 12. (D) Day 12 clone of *S. epidermidis* 155 with evolved *S. aureus* SH1000 day 12. (E) Ancestor *S. epidermidis* 155 with evolved *S. aureus* SH1000 day 15. (F) *S. epidermidis* 155 day 15 clone with evolved *S. aureus* SH1000 day 15.

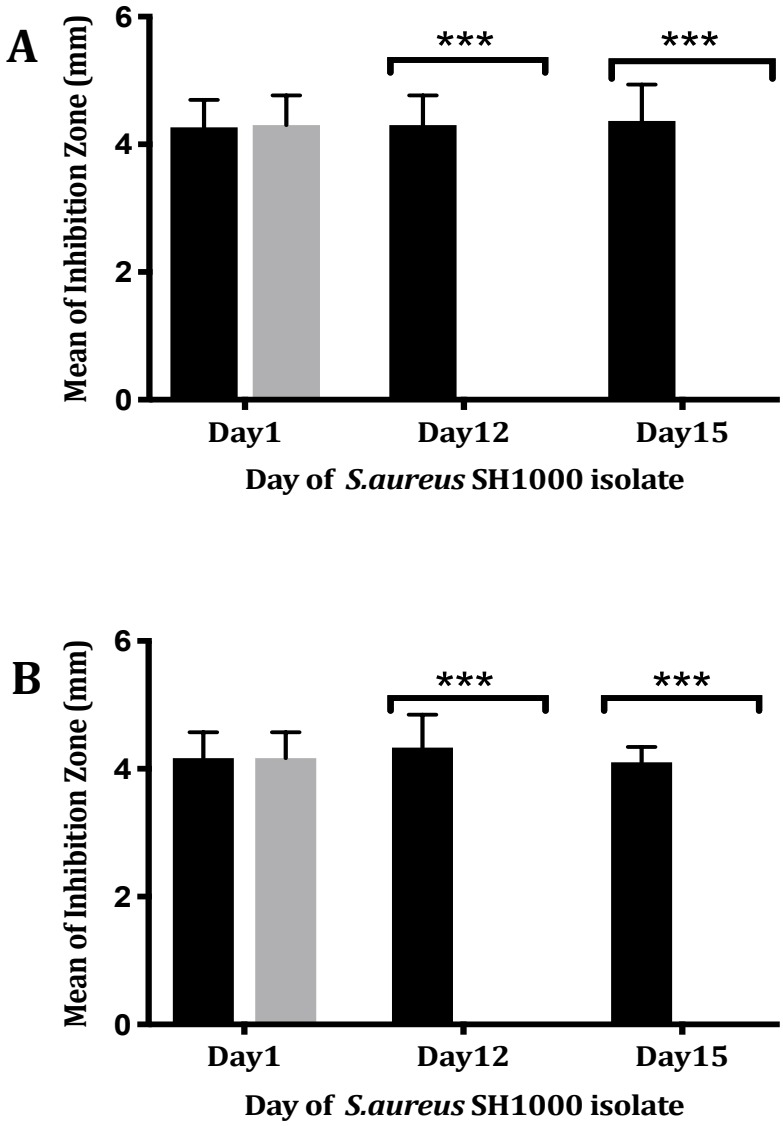

Figure 3.8 Growth inhibition of *S. aureus* SH1000 clones by *S. epidermidis* B155. (A) Inhibition zone diameter (mm) of *S. aureus* SH1000 WT (black bar) and *S. aureus* SH1000 clones from days 1, 12 and 15 (grey bar) of competition tested against ancestor *S. epidermidis* B155. (B) Inhibition zone (mm) of *S. aureus* SH1000 WT (black bar) and its clones from days 1, 12 and 15 (grey bar) tested against *S. epidermidis* B155 clones. Data are the mean ± standard deviation calculated from 6 biological replicates. Asterisks show significance from student's t-test (*** $P \leq 0.001$).

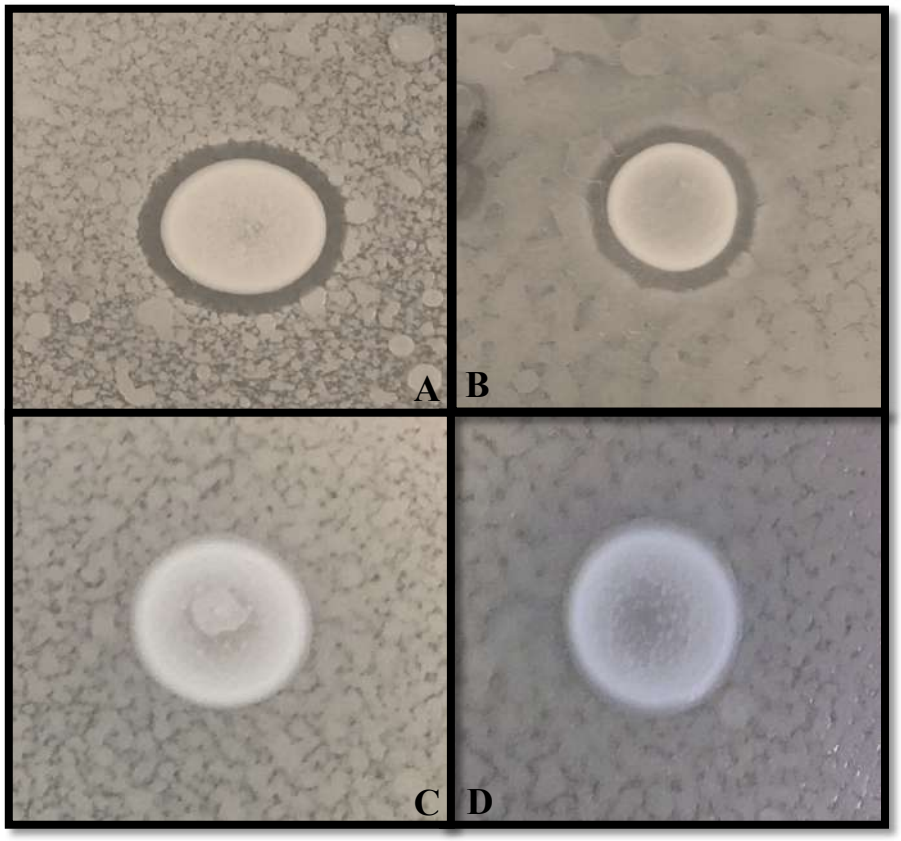

Figure 3.9 *S. aureus* SH1000 developed resistance to *S. epidermidis* B155 inhibitory toxin during competition on agar. Deferred inhibition assays were performed by spotting overnight culture of *S. epidermidis* 155 as either WT or clones isolated from day 1 and 8 of competition. Plates were incubated at 37°C before being sprayed with *S. aureus* SH1000 and incubated overnight. (A) Ancestor *S. epidermidis* 155 with a day 1 clone of *S. aureus* SH1000. (B) Day 1 clone of *S. epidermidis* 155 with day 1 clone of *S. aureus* SH1000. (C) Ancestor *S. epidermidis*155 with day 8 evolved *S. aureus* SH1000 (D) Day 8 clone *S. epidermidis* 155 with day 8 evolved *S. aureus* SH1000.

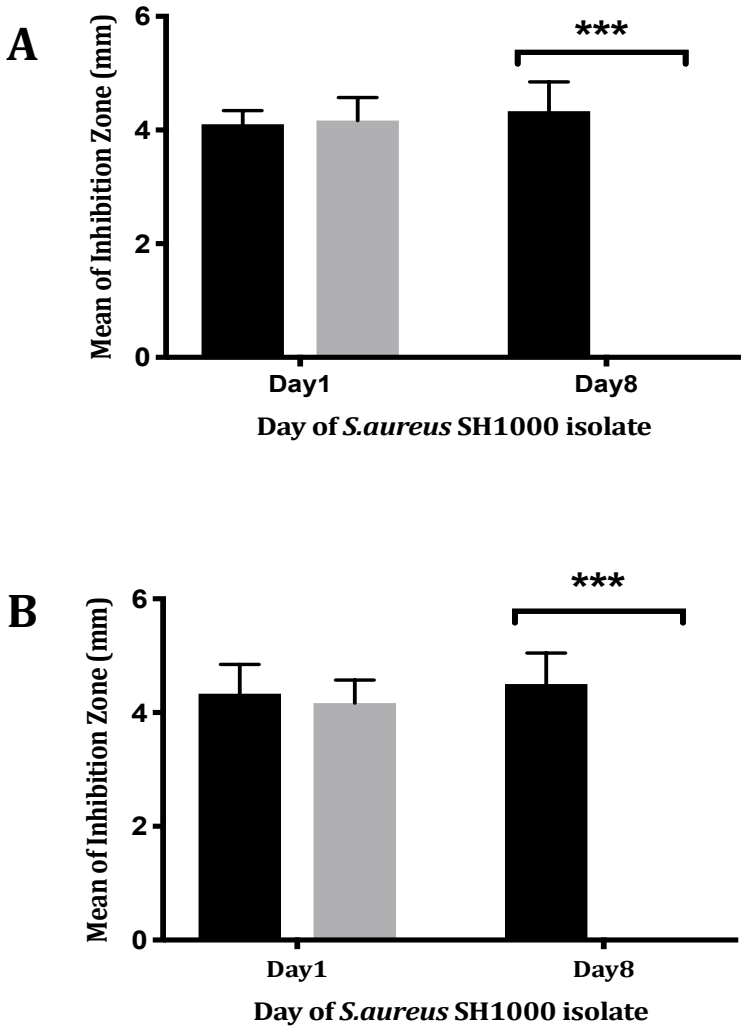

Figure 3.10 Growth inhibition of *S. aureus* SH1000 clones isolated from competition with *S. epidermidis* B155. (A) Inhibition zone (mm) of *S. aureus* SH1000 WT (black bar) and *S. aureus* SH1000 clones from day1 and 8 (grey bar) tested against ancestor *S. epidermidis* B155. (B) Inhibition zone (mm) for the *S. aureus* SH1000 WT (black bar) and *S. aureus* SH1000 clones from days 1and 8 (grey bar) against *S. epidermidis* B155 clones from day 1 and 8. Data represent the mean ± standard deviation calculated from 6 biological replicates. Asterisks show significance from student's t-test (*** $P \leq 0.001$).

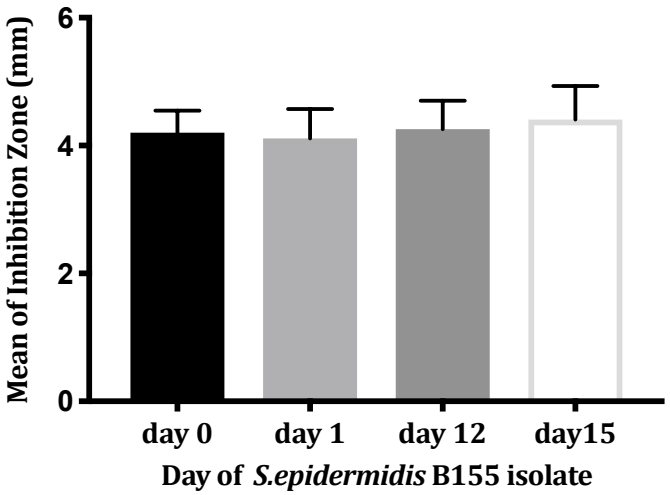

Figure 3.11 Growth inhibition of *S. aureus* SH1000 WT by *S. epidermidis* B155 clones isolated from different days of competition. Inhibition zone (mm) of *S. aureus* SH1000 WT from competition with *S. epidermidis* B155 on day 0 (black bar), or isolated day 1 (light grey bar), day 12 (dark grey bar) or day 15 (empty bar). The data are the mean ± standard deviation calculated from 6 biological replicates. No significant differences were observed measured by student t-test.

3.3.5 Evolved *S. aureus* outcompete *S. epidermidis* B155

To further investigate the ability of evolved *S. aureus* to outcompete *S. epidermidis* B155, *S. aureus* SHG01 (evolved) population fitness that isolated from day 12 during compeition in liquid culutre was assessed by competing isolated clones against ancestral *S. epidermidis* B155. Competitions were conducted using the same medium and environmental conditions for the previous selection following the same method (2.4.1). Both competitors were grown at ratio 1:1 in BHI, shaken for 24 h. Monocultures of *S. aureus* WT or SHG01 (evolved) clones served as a control. The frequency of the competitor species was enumerated by serial dilution on BHI agar plates. Competition by *S. epidermidis* B155 significantly reduced the number of viable *S. aureus* WT cells (1.3×10^8 CFU ml^{-1}) compared with *S. aureus* cultured alone (1.665×10^9 CFU ml^{-1}) ($P < 0.001$, n=3) (Fig. 3.13). There was no significant difference in growth yield between *S. aureus* SHG01 (evolved) clone cocultured with *S. epidermidis* B155 (1.3×10^9 CFU ml^{-1}) compared with its yield of it as a monoculture (1.9×10^9 CFU ml^{-1}) (P=0.11, n=3) (Fig. 3.13). Notably, *S. aureus* SHG01 competed more effectively when mixed with *S. epidermidis* B155 relative to *S. aureus* WT and the difference was statistically significant between dual *S. aureus* WT and dual *S. aureus* SHG01 (evolved) (P=0.002, n=3) (Fig. 3.13). The data presented in Fig. 3.12 clearly illustrates that the *S. aureus* SHG01 (evolved) strain competed very effectively with *S. epidermidis* B155 (ratio ~7:1 of *S. aureus* evolved: *S. epidermidis*) this was based on the number of pigmented *S. aureus* (yellow) compared with non-pigmented *S. epidermidis* colonies (Fig. 3.12), which support the observation that *S. aureus* evolve resistance to toxin producing *S. epidermidis* B155.

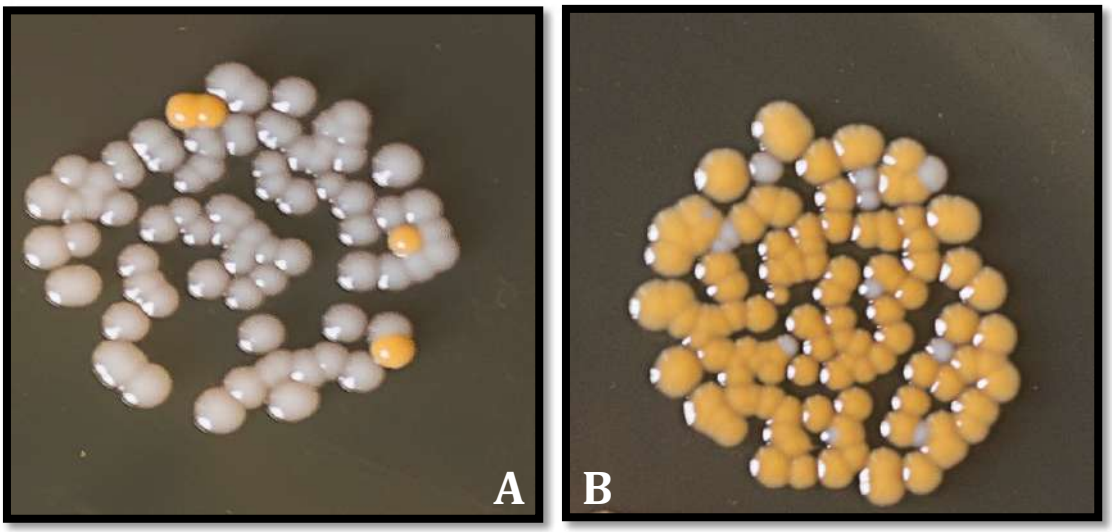

Figure 3.12 *S. aureus* SHG01 (evolved) competes effectively compared with its parent in culture with ancestral *S. epidermidis* B155. Images taken of representative dilutions after coculture for 24 h incubation at 37°C. Serial dilution (A) of cocultured *S. aureus* WT (pigmented colonies) and *S. epidermidis* B155 WT (non-pigmented colonies) taken from dilution 10^{-6} (B) *S. aureus* evolved (pigmented colonies) and *S. epidermidis* B155 WT (white colonies) taken from dilution 10^{-6}.

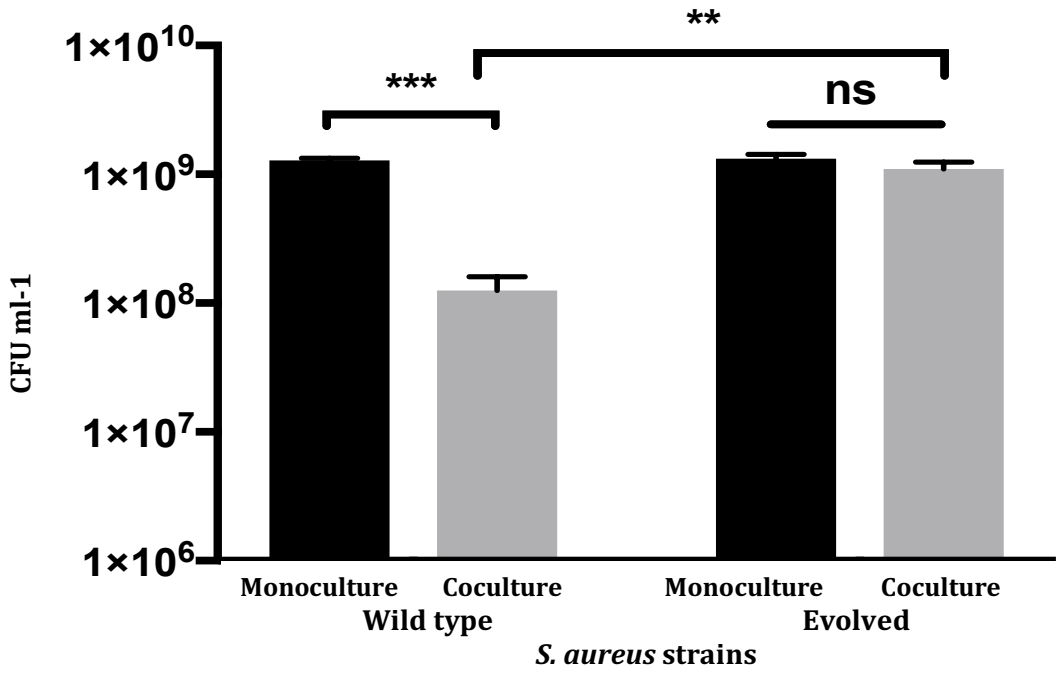

Figure 3.13 Increased competitiveness of *S. aureus* SHG01 (evolved) clone compared with parental wild type in culture with ancestral *S. epidermidis* B155. Both species were inoculated as monocultures (black bar) or coculture at ratio 1:1 (grey bar) in BHI broth, shaken for 24 h and enumerated by serial dilution. *S. aureus* SHG01 (evolved) clone (right) (ns) competed more effectively with *S. epidermidis* B155 compared with wild type parental *S. aureus* SH1000 (left) [($P < 0.001$)]. A significant difference was observed between mix *S. aureus* WT and mix *S. aureus* SHG01 (evolved) [($P=0.002$)] while no significant differences between single and mixed *S. aureus* SHG01 (evolved). These data are the mean ± standard deviation calculated from 3 biological replicates. Significance was measured by Tukey's multiple comparison test.

3.4 Discussion

In this chapter, the research sought to examine the breadth of variability of antimicrobial expression by CoNS, with particular focus on *S. epidermidis*. The antimicrobial action of CoNS was tested against *S. aureus* and was examined using an in vitro deferred inhibition assay. To grade the inhibitory status of isolates, two scores for inhibition were assigned: a qualitative score based on inhibitory zone clarity (zone clarity score) and a quantitative score based on inhibitory zone (Libberton *et al.*, 2014), indicating the presence of different antimicrobial outcomes. The study revealed a large variation of antimicrobial activity in (CoNS) that is likely to also represent simultaneous variability in host sensitivity and expression of antimicrobial by the CoNS isolates. Regardless, the assay revealed the wide difference in outcomes of competition between isolates and hosts. While also the largest study group, of all the (CoNS) screened, *S. epidermidis* was the most effective species with respect to its ability to kill *S. aureus* strains as determined by a clarity score of 4 representing apparent complete killing of the indicator strain.

Regarding *S. epidermidis*, it was found previously to be a negatively associated with *S. aureus,* via several potential mechanisms, ESP-mediated biofilm disruption (Iwase *et al.,* 2010), *agr* interference (Lina *et al.*, 2003) or production of substances such as bacteriocins (Coelho *et al.*, 2007; Bastos *et al.*, 2009). In the study here, *S. epidermidis* isolates B008, B014, B155 and B180 exhibited pronounced inhibitory activity whereby they inhibited all targeted *S. aureus* strains including USA300, a community associated MRSA strain responsible for major outbreaks of staphylococcal skin and soft-tissue infection (SSTI) (King *et al.*, 2006). This inhibitory capacity of these four isolates was associated with the greatest qualitative clarity score in 4/5 isolates that had pronounced activity across all four tested indicator *S. aureus* strains. Similarly, one *S. capitis* (B273) strain had pronounced activity against all *S. aureus* indicator strains. *S. capitis* (B160) was also active against all *S. aureus* but in less degree of inhibition compared to strain (B273). It was presumed likely that the presence and production of a bacteriocin or bacteriocin-like agents in these species, such as epidermin or epicidin which are widely found in (CoNS), especially *S. epidermidis*

would be responsible for the pronounced inhibitory activity, perhaps with high levels of expression. The lower levels of inhibition were considered among other isolates to be a measure of expression level combined with indicator host resistance threshold. Across the panel of isolates tested, 29 of the 62 CoNS strains exhibited no apparent activity towards *S. aureus.* The reasons for this are unclear but could range to conditions of the assay, expression level, absence of antimicrobial genes and indicator strains not being representative of antimicrobial targets.

S. hominis was described as a bacteriocin producer (dos Santos Nascimento *et al.*, 2005) with nukacin KQU-131 found to be secreted by *S. hominis* kqu-131 isolated from fermented fish *(Wilaipun et al.,* 2008). Hominicin was also isolated form S. *hominis* MBBL 2–9. (Kim *et al.*, 2010). This latter bacteriocin was found to be active against antibiotic-resistant *S. aureus* such as VISA and MRSA strains (Kim *et al.*, 2010). Previous work by Nakatsuji *et al.,* (2017) showed that the lack of coagulase-negative staphylococcal (CoNS) species, including *S. hominis* and *S. epidermidis,* that produced antimicrobial activity on the skin of patients with atopic dermatitis (AD) was strongly associated with increased colonisation of *S. aureus* (Nakatsuji *et al.*, 2017). These unknown AMPs were proposed to act synergistically with human AMPs such as LL-37 (Nakatsuji *et al.*, 2017). In relation to the results of the presented study here, most of the *S. hominis* isolates tested affected *S. aureus* growth although they had a limited inhibition activity measured via clarity and size of zone. *S. hominis* isolates B150 and B175 were able to slightly inhibit growth of *S. aureus* SH1000 and Newman strains while 4 out of 6 *S. hominis* isolates showed a low effective inhibition against *S. aureus* B032) However, USA300 strain was not inhibited by either *S. hominis* or *S. warneri* strains from the panel tested. Moreover, based on the target strain there were clear differences in antimicrobial activity by which producing toxin strains had ability to inhibit some *S. aureus* strains but not inhibited others. In the literature similar findings have already been found regarding the production of bacteriocins. Within species, some strains might be susceptible while others would be resistant to a specific bacteriocin (Nascimento *et al.*, 2006). Spontaneously resistant mutants to bacteriocin were reported could be found in

some cells within a bacteriocin-sensitive bacterial population (Jack *et al.*, 1995). Resistance to bacteriocin seems to be a complex phenotype involving multiple cell wall and/or cytoplasmic membrane alterations (Crandall and Montville, 1998; Coelho *et al.*, 2007).

Human skin has a symbiotic relationship with commensal microbes, with one of the most important and ubiquitous members being *S. epidermidis* (Arvidson, 2006). Due to their shared features, establishment of *S. aureus* on the skin or mucous membrane, means it will always compete with resident *S. epidermidis* in the niche. Therefore in this study, competition experiments were performed to focus on the interaction between these two species. The experimental rationale was to investigate the toxin-producing *S. epidermidis* B155 isolate which has antimicrobial activity towards the laboratory strain *S. aureus* SH1000 and further strains tested. In competition with strain SH1000, cell numbers were followed over time as the species vie for resources with each other. In monocultures, the population size of both *S. aureus* and *S. epidermidis* B155 was larger than when grown together indicating that these species compete with each other and that there were finite resources in the BHI growth medium being used. The result clearly showed that the inhibitory activity of *S. epidermidis* B155 when it was co-cultivated with *S. aureus* contributed to its dominance over *S. aureus* particularly in the early, day 1 and 2 stages of competition. This observation was shown under conditions of growth in batch culture and on agar. The reduction of *S. aureus* cell viability by *S. epidermidis* toxin gave the latter a competitive advantage and supports the previously described mechanism that *S. epidermidis* on the skin acts as a defence mechanism against *S. aureus* colonization due to the production of several toxins.

The antagonistic interaction between two species will depend on the effectiveness of secreted inhibitory molecules. In the laboratory, environmental conditions (nutrients, temperature, pH, etc.) can affect the stimulation and production of bacterial bacteriocins that facilitate their effective interaction with sensitive competitor species (Jack *et al.*, 1995). Spatial population structure is

implicated in the interference competition within a bacterial community. A study was conducted by Chao and Levin (1981) to determine how spatial structure affects the invasion by *E. coli* bacteriocin producer strain into a sensitive *E. coli* population. They concluded that in a spatially structured environment, a toxin producer strain will invade at lower frequency into toxin sensitive populations. Whereas, a higher frequency abundance of toxin producing strain is needed to successfully invade into a population of sensitive strain under unstructured environmental conditions (Chao and Levin, 1981). Wloch-Salamon *et al.* (2008) cultured *Saccharomyces cerevisiae* isogenic K1 toxin-producing and sensitive strains together in competition under low and high nutrient conditions. They found that in high nutrient environments, inhibitory toxin-producing strains were able to outcompete sensitive strains, whereas under low nutrient conditions they were out-competed. The authors argued that the lack of toxin production seen in the low nutrient environment is unlikely to be solely due to a nutritional constraint, but rather due to a physiological change in toxin production or resistance developing after the nutrients have been depleted (Wloch-Salamon *et al.*, 2008). Because it was debated that bacteriocin-producer bacteria are favoured in nutrient-rich environments (Xavier and Russell, 2006), in our experiments the *S. epidermidis* producer strain and sensitive *S. aureus* were added at ratio 1:1 in both conditions using a rich BHI media and our producer species dominated the batches culture supporting the idea that nutrient rich media favour the toxin producing bacteria and our data suggested that production of inhibitory toxin of *S. epidermidis* B155 strain can be effective in planktonic or sessile competition.

The effectiveness of toxin produced by *S. epidermidis* B155 during competition could be because the two species was grown together at the same growth rate. It was suggested that if the producer strain was added at high frequency the less any benefit would be because there is insufficient sensitive strains to kill, therefore there are limited nutrients to be obtained from costly toxin production. Similarly, at a low frequency of producer, both strains will share freed up resources and the benefits of reducing competition will benefit the producer

strain (Inglis *et al.*, 2009). However, at intermediate frequency a great fitness advantage can be gained by a bacteriocin producer strain via killing sensitive competitor strains and accordingly freeing-up nutrients via paying off to prevent competitors from growing into unexploited patches and by removing them from their current one (Inglis *et al.*, 2009). Results presented here in this study are consistent with a study showing that *Pseudomonas aeruginosa* produced a molecule that inhibited the growth of *E. coli* when they were cocultured with similar growth rates under planktonic culture to test the interaction between them (Khare and Tavazoie, 2015).

Despite the identification of antagonistic molecules secreted by different species in interspecific competition, species adaptation to such competition is still relatively underdescribed. Certain organisms sharing the same environment can result in changes of: adaptation patterns, growth of organisms, morphology or development of their ability to synthesise components including proteins (de Souza *et al.*, 2017). Through the study presented here, laboratory experimental competitions identified that after competing for a sufficient number of days under planktonic conditions, *S. aureus* evolved resistance after continued exposure to toxin produced by *S. epidermidis* B155; this supports multiple pathways to combat interspecies competition. A similar resistance evolution pattern occurred in *S. aureus* clones from day 8 competed on a solid surface. Comparison of competitiveness of *S. aureus* evolved clones to their common ancestor in competition with *S. epidermidis* B155 ancestor strain revealed that evolved strains cells were had greater fitness to *S. epidermidis* B155. Compared with *S. aureus* wild-type after competition for 24h evolved *S. aureus* clones exhibited a resistance phenotype toward toxin-producing *S. epidermidis* B155 with evidence for fixed genetic variations as the cost of resistance. This outcome supported that antibiotic resistance mechanisms might also play a role in the observed inhibition of antimicrobial activity during co-cultivation (Rice, 2006; Wellington *et al.*, 2013). However, this was not the case in a recent study showing that *S. lugdunensis* which produces lugdunin, seemed to protect against *S. aureus* carriage both in humans and in a cotton rat colonisation model. During coculture

S. aureus was not able to be recovered after day 3, which indicated *S. lugdunensis* effectively killed all *S. aureus* cells in competition (Zipperer *et al.*, 2016).

It is challenging to determine the mechanism by which *S. aureus* resistance functions towards the competitor species component. If the toxin produced by inhibitory *S. epidermidis* strains are cationic antimicrobial peptides (CAMP), such as bacteriocins that are a widespread within CoNS and particularly *S. epidermidis* (Schnell *et al.*, 1988; Héchard and Sahl, 2002), then the resistance of *S. aureus* to a variety of CAMP has been linked to mutations in the *mprF* (Staubitz *et al.*, 2004; Weidenmaier *et al.*, 2004) and *dltABCD* operons (Peschel *et al.*, 1999). Collectively, these mutations lead to modification of cell wall net charge and membrane components (Weidenmaier *et al.*, 2005; Ernst *et al.*, 2009). It could be examined with future experiments whether deletion of *mprF* or *dlt* operons increases sensitivity of *S. aureus* to toxin producing *S. epidermidis* B155. To further investigate the mechanism responsible for the inhibition of *S. aureus* growth by *S. epidermidis,* the toxin should be purified by using high performance liquid chromatography (HPLC) potentially in conjunction with nuclear magnetic resonance (NMR) spectroscopy to identify the chemical structure. The genetic factors facilitating phenotypic alterations, resistance will be discussed in the next chapter.

Further experiments in this chapter examined whether *S. epidermidis* B155 changed phenotype and increased its production of inhibitor or alternative toxins against *S. aureus* by testing *S. epidermidis* clones selected from different days of competition using the deferred inhibition assay with *S. aureus* SH1000. No changes in phenotype were seen in any tested clone compared with wild type, supported by no significant difference in diameter of inhibition zone. The outcome could indicate that *S. epidermidis* B155 became a less-fit competitor due to the reduction of cell number over time, particularly towards the end of the experiment. Habets *et al.*, 2007 suggested increasing numbers of invader producing species may increase the intraspecific competition compared with interspecific competition leading to a decrease in the level of fitness (Habets *et al.*, 2007). The results obtained here are not supportive with what was observed

previously by Libberton *et al.*, 2015 who found that inhibitor-producing *S. epidermidis* co-evolved when invading resident *S. aureus*, which developed resistance. The invader *S. epidermidis* in their described case displayed a greater inhibition activity around the *S. aureus* parent strain, however, the reason for this observation was not investigated (Libberton *et al.*, 2015). The outcomes of the study presented here by detection and characteristics of genetic variations between *S. epidermidis* clones and wild type is described in the following chapter. *S. aureus* SH1000 was observed to be a more successful competitor when co-cultured with *S. epidermidis* non-inhibitory strain B115 since it had a comparatively high growth yield. Perhaps it grows faster than *S. epidermidis* B115 under the co-culture conditions, however no data was obtained to support this idea. Serial culture also saw the ratio of both species stay relatively constant, at least in the first few days which would suggest either there is a degree of antagonism or resource sharing. Each species grew well in monoculture thus the presence of *S. epidermidis* did not affect the population size of *S. aureus*. *S. epidermidis* B115 showed progressively reduced yield until the end of experiment. Therefore it is likely that this isolate can coexist with *S. aureus* when they occupy the same environments since coexistence may occur if one species grows faster when resources are abundant while the another one grows at low resources level (Pekkonen *et al.*, 2013). Therefore, the availability of resources could affect this type of interaction between species and the lower yield of *S. epidermidis* B115 would support this explanation.

Chapter 4: Identification of genetic determinants associated with competition between *S. aureus* and *S. epidermidis*

4.1 Introduction

In many laboratories, the use of whole-genome sequencing technologies has become an attractive tool to gain insight into small bacterial genomes, including their evolution and species epidemiology (Jamrozy *et al.*, 2017). This advance was facilitated by high-throughput data acquisition from massively parallel short-read sequencing with greater sequencing depths generated by the second generation Illumina sequencing platform. With the advent of third generation sequencing, the single molecule real time sequencing (SMRT) PacBio platform is able to produce very long reads up to and exceeding 10 kb in length, with unbiased genome coverage (Ferrarini *et al.*, 2013) (Heather and Chain, 2016). The disadvantage of using PacBio is its 15-18% error rate, therefore these errors must be corrected before use in genome assembling or other applications (Li *et al.*, 2015). Overall, next generation sequencing is hugely beneficial for the ease of complete *de novo* genome assembly as well as for discovery of single nucleotide differences between two or more genomes (Benjak *et al.*, 2015).

Whole-genome comparisons enable powerful genetic approaches, such as; detection of genetic determinants associated with drug resistance (Friedman *et al.*, 2006); comparing transmission dynamics; phylogenetics; molecular epidemiology; estimations of mutation rates; and phylogeography (Benjak *et al.*, 2015). The comparative DNA analysis between resistant and susceptible or parent *S. aureus* strains has determined suites of genes that are responsible for *S. aureus* resistance and virulence phenotypes (Friedman *et al.*, 2006). A good example of the resolving power of using this technique was the identification of the genetic basis for resistance in glycopeptide intermediate *S. aureus* (GISA), vancomycin intermediate *S. aureus* (VISA) and daptomycin resistant *S. aureus* (Friedman *et al.*, 2006; Mwangi *et al.*, 2007; Renzoni *et al.*, 2011; Song *et al.*, 2013).

Developing resistance to antimicrobials often protects bacterial cells via different mechanisms though, generally, resistance of Gram-positive bacteria occurs by

changing the target to make it less sensitive to drug action (Andersson *et al.*, 2016). For instance, methicillin-resistant *S. aureus* strains utilise phospholipid cell membrane adaptations via PgsA (phosphatidylglycerol synthase), Cls (cardiolipin synthase), MprF (multiple peptide resistance factor) among others to change its negative surface charge as a protective tactic, evolved possibly against the insertion of positively charged cationic AMPs (CAMPs) that also calibrates fluidity versus rigidity of cell membrane to resist the AMPs action (Maria-Neto *et al.*, 2015). In addition, resistance could be achieved by extruding the antimicrobial outside the bacterial cells. This resistance mechanism is controlled by the expression of efflux pumps, for example tetracycline efflux pumps that confer tetracycline resistance this phenomenon, as described in *E. coli* (Wang *et al.*, 2014; Munita and Arias, 2016). Another mechanism used by bacteria to dampen the effect of antimicrobial agents is enzymatic cleavage of the antimicrobial or via modification. For example, the penicillinases are a group of β-lactam hydrolytic enzymes that are active against the penicillin (Chambers and DeLeo, 2009).

4.1.1 Mobile genetics elements in staphylococci

Acquisition of various adaptive traits that enhance fitness of their hosts has been linked to MGEs, which can move between microbial cells (Frost *et al.*, 2005). Research identified that many plasmids carry resistance genes, which make bacterial host cells capable of growth in the presence of antimicrobials including heavy metals, which likely have spatially or temporarily variable distributions (Eberhard, 1990). Phages were reported to have a crucial role with increased virulence of bacteria, such as temperate bacteriophage (CTXϕ) chracterised in *Vibrio cholerae* (Rankin *et al.*, 2011; Faruque and Mekalanos, 2012). Although bacteriocins are an important class of antimicrobials, they were found to be encoded on plasmids and are rarely present within the core genome of species, being readily horizontally transferred as MGEs (Janek *et al.*, 2016).

A wide variety of MGEs have been identified in *S. aureus* and they represent up to 25% of the *S. aureus* genome and are mostly found to encode several virulence

factors, while these accessory genetic materials are not well described in CoNS (Malachowa and DeLeo, 2010; Otto, 2014). Secreted virulence factors include Panton-Valentine Leucocidin [PVL], which is prophage-encoded and contributes to necrotic skin lesions caused by *S. aureus*. In the USA, around 53–62% of *S. aureus* isolated from skin and soft tissue infections possess PVL genes (Amissah *et al.*, 2017). Contrastingly, in CoNS few prophages are observed in clinical isolates, including *S. epidermidis* and *S. hominis,* with closely related phages to those found in *S. aureus*. Plasmids are involved in acquisition by *S. aureus* of many genes responsible for resistance to multiple antibiotics and they can carry toxin genes. Similarly, plasmids were also described among *S. epidermidis* strains while they are rarely described for other CoNS but may be equally frequent (Argemi *et al.*, 2017). Recently, the plasmids and prophages were identified in *S. lugdunensis* to horizontally transfer genes from *S. aureus,* which means this commensal species potentially could accept some virulence determinants (Argemi *et al.*, 2017). Finally, many pathogenicity islands identified in *S. aureus* encode superantigens and virulence factors (Gal-Mor and Finlay, 2006) while few toxin genes are found on CoNS pathogenicity islands, although it was reported that an enterotoxin C-like-bearing pathogenicity island was identified in three *S. epidermidis* strains (Madhusoodanan *et al.*, 2011; Nanoukon *et al.*, 2017).

4.1.2 Polyketides and secondary metabolite producing bacteria

In the genomic era, the potential of one bacterium to produce bioactive molecules can be assessed by molecular methods. A wide variety of secondary metabolites can be encoded and then identified by comparative genome analysis, including antibiotics, antineoplastics and immunosuppressants (Challis *et al.*, 2000; Hahn and Stachelhaus, 2004). The majority of these secondary metabolites are formed by enzymatic activities, including polyketide synthases (PKSs) and non-ribosomal peptide synthetases (NRPSs) or hybrid clusters (PKS/NRPS) (Morris *et al.*, 2009; Singh *et al.*, 2017). NRPS can be as small as one module or consist of multi-modular units with molecular weights > 2 MDa (Bloudoff and Schmeing, 2017). Typically, the peptide elongations required module comprises three essential domains: adenylation (A), which is responsible for the amino acid

activation, peptidyl carrier protein (PCP) domain, or known as the thiolation domain (T) which transports the aminoacyl and peptidyl substrates to different domains of the NRPS, condensation (C) domain that is involved in peptide bond formation to grow the peptide chain and is about 450 amino acids in length and found in the N-terminus of each module (Roongsawang *et al.*, 2005; Jenke-Kodama and Dittmann, 2009; Strieker *et al.*, 2010). Thioesterase (TE) is an additional domain located in the termination module and involved in product release (Strieker *et al.*, 2010).

While PKSs are synthesised by a stepwise chain elongation mechanism and use acyl-CoA substrates as precursors, the growing chain is attached to the complex by a β-ketothioester linkage. Modules consist of essential and accessory domains with different catalytic activities responsible for each step in chain extension and modification (Hildebrand *et al.*, 2004). The core domains consisting of a β-ketoacyl synthase (KS) and an acyl carrier protein (ACP) responsible for condensing successive acyl-CoA substrates that are selected and activated by an acyltransferase (AT) (Hopwood and Sherman, 1990; Donadio *et al.*, 1991; Khan *et al.*, 2014). There are other additional domains that may be present in the module to activate the substrate to form the chemical structure diversity, such as ketoreductase (KR), enoylreductase (ER) and dehydratase (DH) (Liou and Khosla, 2003; Khan *et al.*, 2014; Aleti *et al.*, 2015). Within modules, the variability of the interdomains and intradomains together with the differences in module arrangements resulting in the production of chemically diverse compounds synthesised by NRPS and PKS (Fischbach and Walsh, 2006).

The PKSs can be classified into three different types: type I are multifunctional enzymes organised into modules (e.g. 6-deoxyerythromycin B synthase, DEBS); type II are multienzyme complexes that carry only a module with iteratively acting activities, such as tetracycline biosynthetic cluster and tetracenomycin C; and type III often referred to as chalcone synthase-like PKSs are homodimeric enzymes that essentially are iteratively acting as condensing enzymes, such as flavolin biosynthetic cluster (Planson *et al.*, 2011). The richness and diversity of secondary metabolism in this PKS group add valuable bioactive molecules with

pharmaceutical activity. Among the large number of industrial uses of polyketide drugs are: β lactams, cephalosporins, rifamycins, tetracyclines, erythromycin and anthracyclines; many polyketides have potential for the development of commercial drugs (Arteaga *et al.*, 2017).

In recent years, to identify novel microbial secondary metabolites, several bioinformatics tools have been developed with information on biosynthetic gene clusters and secondary metabolites. Several of the major web-based tools, such as NaPDoS (Ziemert *et al.*, 2012), antiSMASH (Medema *et al.*, 2011) and NP.searcher (Li *et al.*, 2009), were developed using hidden Markov models for idintification of NRPS and PKS encoding loci in bacterial genomes. Further information about cluster prediction can be obtained by antiSMASH, which enables BLAST searches with the predicted gene cluster to detect its closest sequences in the database (Aleti *et al.*, 2015). Another useful tool is ClustScan which provides a rapid detection of biosynthetic gene clusters with prediction of the chemical structures of the products (Starcevic *et al.*, 2008).

Although these bioinformatic tools provide useful high quality manually curated annotations, they come at the cost of narrow specificity and often have no or limited maintenance. Most of these systems are focused on specific classes of species, such as streptomycetes or types of biosynthetic clusters (e.g., PKS/ NRPS). In addition, some analyses have relatively few records and do not provide the tools for in-depth sequence study, while others are no longer updated (Hadjithomas *et al.*, 2015).

4.2 Aims

The data from the previous chapter revealed that *S. aureus* becomes resistant to an antimicrobial produced by *S. epidermidis* B155 confirming that evolution of resistance contributes to interspecific bacterial competition. The specific aim of this chapter was to use genome sequencing to narrow the focus on the genes and mutations responsible for variations in *S. aureus* resistance to the antimicrobial produced by *S. epidermidis* B155. In addition, the entire *S. epidermidis* B155 genome would be sequenced using PacBio technology and from its assembly the contributions of mobile genetic elements, particularly plasmids, in shaping the antimicrobial properties of this strain would be assessed in detail.

4.3 Results

4.3.1 Sequencing QC and alignment statistics

S. aureus SH1000 DNA was extracted and purified from clones selected from days (1, 3, 9, 12, 13 and 15) following the start of competition experiments in liquid culture. DNA sequencing was performed using the Illumina platform methods to identify mutations that accrued in experimentally evolved *S. aureus* genomes compared with wildtype. Before sequencing, all genomic DNA samples were verified to ensure their high quality with a sufficient quantity for sequencing. DNA samples used for sequencing were purified for low protein, salts and solvent contamination. The purity of DNA was assessed to have the ratio of absorbance at 260/280 and 260/230 nm greater than 1.8 (Table 4.1). Qubit spectrophotometer reads and gel electrophoresis were also used to confirm that DNA samples contained a sufficient yield of intact gDNA.

Table 4.1 Quality control analysis results for DNA samples of *S. aureus* SH1000 and *S. epidermidis* B155 submitted for sequencing. Table shows the values of required quality checks for DNA prior to sequencing. Concentration was assessed using Qubit and absorbance 260/280 and 260/230 using Nanodrop.

Strain	Sample ID	Concentration (ng/ul)	Absorbance 260/280	Absorbance 260/230
***S. aureus* SH1000 WT (Single culture)**	A1-day01	104.0	1.9	1.8
	A2-day15	84.6	1.8	1.8
***S. aureus* SH1000 clones (Co-culture)**	B1-day01	103.7	1.9	1.9
	B2-day03	65.0	1.9	1.9
	B3-day09	69.7	1.8	1.8
	B4-day12	71.5	1.9	1.8
	B5-day13	59.4	1.8	1.9
	B6-day15	50.4	1.9	1.8
***S. epidermidis* B155 clones (Co-culture)**	C1-day01	131.4	1.9	1.8
	C2-day03	92.0	1.9	1.8
	C3-day09	85.0	1.9	2.2
	C4-day12	130.5	1.9	2.2
	C5-day13	115.5	1.8	2.0
	C6-day15	80.4	1.9	1.8

4.3.2 Selection SNPs/INDELs in evolved clones of *S. aureus* SH1000

After sequence reads were aligned to their reference genome, the SnpEff tool was used to detect genomic variants, including single nucleotide polymorphism (SNPs) and insertions and deletions (INDELs) because this algorithm can rapidly analyse and annotate thousands of variants and predict their possible genetic effects (Cingolani *et al.*, 2012). Polymorphism filtering was done by using a bespoke perl script (unique_SNPs.pl) to exclude any identical variants found in wild type compared with evolved isolates. SNPs and INDELs retained were considered as the allelic variants causing the changes leading to resistance evolution of *S. aureus* in the presence of the antimicrobial. Changes in genes that were present in both competition control and evolved clones were discounted. All non-synonymous SNPs are listed in (Table 4.3) and SNPs and INDELs were considered heterogeneous if < 80 % of reads had different bases compared with the reference genome and were therefore disregarded during analysis of *S. aureus* SH1000 clones.

The prediction for the comparative analysis was that sequence changes would be identified that accounted for increased competitive fitness and these changes would include alterations to nutrient acquisition and metabolism. With respect to *S. aureus* antimicrobial resistance, additional mutations were predicted corresponding to known BraRS, GraRS and VraRS antimicrobial peptide resistance loci (Kawada-Matsuo *et al.*, 2013).

The *S. aureus* genetic polymorphisms detected in resistance evolved SH1000 comprised 7 SNPs and 14 INDELs. Of these, 4 SNPs out of 7 were found to be synonymous SNPs located in the *sdrC* and *sdrD* MSCRAMM-encoding, clumping factor B (*clfB*) and hypothetical protein (SAOUHSC_00274) genes (Table 4.2). Since these mutations were expected to be silent they were disregarded from analysis. Remarkably, three SNPs were identified that could be associated with antimicrobial resistance, within the reads of the SH1000 clones associated with SAOUHSC_01313, SAOUHSC_01314 and *fabI* genes. The latter gene, *fabI* that is essential for *S. aureus* viability, encodes enoyl-acyl carrier protein (ACP) reductase associated with fatty acid biosynthesis; in *S. aureus* and *E. coli* this enzyme is an antibacterial target (Payne *et al.*, 2002). The *fabI*-associated SNP

was found in clones isolated from day 13 and 15 but was not present in either previous days or in the control. This SNP was a C to T base change located at chromosome position 919997 upstream of the *fabI* gene.

The most notable observation was that 100% of reads from day 12, day 13 and day 15 clones that were resistant to antimicrobial produced by *S. epidermidis* B155 had SNPs in genes that encode a two component system (TCS). Base change T → A was found in SAOUHSC_01313 that encodes the histidine kinase of the TCS. The SNP caused amino acid change from tyrosine to asparagine (Tyr137Asn) and was found in clones resistant to antimicrobial produced by *S. epidermidis* B155 that were isolated from day 13 and 15 (Table 4.3). Another SNP found in SAOUHSC_01314 gene which encodes the response regulator. The SNP introduces an amino acid change from proline to isoleucine (Phe90Ile). This TCS is a homologue of *Bacillus subtilis* DesKR TCS, which controls expression of a fatty acid desaturase (*des*) gene at low temperatures to modify membrane lipid composition and regulate membrane fluidity (Aguilar *et al.*, 2001).

Further identified polymorphisms (Table 4.3) included INDELs located in genes associated with metabolism, including utilisation of carbohydrates, or the cell membrane and these could also be associated with *S. aureus* fitness: deletion of a C nucleotide at position 1283783 located upstream of *opuD*, encoding a transporter involved in the uptake of glycine betaine; detection of a C nucleotide at chromosome poisition 947897 in the *tarM* gene involved with cell wall teichoic acid (WTA) modification (Xia *et al.*, 2010) and it is located upstream of the hypothetical protein SAOUHSC_00971 (Table 4.3). A further deletion of a C nucleotide was within the *scrA* gene encoding phosphoenolpyruvate-dependent sucrose phosphotransferase system (PTS). Others mutations occurs at regions 1041999 and 1180884 within loci encoding for *rpmF* and *rpsB* genes, respectively. Both genes are involved in protein biosynthesis. All *S. aureus* clones contained a deletion of A nucleotide upstream of the *gntK* gene (gluconate kinase); it was present in 100% of reads covering the chromosome at the position 2592011. Deletion of C (position 2782815) in the *hisF* gene encoding a multifunctional imidazole glycerol phosphate synthase subunit/phosphoribosyl-AMP cyclohydrolase/phosphoribosyl-ATP pyrophosphatase was also identified.

Deletion of T at chromosome position 2296653 resulted in a frameshift mutation in a gene encoding a hypothetical protein with unknown funtion thus, it is difficult to predict its role in *S. aureus* resistance.

Table 4.2 Synonymous, SNPs and INDELs from evolved *S. aureus* SH1000 clones with resistance to *S. epidermidis* B155. SNPs and INDELs from *S. aureus* SH1000 clones were selected after competition experiment in planktonic culture from day 1, 3, 9,12,13,15.

Gene ID	Gene description	Genome Position	Base Change	Codon change	SNP effect	Day of change
SAOUHSC_00274	Hypothetical protein		A→ G	Glu150Glu	Synonymous variant	3,9,12
SAOUHSC_00544	SdrC (fibrinogen-binding protein SdrC)		T → C	Ser854Ser	Synonymous variant	1,3,9,12,13,15
SAOUHSC_00545	SdrD (fibrinogen-binding protein SdrD)		G → A	Ser1192Ser	Synonymous variant	1,3,9,12,13,15
SAOUHSC_02963	Clumping factor B		C→ T	Ser730Ser	Synonymous variant	9,12,13,15

Table 4.3 Non-Synonymous SNPs and INDELs of evolved *S. aureus* SH1000 with resistance to *S. epidermidis* B155. SNPs and INDELs from *S. aureus* SH1000 clones selected after competition experiment in planktonic culture from day 1, 3, 9, 12, 13, 15. All mutations classified as homozygous if > 80 % of reads which have different bases to the references genome.

Gene ID	Gene product description	Genome Position	Base Change	Codon change	SNP effect	Day of change
SAOUHSC_00039	Hypothetical protein	47648	Deletion of T nucleotide		Upstream gene variant	1,3,9,12,13,15
SAOUHSC_00409	Hypothetical protein	412759	Insertion of T nucleotide		Upstream gene variant	1,3,9,12,13,15
SAOUHSC_00591	Hypothetical transmembrane protein	590401	Deletion of G nucleotide	Arg189fs	Frameshift variant	1,3,9,12,13,15
SAOUHSC_00947	FabI (enoyl-(acyl carrier protein) reductase)	919997	C → T	--	Upstream gene variant	13,15
SAOUHSC_00971	Hypothetical protein	947897	Deletion of C nucleotide		Upstream gene variant	1,3,9,12,13,15
SAOUHSC_01071	Glycerophosphoryl diester phosphodiesterase	1041999	Deletion of T nucleotide	--	Upstream gene variant	1,3,9,13,15
SAOUHSC_01233	Hypothetical protein	1180884	Deletion of T nucleotide		Upstream gene variant	1,3,9,12,13,15
SAOUHSC_01313	Histidine kinase	1257634	T → A	Tyr137Asn	Missense variant	13,15

Gene	Gene product description	Genome Position	Base Change	Codon change	SNP effect	Day of change
SAOUHSC_01314	Response regulator	1258581	T → A	Phe90Ile	Missense variant	12
SAOUHSC_01346	OpuD (glycine betaine transporter)	1283783	Deletion of C nucleotide	--	Upstream gene variant	1,3,9,12,13,15
SAOUHSC_01722	AlaS (alanyl-tRNA synthetase)	1632624	Insertion of A nucleotide	--	Upstream gene variant	1,3,9,12,13,15
SAOUHSC_01724	Hypothetical protein	1636250	Deletion of -T nucleotide		Upstream gene variant	1,3,9,12,13,15
SAOUHSC_02416	Hypothetical protein	2244931	Deletion of CT nucleotide		Upstream gene variant	1,3,9,12,13,15
SAOUHSC_02473	Hypothetical protein	2296653	Deletion of T nucleotide		Frameshift variant	1,3,9,12,13,15
SAOUHSC_02661	ScrA (PTS system sucrose-specific transporter subunit IIBC)	2446160	Deletion of C nucleotide	Asn7fs	Frameshift variant	1,3,9,12,13,15
SAOUHSC_02808	Gntk (gluconate kinase)	2592011	Deletion of A nucleotide	--	Upstream gene variant	1,3,9,12,13,15
SAOUHSC_03008	HisF (multifunctional imidazole glycerol phosphate synthase subunit/phosphoribosyl-AMP cyclohydrolase/phosphoribosyl-ATP pyrophosphatase)	2782815	Deletion of C nucleotide	Tyr249fs	Frameshift variant	1,3,9,12,13,15

4.3.2.1 Validation of *desK* and *desR* SNPs

The presence of SNPs in the *desK* and *desR* genes was confirmed by sequencing amplified PCR products spanning the alleles. Primers were designed to achieve a product size of 777 bp and 560 bp for *desk* and *desR* genes, respectively, and these primers were used to amplify these regions from 50 *S. aureus* evolved clones isolated from day 12 (SHG02 strain) and day 15 (SHG01 strain) (Fig 4.1). Subsequently, the purified PCR products were Sanger sequenced using the PCR amplification primers (DesR-FW and DesR-RV) (Chapter 2, Table 2.2). All sequences were compared to the original *desk* and *desR* genes found in the NCBI database (http://www.ncbi.nlm.gov), *S. aureus* reference Sequence: NC_007795.1 and the sequences were aligned with *S. aureus* WT. Pairwise sequence alignment was preformed using EMBOSS (European Molecular Biology Open Software Suite), Global Needle tool (https://www.ebi.ac.uk/Tools/psa/emboss_water/nucleotide.html) (Fig 4.2).

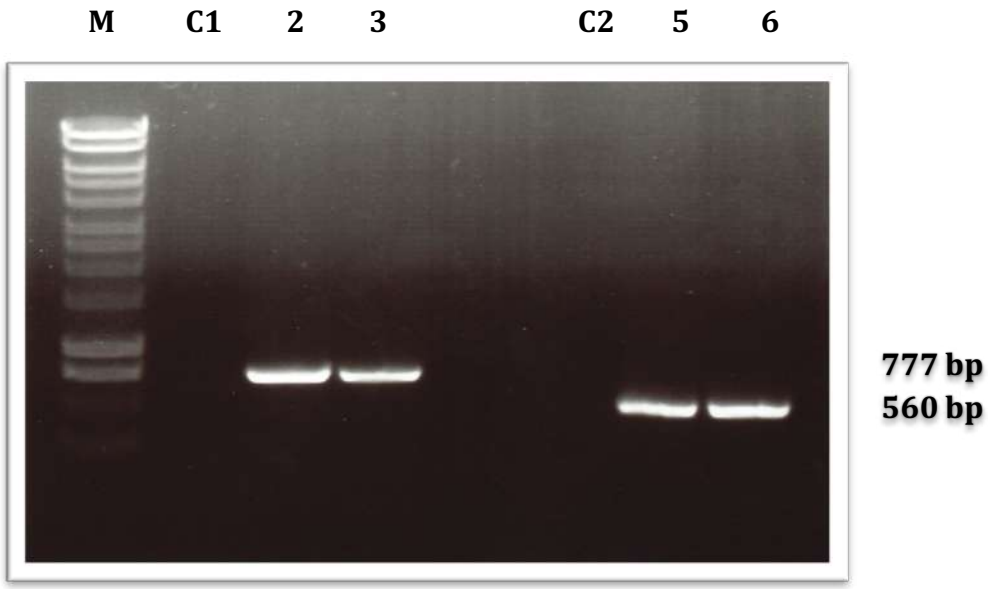

Figure 4.1 Electrophoresis gel image of products of PCR amplification for *desK* and *desR* locus. (C1) negative amplification control (*desK*) (1) *desK* gene of *S. aureus* SH1000 WT (2) *S. aureus* evolved clone with SNP in *desK* gene (SHG02) (C2) negative amplification control (*desR*) (5) *desR* gene of *S. aureus* SH1000 WT (6) *S. aureus* evolved clone with SNP in *desR* gene (SHG01) (M) is molecular size marker (Bioline).

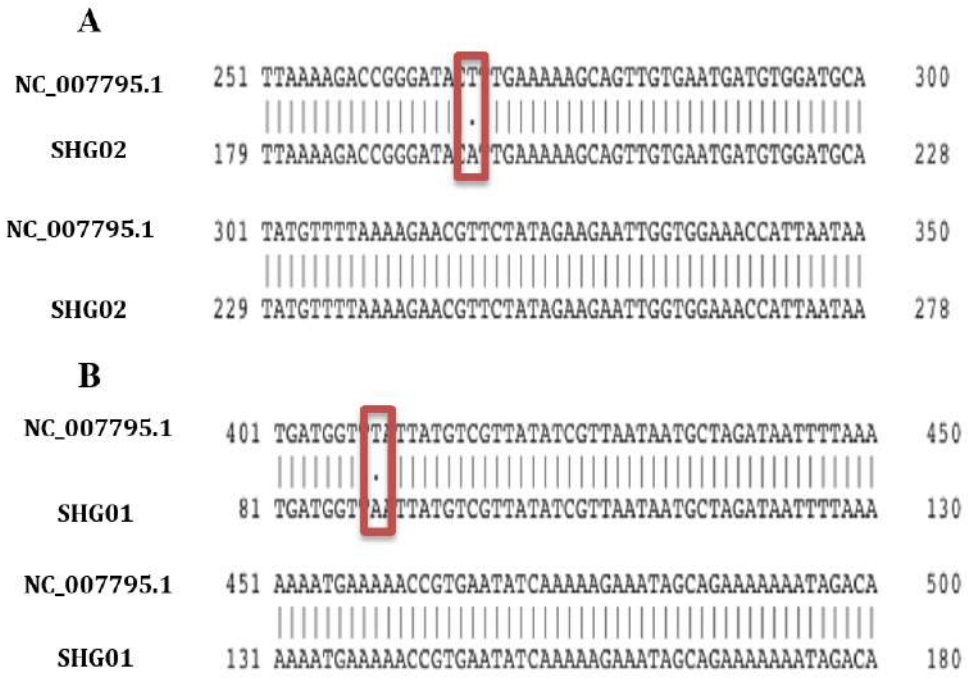

Figure 4.2 Pairwise sequence alignment of both *desk* and *desR* genes of *S. aureus* evolved clone SHG01 and SHG02 with reference sequences genes from *S. aureus* reference sequence: NC_007795.1 available in NCBI. (A) Shows SNP nucleotide change from T to A in *desK* gene of SHG02 strain (B) Shows SNP nucleotide change from T to A in *desR* gene of SHG01 strain. Alignment was performed using EMBOSS Needle alignment.

4.3.3 WGS and SNPs/INDELs analysis of *S. epidermidis* B155

4.3.3.1 *S. epidermidis* B155 genome sequencing using PacBio

PacBio sequencing was used to produce a high-quality assembly of *S. epidermidis* B155 to improve study of its genome. Final genome *de novo* assembly from the total reads was performed using the PacBio HGAP2 assembly pipeline with default filter parameters. Sequencing reads in the final polished assembly yielded 6 contigs generating a draft genome with a size of 2.6 Mb. The largest contig was 2,465,115 bp in length with coverage of 421.66X and it represents the bacterial chromosome (Table 4.4). A further 5 smaller contigs sequences were independent assemblies (Table 4.4). The small number of contigs generated for the B155 genome indicated a quality assembly. The smaller contigs were further examined to confirm whether they represented circular molecules or not. Each contig was considered to be a putative plasmid if there was the presence of a *rep* gene and by using Blastn of about 5000-15000 bp from the beginning of the contig to compare against the same contig. If this produced significant match with both the start and end, the contig was considered to be circular. Artemis Comparison Tool (ACT) was also used to confirm the repeated regions in both the start and the end of the sequences. Using these criteria, it was found that contigs 2 and 3 represented complete circlular plasmids. Contig 6 was considered circular since it had the same genes at beginning and the end of the sequence despite the repeated genes found (Fig. 4.3), while contigs 4 and 5 were found to be circular with little repeat overlapping sequences.

Table 4.4 Sequence length and read coverage for each contig generated from PacBio assembly of *S. epidermidis* B155.

Contig	Contig length	Coverage (X)
1	2,465,115	421.66
2	59,987	206.56
3	59,882	93.55
4	24,173	81.02
5	5,714	243.35
6	17,019	148.19

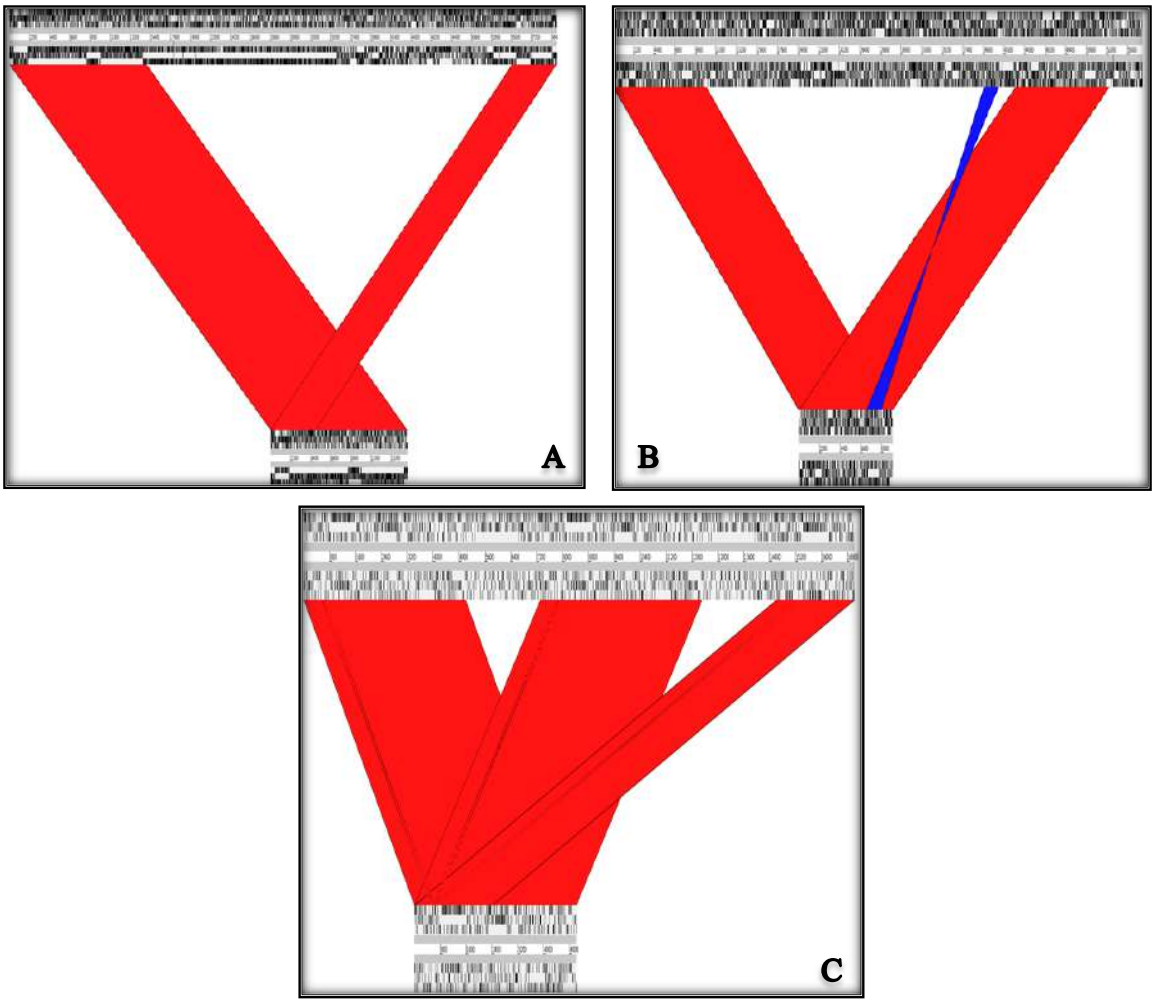

Figure 4.3 Confirmation of circularity for contigs resulting from PacBio assembly of *S. epidermidis* B155 strain. (A) Shows the first 10,000 bp of contig 2 against contig 2 itself. (B) Shows the first 10,000 bp from contig 3 against contig 3 itself (C) Shows the first 5000 bp from contig 6 against contig 6 itself indicating likely duplication. Results visualisation by using Artemis Comparison Tool (ACT).

4.3.3.2 Functional annotation of *S. epidermidis* B155 genome features

The assembly of *S. epidermidis* B155 genome was annotated using PROKKA software that generates gene annotations rapidly by predicting coding regions, translating those regions into amino acid sequences, and comparing these with databases of known proteins using BLASTp (Seemann, 2014). The draft *S. epidermidis* B155 genome is 2,631,766 bp in length with overall GC content of 31.98 %. It consists of 2,411 protein-coding genes CDSs that were predicted using Prodigal (7) 61 tRNA genes, 19 copies of rRNA and one transfer-messenger RNA (tmRNA) gene. The properties of the genome are summarised in (Table 4.5).

Table 4.5 The properties of *S. epidermidis* B155 genome

Species	*S. epidermidis*
Isolate ID	B155
Protein CDS	2411
tRNA	61
rRNA	19
tmRNA	1
GC%	31.98
Source	Nasal

4.3.3.3 Genetics polymorphisms in *S. epidermidis* B155 clones from competition

The SnpEff tool was used to construct a reference database for *S. epidermidis* B155 using .gff files created as PROKKA output. To identify whether SNPs or INDELS were found in *S. epidermidis* B155 after competition with *S. aureus,* Illumina DNA sequence reads from *S. epidermidis* clones were aligned with the constructed reference genome assembly described above. SNP analysis was then carried out by using the SNPs calling pipeline as described previously in the analysis of *S. aureus* SH1000 isolates (Chapter 2, section 2.10).

From the SnpEff analysis, there was a single non-synommous SNPs identified in a clone of *S. epidermidis* B155 isolated from day 13 consisting of a base change C

→ A resulting in change of amino acid from histidine to asparagine in Epi_01052 gene at the position 1073479 in the genome (Table 4.6). This gene was annotated by Prokka as a hypothetical protein though it shares 99% sequence similarity with the gene encoding EbhA protein *in S. epidermidis* ATCC 12228 strain, revealed by Blastn. EbhA is a cell surface extracellular matrix binding protein that in *S. aureus* has a role in osmotic stress tolerance (Kuroda *et al.*, 2008).

Table 4.6 Mutations selected in *S. epidermidis* B155 clones during competition with *S. aureus* SH1000. SNPs and INDELs from *S.epidermidis* B155 clones selected after competition experiment in planktonic culture from day 1, 3, 9, 12, 13, 15. All mutations classified as homozygous if > 80 % of reads had different bases compared with the reference genome.

Gene ID	Gene description	Genome position	Base Change	Codon change	SNP effect	Day of change
Epi_ 0105	EbhA	1073479	C → A	His2905Asn	Missense variant	13

4.3.3.4 Characteristics of *S. epidermidis* B155 plasmids

An important genetic feature found in *S. epidermidis* B155 genome was the presence of five putative plasmids within the genome. This was determined from their circularity and/or by finding genes encoding a replication protein. Open reading frames were identified and annotated using PROKKA. The coding genes were analysed further by extracting sequences and then using local alignment withBLASTp to smaller, manually curated database. This aided annotation since PROKKA curates genes as "hypothetical proteins" if the predicted gene cannot be matched with a reference within the large protein databases UniProt or Pfam (Seemann, 2014). Plasmid map visualisation for circle contigs was performed using SnapGene (SnapGene software (from GSL Biotech; available at http://www.snapgene.com).

Plasmid of contig 2 (pEPI155_2) was trimmed and sequence duplications were removed and then annotated again using PROKKA such that the full-length was 55.108 kb. Blastn identified that plasmid of contig 2 (pEPI155_2) shares 94%

identity over a very low coverage region (3%) with *S. epidermidis* PM221 plasmid 1 (Table 4.7A). Overall this reveals that this contig is largely absent from the genome database. Contig 2 consists of two genes that encode PKS (Epi_00004 and 00005) and two genes that encode NRPS (Epi_00002 and Epi_00007) based on PROKKA annotation that revealed these genes have low sequence similarity with known polyketide synthases (PKS)/non-ribosomal peptide synthases (NRPS). Both enzymes are involved in the synthesis of a wide range of structurally variable secondary metabolites, such as plipastatin, gramicidin and bacillaene. BlastP analysis supported the low level of sequence identity of those proteins to databse entries (Table 4.7A). The *fenF* gene (Epi_00006) is predicted to encode malonyl CoA-acyl carrier protein transacylase that is likely to be associated with polyketide/NRP modification. In addition, the presence of accessory proteins, such as thioesterase (Epi_000026), phosphopantetheinyl transferase (Epi_000027) and multidrug resistance ABC transporter ATP binding permease proteins in the same plasmid indicates the antimicrobial products are likely to be NRPS or PKS since those proteins are required for their synthesis and export/innate resistance. Multiple genes encoded hypothetical proteins of unknown function. Whether the presence of PKS or NRPS genes are associated with the production of antimicrobial in *S. epidermidis* B155 strain requires characterisation of the purified compounds produced by the proteins encoded at this locus in the *S. epidermidis* B155 strain. Further, experiments will need to be performed before a definitive function can be assigned. To our knowledge PKS production has not been reported in staphylococci and the plasmid would appear to encode a combination of PKS and NRPS activities that might be combined to synthesis a novel molecule. A map of plasmid contig2 (pEPI155_2) is shown in Fig. 4.4 with the major genes and selected restriction sites.

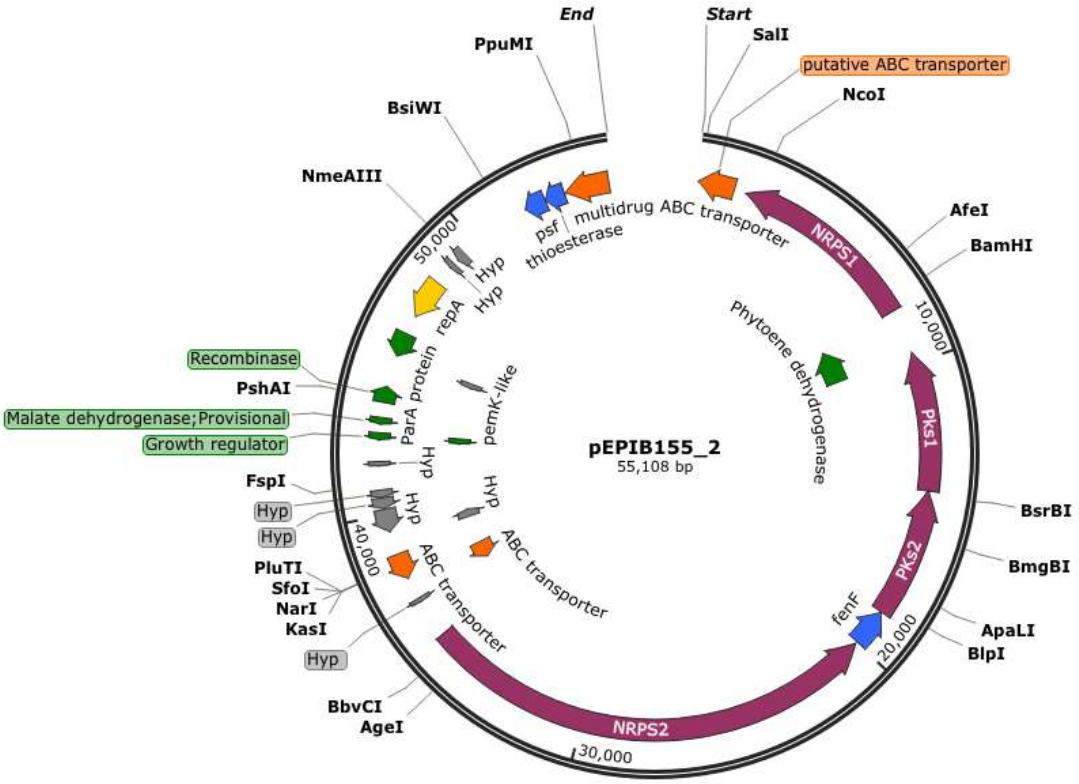

Figure 4.4 Plasmid map of pEPI155_2. The DNA sequence of contig 2 was annotated with ORFs using PROKKA and Blastp analysis. Gene products: **NRPS** non-ribosomal peptide synthetases, **PKS** Polyketide synthase, **FenF** Malonyl CoA-acyl carrier protein transacylase, **Hyp** hypothetical protein, protein, **RepA** Replication initiator protein A, **Psf-1** 4'-phosphopantetheinyl transferase**,** thioesterase, malate dehydrogenase; Provisional, growth regulator, ParA family protein, PemK-like family protein, ABC transporter ATP-binding protein and putative multidrug resistance ABC transporter ATP-binding/permease protein. Colours represent the putative functions of the genes: magenta, genes involved in PKS/NRPS synthases; blue, accessory genes associated with PKS/NRPS biosynthesis; grey, hypothetical proteins; orange, transport; yellow, replication; dark green, the remaining genes. Figure created using Snapgene (GSL Biotech).

Plasmid contig 3 (pEPI155_3) displayed 90% DNA sequence homology with *S. epidermidis* PM221 plasmid 1 with a query coverage 19% (Table 4.7B), making it largely unrepresented in the genome databases. This plasmid carries a variety of gene functions, including a toxin-antitoxin (TA) locus belonging to the YefM-YoeB family known to act as plasmid maintenance or stability modules. Normally a pair of toxin and antitoxin genes is encoded within a single operon (Kędzierska and Hayes, 2016). The *yefM-yoeB* operon organisation (Epi_02381 and Epi_02382) in pEPI155_3 is similar to other bacterial toxin-antitoxin system module (100% identity) in which the first gene encodes the antitoxin and overlaps the toxin gene. Transposases (Epi_02380) encoded by IS110/IS492 family elements are also found in this plasmid.

Plasmid contig 4 (pEPI155_4) shares greatest sequence identity with *S. epidermidis* strain ATCC 12228 plasmid pAMT2 (Table 4.7C). Genes associated with heavy metal ion resistance are encoded on pEPI155_4, including *czcD*, *copZ* and *copA*. CopA is a transmembrane ATPase responsible for transporting copper ions into and out of the cell (Lu and Solioz, 2001). CzcD protects the cell against the toxicity of cobalt, zinc, and cadmium (Nies, 1992) and has a role in regulation of the $CzcCB_2A$ efflux system expression (Anton *et al.*, 1999).

A β-lactamase *blaZ* gene and its regulator genes *blaR1* and *blaI* were identified on the pEPI155_4 plasmid. Their translation products are required for ampicillin resistance, which is mediated by the production of a penicillinase encoded by the *bla*Z gene, which inactivates penicillin by hydrolysis of the beta-lactam ring (Jensen and Lyon, 2009; Ferreira *et al.*, 2017). In addition, a copy of a gene encoding enoyl-acyl-carrier-protein reductase I (*fabI*) was also identified (100% identity). This protein is involved in the pathway of fatty acid biosynthesis, which is part of lipid metabolism. FabI catalyzes the last step in the essential bacterial fatty acid biosynthetic pathway and is the sole form of enoyl-acyl carrier protein (ACP) reductase present in *S. aureus*, *S. epidermidis*, and other staphylococci (Karlowsky *et al.*, 2009). Fig 4.5 presents the plasmid pEPI155_4 with the important genes mapped together with restriction sites.

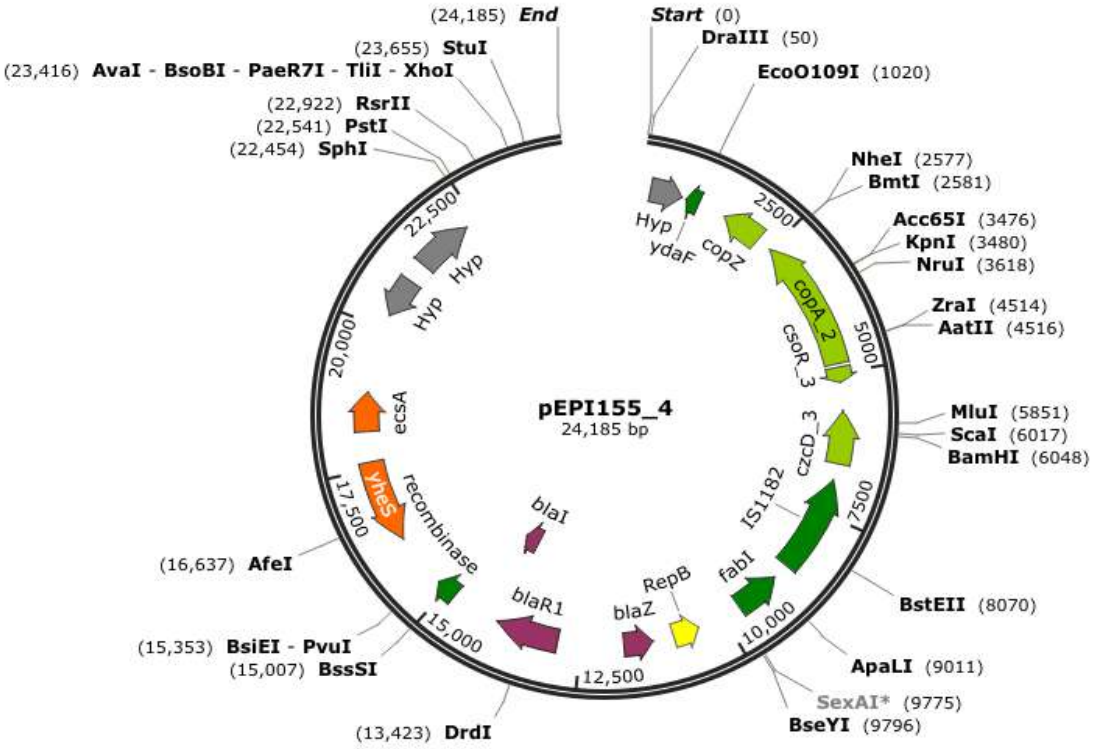

Figure 4.5 Plasmid map of pEPI155_4. The DNA sequence of contig 4 was annotated with ORFs from PROKKA and Blastp analysis. Gene products: **Hyp** hypothetical protein, **YdaF** putative ribosomal N-acetyltransferase, **CopZ** Copper chaperone CopZ, **CopA_2** Copper-exporting P-type ATPase A, **CsoR_3** Copper-exporting P-type ATPase A, **CzcD_3** Cadmium%2C cobalt and zinc/H(+)-K(+) antiporter, **IS1182** IS1182 family transposase, **FabI** Enoyl-[acyl-carrier-protein] reductase [NADPH], **RepB** Replication protein, **BlaZ** Beta-lactamase precursor, BlaR1 Regulatory protein, BlaI Regulatory protein, **YheS** Putative ABC transporter ATP-binding protein, recombinase, **EcsA** ABC-type transporter ATP-binding protein, **RepA** Replication initiator protein A. Colours represent the putative functions of the genes: magenta, genes involved in beta-lactam antibiotic resistance; light green, genes associated with heavy metal resistance; grey, hypothetical proteins; orange, transport; yellow, replication; dark green, the remaining genes. Figure created using Snapgene from GSL Biotech.

Plasmid contig 5 (pEPI155_5) is 98% identical to *S. epidermidis* ATCC 12228 plasmid pSE-12228-06 with query coverage 75% (Table 4.7D). pEPI155_5 is a small plasmid comprised of 5,714 bp and it contains mobilisation and replication regions. The final identified contig contains multiple duplication genes. Plasmid contig 6 (pEPI155_6) has homology with *S. epidermidis* PM221 plasmid 3 with 98% identity and 83% query coverage (Table 4.7E). The plasmid contains multiple copies of signal peptidase encoding genes *spsB_4* and *spsB_3* plus a pre_mob gene for plasmid recombination and mobilisation (Table 4.7E). Plasmid contigs 5 and 6 may represent one single plasmid that was misassembled since contig 5 is very small compare to others contigs.

Table 4.7A Genes present in pEPI155_2 that are homologous with *S. epidermidis* PM221 plasmid 1. Identity 94%, E-value 0, Query coverage 3%. Blast homolgy was preformed against the NCBI BLAST databases and the number in bracket indacte the the percent of identity.

Gene product	Coding sequence (Prokka)	Putative function or annotation	Coordinates	Protein size (bp)	Blast homology (%)
	Epi_00001	putative ABC transporter ATP-binding/permease	95-1309	404	ATP-binding cassette domain-containing protein (99.27%)
NRPS1	Epi_00002	Non-Ribosomal Peptide Synthesis	1738-8130	2130	Non-ribosomal peptide synthetase (37%)
	Epi_00003	phytoene desaturase	8142-9644	500	FAD-dependent oxidoreductase (100%)
PKs1	Epi_00004	Polyketide synthase	9637-14322	1561	Polyketide synthases (46%)
PKs2	Epi_00005	Polyketide synthase	14325-18683	1452	Polyketide synthases (38%)
FenF	Epi_00006	Malonyl CoA-acyl carrier protein transacylase	18717-19988	423	ACP S-malonyltransferase (46%)
NRPS2	Epi_00007	Non-Ribosomal Peptide Synthesis	20037-35558	5173	Non-ribosomal peptide synthetase (32.37%)
Hyp	Epi_00008	Hypothetical protein	36836-36994	52	Hypothetical protein (52.94%)
	Epi_00009	ABC-2 family transporter protein	36994-37743	249	ABC transporter permease (55.66%)
	Epi_00010	ABC transporter ATP-binding protein	37727-38599	290	ABC transporter ATP-binding protein (62.46%)
Hyp	Epi_00011	Hypothetical protein	39064-39408	114	ParA family protein (78.95%)
Hyp	Epi_00012	Hypothetical protein	39393-40166	257	Hypothetical protein (92.22%)
Hyp	Epi_00013	Hypothetical protein	40178-40561	127	Hypothetical protein (100%)

Gene product	Coding sequence (Prokka)	Putative function or annotation	Coordinates	Protein size (bp)	Blast homology (%)
Hyp	Epi_00014	Hypothetical protein	40563-40826	87	Hypothetical protein (98.85%)
Hyp	Epi_00015	Hypothetical protein	41622-41768	48	Hypothetical protein (86.05%)
	Epi_00016	PemK-like family protein	42153-42485	81	MazF anti-toxin (93.83%)
	Epi_00017	Growth regulator	42482-42727	228	Hypothetical protein (85%)
	Epi_00018	Malate dehydrogenase; Provisional	43010-43237	75	Malate dehydrogenase; Provisional (82.54%)
	Epi_00019	Putative site-specific recombinase	43742-44299	185	Recombinase family protein (98.90%)
Hyp	Epi_00020	Hypothetical protein	45161-45361	66	Plasmid replication-associated protein (93.48%)
	Epi_00021	ParA family protein	45361-46161	266	ParA family protein (93.61%)
repA	Epi_00022	Replication protein	46819-48177	452	Replication protein (69.64%)
Hyp	Epi_00023	Hypothetical protein	48810-49016	68	LPXTG cell wall anchor domain-containing protein (35%)
Hyp	Epi_00024	Hypothetical protein	49171-49476	101	Hypothetical protein (51.55%)
Psf-1	Epi_00025	4'-phosphopantetheinyl transferase	51992-52717	241	4'-phosphopantetheinyl transferase (36.48%)
	Epi_00026	Thioesterase subunit	52731-53417	228	Thioesterase (48.23%)
	Epi_00027	Multidrug ABC transporter ATPase	53439-54950	508	ABC transporter ATP-binding protein (36.21%)

Table 4.7B Annotation of pEPI155_3 homologous to *S. epidermidis* PM221 plasmid 1. DNA identity 90%, E-value 0, Query coverage 19%. Blast homolgy was preformed against the NCBI BLAST databases and the number in bracket indacte the the percent of identity.

Gene Product	Coding sequence (Prokka)	Putative function or annotation	Coordinates	Protein size (bp)	Blast homology (%)
Hyp	Epi_02371	Hypothetical protein	760-990	81	Hypothetical protein (100%)
Soj_2	Epi_02374	Sporulation initiation inhibitor protein	1672-2466	264	ParA family protein (100%)
	Epi_02380	Transposase IS116/IS110/IS902 family	7336-8409	358	IS110 family transposase (100%)
YefM	Epi_02381	Antitoxin YefM	8978-9232	84	Type II toxin-antitoxin system Phd/YefM family antitoxin (100%)
YoeB	EPi_02382	Toxin YoeB	9225-9491	89	Txe/YoeB family addiction module toxin (100%)
	Epi_02400	ABC-type transport system involved in multi-copper enzyme maturation, permease component	21457-22158	234	ABC transporter permease (90.99%)
TrpS2	Epi_02411	Tryptophan-tRNA ligase 2	28116-29123	337	Tryptophan--tRNA ligase (90.70%)
PGA_cap	Epi_02414	Bacterial capsule synthesis protein	32805-33179	124	Hypothetical protein (100%)

Gene Product	Coding sequence (Prokka)	Putative function or annotation	Coordinates	Protein size (bp)	Blast homology (%)
Bin3_1	Epi_02415	Putative transposon Tn552 DNA-invertase bin3	33926-34237	103	Resolvase-like protein (80.95%)
	Epi_02422	Plasmid recombination enzyme	41211-41450	433	Plasmid recombination enzyme type 3 (79.45%)
	Epi_02429	Hypothetical protein	46015-47019	335	Replication initiator protein A (100%)
YvdD_3	Epi_02430	LOG family protein yvdD	47338-47898	186	TIGR00730 family Rossman fold protein (100%)

Table 4.7C Annotation of pEPI155_4 homologous to S. *epidermidis* strain ATCC 12228 plasmid pAMT2. DNA identity 99%, E-value 0, Query coverage 82%. Blast homolgy was preformed against the NCBI BLAST databases and the number in bracket indacte the the percent of identity.

Gene Product	Coding sequence (Prokka)	Putative function or annotation	Coordinates	Protein size (bp)	Blast homology (%)
	Epi_02448	Hypothetical protein	184-732	182	Hypothetical protein (100%)
YdaF_2	Epi_02449	Putative ribosomal N-acetyltransferase	809-1336	77	N-acetyltransferase (99.43%)
CopZ	Epi_02451	Copper chaperone CopZ	2249-2458	70	Copper chaperone CopZ (98.55%)
CopA_2	Epi_02452	Copper-exporting P-type ATPase A	2492-4879	796	Copper-translocating P-type ATPase (99.75%)
CsoR_3	Epi_02453	Copper-sensitive operon repressor	4894-5169	92	Metal-sensing transcriptional repressor (98.90%)
CzcD_3	Epi_02455	Cadmium, cobalt and zinc/H(+)-K(+) antiporter	5660-6601	313	Cation transporter (100%)
	Epi_02456	IS1182 family transposase	6891- 8600	570	IS1182 family transposase (100%)
FabI	Epi_02457	Enoyl-[acyl-carrier-protein] reductase [NADPH]	8886- 9656	257	Enoyl-[acyl-carrier-protein] reductase FabI (100%)

Gene Product	Coding sequence (Prokka)	Putative function or annotation	Coordinates	Protein size (bp)	Blast homology (%)
RepB	Epi_02459	Replication protein	10459- 10962	148	Initiator RepB protein (99.40%)
BlaZ	Epi_02460	Beta-lactamase precursor	11271- 12116	164	Penicillin-hydrolyzing class A beta-lactamase BlaZ (99.29%)
BlaR1	Epi_02461	Regulatory protein	12223- 12702	427	Regulatory protein BlaR1 (100%)
BlaI	Epi_02463	Regulatory protein	13969- 14349	126	Penicillinase repressor BlaI (99.21%)
	Epi_02464	Recombinase	14613-15191	192	Recombinase family protein (98.96%)
YheS	Epi_02466	Putative ABC transporter ATP-binding protein	16154-17620	488	ABC-F type ribosomal protection protein Msr (A) (100%)
EcsA	Epi_02467	ABC-type transporter ATP-binding protein	18157-18852	231	ATP-binding cassette domain-containing protein (100%)
Hyp	Epi_02470	Hypothetical protein	21349-22302	333	Replication initiator protein A (100%)

Table 4.7D Annotation of pEPI155_5 homologous to *S. epidermidis* ATCC 12228 plasmid pSE-12228-06. DNA identity 98%, E-value-0, Query coverage 75%. Blast homolgy was preformed against the NCBI BLAST databases and the number in bracket indacte the the percent of identity.

Gene Product	Coding sequence (Prokka)	Putative function or annotation	Coordinates	Protein size (bp)	Blast homology (%)
Hyp	Epi_02472	Hypothetical protein	23-880	285	RepB family plasmid replication initiator (100%)
Hyp	Epi_02473	Hypothetical protein	1507- 1701	85	Hypothetical protein (98.44%)
	Epi_02474	ABC-2 type transporter	1797- 2597	266	Teichoic acid ABC transporter permease (100%)
MobC	Epi_02475	Bacterial mobilisation protein	2932- 3312	126	Plasmid mobilization relaxosome protein MobC (98.41%)
	Epi_02477	Relaxase/Mobilisation nuclease domain protein	3472- 4482	338	Relaxase/mobilization nuclease domain protein (88.39%)
Hyp	Epi_02478	Hypothetical protein	5079- 5258	296	Hypothetical protein (98.31%)

Table 4.7E Annotation of pEPI155_6 homologous to *S. epidermidis* PM221 plasmid 3. DNA identity 98%, E-value-0, Query coverage 83%. Blast homolgy was preformed against the NCBI BLAST databases and the number in bracket indacte the the percent of identity.

Gene product	Coding sequence (Prokka)	Putative function or annotation	Coordinates	Protein size (bp)	Blast homology (%)
Rep	Epi_02480	Replication protein	767- 1633	288	RepB family plasmid replication initiator protein (99.65%)
SpsB_4	Epi_02481	Signal peptidase IB	2301- 2867	188	Signal peptidase (98.84%)
IsaB_3	Epi_02482	Immunodominant staphylococcal antigen B precursor	3535- 4020	171	Hypothetical protein (98.76%)
Hyp	Epi_02483	Hypothetical protein	4568- 4987	139	Hypothetical protein (98.56%)
Mob_pre	Epi_02484	Plasmid recombination enzyme	5442- 6650	426	Recombination (98.76%)
SpsB_5	Epi_02487	Signal peptidase IB	9606-10172	188	Signal peptidase (98.40%)
IsaB_4	Epi_02488	Immunodominant staphylococcal antigen B precursor	10840-11325	171	Hypothetical protein (98.76%)
Hyp	Epi_02489	Hypothetical protein	11873-12292	139	Hypothetical protein (98.56%)

4.3.4 Screening for species that inhibit *S. aureus* SH1000 but not the evolved strain SHG01.

Over 200 different species/isolates, including Coagulase-negative staphylococci (CoNS), *Bacillus* strains from previous skin and nasal culture experiments (Table 2.1, chapter 2) and *S. epidermidis* strains (Appendix Table A1) were tested for antimicrobial activity towards *S. aureus* SH1000. Species were tested against *S. aureus* parental wild-type and evolved strain SHG01 using deferred inhibition assays and agar overlay assays to find species with a similar effect as *S. epidermidis* B155 against *S. aureus,* i.e. inhibit *S. aureus* wild-type but unable to inhibit evolved *S. aureus desR* evolved (SHG01) strain. After screening, *S. aureus* SHG01 displayed a resistance phenotype when tested with a single isolate of a *Bacillus* species that inhibited SH1000, indicating that this may have a similar inhibition activity as *S. epidermidis* B155 Fig 4.6. Sequencing of 16S rDNA identified the species as *Bacillus flexus,* which appears poorly studied relative to the many species screened for antimicrobial activity. *S. aureus* SH1000 was growth inhibited by the *B. flexus* B003 revealing a small, reproducible inhibition zone of 2.50 ± 0.5 mm, n=6. The *S. aureus* evolved SHG01 strain showed no inhibition zone, which represents a significant difference between the two strains (t.test, $P < 0.05$) Fig 4.7.

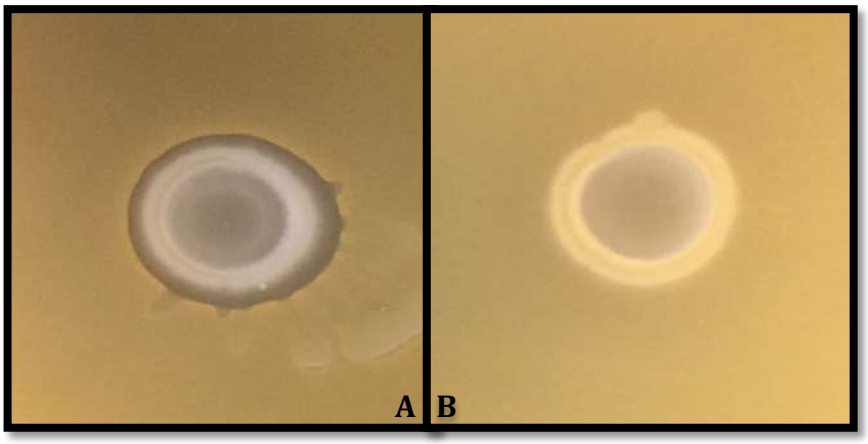

Figure 4.6 *S. aureus* SHG01 evolved strain displayed resistance to antimicrobial produced by *Bacillus flexus* B003 compared with WT. Agar overlay assay was performed by spotting overnight *Bacillus flexus* B003 culture onto the middle of the plates, which were incubated at 37°C for 18 h. A dilution (~0.1) of overnight culture of evolved and WT *S. aureus* strains were spray overlaid onto plates. The plates were re-incubated at 37°C for 24 h. (A) *S. aureus* WT and (B) *S. aureus* evolved (SHG01) with *B. flexus* B003.

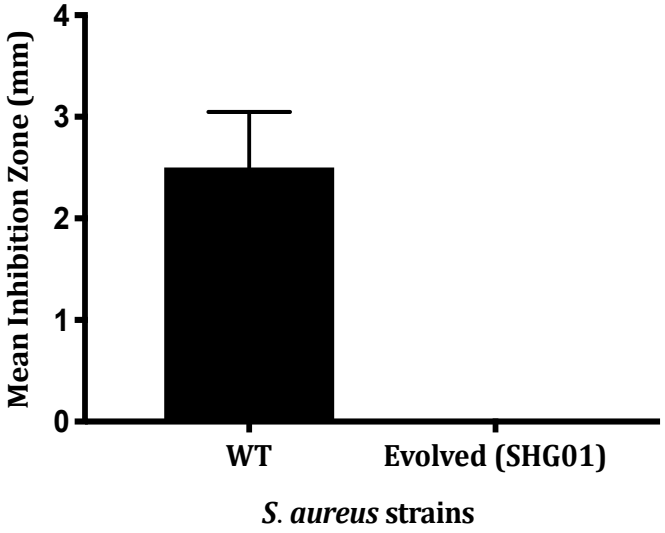

Figure 4.7 Quantitative growth inhibition of *S. aureus* SH1000 WT and evolved *desR* strain (SHG01) by *Bacillus flexus* B003. Inhibition zone (mm) shown for the sensitive *S. aureus* SH1000 WT (black bar) and resistance-evolved *S. aureus* SHG01 against *B. flexus* (B003). The data are the mean ± standard deviation calculated from 6 biological replicates.

4.3.5 *Bacillus flexus* B003 WGS using PacBio and genome annotation

The PacBio RS II platform was used for whole genome sequencing of the *Bacillus flexus* B003 strain to seek the basis for the inhibitory phenotype towards *S. aureus* SH1000, similar to the phenotype of *S. epidermidis* B155. For sequencing, 1 SMRT cell was used, achieving average 115.27x sequencing coverage. Following use of the HGAP3 assembly pipeline it was determined that the bacterial genome has 4.3 Mb in length and consists of 3 contigs including the circular chromosome with size around 4.1 Mb and two large plasmids of 127 kb and 46 kb (Table 4.8).

Table 4.8 Summary of *Bacillus flexus* B003 genome assembly statistics using HGAP3 comprising 3 contigs.

Sequence platform	PacBio
Assembler	HGAP3
No. of contigs	3
Total length	4273992
GC (%)	37.98
N50	4,100,230
L50	1
Coverage (X)	115.27
Largest contig	4,100,230

The genome was then annotated using the PROKKA tool. The general features of the annotated genome that were observed are presented in (Table 4.9). The complete genome of *Bacillus flexus* B003 was obtained as individual chromosomal and extrachromosomal contigs, which consist of 4362 coding sequences (CDS), 36 rRNA, 98 tRNA and one tmRNA with the average G+C content of 38 %.

Table 4.9 The sequence properties of the *Bacillus flexus* B003 genome obtained by Prokka annotation.

Species	*B. flexus*
Isolate ID	B003
Protein CDS	4362
tRNA	98
rRNA	36
tmRNA	1
GC%	38 %
Source	Skin

4.3.6 Prediction of secondary metabolite biosynthetic gene clusters

Secondary metabolite biosynthetic gene clusters (BGCs) found in both the *S. epidermidis* B155 and *B. flexus* B003 genomes were predicted by using AntiSMASH 4.0.2. The output annotation identified 3 candidate gene clusters related to secondary metabolite production in *S. epidermidis* B155 (Table 4.10). Cluster 1 includes siderophore biosynthesis activity, which showed 100% similarity with the genes responsible for producing the natural product staphyloferrin in *S. aureus*. *S. aureus* synthesises two siderophores, staphyloferrin A (SA) and staphyloferrin B (SB), and both are secreted into the extracellular milieu. Notably, while commonly produced by *S. epidermidis,* there were no lantibiotic genes predicted in the *S. epidermidis* B155 genome.

Cluster 2 was identified to comprise a NRPS with sequence size of 47,163 bp. The domain organisation of this cluster consisted of: module 1 (A PCP C A PCP NAD) and module 2 (ACPs). No similar clusters were found in the MIBiG database based on the prediction of antiSMASH. Alternatively, searching the core biosynthetic genes using BlastP revealed that it was 100% similar to putative linear gramicidin synthetase LgrC. Because NRPS clusters terminate with a TE domain this domain pattern probably is not complete. Of particular interest to the study, cluster 3 present in contig 2 is notable because it is predicted to comprise a Non-

Ribosomal Peptide Synthetase (NRPS) and trans-Acyl Transferase Polyketide Synthetase (NRPS-TransATPKS) gene cluster. Remarkably, this cluster shared around 75% to 81% sequence similarity to gene clusters found in *Streptococcus mutans* strains (Fig 4.8). Based on the MIBiG database it showed a very low similarity to macrolactin, surfactin, bacillaene, plipastatins (fengycins), bacitracin and iturins (bacillomycins).

Within the NRPS-TransATPKS cluster, 6 genes encode NRPS/PKs core structure genes, 4 transporter genes, a dehydrogenase, and another gene could encode for a transcriptional regulator. The functional activity domains found to define the structure of NRPS-TransATPKS were the following: (KS PCP C A A PCP C) (KS DH KR PCP) (KS DH KR PCP) (AT) (A C PCP E C A PCP C A PCP E C A PCP) (ACPs) and (TE) (Fig. 4.9 with legend description of functions).

Table 4.10 AntiSMASH 4.0 annotation of secondary metabolite gene clusters. AntiSMASH uses profile hidden Markov models (profile HMM) for identification. These models turn multiple sequence alignments into a position-specific scoring system that can be used to search databases for remotely homologous sequences. The clusters are colour coded based on prediction of secondary metabolite type.

Cluster	Type	Position	Metabolites (MIbiG similarity)	Contig
Cluster 1	Siderophore	411084-426076	Staphyloferrin (100%)	1
Cluster 2	NRPS	2306195 - 2353358	--	1
Cluster 3	Transatpks-Nrps	1- 59998	--	2

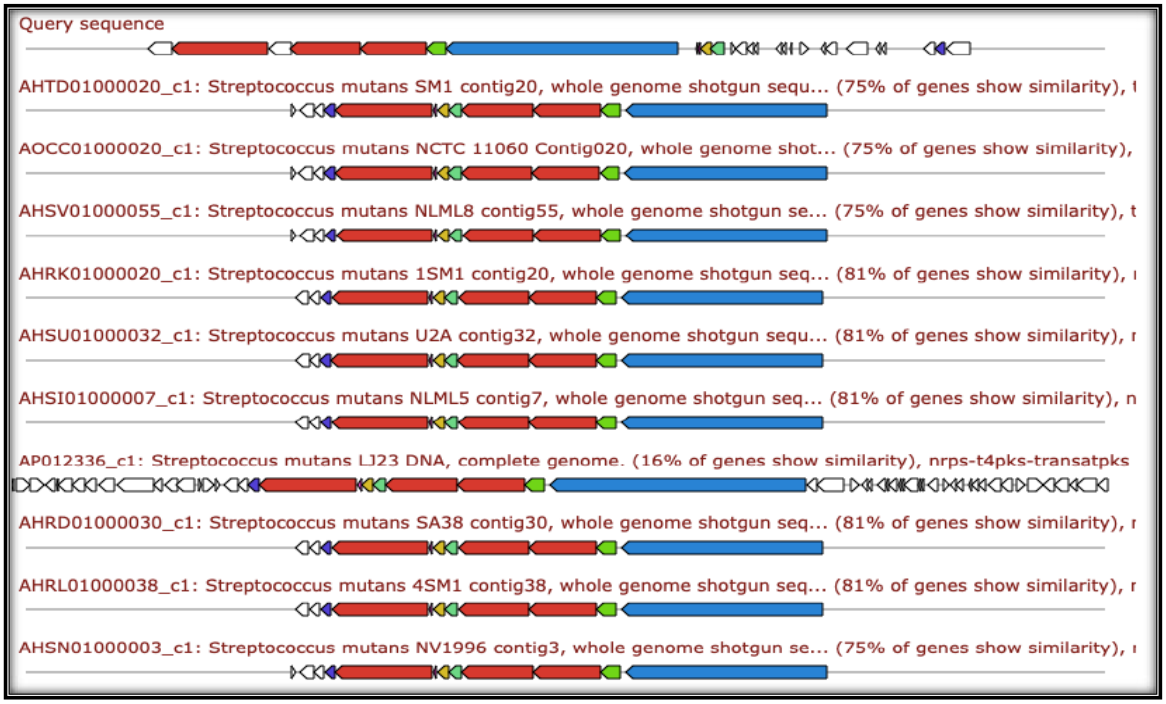

Figure 4.8 Alignment of the biosynthetic gene cluster of the *S. epidermidis* B155 NRPS-TransATPKS to clusters present in the genome sequences of *Streptococcus mutans* strains using AntiSMASH 4.0.

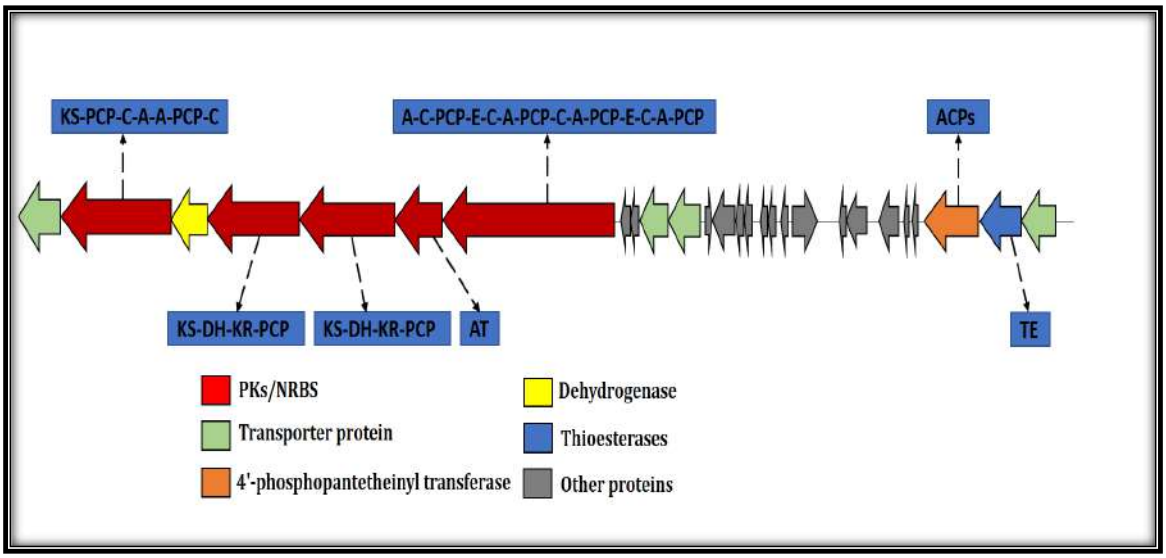

Figure 4.9 The activity domain pattern identified in cluster 3 of a Transaptks-NRPS found in *S. epidermidis* B155 genome contig2. A adenylation; C condensation; E epimerisation; PCP peptidyl carrier protein; AT acyltransferase; KR ketoreductase; KS ketosynthase; TE thioesterase; ACPs 4'-Phosphopantetheinyl transferases. Transporters, other proteins and functional enzymes are indicated by arrows of different colours.

The *B. flexus* B003 genome was similarly annotated by antiSMASH and the analysis of gene clusters revealed that the genome encodes 5 relevant gene clusters and all of these are located on contig 1, the main chromosome. The clusters include: one PKS (type III), one siderophore and two terpenes (Table 4.11). Of these, cluster 1 contains genes encoding linear azol(in)e-containing peptides (LAP) that has 91 % similarity with plantazolicin/plantathiazolicin biosynthesis pathway (Table 4.11). Plantazolicin is a ribosomally synthesised and post-translationally modified peptide (RiPP) natural product (Molohon *et al.*, 2016). This gene cluster is closely related to the *B. amyloliquefaciens* (100 % similarity) which is known to produce plantazolicin (Dunlap *et al.*, 2015) and also shares a low cluster similarity (25 %-31 %) with those found in others Bacilus species including *B. badius*, *B. pumilus* and *B. subtilis* (Fig. 4.10).

Cluster 3 contains genes encoding PKSs (type III), which are of interest. This is an unknown gene cluster but it is homologous with clusters of *Bacillus megaterium* (68 % of genes show similarity) and to several *Bacillus spp*. (65% of genes show similarity) (Fig. 4.11). Both clusters 2 and 4 encode terpene synthase. Cluster 2 shares 31% homology with *Streptomyces coelicolor* genes for biosynthesis of the terpene natural product, hopene. Cluster 5 contains genes that encode siderophore that shares 37% similarity with the genes encoding acinetoferrin synthesis of *Acinetobacter haemolyticus* (Table 4.11). Overall, the presence of these gene clusters shows that the *B. flexus* B003 strain has the potential to biosynthesise several natural products and of relevance encodes capacity for polyketide biosynthesis.

Table 4.11: AntiSMASH 4.0 annotation of secondary metabolite gene clusters. AntiSMASH uses profile hidden Markov models (profile HMM) for identification. These models turn multiple sequence alignment into a position-specific scoring system that can be used to search databases for remotely homologous sequences. The clusters are colour coded based on prediction of secondary metabolite type

Cluster	Type	Location	Metabolites (MIbiG similarity)	Contig
Cluster 1	LAP	694911- 717 095	Plantazolicin (91%)	1
Cluster 2	Terpene	756183- 778039	Hopene (31%)	1
Cluster 3	T3pks	999798- 1040886	--	1
Cluster 4	Terpene	1713873- 1734589	--	1
Cluster 5	Siderophore	3871244- 3887224	Acinetoferrin (37%)	1

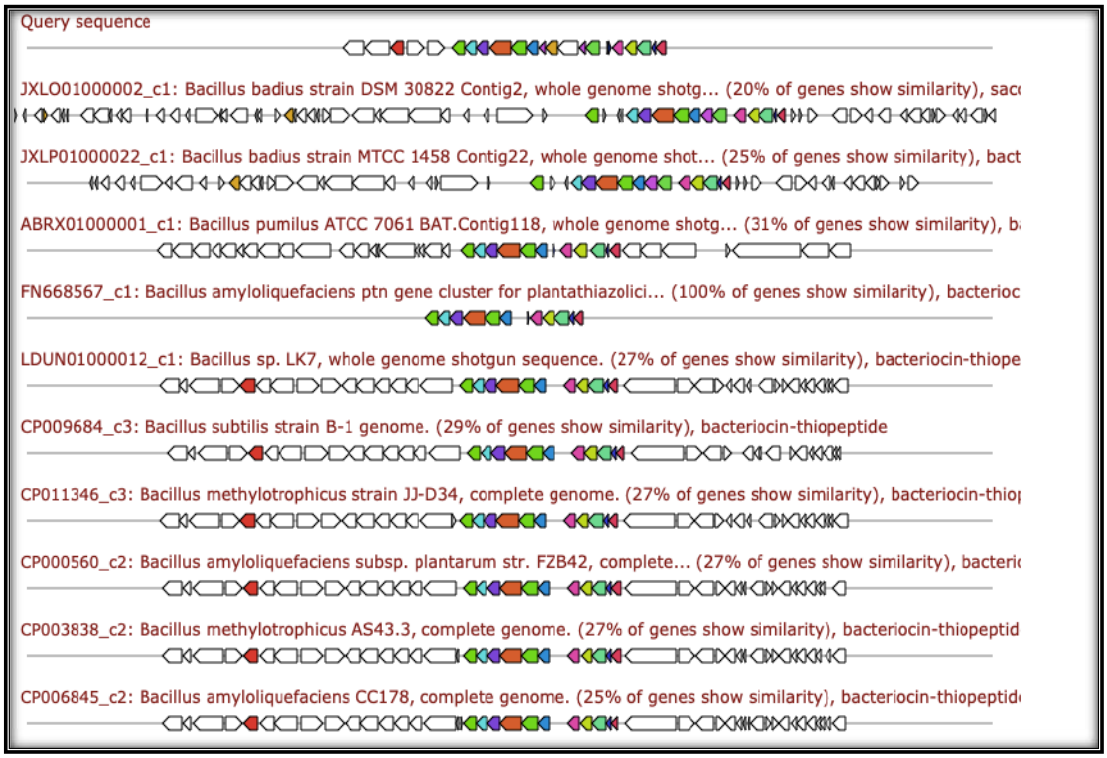

Figure 4.10 Alignment of biosynthetic gene clusters of linear azol(in)e-containing peptides to clusters present in the genome sequence of different *Bacillus species*: *B. badius, B. pumilus, B. amyloliquefaciens, B. subtilis* and *Bacillus* Spp. using AntiSMASH 4.0.

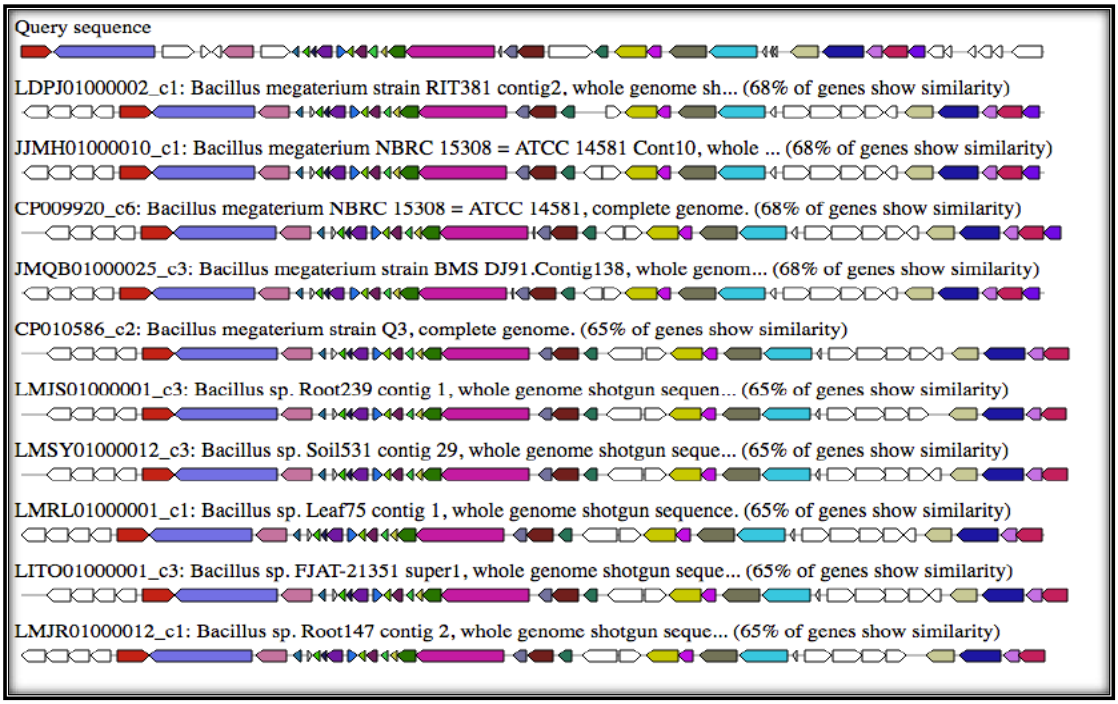

Figure 4.11 Alignment of biosynthetic gene clusters of unknown polyketide type III to clusters present in the genome sequence of *Bacillus megaterium* and *Bacillus* Spp. using AntiSMASH 4.0.

4.4 Discussion

In the previous chapter, it was found that *S. aureus* evolved resistance under selective pressure from the bioactive agent secreted by *S. epidermidis* B155. The data revealed that *S. aureus* potentially used novel and multiple genetic mechanisms to compete with *S. epidermidis*. In this chapter, the *S. aureus* genetic determinants that enabled the resistance were interrogated. In addition, the genes encoding the antimicrobial property of *S. epidermidis* B155 were investigated.

4.4.1 Genome sequencing of evolved *S. aureus* highlighted mutation of the DesKR homologous TCS system

Whole genome sequencing was performed to interrogate the fixed genetic changes in the genomes of clones selected from different days of the competition experiment. SNPs and INDELs were predicted and those found in both control WT SH1000 strains and selected clones were discarded. Somewhat unexpectedly, annotation identified the presence of SNPs in SAOUHSC_01313 (*desK)* and SAOUHSC_01314 (*desR*) genes in evolved *S. aureus.* The SAOUHSC_01313 (*desK*) gene encodes a putative sensor kinase proposed to form part of a two component system (TCS) with the histidine kinase encoded by SAOUHSC_01314 (*desR*). This TCS demonstrates homology with *B. subtilis* DesKR (Kim *et al.*, 2016). DesKR of *B. subtilis* is a regulator that controls the expression of a fatty acid desaturase (*des*) gene at low temperatures that modifies membrane lipid saturation to adjust membrane fluidity (Aguilar *et al.,* 2001). In *B. subtilis*, *des* expression is also indirectly repressed by WalKR, an essential TCS regulator of cell wall integrity (Utsumi, 2008).

From these data it was proposed that the SNPs identified in this TCS contributed to *S. aureus* resistance because these SNPs were present in *S. aureus* evolved strains isolated from day 12, day 13 and day 15 compared with the parent WT and a SH1000 isolate from the first day of competition. These SNPs in the TCS genes may be associated with membrane function and are not linked to those known loci for cell surface antimicrobial peptide resistance BraRS, GraRS (Meehl *et al.*, 2007), AgrCA and VraRS (Howden *et al.*, 2010). The finding here implicates

an additional TCS in antimicrobial resistance, which was not expected from the large amount of *S. aureus* data associated with resistance and the multiple TCS already characterised. There is potential precedent for an association with membrane fluidity regulation and antimicrobial resistance. In *S. aureus*, resistance to pediocin produced by *Pediococcus pentosaceus* was reported to be associated with increased membrane fluidity that inhibits the lantibiotic oligomerisation, preventing pore formation (Lather *et al.*, 2015). The genetic basis for this resistance has not been determined. Resistance to aureocin A70 was reported to potentially associated with changes in cell membrane lipid composition and cell wall thickness (Ceotto *et al.*, 2009). In *L. monocytogenes* resistance to class II bacteriocins is linked to modified cell membrane fluidity and cell surface charge (Ceotto *et al.*, 2009). The *S. aureus* DesKR gene operon comprises four genes, with two putative antimicrobial export membrane proteins SAOUHSC_01311 and SAOUHSC_01312. Furthermore upstream of the desKR operon there is cardiolipin synthetase gene *cls1* (SAOUHSC_01310) and this is positionally associated with the TCS operon. In one previous study, it was reported that cardiolipin (CL) was associated with resistance to antibiotics (Zhang *et al.*, 2014). This result demands further experiments to identify the antimicrobial, and confirm the results with genetic linkage studies in *S. aureus*. In the next chapter, it will be examined whether the expression of the operon-encoded transporters is linked with the resistance phenotype. These outcomes also require further experiments to identify the antimicrobial and its potential to induce expression of the TCS operon making it a direct environmental sensor.

A further association was identified that may link resistance of *S. aureus* to the *S. epidermidis* B155 antimicrobial with potential changes in cell membrane lipids composition. A SNP was found upstream of the essential *fabI* gene of *S. aureus* SHG01, which encodes enoyl-acyl carrier protein (ACP) reductase integral to fatty acid biosynthesis (Grandgirard *et al.*, 2015). Inhibition of the biosynthetic pathway of type II fatty acid that is responsible for *de novo* production of phospholipid precursor molecules is a therapeutic strategy that targets the bacterial cell envelope (Payne *et al.*, 2002). The pathway of fatty acid synthesis in

plants, bacteria and protozoa consists of individual monofunctional enzymes allowing for their selective inhibition (Payne *et al.*, 2001). In this pathway, the fatty acid chain, which is attached to the acyl carrier protein (ACP), is elongated by two carbon atoms per cycle. The final reduction is catalysed by the NAD (P) H-dependent trans-2-enoyl-ACP reductase (FabI), which is known to play a key regulatory role in this pathway (Heath and Rock, 1995; Xu *et al.*, 2008). This enzyme is highly conserved across several pathogenic bacteria but *S. aureus* enoyl-ACP reductase is the only known FabI with a clear preference for NADPH (Heath *et al.*, 2000; Priyadarshi *et al.*, 2010). In *E. coli* and *S. aureus* this enzyme was identified as an antimicrobial target (Payne *et al.*, 2002). Of note, the antimicrobial producing *S. epidermidis* 155 has an additional plasmid-encoded copy of *fabI* (section 4.2). How this relates to production and self-resistance is unclear. Reports revealed that in *S. aureus,* increased expression of *fabI* due to upstream polymorphisms and point mutations in the gene confer resistance to triclosan and diazoborine, indicating that *fabI* is the cellular target for these antimicrobials (Grandgirard *et al.*, 2015). Recently, AFN-1252 was reported as a novel inhibitor of the fatty acid biosynthesis pathway, specifically inhibiting the essential staphylococcal FabI enoyl-ACP reductase (Hafkin *et al.*, 2015), supported by the presence of missense mutation in *fabI* of *S. aureus* leading to resistance to AFN-1252 (Yao *et al.*, 2013).

Because the identified *S. aureus* genes associated with resistance to *S. epidermidis* B155 antimicrobial are not those known TCS mechanisms (i.e. GraSR, BraSR, VraSR, WalKR) we predicted that the antimicrobial produced by *S. epidermidis* B155 is unique among the antimicrobials secreted by staphylococci, particulary *S. epidermidis* that are known to secrete epidermin, pep5 epilancin K7 and epicidin 280 (Sahl and Bierbaum, 1998).

4.4.2 Genome sequencing of *S. epidermidis* B155

Whole genome sequencing of *S. epidermidis* B155 was completed using PacBio to improve its assembly and help to find the genomic basis for the antimicrobial activity of this strain toward *S. aureus*. A SMART single, large-insert template library to generate coverage of 80-100x was used followed by HGAP2 analysis,

which was developed by Chin *et al.,* 2013 who concluded that assembling a complete genome using only long SMRT sequencing reads achieves comparable or even higher performance compared with other sequencing platforms (99.999% accuracy in three organisms with known reference sequences), including 11 corrections to the Sanger reference of studied genomes (Chin *et al.*, 2013). Koren *et al.* (2012) reported that genome assembly into a single contig per chromosome for most microbial genomes could be achieved using this platform (Koren *et al.*, 2012). Here the analysis of *S. epidermidis* B155 generated excellent *de novo* assembly for the genome with size 2.6 Mb into six contigs, the largest representing the bacterial chromosome 2,465,115 bp and plasmids of 59,987 bp (pEPI155_2), 59,882 bp (pEPI155_3), 24,173 bp (pEPI155_4), 5,714 bp (pEPI155_5), and 17,019 bp (pEPI155_6). The long-read complete sequence method using PacBio was performed previously for the *S. epidermidis* ATCC 12228 genome (MacLea and Trachtenberg, 2017). Assembly of its genome identified five plasmids and a slightly smaller chromosome was obtained compared with the assembly of *S. epidermidis* ATCC 12228 using Illumina (Zhang *et al.*, 2003). The high quality of genome sequence of *S. epidermidis* strains including ATCC 12228 and B155 will provide better understanding of the capacity of some *S. epidermidis* strains to cause diseases in humans and animals or to adapt as commensal bacteria.

4.4.3 Only single SNP found in *S. epidermidis* B155 clones resulting from competition with *S. aureus*

The genome of *S. epidermidis* B155 was annotated using PROKKA and then a reference genome was generated using the SnpEff tool. SNPs in the *S. epidermidis* B155 clones chosen from different days of selection were then compared with the reference genome and SNPs were predicted as described above for *S. aureus*. Only a single SNP was detected in a clone isolated from day 13 of competition. The SNP is in a gene encoding Epi_01052 hypothetical protein that shares 99% sequence similarity with the extracellular matrix protein (EbhA) gene of *S. epidermidis* ATCC 12228 strain, revealed by Blastn. It was uncertain if the change in the *S. epidermidis* B155 genome was a result of competition, however this finding of a near absence of sequence changes supported the unchanged

phenotype of *S. epidermidis* B155 clones selected from different days and tested against *S. aureus* WT using inhibition assays.

4.4.4 *S. epidermidis* B155 plasmids identification

In bacteria, plasmids contribute majorly to horizontal gene transfer and notably with antibiotic resistance genes that are widespread in *Firmicutes* (Shintani *et al.*, 2015). Within staphylococci the most described plasmids have been found in *S. aureus* (European Nucleotide Archive 2016). The most studied CoNS is *S. epidermidis* regarding its pathogenicity and until now, 21 plasmids have been identified (Argemi *et al.*, 2017). The second most studied CoNS in terms of known plasmids after *S. epidermidis* are *S. simulans* and *S. haemolyticus* with 5 identified plasmids. Regarding *S. epidermidis*, the transmission of MGE from *S. epidermidis* to *S. aureus* has been frequently described, however, no genetic material has been reported to be transferred from *S. aureus* to CoNS (Otto, 2009). Here, we identified 5 plasmids in *S. epidermdis* B155. Importantly for the study, plasmid pEPI155_2 represents the largest extrachromosomal elements in *S. epidermidis* B155 sequence and it carries a ~45.5-kb locus encoding proteins showing similarity to non-ribosomal peptide synthases (NRPS)/polyketide synthases (PKS) genes. This family of proteins are involved in biosynthesis of several structurally variable secondary metabolites including toxins (e.g. the *Pseudomonas syringae* phytotoxin syringomycin), antibiotics (e.g. penicillin and vancomycin) and siderophores (e.g. pyoverdine and yersiniabactin) (De Maayer *et al.*, 2012). However, because of the low sequence similarity to known PKS/NRPS proteins, the compounds produced by this locus in the *S. epidermidis* B155 strains needs further characterisation before a definitive function can be assigned. The newly sequenced plasmid suggests that there is a more extensive repertoire of plasmids with unique genes in staphylococci.

Plasmid pEPI155_3 is predicted to encode toxin-antitoxin TA stabilisation systems, comprising a putative toxin recognising a specific cellular target and a putative antitoxin, counteracting its toxic effect. The persistence of these systems in genomes is proposed in many models where they may have a contribution to genome and plasmid stability and may work as anti-addiction modules by

preventing post-segregational killing (Van Melderen and De Bast, 2009; Van Melderen, 2010). Five types of TA systems were classified based on the antitoxin nature and the mode of action (Schuster & Bertram, 2013). This work suggested that beside the role of TA systems in plasmid and mobile genetic element stabilisation, they can contribute to growth control, phage defence, protective responses to adverse conditions, programmed cell death or cell arrest and formation of drug-tolerant persister cells (Nolle *et al.*, 2013). The MazEF TA system was found to control processes beyond pathogenicity in *S. aureus* (Zhu *et al.*, 2009). The antitoxin identified in plasmid pEPI155_3 shows considerable similarity with the type II toxin-antitoxin system YefM family and the toxin is similar to YoeB toxin. The TA system YefM/YoeB is located in the chromosome or in some plasmids of many bacteria such as *E. coli* (Nieto *et al.,* 2007). In *S. aureus,* two YoeB homologues of the *E. coli* yefM-yoeB TA system were identified with translation initiation inhibitor function. This system contributes to the transition to persister cell formation in the bacterial biofilms. Constructed mutant strains that lack TA systems like YoeB/YefM, MazF/MazE and RelE/RelB show less biofilm formation in *E. coli* (Kim *et al.*, 2009).

β-lactamase *blaZ* and its transcriptional regulators *blaR* and *blaI* were identified on the plasmid pEPI155_4. Their translation products are very well-characterised and are normally required for β-lactam antibiotic resistance e.g. penicillin (Tasara *et al.*, 2013). The plasmid pEPI155_4 also carries a locus that can confer resistance to heavy metals. While divalent catons such as zinc, nickel and iron are required for bacterial growth and its replication, (Sabala *et al.*, 2014) heavy metal ions are often added as supplements to feed stocks to prevent gastrointestinal diseases in livestock as a result resistance to heavy metal is common among livestock-associated bacterial strains (Cavaco *et al.*, 2010). Resistance mechanisms to several toxic heavy metals have evolved within many located to either plasmids or chromosome. Cobalt, zinc and cadmium (Czc system) was found on the *S. aureus* chromosome (Poston and Hee, 1991; Kuroda *et al.*, 1999). A putative permease and a cobalt/zinc/cadmium exporter (*czcD*) gene is encoded on pEPI155_4 similar to the previous resistance cadmium/zinc^{+2} mechanisms encoded on pi258 plasmid of *S. aureus* (Ye *et al.*, 2005). A *czrC* gene

encoding resistance to zinc and cadmium in *S. aureus* was found genetically located within the type V SCC*mec* elements widespread among CC398 MRSA (Cavaco *et al.*, 2010). Copper resistance genes *copZ* and *copA* were also encoded in pEPI155_4. It is common that the chromosome of *S. aureus* comprises a conserved copper resistance operon including of *copA* and *copZ* genes (Sitthisak *et al.*, 2007). While copper may contribute to innate immunity via enhancing the bactericidal activity of of macrophages, copper resistance has been linked to virulence in many bacterial pathogens such as *Streptococcus pneumoniae Neisseria gonorrhoeae* and *Mycobacterium tuberculosis* (Jamrozy *et al.*, 2017). Resistance to copper might also be associated with *S. aureus* antibiotic resistance as methicillin resistance is higher in copper-resistant strains (Pal *et al.*, 2017).

4.4.5 Prediction of antimicrobial secreted by *S. epidermidis* B155

Based on the resistant phenotype of *S. aureus* clones that evolved after competition with *S. epidermidis* B155, ~150 isolates of *Staphylococcus* and *Bacilllus* that were identified as antimicobial producers were tested to identify any that inhibited the wild type but not the evolved *S. aureus* clones. Among those isolates tested, a single *Bacillus flexus* strain (B003) was found with a similar inhibition phenotype as *S. epidermidis* B155 against *S. aureus* and the evolved clone SHG01. To test whether there was a correlation between *S. epidermidis* B155 and *B. flexus* B003 in terms of their inhibitory activity, whole genome sequencing using PacBio was performed for the latter species after its identifcation using 16S rDNA sequencing. To identify whether there was similarity between the antimicrobials secreted by both *S. epidermidis* B155 and *B. flexus* B003 the antiSMASH tool was first used. AntiSMASH has become the standard tool to analyse bacterial and fungal genomes to predict the production of secondary metabolites including (non-ribosomal peptides, polyketides type I, II and III, bacteriocins, lantipeptides, β-lactams, terpenes, siderophores, aminoglycosides/aminocyclitols, aminocoumarins, ectoines, indoles, phosphoglycolipids, melanins, butyrolactones, and a generic class of clusters encoding unusual secondary metabolite biosynthesis genes) (Blin *et al.*, 2013).

Bacteria with small genomes have been considered generally to be a poor source of PKS and NRPS synthesised natural products (Jenke-Kodama *et al.*, 2005; Wang *et al.*, 2014). There were 3 co-located secondary metabolite gene clusters identified in the *S. epidermidis* B155 genome, one encoding NRPS-TransATPKS hybrid, one NRPS and one siderophore. The NRPS-TransATPKS cluster shared a very low similarity with clusters responsible for the synthesis of plipastatins (fengycins), bacillaene, surfactin, macrolactin, bacillibactin and iturins (bacillomycins). All of these metabolites are produced by *Bacillus* genus and contribute to biocontrol processes (Hiradate *et al.*, 2002; Chen *et al.*, 2006; Ongena *et al.*, 2007). However, due to the low similarity of the *B. flexus* B003 gene clusters referred to above to the genes encoding proteins for the biosynthesis of compounds deposited in the the minimum information about a biosynthetic gene cluster (MIBiG) database, this indcates the potential for a new structure to be resolved in the future.

Notably, the unknown cluster of *S. epidermidis* shared a high sequence homology with a cluster widely found in *Streptococcus mutans* strains. Different bioactive compounds have recently been isolated from *S. mutans*, including mutacins I-IV and mutanobactins (Liu *et al.*, 2016). Mutanobactins are compounds of hybrid PKS/NRPS origin that inhibit the morphological transition of *Candida albicans*, a commensal and opportunistic human pathogen. More recently, Liu *et al.,* (2016) studied 169 *S. mutans* genomes and they reported the detection of of 144 natural product gene clusters including NRPS, PKS, and hybrid PKS/NRPS (Liu *et al.*, 2016). These data raise the possibility that *S. epidermidis* B155 acquired its antimicrobial properties from *S. mutans* via horizontal gene transfer, particularly as the NRPS-TransATPKS cluster is located on plasmid pEPIB155_2. The location indicates this antimicrobial activity is not encoded on the core genome, but rather encoded on a mobile genetic element (MGE) exchanged through horizontal gene transfer. Accessory traits, such as the production of antimicrobial substances, are widely found to be encoded on MGEs in staphylococci (Schoenfelder *et al.*, 2010; Alibayov *et al.*, 2014). Furthermore, as there was no known bacteriocin found to be encoded in the accessory genome of *S. epidermidis* B155 it is possible that this

strain employs unknown or novel mechanisms of niche competition and invasion.

There were 5 secondary metabolite clusters found in the *B. flexus* B003 genome, one linear azol(in)e-containing peptides (plantazolicin/plantathiazolicin), two terpene, one T3pks and one siderophore cluster. Plantazolicin is an antibiotic compound that has inhibitory activity against Gram-positive bacteria closely related to its producer, *B. amyloliquefaciens* inlcuding human patogens (Scholz *et al.,* 2011) (Molohon *et al.,* 2016). Notebly, plantazolicin was found to alter the expresstion of DesKR TCS in *B. anthracis*, suggesting it has implications in bacterial cell membrane homeostasis (Molohon *et al.*, 2016). Genome analysis revealed the presence of a type three polyketide (PKS III) cluster which is also likely source of the inhibition trait associated with *B. flexus* B003. PKS III are secondary metabolites, originally thought to be found only in plants but in 1999 discovered in bacteria (Funa *et al.*, 1999). After then, the roles of this type of secondary metabolite cluster were determined from several species ranging from those concerned with formation of pigment in *Streptomyces griseus* to phenolic lipid biosynthesis associated with the cell membrane of dormant cells of *Streptomyces* and *Azotobacter vinelandii* (Yu *et al.*, 2012). The fact that PKS III are associated with lipids inserted into cell membranes lends support to the hypothesis that the mechanism is used by some bacteria for competitive inhibition. To confirm this theory further genetic experiments using gene knock outs or SNPs would need to be performed in combination with physiological assays.

The results from the study to date clearly show that despite *S. epidermdis* B155 and *B. flexus* B003 not sharing the exact same genetic basis for inhibition, their inhibitory mechanisms are expected to be closely related. Both species inhibit growth of *S. aureus* but not the *desKR* evolved variant. More investigations are needed to characterise the antimicrobial production in both species that will improve understanding of the newly identified resistance mechanisms that appear to relate to an inhibitory mechanism of *S. aureus* not previously studied.

Chapter 5: The contribution of the DesKR TCS and associated ABC transporter to antimicrobial resistance of *S. aureus*

5.1 Introduction

S. aureus is able to survive and thrive due to its evolution of a range of responsive mechanisms and adaptations to stressful environments including antibiotics, temperature, oxidative, pH and osmotic stressors (Singh *et al.*, 2012). The adaptation patterns to altered environmental conditions are controlled by signal transduction systems (TCS) (Cybulski *et al.*, 2004; Eguchi and Utsumi, 2008; Martín and de Mendoza, 2013) which consist of a sensory histidine-kinase and a regulator that encodes a cognate response regulator (Cybulski *et al.*, 2004; Mitrophanov and Groisman, 2008). In *S. aureus,* most of these TCS identified have been studied extensively while the function of several remain poorly characterised. Previous reports by Kim *et al.* (2016) identified that a member of the *S. aureus* TCS repertoire shares high sequence homology with a TCS of *B. subtilis*, known as DesKR (Kim *et al.*, 2016).

In *B. subtilis,* the DesKR TCS regulates the maintenance of cell membrane fluidity at low temperature (Aguilar *et al.,* 1998*;* Aguilar *et al.,* 2001; Cybulski *et al.,* 2002). At low temperature, DesK senses decreased membrane fluidity which phosphorylates the response regulator DesR leading to activation of *des* gene transcription that encodes acyl lipid desaturase Δ^5-Des. Subsequently, the Δ^5-Des enzyme converts saturated membrane fatty acids into unsaturated fatty acids, which increases membrane fluidity (Fig. 5.1) (Aguilar *et al.*, 2001; Martín and de Mendoza, 2013; Cybulski *et al.*, 2015). Several biophysical lines of evidence support the idea that lower environmental temperature leads to increased membrane bilayer thickness due to the lipids becoming more ordered revealing a link between variations in membrane fluidity and alterations in thickness of the cell membrane (Saita *et al.*, 2016).

It can be predicted that this locus might enhance the flexibility and adaptability of *S. aureus* to a wide variety of ecological niches. Kim *et al.* (2016) proposed the importance of a homologous DesKR system in virulence, antimicrobial resistance

and temperature adaptation in a multi-drug resistance *S. aureus* strain (Mu50) (Kim *et al.*, 2016).

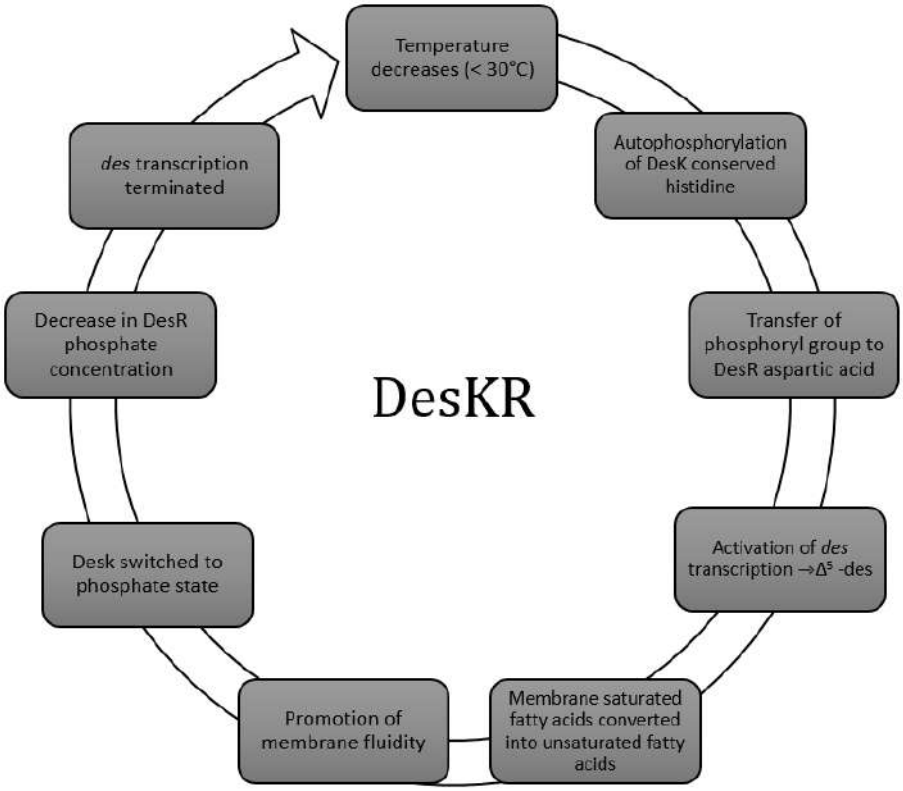

Figure 5.1 The *B. subtilis* DesKR system mediates regulation of membrane function in response to temperature downshift. Low temperature is sensed by an integral membrane-associated DesK histidine kinase, which phosphorylates the response regulator DesR to activate expression of the acyl lipid desaturase Δ5-Des. The Δ5-Des converts saturated fatty acids into unsaturated fatty acids to promote membrane fluidity. DesK activation to the phosphatase state next occurs and the phospho-DesR concentration declines thereby reducing transcription of *des*. The information was obtained from (Cybulski *et al.*, 2004; Martín and de Mendoza, 2013; Saita *et al.*, 2016).

In the previous chapter 4, it was identified that single nucleotide polymorphisms (SNPs), in the *desKR* homologous operon of *S. aureus* SH1000, resulted from evolution of resistance to secreted antimicrobial of *S. epidermidis* B155. According to KEGG databases (Kyoto Encyclopedia of Genes and Genomes) the *desKR* operon consists of two upstream genes *SAOUHSC_01311* and *SAOUHSC_01312* that share significant homology with ABC type transport system

ATP-binding proteins (Fig. 5.2). ABC transporters are importers of essential substrates, including organic and inorganic ions, amino acids, mono- and oligosaccharides, iron-siderophore, peptides, vitamins, polyamine cations and metals. Their transport roles can also be that of exporters via secretion of diverse molecules, such as lipids, peptides, polysaccharides, hydrophobic drugs, and proteins, including toxins. (Davidson *et al.*, 2008; Wilkens, 2015). A possible role for these two ABC transporter proteins could be with *S. aureus* resistance to the *S. epidermidis* B155 antimicrobial. This scenario is similar to the ABC transporters adjacent to GraSR TCS that are upregulated by the TCS to export antimicrobial peptides (Yang *et al.*, 2012). Furthermore, a *cls1* (SAOUHSC_01310) gene encoding a cardiolipin synthase in a monocistronic operon is located upstream of the *desKR* locus (Fig 5.2), which might be related to the transporters. The *cls1* gene is positionally located upstream of *desKR* in staphylococci. At stationary phase, cardiolipin represents around 30% of cell membrane lipids of *S. aureus.* This anionic lipid has a role in greater resistance to high salt environments (De Leo *et al.*, 2009; Tsai *et al.*, 2011). Cardiolipin contributes to the physiology of bacterial plasma membranes through organisational roles, such as localisation of transporters, bacterial cell division in *E. coli* and the triggering of compensatory changes in the membrane phospholipid composition, which affect bacterial adaptive mechanisms (Arias *et al.*, 2011).

Gene function	Cardiolipin synthase	ABC transporter ATP-binding protein	ABC transporter protein	TCS histidine Kinase	TCS response regulator	Hypothetical protein
Gene size(bP)	1482	909	732	1092	603	189
Protein size (aa)	493	302	243	363	200	62

Figure 5.2 The two-component system *desKR* homologous operon of *S. aureus* SH1000. The diagram represents the *desKR* locus and location of a cardiolipin synthase gene. Gene information was obtained from the KEGG database. SAOUHSC_01310 encodes cardiolipin synthase (*cls1*), SAOUHSC_01311 encodes an ABC-2 type transport system ATP-binding protein, SAOUHSC_01312 encodes an ABC-2 type transport system permease protein, SAOUHSC_01313 (*desK*) encodes a TCS histidine kinase, SAOUHSC_01314 (*desR*) encodes a response regulator and SAOUHSC_01315 is a hypothetical protein. Gene sizes are shown as numbers of base pairs, and protein sizes as numbers of amino acid residues.

5.2 Aims

The main aim of this chapter was to investigate the role of the TCS *desK* histidine kinase (SAOUHSC_01313) and the putative ABC transporter SAOUHSC_01312 genes in the resistance of *S. aureus* SH1000 to *S. epidermidis* B155 secreted antimicrobial. This aim is based on the observations in Chapter 4 using *desK* and *SAOUHSC_01312* mutant strains constructed previously. In addition to the main aim, the phenotypic differences between *S. aureus* wild-type and these mutant strains would be examined using different assays such as temperature responses, based on the findings of the *B. subtilis* homologous system, and carotenoid production.

5.3 Results

5.3.1 Constructing allelic replacement SNP variants of *desR*

To identify the effect of the single nucleotide changes in the *desKR* operon that were identified in Chapter 4, allelic replacements were performed to define the contribution of specific SNPs in future experiments. The *desR* SNP variant identified in the *S. aureus* evolved strain (SHG01) resulting from competition with *S. epidermidis* B155 was introduced into the parent *S. aureus* SH1000 strain, to generate strain *S. aureus* H001 (Fig 5.3). Allelic replacement of *desR* SNP gene began with amplification of a 1019 bp region of the target gene using primers pairs desR(F)/desR(R) (Chapter 2, Table 2.2). The PCR product was digested with the restriction enzymes *Eco*RI/*Bam*HI recognising PCR product ends. Subsequently, this digested fragment was ligated into pMUTIN4 vector (8610 bp) which also digested with *Eco*RI/*Bam*HI. The resulting ligation reactions were used to transform *E. coli* TOP10. Ampicillin-resistant colonies were identified, and plasmids were purified and digested with restriction enzymes *Eco*RI and *Bam*HI. Identification of correctly sized fragments indicated the desired allelic replacement plasmid was constructed successfully (Fig. 5.4). These correctly cloned plasmids and pMUTIN4, which served as a control, were used to transform *S. aureus* RN4220. Colonies obtained from this step were used to prepare a phage ϕ11 lysate for transduction into the SH1000 wild type strain. A single transductant clone, named H001, was chosen for further study based on phenotypic properties that matched the *S. aureus* SNP donor strain used for DNA amplification.

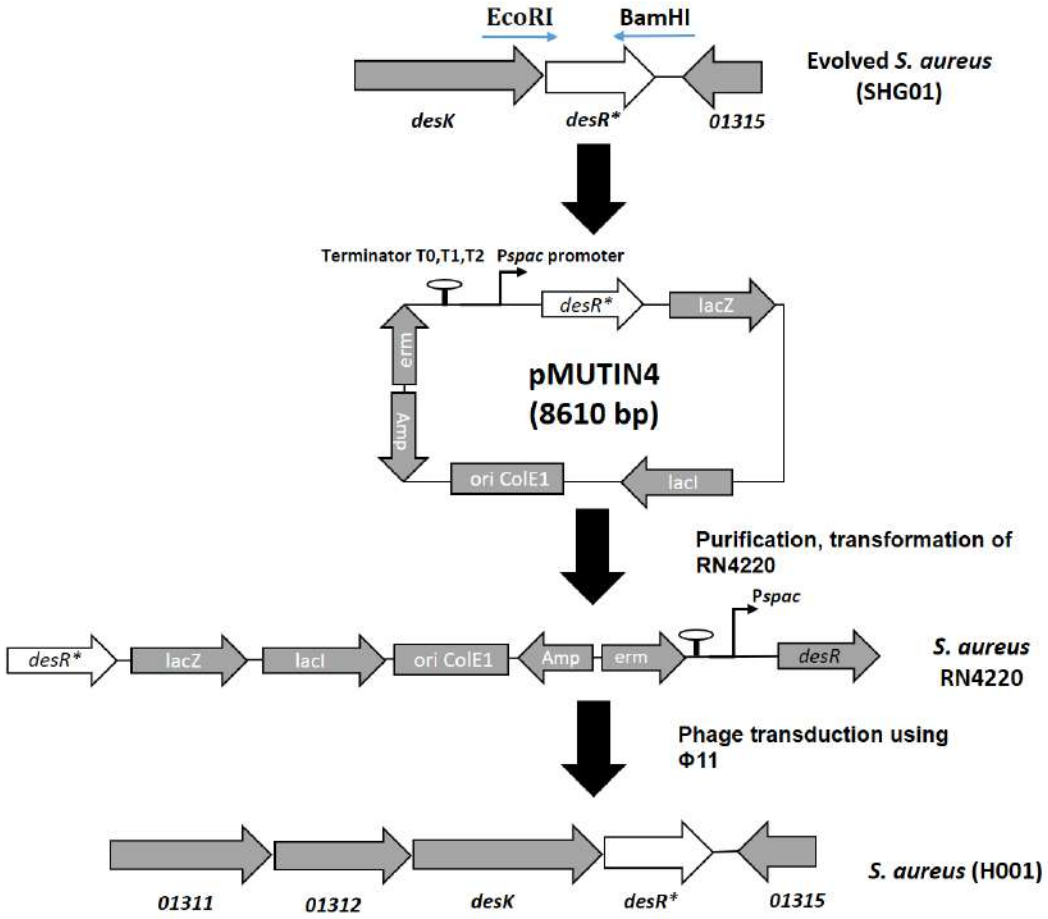

Figure 5.3 Schematic of allelic replacement construction of *desR* SNP in *S. aureus* SH1000 wild type. Allelic replacement plasmid of the *SNP desR* gene of *S. aureus* SH1000 was constructed using the suicide plasmid pMutin4. The SNP *desR* region was amplified by primers desR(F)/desR(R) including *Eco*RI and *Bam*HI, respectively. Both the insert DNA and pMutin4 were digested and then ligated together. The ligated product was used to transform *E. coli* TOP10 to select for the correct recombinant plasmid. Purified, correctly cloned plasmid was next used to transform *S. aureus* RN4220. A selected clone was used to prepare a phage ϕ *11* lysate to trasnduce marked SNP *desR* to *S. aureus* SH1000 that was resolved by recombination to remove the plasmid and generate *S. aureus* H001 strain.

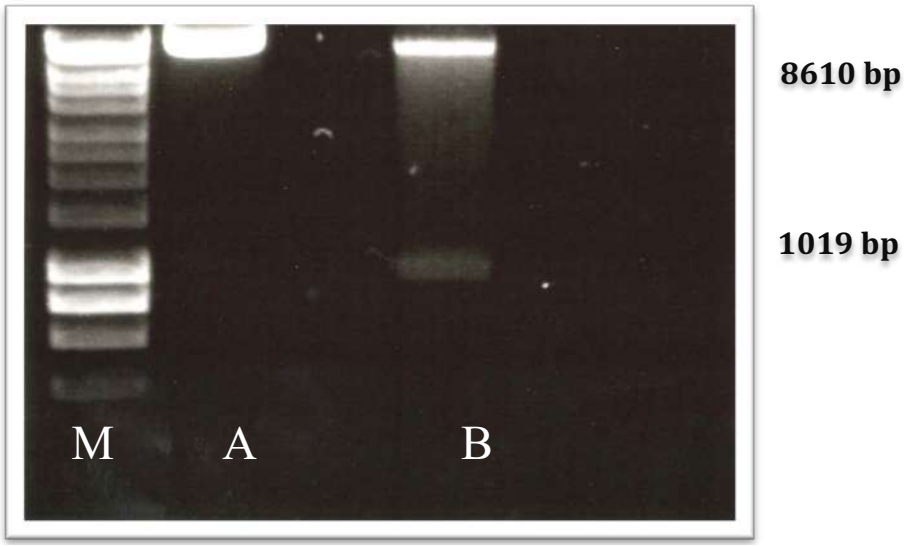

Figure 5.4 Confirmation of recombinant plasmid by restriction enzyme digest. (A) pMUTIN4+*desR* SNP plasmid (undigested control); (B) pMUTIN4+*desR* SNP plasmid digested with restriction enzymes *Bam*HI and *Eco*RI. The upper band represents pMUTIN4 plasmid (8610 bp) and the bottom band represents the SNP *desR* gene (1019 bp), (M) shows 1 kb molecular weight marker.

The constructed strain *S. aureus* H001 was first phenotypically confirmed using *S. epidermidis* B155 in an inhibition assay (chapter 2, section 2.2). *S. aureus* H001 was resistant to the antimicrobial produced by *S. epidermidis* B155 compare to *S. aureus* parant strain (4.40 ± 0.76 mm) (Fig. 5.5 & 5.6). This supporting that the *desR* SNP was introduced successfully to the genome of *S. aureus* SH1000. Given that the *desR* SNP was not identified in isolation as the only change in the evolved *S. aureus* strain it was deemed important to investigate the whole genome for changes, therefore the *S. aureus* H001 genome was sequenced to determine if any other mutations were introduced during or as a consequence of the pMUTIN4-mediated allelic exchange process. Genome sequencing was performed using the Illumina platform (chapter 2, section 2.9.1) and SNPs were obtained using method described in chapter 2 (section 2.10). *S. aureus* H001 was compared with

S. aureus SH1000 wild-type and from this data analysis, *S. aureus* H001 was confirmed to be modified by replacing its *desR* gene with the allele from the evolved strain (conferring the p.Phe90Ile amino acid change) with the desired SNP at position 1258581 (Table 5.1). Additionally, however SNPs were obtained using the strain carried an additional 13 SNPs/INDELs present in > 80% of reads (Table 5.1). All these SNPs/INDELs matched changes found in the evolved strain (SHG01) and described in chapter 4 (Table 4.3) with exactly the same position, including changes in genes: SAOUHSC_00039, SAOUHSC_00409 that encode hypothetical proteins, *hisF* encoding multifunctional imidazole glycerol phosphate synthase subunit/phosphoribosyl-AMP cyclohydrolase/phosphoribosyl-ATP pyrophosphatase; and *scrA* encoding PTS system sucrose-specific transporter subunit IIBC. A further six SNPs/INDELS were identified at chromosomal locations already observed in the SHG001 evolved variant but in this instance the SNPs were called as upstream gene variants, while in the H001 strain the SNP effect was frameshift variants. Despite the nomenclature discrepancy, the common variants were annotated to genes including: *tarM* that encodes a group 1 family glycosyltransferase that modifies teichoic acid to modulate its roles in colonisation and phage resistance (Xia *et al.,* 2010; Winstel *et al.,* 2015; Li *et al.,* 2015); *rspB,* encoding a conserved ribosomal protein; rpmF that also encodes for a ribosomal protein*; sbcC,* encoding a protein with recombinational repair function; *mnmA,* encoding a (5-methylaminomethyl-2-thiouridylate) methyltransferase; *cymR*, encoding a global regulator of cysteine metabolism; and *salA,* which encodes an ATP-binding Mrp/Nbp35 family protein; two genes (*SAOUHSC_02473* and *SAOUHSC_02813*) are located in genes encoding hypothetical proteins at position 2296653 and 2592011, respectively. Since those SNPs/INDELs were present in common between the evolved and constructed strains, it is proposed that these are compensatory mutations associated with *desR* mutation.

By comparing the constructed strain (H001) with the original *S. aureus* evolved strain (SHG01), there were two mutations identified that were only present in strain H001; insertion of two A nucleotides located upstream *SAOUHSC_02297* gene which encoding S1 RNA binding domain protein and another mutation

upstream *rrlF* gene that encodes ribosomal proteins 5S at the position 2244413 (Table 5.2). Sanger sequencing of PCR products of the identified SNP/INDELS in all of the genes confirmed the alterations were correct. Because of these extra mutations found in *S. aureus* strain H001, it was not used for further studying the effects on resistance to the antimicrobial secreted by *S. epidermidis* B155. It was deemed that there was no clear benefit of switching from the original clone of the evolution experiment to the newly constructed strain.

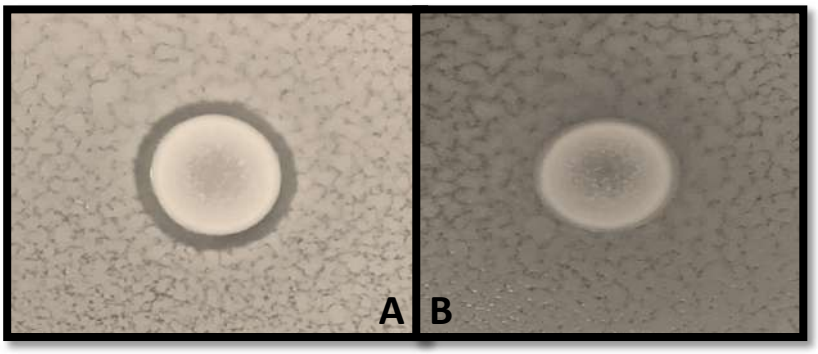

Figure 5.5 *S. aureus* H001 single SNP mutant strain displayed resistance to antimicrobial produced by *S. epidermidis* B155 compared with WT. Deferred inhibition assays were performed by spotting overnight culture of *S. epidermidis* B155 WT. Plates were incubated at 37°C before being sprayed with *S. aureus* strains and incubated overnight. (A) *S. aureus* WT and (B) *S. aureus* single SNP mutant (H001) with *S. epidermidis* B155*.*

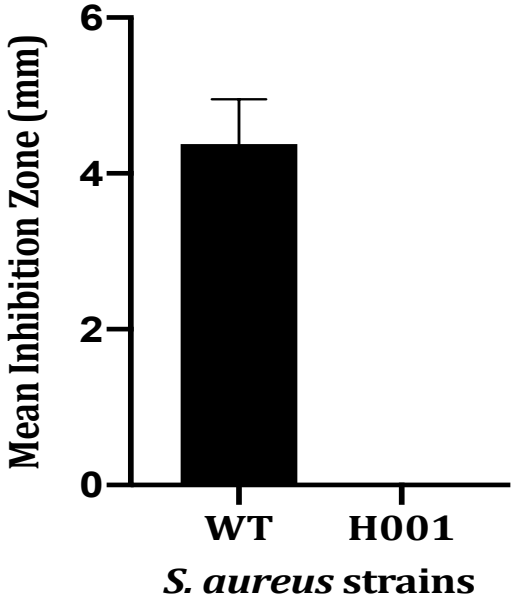

Figure 5.6 Quantitative growth inhibition of *S. aureus* SH1000 WT and single SNP strain (H001) by *S epidermidis* B155. Inhibition zone (mm) shown for the sensitive *S. aureus* SH1000 WT (black bar) and single SNP *S. aureus* strain H001 against *S. epidermidis* (B155). The data are the mean ± standard deviation calculated from 6 biological replicates.

Table 5.1 Identified sequence changes in *desR* SNP allelic variant strain H001. SNPs and INDELs identified in *S. aureus* H001 SNP *desR* mutant compared with *S. aureus* SH1000 wild-type. All mutations classified as homozygous if > 80 % of reads had different bases to the reference genome**.**

Gene ID	Position	Gene name	Base change	Codon change	SNP effect
SAOUHSC_00039	47648	Hypothetical protein	Deletion of T nucleotide	__	Upstream gene variant
SAOUHSC_00409	412759	Hypothetical protein	Insertion of T nucleotide	__	Upstream gene variant
SAOUHSC_00973	947897	*tarM*	Deletion of C nucleotide	p.Asn234fs	Frameshift variant
SAOUHSC_01078	1041999	*rpmF*	Deletion of T nucleotide	p.Arg35fs	Frameshift variant
SAOUHSC_01232	1180884	*rpsB*	Deletion of T nucleotide	p.Val10fs	Frameshift variant
SAOUHSC_01314	1258581	*desR*	T → A	p.Phe90Ile	Missense variant
SAOUHSC_01343	1283783	*sbcC*	Deletion of C nucleotide	p.Asp943fs	Frameshift variant
SAOUHSC_01726	1632624	*mnmA*	Insertion of A nucleotide	p.Ter101fs	Frameshift variant
SAOUHSC_01732	1636250	*cymR*	Deletion of T nucleotide	p.Thr102fs	Frameshift variant
SAOUHSC_02417	2244931	*salA*	Deletion of CT nucleotides	p.Ter296fs	Frameshift variant

Gene ID	Position	Gene name	Base change	Codon change	SNP effect
SAOUHSC_02473	2296653	Hypothetical protein	Deletion of T nucleotide	p.His16fs	Frameshift variant
SAOUHSC_02813	2592011	Hypothetical protein	Deletion of A nucleotide	p.Ser12fs	Frameshift variant
SAOUHSC_02661	2446160	*ScrA*	Deletion of C nucleotide	Asn7fs	Frameshift variant
SAOUHSC_03008	2782815	*hisF*	Deletion of C nucleotide	Tyr249fs	Frameshift variant

Table 5.2 Unique sequence changes in *S. aureus* H001. SNPs and INDELs identified in SNP *desR* mutant *S. aureus* H001 compared with *S. aureus* SHG01. All mutations were classified as homozygous if > 80 % of reads had different bases to the reference genome**.**

Gene ID	Position	Gene name	Base change	Codon change	SNP effect
SAOUHSC_02297	2134726		Insertion of AA nucleotides	_	Upstream gene variant
SAOUHSC_R00010	2244413	*rrlF*	Deletion of T nucleotide	_	Upstream gene variant

5.3.2 *S. aureus desK::tet* allelic replacement and *SAOUHSC 01312* deletion mutants exhibit increased susceptibility from *S. epidermidis* 155

To determine if the histidine kinase -encoding *desK* gene and the co-transcribed ABC transporter *SAOUHSC_01312* have a contribution in resistance to the antimicrobial produced by *S. epidermidis* B155, deferred growth inhibition assays were performed, as described in chapter 2 (section 2.2). The *S. epidermidis* B155 inhibitor-producing strain was cultured on agar plates prior to spraying over the wild type *S. aureus* SH1000, or either of the two *desK::tet* replacement and *SAOUHSC_01312* deletion mutant strains, which were constructed previously. Based on their degree of inhibition, a score of clarity was recorded and the mean values of the zone of inhibition calculated (Fig. 5.7 and Fig. 5.8). The putative *SAOUHSC_01312* ABC transporter mutant had a larger zone of clearance, compared with the *S. aureus* parent strain (7.96 ± 1.07 mm and 4.57 ± 0.89 mm, respectively) with a clarity score 4 (Fig. 5.7 and Fig. 5.8). Similarly, a greater size of inhibition zone (8.46 ± 0.92 mm) of the *desK* mutant compared with *S. aureus* wild-type was observed with clarity score 4. One-way ANOVA tests confirmed a significant difference in inhibition zone size between both of mutant strains and wild type (Tukey's test $P < 0.001$) while there was no significant difference between *desK* and *SAOUHSC_01312* mutants ($P=0.15$). These values support that both TCS genes have considerable roles in antimicrobial resistance.

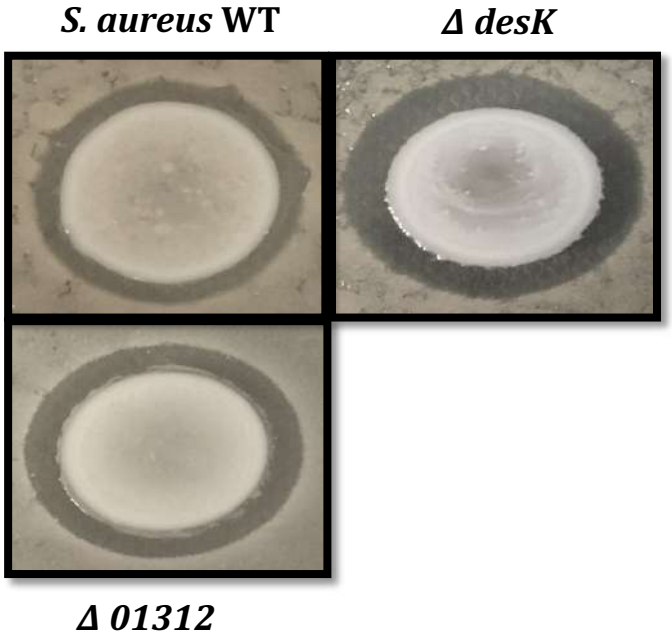

Figure 5.7 *S. aureus desK* and *SAOUHSC_01312* mutant strains displayed more susceptibility to antimicrobial produced by *S. epidermidis* B155 compared to wild type. Deferred inhibition assay were performed by spotting overnight culture of *S. epidermidis* 155 on BHI agar plates, which were incubated at 37°C before being sprayed with *S. aureus* SH1000 (WT), *SAOUHSC_01312* mutant (∆01312) and *desK* mutant (*desK::tet*) over the plates that were re-incubated overnight. Images were taken from representative agar plates following overnight incubation at 37°C.

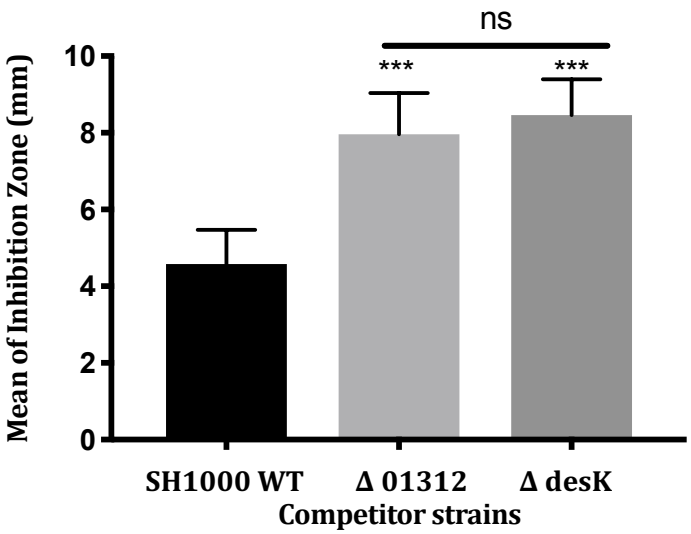

Figure 5.8 Growth inhibition of *S. aureus* SH1000 wild type, and mutants of *desK* and *SAOUHSC_01312* by *S. epidermidis* B155. Inhibition zone (mm) of the *S. aureus* SH1000 WT (black bar), *SAOUHSC*_01312 mutant (Δ01312) (light grey) and *desK::tet* mutant (ΔdesK) (dark grey) challenged *S. epidermidis* B155. The data presented are the mean ± standard deviation calculated from 6 biological replicates (18 plates). Asterisks show significance as measured by Tukey's correction of One-way ANOVA (*** $P \leq 0.001$) and ns, indicates no significant difference.

5.3.3 A *S. aureus* SH1000 *desK* mutant demonstrates an altered growth rate across different temperatures

To assess the role of the DesKR TCS in response to different temperatures, the growth rates of *S. aureus* SH1000 wild-type, ABC transporter *SAOUHSC_01312* deletion mutant and *desK::tet* mutant were compared at 25°C, 37°C and 42°C. The growth rate was examined for each of the strains during equivalent exponential growth phases and their doubling times were calculated (Table 5.2). At 37°C, the growth of *SAOUHSC_01312* mutant did not greatly differ from wild type (*P*=0.21) and both had relatively similar exponential growth rates (doubling time: 0.89 h, 0.92h respectively). In contrast, the *desK* mutant had a greater doubling time (1.01 h) with a significantly lower growth rate in comparison with wild -type (*P*= 0.001) (Fig 5.9 B). At 25°C, growth rate of the *desK* mutant was significantly lower than wild-type with a doubling time of 2.32 h (*P*=0.006) (Table 5.2, Fig 5.9 A). Statistical analysis supported the reduction of *desK* mutant compared with *SAOUHSC_01312* (Fig 5.9 A). However, growth rate was not significantly different for the *SAOUHSC_01312* mutant compared with wild type (*P*=0.26) (Fig 5.9 A). At a higher temperature of 42°C, the *desK* mutant had reduced growth rate, with doubling time 0.97 h (*P*=0.02). While the *SAOUHSC_01312* mutant apparently grew more than wild type at this higher temperature, the *SAOUHSC_01312* mutant exhibited a growth rate with doubling time (0.89 h) with raised temperature (42°C) (doubling time 0.91 h) (*P*=0.22) (Fig 5.9C; Table 5.2) revealing no obvious difference from the wild type. There was a significant difference between growth rates of the *desK* mutant and *SAOUHSC_01312* mutant (*P*=0.009) (Fig 5.9C). Overall, the *desK* mutant exhibited reduced growth rate at both 25°C, 37°C and 42°C while there was no statistically significant difference in growth rates of the *SAOUHSC_01312* mutant across temperatures.

Table 5.3 Growth rates of *S. aureus* strains during exponential growth phase at 37°C, 25°C and 42°C. Strains SH1000 wild type, *SAOUHSC_01312* deletion mutant, and *desK::tet* mutant were cultured in BHI medium. Data are expressed as the mean doubling time for 6 biological replicates during exponential growth phase.

Strain	Duration of exponential growth (h)	Doubling time (h)
25°C		
WT	4	1.26
Δ *desK*	4	2.32
Δ 01312	4	1.20
37°C		
WT	4	0.92
Δ *desK*	4	1.01
Δ 01312	4	0.89
42°C		
WT	3	0.90
Δ *desK*	3	0.97
Δ 01312	3	0.89

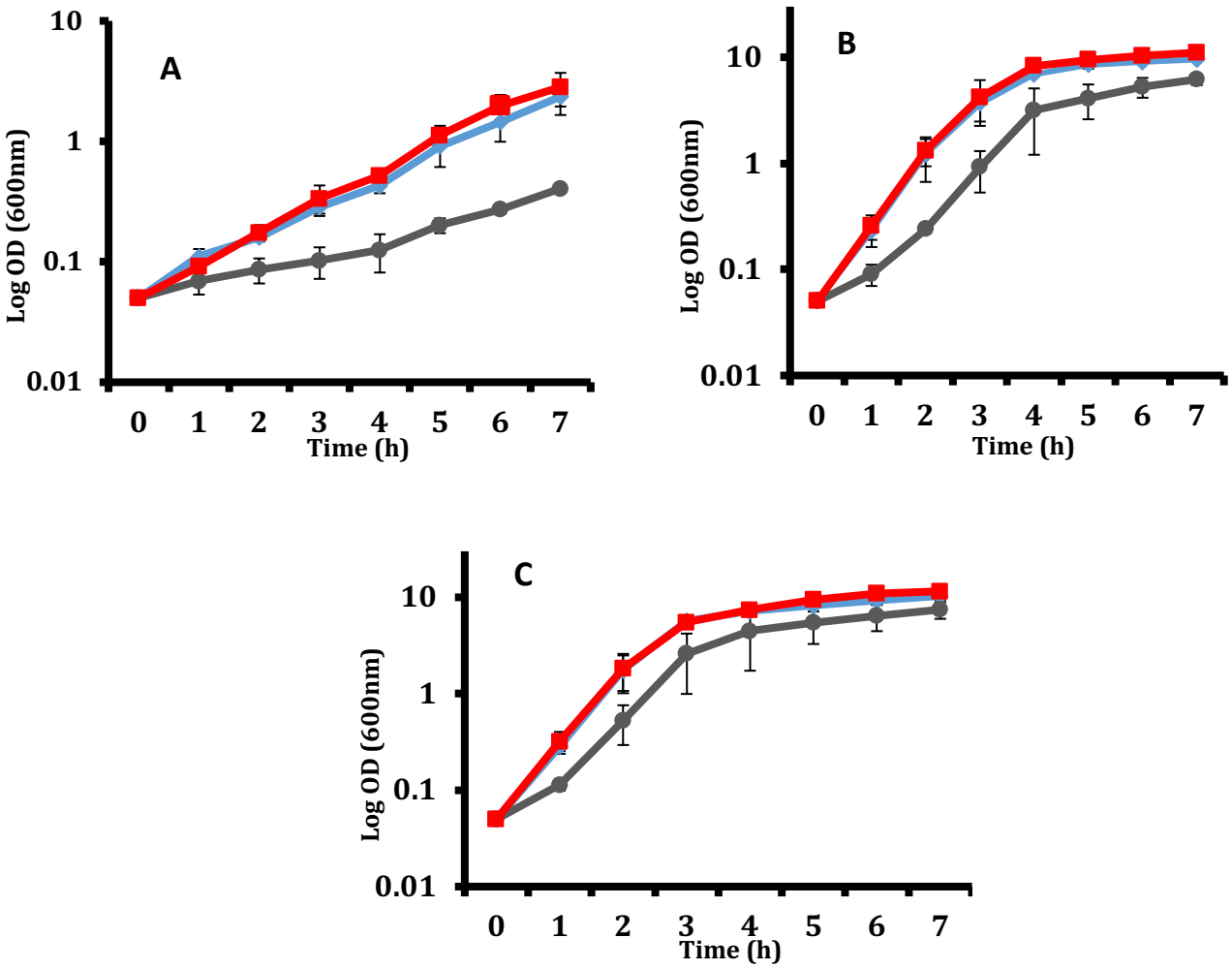

Figure 5.9 Growth of *S. aureus* wild type, *desK::tet* mutant and *SAOUHSC_01312* deletion mutant strains at 25°C, 37°C and 42°C. SH1000 wild type (blue triangles), *SAOUHSC_01312* mutant (red squares), and *desK* mutant (grey circles) strains were cultured in BHI medium with initial optical density =0.05 and then turbidity was measured hourly. Growth is shown for the three strains at (A) 25°C; (B) 37°C and (C) 42°C. All values represent the mean absorbance at 600 nm for 3 biological replicate cultures. The values are expressed as mean ± standard deviation.

5.3.4 Staphyloxanthin production

The expression of staphyloxanthin was measured to determine the contribution of the *desK* and *SAOUHSC_01312* transporter genes to carotenoid biosynthesis of *S. aureus*. Staphyloxanthin pigment production was assayed from overnight culture cells of *S. aureus* WT, *desK* and *SAOUHSC_01312* mutants. Cells pellets were extracted using 100% methanol (v/v) to recover pigment and their absorbance was measured across a full spectrum of light wavelengths using an optical spectrum analyser plate reader, with scanning at 1 nm intervals from 350 nm to 550 nm. The *desK* and *SAOUHSC_01312* mutants showed reduced production of staphyloxanthin pigment compared with wild-type *S. aureus*. This was clearly visualised by comparing cell pellets *SAOUHSC_01312* mutant that were bright yellow and *desK* mutant was non- pigmented compared with their parent strain which was golden-yellow (Fig 5.10 A). The differences between wild-type and mutant strains were confirmed by absorbance measurements. Both mutants showed decreased staphyloxanthin absorbance spectrum from around 370 nm to 500 nm compared to parent strain (Fig 5.10 B). The *S. aureus* wild type shows two absorbance maxima at 449 nm and 447 nm and these absorption peak*s* were reduced in *SAOUHSC_01312* mutant and absent in the *desK* mutant (Fig 5.10B). These data confirm that loss of *desK* and *SAOUHSC_01312* expression alters the expression of carotenoid pigmentation of *S. aureus*.

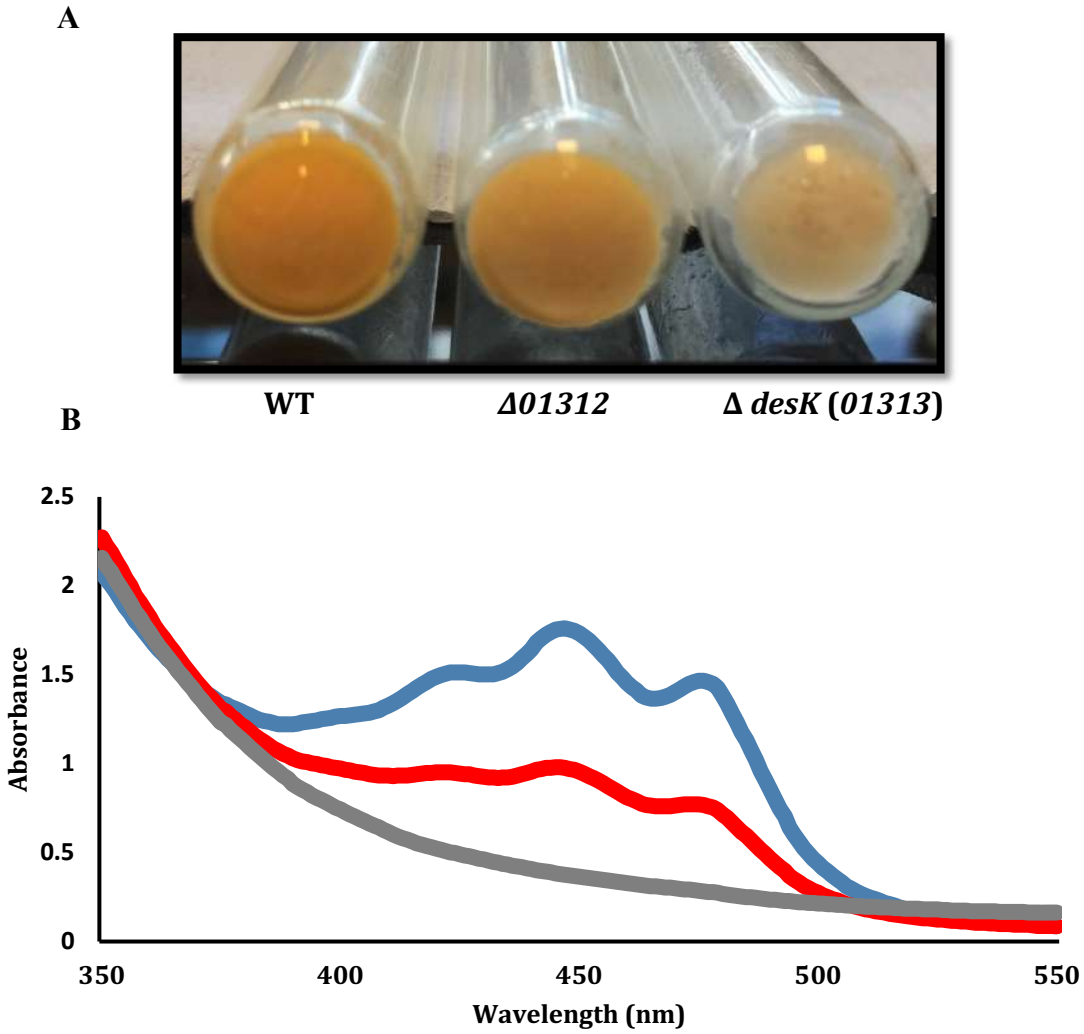

Figure 5.10 The contribution of *desK* and *SAOUHSC_01312* genes to carotenoid staphyloxanthin production in *S. aureus*. (A) Cells of *S. aureus* SH1000 wild-type, plus *01312* and *desK* mutants were cultured overnight at 37°C in 10 ml BHI broth and cells were pelleted. (B) Pellets were extracted with 100% (v/v) methanol prior to the absorbance of the solvent being measured at wavelengths 350-550 nm for *S. aureus* SH1000 wild type (blue line), *01312* mutant (red line), and *desK* mutant (grey line). The mean absorbance calculated at wavelengths from 350-550nm (1 nm intervals) was taken from three technical replicates.

5.4 Discussion

The two-component system DesKR of *S. aureus* is poorly understood compared with its homologous TCS in *B. subtilis.* The encoding genes are collectively transcribed as an operon: *SAOUHSC_01311-01312- desK-desR.* In this chapter, phenotypic changes were investigated following the deletion of genes *desK* (*SAOUHSC_01313*) and the putative ABC transporter gene (*SAOUHSC_01312*). To characterise the functions and contributions of these genes, firstly, a single SNP *desR* mutant was created by replacing *desR* gene in *S. aureus* SH1000 wild–type with SNP *desR* gene taken from evolved strain (SHG01) that was selected during experimental evolution in Chapter 4. The constructed SNP *desR* mutant (H001) was confirmed firstly by its resistance to antimicrobial produced by *S. epidermidis* B155 and also by whole genome sequencing. However, in addition to the introduced *desR* SNP, further SNPs/INDELS were found in the genome of strain H001. Mostly, these variants in the newly constructed strain were present in the original experimentally evolved strain (SHG01) and occurred at the same regions, therefore it was proposed that they were compensatory mutations due to *desR* mutation. The *cymR* gene encodes a key regulator of cysteine biosynthesis that senses oxidative stress through its sole cysteine residue Cys25. The identified frameshift mutation at amino acid 102/141 will prevent dimerisation of the regulator via its C-terminus and likely renders the protein inactive (Tanous *et al.*, 2008; Ji *et al.*, 2012). In *S. aureus,* the *cymR* mutant showed increased susceptibility to copper, tellurite, disulfide, and H_2O_2-induced oxidative stresses (Soutourina *et al.*, 2010). Potentially, the single SNP mutant strain (H001) together with the original evolved resistant strains have a similar pattern against oxidative stresses. Collectively, *cymR* and the other identified genes, such as *sbcC* (encoding a Fe-4S scaffold protein) and *salA* (encoding a repair exonuclease) could have roles in the resistance of *S. aureus* to the secreted antimicrobial of *S. epidermidis* B155 and therefore be associated directly or more likely indirectly with DesKR TCS function. There were two SNPs/INDELs not found in the evolved strain that were found in the constructed strain H001. These could be coincidental mutations that occurred during sub-culturing of *S. aureus* in X-Gal plates to confirm the deletion of the plasmid. Alternatively, since the evolutionary selection was different between the initially isolated strain and the constructed

SNP variant the additional mutations could represent their differing origins. The same observation of additional mutations was shown in the previous study by Howden *et al.,* 2011 when mutations in the essential sensor histidine kinase (*walK)* gene was introduced to a parent strain. This created a strain with the desired mutation in *walK* but there were four additional SNPs upon genome sequencing (Howden *et al.*, 2011). Because of the unexpected SNPs/INDELs identified in H001 strain (*desK* and *desR* are not essential) it would complicate future interpretation of phenotypic results to use the strain for the original purposes it was designed for, consequently the strain was not used for further study. These data also indicate that it is unlikely that a straightforward single SNP variant strain of the versions identified in *desK* or *desR* could be constructed without compensatory mutations being generated.

To examine if the *desKR* operon contributes to antimicrobial resistance, deferred antagonism assays were performed. *S. aureus* wild type was compared with *desK* TCS mutant and the putative ABC transporter *SAOUHSC_01312* mutant against the antimicrobial-producing *S. epidermidis* B155. The data showed increased susceptibility to antimicrobial of both mutants in comparison with the wild type. While there was no significant difference between the *desK* mutant and *SAOUHSC_01312* mutant there was a trend for the *desK* mutant to exhibit a diameter of inhibition zone that was greater. The results supported that the *desKR* locus contributes to *S. aureus* survival from antimicrobial(s). TCS of bacteria are viewed as credible targets for the development of novel antibacterial agents (Worthington *et al.*, 2013). The importance of ABC transporters for bacterial survival has been determined in several studies. In *S. aureus, SAOUHSC_01311* and *SAOUHSC_01312* were recently identified to be strongly expressed in response to UM-C162 which has a role in inhibition of *S. aureus* virulence factors, including biofilm formation. The induction of these two transporter genes were proposed to be related to transport of this compound in and out of the bacterial cell (Kong *et al.,* 2018). The transcription of the *braDE* and *vraDE* operons are activated by the well-characterised BraRS TCS. Both operons encode ABC transporters that have roles in resistance to nisin, bacitracin and daptomycin (Hiron *et al.*, 2011; Popella *et al.*, 2016). It is still unknown how

VraDE is associated with resistance but this ABC transporter resistance mechanism is proposed to be an ATP-driven efflux pump (Popella *et al.*, 2016). The GraSR TCS regulates a downstream ABC-transporter-dependent efflux pump (*VraFG*) (Li *et al.*, 2007; Meehl *et al.*, 2007). VraFG transporter itself was not implicated directly in resistance, however instead it senses CAMPs by transferring signal to sensor *graS*, which causes activation of *graR*-dependent transcription (Falord *et al.*, 2012; Yang *et al.*, 2012). In *S. aureus*, it was also suggested that the ABC transporter permease VraE was associated with AFA resistance (Kenny *et al.*, 2009) therefore, *vraE* mutation can lead to decrease *S. aureus* survival in the presence of linoleic acid (Kenny *et al.*, 2009). It is possible that the *SAOUHSC_01312* encoded ABC transporter permease acts similarly to the VraFG ABC transporter in the GraSR TCS by detecting and sensing the stimulus of antimicrobial and signaling is subsequently transferred to the response regulator DesR. The phosphorylation of DesR could then activate antimicrobial resistance gene expression. The greater sensitivity of the *desK* mutant to antimicrobial could arise from roles other than sensing mechanisms. Such multi-funtionality of the TCS and adjacent transporter would mirror the stimulus of CAMPs by GraSR TCS detected by sensor protein GraS together with the VraFG ABC transporter (Falord *et al.*, 2012; Yang *et al.*, 2012). In the DesKR TCS scenario, inactivation of ABC transporter 01312-dependent antimicrobial stimulus could result in sensing by DesK, whereas inactivation of the response regulator may negate transcription of the operons encoding mechanisms responsible for antimicrobial resistance (Beier and Gross, 2006). The activation mechanisms may depend on the mode of action and charge or structural features of antimicrobial and whether it is located in the membrane. Further experiments are needed to establish if there is a transporter sensing mechanism and to uncover stimulus of specificity DesKR TCS. Broad testing could reveal stimulus acting antimicrobial compounds, including antibiotics and inhibitor-producing species isolated from the human microbiome being tested on DesKR operon mutant strains. Kim *et al.* (2016) identified the susceptibility of a *desR* (SAV1322) mutant of *S. aureus* strain Mu50, a vancomycin-intermediate resistant MRSA, to gentamicin, tetracyclines and glycopeptides which had lower MICs than parent strain, however complementation of *desR* mutant did not restore this phenotype leaving a degree

of uncertainty (Kim *et al.*, 2016). Inactivation of *desK* or *desR* genes in *S. aureus* SH1000 may have a similar role in antibiotic resistance to antibiotics, as observed in strain Mu50.

Next, the growth rate of *S. aureus desK* mutant and *SAOUHSC_01312* mutant were compared with their isogenic wild-type at different temperatures: 25°C; 37°C and 42°C. It was noted that the growth of the *desK* mutant was significantly reduced at all temperatures with increased of doubling time. However, the *SAOUHSC_01312* mutant showed no significant difference in growth rate at all temperatures tested. These data support that desKR operon contributes to the temperature response in *S. aureus* SH1000. Previous work by Kim *et al.* (2016) showed that there was a reduction in the growth of *desR* mutant in *S. aureus* Mu50 under low (25°C) and high (46°C) temperature while both *desR* mutant and wild type had similar growth rate at 37°C suggesting its important role in reduced and increased temperature. Their data matches findings here, regarding reduced growth rate at lower and higher temperature, but is inconsistent with the SH1000 *desK* mutant data at 37°C. These differences might indicate that the observed phenotypes of the response regulator mutant could be highly strain specific (Kim *et al.*, 2016). Unfortunately, the Kim *et al* group were unwilling to share their strain to compare these discrepancies and future investigation involving transfer of the deletion to other *S. aureus* strains such as Newman and USA300 would be required to confirm this hypothesis. One curiosity though is that reduced growth rate across all temperatures of the *desK* mutant was not observed with the *SAOUHSC_01312* mutant strain. Given the small regulon of the DesR TCS (operons *SAOUHSC_01311-01312-01313-01314* and *01315*) an explanation for the difference in growth rate might come from the gene *01315* encoding a short hydrophobic protein and this needs further study.

The extent of homology with the DesKR TCS proteins of *S. aureus* and those of the *B. subtilis* proteins suggests that both TCS could have the same primary function. Conceivably, in *S. aureus,* the TCS may direct changes to membrane composition to adapt to changing temperature. In contrast to *B. subtilis*, Δ5-Des desaturase is not encoded and no discernible equivalent expressed in *S. aureus*. Under all

temperatures tested, the observation of defective growth rate with the *desK* mutant may indicate that the DesKR functions similarly to that in *B. subtilis,* which directly regulates cell membrane physiology. In *B. subtilis*, DesK is activated at lower temperature (Martín and de Mendoza, 2013). A previous study revealed that if the fluidity of the plasma membrane is decreased as result of high temperature, DesK is activated via restricted incorporation of low melting point, anteiso fatty acids (branched chain) which supports the idea that DesK directly responds to the physical properties of the cell membrane rather than to temperature itself (Cybulski *et al.*, 2002). The data obtained in this study supports that the SAOUHSC_01312 transporter is not required for growth at low temperature. Notably, there is a *cls1* gene encoding cardiolipin synthase located upstream of the *desKR* locus in *S. aureus*. Cardiolipin is essential for maintaining the integrity of the bacterial membrane in response to environmental stressors (Unsay *et al.*, 2013) and an important lipid to enhance membrane fluidity (Unsay *et al.*, 2013). Cardiolipin has a role in *S. aureus* resistance to high salinity (Tsai *et al.*, 2011) based on previous studies that reported cardiolipin increases survival of *B. subtilis* and *E. coli* in high salt conditions (Lopez *et al.*, 2006; Romantsov *et al.*, 2007). In *E. coli*, the activity of cardiolipin synthase increases about ten-fold after at the stationary growth phase (Hiraoka *et al.*, 1993). Mutation of the cardiolipin synthase gene can lead to longer generation times, low viability, and low final cell density (Nishijima *et al.*, 1988; Hiraoka *et al.*, 1993). In *S. aureus,* it is unclear if there is a relationship between expression of cardiolipin synthase and elevated temperature**.** Taking into consideration the positional gene location of *cls1* upstream of the *desKR* operon in *S. aureus*, cardiolipin expression might be associated with membrane lipid composition and associated with normal homeostasis. Particular changes in lipids (exogenous or endogenous) may be sensed and/or transported. For example, the ABC transporter *SAOUHSC_01312* could sense the presence of a higher level of anionic cardiolipin, which may pose a negative feedback to indirectly control the synthesis of cardiolipin or compensatory property of the membrane to ensure physiological preferences are maintained. It was suggested previously that temperature sensitivity is associated with cardiolipin synthase gene deletion (Zhong *et al.*, 2004).

Therefore, it would be of interest to assess whether *cls* mutant strains alter expression of the DesKR TCS.

Analysis of pigmentation revealed that there was a decreased expression of staphyloxthin in both *desK* and *SAOUHSC_01312* mutant strains compared with wild type. The staphyloxanthin spectral profile of *S. aureus* has absorption maxima at wavelengths 440nm, 462 nm and 491 nm (Liu *et al.*, 2005) and at 460 nm and 490 nm in *S. carnosus* (Pelz *et al.*, 2005). These three peaks were observed in wild type and reduced absorption was revealed for these peaks in the *SAOUHSC_01312* mutant and were absent in the *desK* mutant. These reductions confirmed diminished staphyloxanthin expression in both mutant strains. From these results it can be predicted that DesKR has an indirectly regulates production of *S. aureus* pigment. Recently, it was proposed that the oxygen-sensing and redox-signaling AirSR TCS modulates expression of the staphyloxanthin biosynthetic operon *crtOPQMN,* which alters antioxidant capability of the cell (Hall *et al.*, 2016). *S*taphyloxanthin antioxidant activity provides protection from attack by reactive oxygen species (ROS) and phagocytic killing (Liu *et al.*, 2005; Clauditz *et al.*, 2006). The pigment also increases antimicrobial fatty acid resistance by altering the rigidity of the cell membrane (Mishra *et al.*, 2011). There is no clear link yet between the pigmentation reduction of the *SAOUHSC_01312* and *desK* mutants. There is also no knowledge about the interaction of the DesKR TCS and response and other TCS system involving in regulation of cell membrane and pigment expression.

Chapter 6: Transcriptome characterisation of *S. aureus desK* and *SAOUHSC_01312* mutant strains

6.1 Introduction

Transcriptomics is one of the key methods for identification of gene expression and regulation in the research field of functional genomics. Over the last two decades, microarray technology was commonly used for any transcriptomics investigation. Based on using nucleic acid probes, typically 60-mers, covalently bound to glass slides, fluorescently labelled target sequences are hybridised to the probes and scanned. The images are then converted to signal intensities and these data are processed using software specific to the application of the array (Mantione *et al.*, 2014). Although experiments that are performed using microarrays are high throughput and considerably less expensive (Dong and Chen, 2013), these methods have several limitations. Microarrays are able to detect only known sequences in genomes and can suffer from high background levels owing to cross-hybridisation (Okoniewski and Miller, 2006; Royce *et al.*, 2007; Wang *et al.*, 2009). Furthermore, it is often difficult to compare the level of expression across different experiments where complex normalisation methods are required (Wang *et al.*, 2009).

Mapping and quantifying transcriptomes has expanded with the development of high-throughput next generation sequencing (NGS). RNA sequencing (RNA-Seq) is more commonly used for transcriptome studies as a replacement for microarray technology because of its advanced features, such as a high technical reproducibility, the large dynamic range, and a reference transcriptome is not required (Van Vliet, 2009; Wang *et al.*, 2009) enabling novel sequences to be detected (Howard *et al*., 2013). The cost of RNA-Seq is more expensive compared with microarray therefore, RNA-Seq may be impractical for large studies.(Zhao *et al.,* 2014) Beneficially, RNA-seq is able to detect single-nucleotide polymorphisms (SNPs) and somatic mutations, allele-specific expression (ASE), RNA editing events, identifying exogenous RNA and quantification of noncoding RNAs (Han *et al.*, 2014).

Multiple research studies have compared microarray and RNA-Seq in parallel and these showed concordance between them with respect to relative values (Bottomly *et al.*, 2011; Sîrbu *et al.*, 2012). A study performed by Marioni, et al estimated the technical variance related to Illumina RNA-Seq technology and its capacity to detect differentially expressed genes compared with existing array platforms. Data collected from RNA-Seq were highly reproducible, with relatively little technical variation. 30% more differentially expressed genes were revealed by using this approach compared with those genes identified from a standard analysis of the array data, at the same false discovery rate (Marioni *et al.*, 2008).

In *S. aureus*, a variety of transcriptional data studies have been established using RNA-Seq. Studies include the role of anti-sense transcription (Lasa *et al.*, 2011) and the identification of small non-coding RNAs (Beaume *et al.*, 2010). The advantages of RNA-Seq were exploited to reveal differentially expressed (DE) genes between isolated sensitive and resistant strains (Song *et al.*, 2013), wild type and gene mutant cells (Truong-Bolduc *et al.*, 2011), and between treated and untreated cells (Pietiäinen *et al.*, 2009; Campbell *et al.*, 2012; Muthaiyan *et al.*, 2012; Cuaron *et al.*, 2013). Furthermore, the transcriptional response of bacteria to antimicrobial was used to gain insight into the mechanisms of action of specific antimicrobial (Muthaiyan *et al.*, 2008). Transcriptional profiling studies of the methicillin-susceptible strain RN450 (8325-4) identified up-regulated genes in response to antibiotics that target the cell wall, including oxacillin, bacitracin and D-cycloserine, which inhibit different steps in peptidoglycan biosynthesis (Utaida *et al.*, 2003).

Bioinformatics skills and extensive experience are required for RNA-Seq data analyses to process the data files (Drewe *et al.*, 2013). Generally, two main steps are involved in the identification of differentially-expressed genes from RNA-Seq data: model parameters estimation from data; and differentially expressed (DE) genes detection from test statistics. Normalisation of the sequenced library is also considered a step of DE analysis (Finotello and Di Camillo, 2015).

For RNA-Seq, statistical tests should be used to evaluate the null hypothesis that a gene is not differentially expressed between two treated samples after calculating P values (Marioni *et al.*, 2008). Typically this is done using a Fisher Exact Test with a great resolution, which can accurately measure a 1.05 fold change. There are different methods for the analysis of differentially expressed genes and they differ on their normalisation procedures: edgeR (Robinson *et al.*, 2010), Cuffdiff2 (Trapnell *et al.*, 2013), Two-stage Poisson Model (TSPM) (Auer and Doerge)and DESeq2 (Anders and Huber, 2010). The calculation of p values in DESeq2, Cuffdiff2 and EdgeR based on a generalised linear model (GLM) likelihood ratio test GLM Wald test and t-test, respectively, while quasi or standard likelihood ratio tests are utilised in TSPM method, based on whether genes are classified as over-dispersed or not. Cuffdiff can estimate false positive, statistically significant p values, when the expression of a gene is detected in only one group (Rajkumar *et al.*, 2015).

6.2 Aims

This chapter is aimed towards further investigation of the regulatory control of the DesKR TCS at the transcriptional level, through use of high-throughput Illumina sequencing to study the differential gene expression. The strains chosen for this part of the study consisted of evolved *S. aureus* (SHG01) from Chapter 4 compared with wild type to identify changes in genes forming the DesKR regulon. In addition, by comparing the transcriptome profile of a *desK::tet* allelic replacement mutant, the effect of the DesKR TCS activity was compared. Finally, since the contribution of the ABC transporter SAOUHSC_01312 to the sensory input of the DesKR TCS is unclear, the *SAOUHSC_01312* ABC mutant in-frame deletion mutant was compared with wild type. The subsequent pairwise comparison of these separate datasets was anticipated to generate considerable insights of the DesKR role and regulon.

6.3 Results

RNA-Seq was carried out for *S. aureus* WT, and isogenic *desK:tet*, evolved desR SNP (SHG01) and *SAOUHSC_01312* mutants to characterise relative gene expression profiles between these strains. Overnight cultures were diluted and grown exponentially to an OD_{600} of 0.5, then cells were harvested. RNA was stabilised using RNAlater (Qiagen, Hilden, Germany) and incubated overnight at 4°C. Next day, total RNA was purified from cells using the method described in chapter 2 (section 2.16.3).

6.3.1 RNA quality control

Before preforming RNA-Seq, RNA samples must pass strict quality requirements. Prior to submission of the samples to the Centre for Genome Research (CGR), University of Liverpool, the absorbance of extracted RNA was measured using NanoDrop® (Thermo Scientific) to ensure that all samples had low salt, protein and solvent contaminations. Acceptable purity was achieved with A_{260}/A_{280} and A_{260}/A_{230} ratios all greater than the threshold of 1.8 (Table 6.1). Furthermore, Qubit Fluorometric (Invitrogen) quantitation was used to determine the concentration of the RNA samples, which should be above the minimum threshold concentration of 30 ng μl^{-1} with a yield of at least 3 µg (Table 6.1). In addition to the quality and the quantity, because RNA is extremely susceptible to degradation, it was important to confirm that sufficiently intact RNA was obtained. This was assessed using an Agilent bioanalyser (Agilent technologies) by verifying RNA integrity (RIN) scores which were all greater than 7.0 with negligible evidence of degradation on the output traces (Fig 6.1).

Table 6.1. Assessment of RNA quality control. RNA sample purity was assessed using NanoDrop, RNA concentration was measured using Qubit and the integrity of RNA samples was assessed using a bioanalyser. RIN: RNA integrity, C: Control (wild type), D: *desK* mutant, E: Evolved desR strain (SHG01), T: *SAOUHSC_01312* mutant.

Sample	ID	Nanodrop 260/280	Nanodrop 230/260	Concentration (ng µl-1)	Sample volume (µl)	RIN
***S. aureus* WT**	C1	2.22	2.10	848	16	9.7
	C2	2.18	2.39	551	22	9.6
	C3	2.14	2.36	796	10	9.9
Δ *desK*	D1	2.15	2.28	1100	10	9.9
	D2	2.18	2.24	928	19	9.8
	D3	2.15	2.32	791	12	9.9
Evolved *S. aureus* (SHG01)	E1	2.19	2.23	510	15	9.1
	E2	2.20	2.14	888	22	9.8
	E3	2.18	2.15	930	12	9.9
Δ *01312*	T1	2.19	2.18	601	12	9.4
	T2	2.21	2.46	914	10	9.4
	T3	2.21	1.91	704	20	9.3

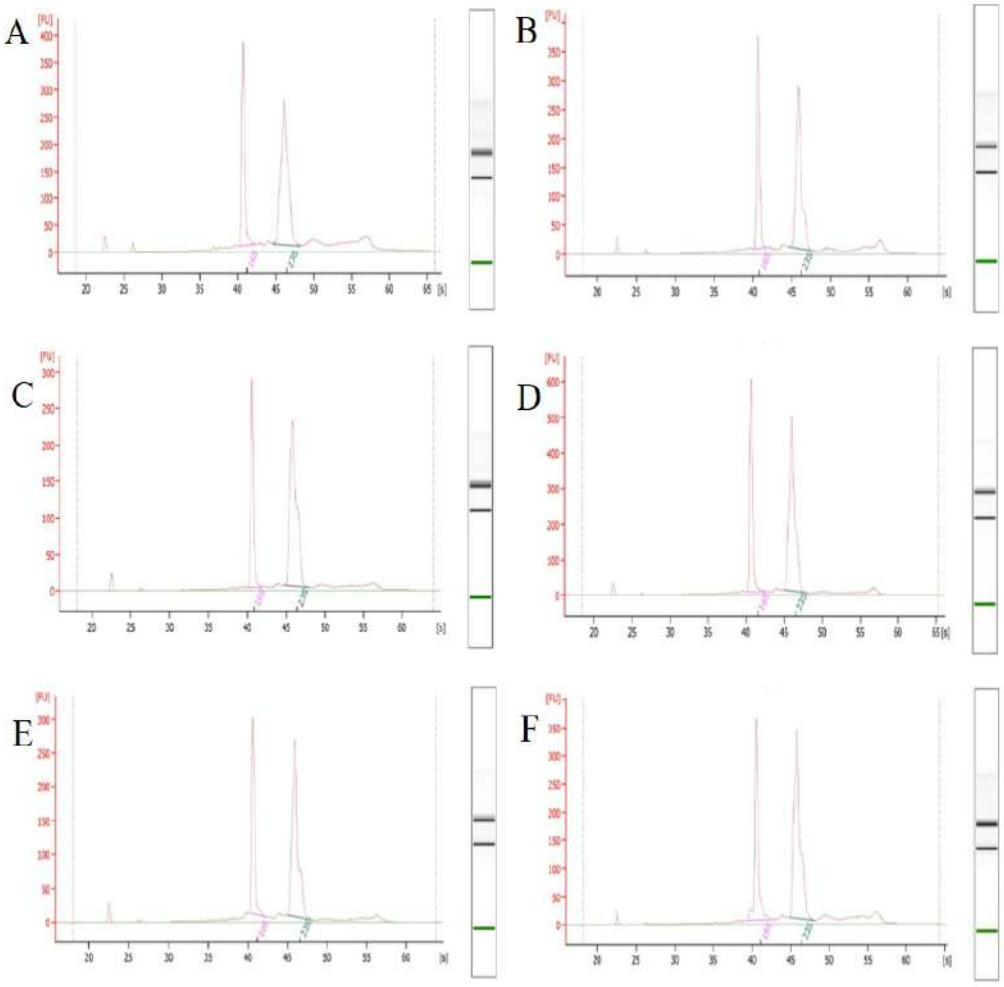
A
B
C
D
E
F

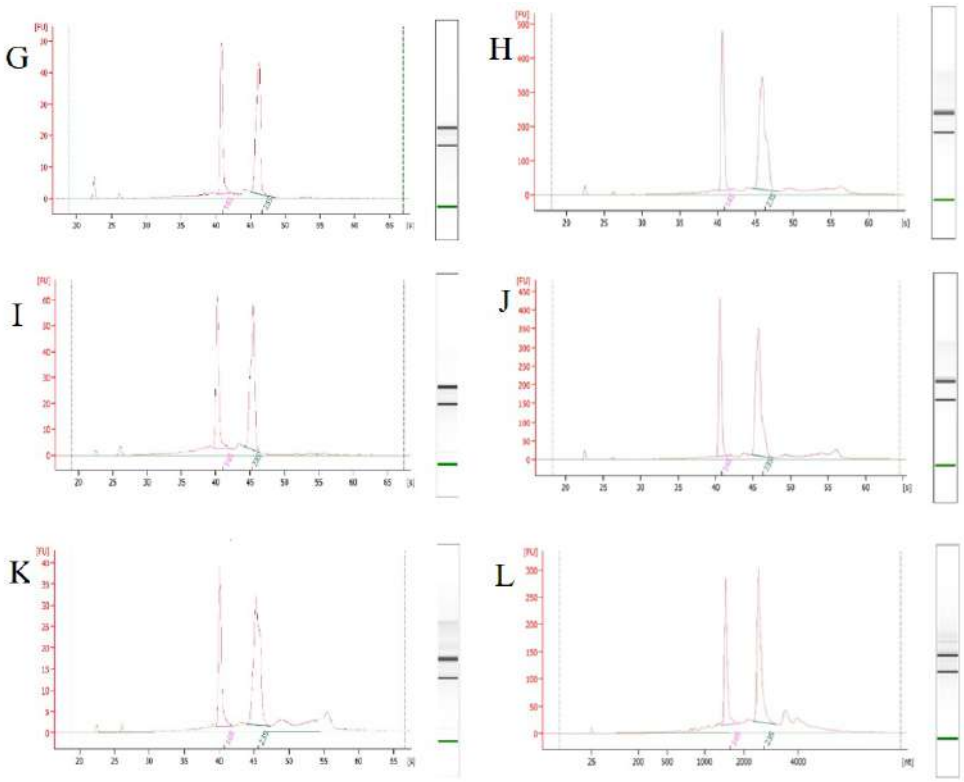

Figure 6.1: Bioanalyser traces of RNA samples processed for sequencing. RNA integrity using the Agilent bioanalyser. Intact RNA was determined by the presence of the two large ribosomal peaks of 23S and 16S RNA while other small peaks indicate 5S RNA, mRNA and their degradation. The three bands in gel image on the right shown the presence of 23S RNA, 16S RNA and the assay marker. (A, B and C) *S. aureus* wild type; (D, E and F) *desK* mutant, (G, H and I) Evolved *desR S. aureus* (SHG01) (J, K and L) *SAOUHSC_01312* mutant.

6.3.2 Alignment of reads to references sequences

Sequencing of the generated libraries was performed with the second generation Illumina HiSeq-2000. Following sequencing, reads were curated by adapter trimming, filtering and bioinformatically analysed by CGR. Transcript reads were aligned to the reference genome sequence using Tophat version 2.1.0 (Langmead and Salzberg, 2012). Tophat essentially uses Bowtie to align the reads; after aligning, Tophat takes all unmapped reads and splits them into shorter segments which are then realigned with Bowtie. The genome reference for *Staphylococcus aureus subsp aureus* NCTC 8325 was downloaded from the Ensembl genome database in FASTA format. The overall proportion of reads alignment to the *S. aureus* reference genome attained by TopHat ranged between 94.44% to 95.76% (Table 6.2). These data indicated a high consistency between samples for the number of and proportion of mapped reads. The results of the read alignments are summarised and shown in Table 4 and show that read mapping percentages vary from 94.44% to 95.76%.

Table 6.2. Summary of sequence alignment to the reference genome sequences. (Sample 1, 2 and 3) *S. aureus* wild type; (Sample 4, 5 and 6) *desK* mutant, (Sample 7, 8 and 9) Evolved *desR S. aureus* (SHG01) (10, 11 and 12) *SAOUHSC_01312* mutant**.**

Samples	Total Reads	Mapped Reads	% Mapped Reads	Reads Mapped as a pair	% Reads Mapped as a pair
Sample_1-C1	48,915,876	46,450,058	94.96	45,482,392	92.98
Sample_2-C2	46,866,584	44,262,221	94.44	43,156,650	92.08
Sample_3-C3	50,038,222	47,498,829	94.93	46,459,126	92.85
Sample_4-D1	49,166,394	46,832,819	95.25	45,770,680	93.09
Sample_5-D2	52,323,064	49,901,915	95.37	48,800,312	93.27
Sample_6-D3	42,513,266	40,290,930	94.77	39,302,756	92.45
Sample_7-E1	54,181,262	51,354,044	94.78	50,205,814	92.66
Sample_8-E2	45,606,190	43,222,430	94.77	42,248,890	92.64
Sample_9-E3	52,200,086	49,818,147	95.44	48,787,470	93.46
Sample_10-T1	44,308,384	42,335,953	95.55	41,392,298	93.42
Sample_11-T2	43,311,856	41,391,935	95.57	40,475,852	93.45
Sample_12-T3	58,308,182	55,836,031	95.76	54,626,208	93.69

6.3.3 Quantification of expression

Following RNA-Seq reads alignment, the datasets were translated into a quantitative measure of gene expression. This was achieved by HTSeq-count (Anders *et al.*, 2015), which counts the number of reads that map to a given gene. To perform this, a reference file that contains all the annotated protein coding genes was downloaded from the Ensembl database as a GTF file.

6.3.4 Differential expression analysis

The raw count data were converted into FPKM (Fragments per Kilobase per Million reads) values. The count numbers per gene were used during the subsequent differential expression analysis. The main processes of this analysis include: data variation assessment; data modelling; model fitting; testing; and DE (Differentially Expressed) gene detection. R (version 3.3.3) environment using the DESeq2 package was performed to analyse DGE (Differential Gene Expression) (Love *et al.*, 2014).

6.3.4.1 Assessment of variation in the count data

6.3.4.1.1 Pairwise scatterplot

To assess the correlation coefficients within and between sample groups for their poor or nonlinear intensity patterns, they were analysed using pairwise scatterplots. Normally, the differences between samples within groups are smaller than between samples from different groups. The plots (Fig 6.2A, B and C) shows the correlation within samples for group wild type, *desK* mutant and evolved *desR* (SHG01) strain, the plots indicate a fairly good reproducibility within these groups. All points are aligned along the diagonal, but there is a greater dispersion at the bottom left, corresponding to a small number of fluctuations. A greater variance was observed in the relationship between *SAOUHSC_01312* mutant samples (Fig 6.2D), which shows as points further from the principal diagonal, compared with other samples (Fig 6.2A, B and C). Across all sample groups means in Fig 6.5 (E), there is observable points (genes) deviating from the diagonal.

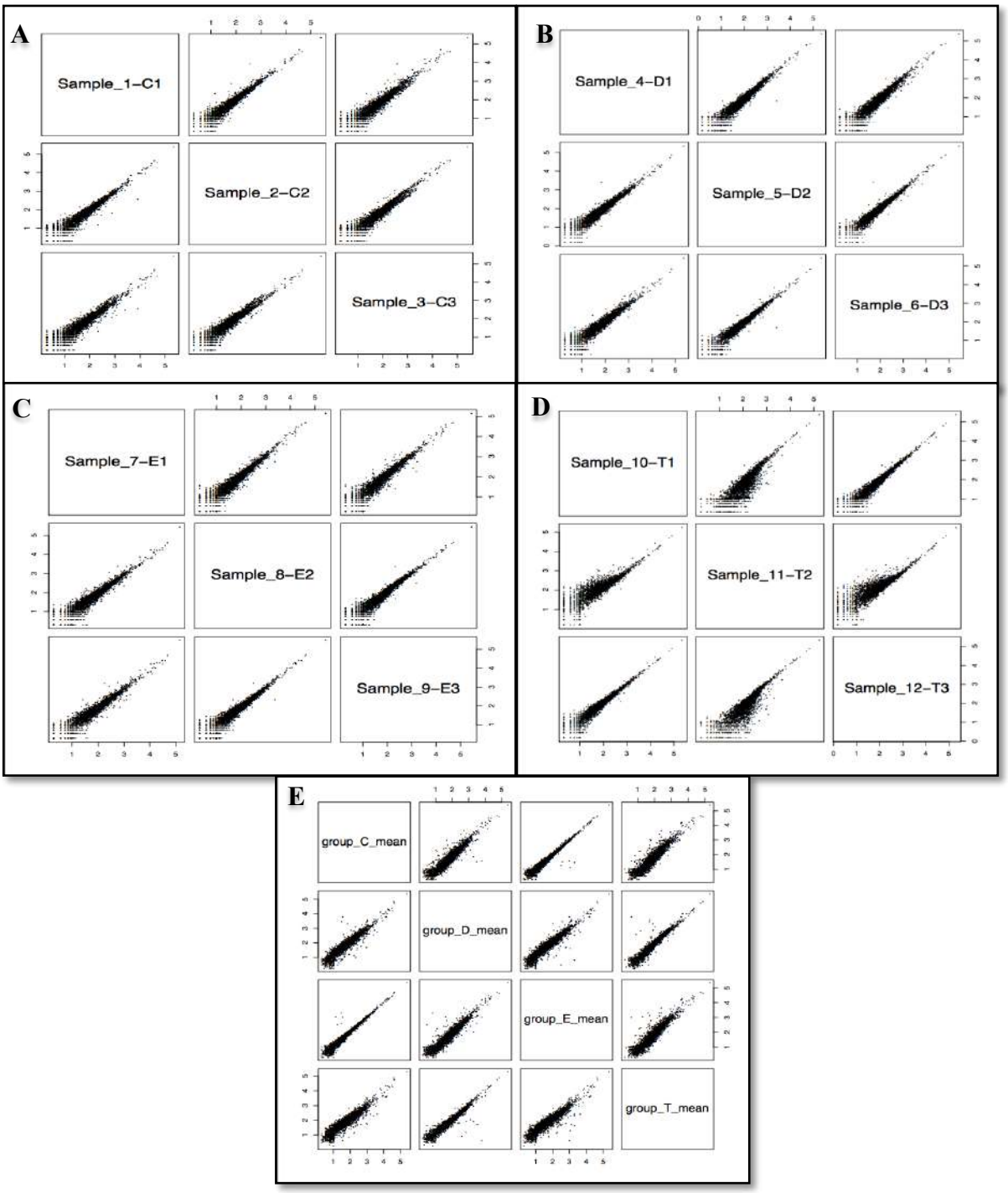

Figure 6.2. Pairwise scatter plots demonstrating the expression of genes for biological replicates within and between groups (log10 scale). (A) *S. aureus* wild type; (B) *desK* mutant, (C) Evolved *desR* (SHG01) (D) *SAOUHSC_01312* mutant and (E) showing the expression of mean values between the four groups.

6.3.4.1.2 Samples correlation Heatmap

A heatmap was also generated for all expression values to estimate the degree of correlation between and within sample groups. The plot (Fig 6.3) visualises the outcome of the variation assessment within and between samples groups. The diagonal blocks from bottom left to top right present the samples within group correlations for each of the two groups. The remaining blocks represent the correlations between two sample groups. From these, it is evident that broadly the samples show a good correlation within their group. For example, samples from group (E), which represent the evolved desR (SHG01) strain, were quite similar with moderate degree of correlation. The *desK* group (D) samples are also similar to each other with equivalent extent of similarity. The greatest variation in correlation within and between samples was determined for the *SAOUHSC_01312* samples (T) where there was a low correlation, relative to others in the entire set, with respect to sample 11 (Fig 6.3). The reasons for this are not clear given the parallel RNA processing and sample quality thresholds being met.

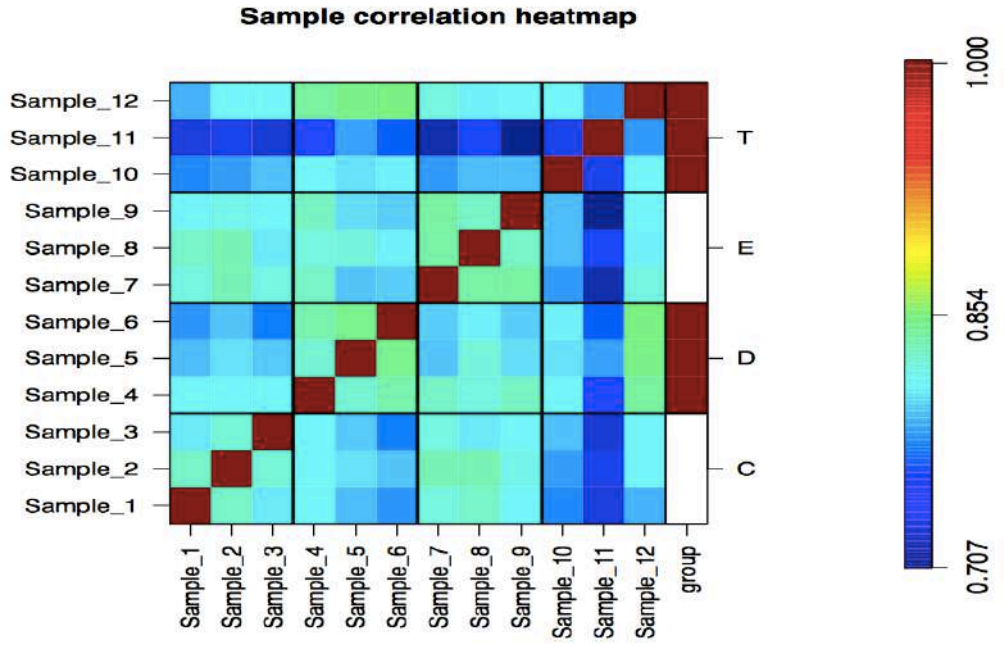

Figure 6.3 Correlation between and within sample groups. Heatmap illustrates the correlation between samples compared with every other samples. Red colour indicates a close correlation while dark blue colour indicates a more distant correlation between or within samples. (C) *S. aureus* wild type; (D) *desK* mutant, (E) Evolved *desR* (SHG01) (T) *SAOUHSC_01312* mutant.

6.3.4.1.3 Principle component analysis (PCA)

A principal component analysis (PCA) was also performed using log10 of read counts from the values of expression of all samples to give an overview of the differences between all samples tested. (Fig 6.4A) illustrates the first and second PCA component accounted for 91.8% and 2.07% of the variance in the samples respectively. Overall, the samples are closely correlated by PCA, with the exception of sample 11 from *SAOUHSC_01312* mutant (T) group. Additionally, it is shown that the control group (C) is very close to the evolved desR (SHG01) group (E) and this linked to the result from the heatmap correlation while both mutants *desK* and *SAOUHSC_01312* groups are quite similar except for one sample from the *SAOUHSC_01312* group. The second and third PCA components account for 2.0% and 0.99 % of the variance, respectively (Fig 6.5B). It can be noticed here that one sample from *SAOUHSC_01312* mutant group (T) appears to be an outlier. Each of the *SAOUHSC*_01312 samples shows a discrete separation from the WT and evolved strain, being more closely associated with the *desR* mutant strain, while the WT (C) group associates more closely with the evolved group (E) (Fig 6.5B).

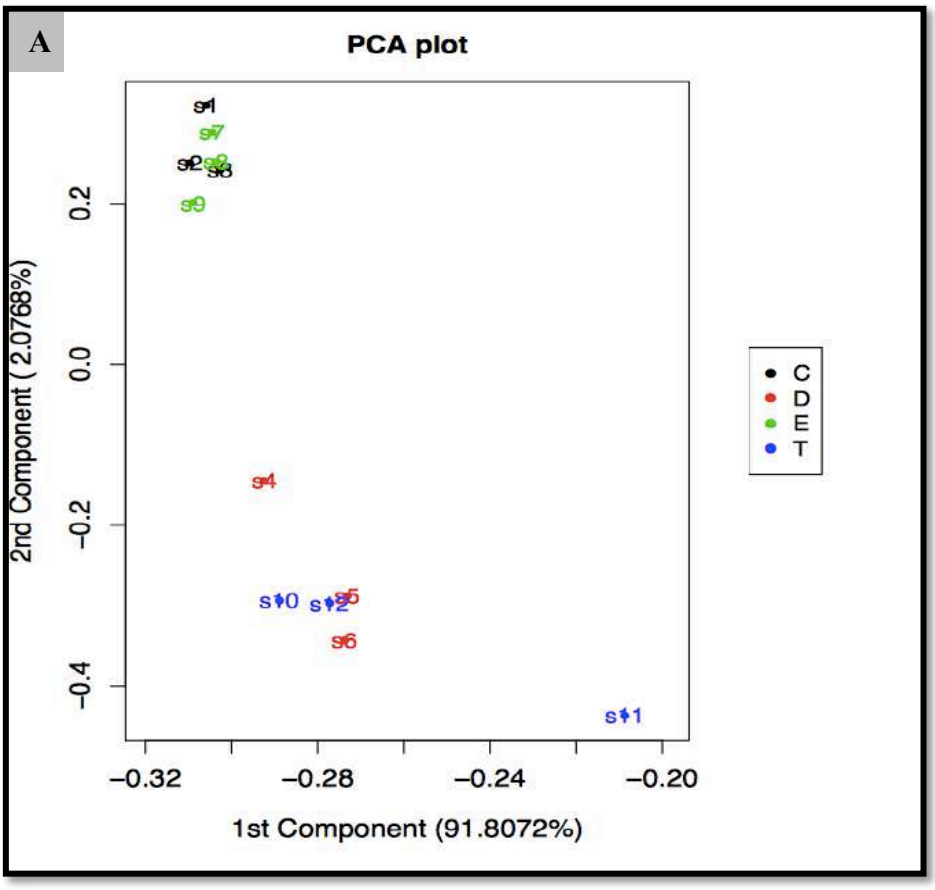

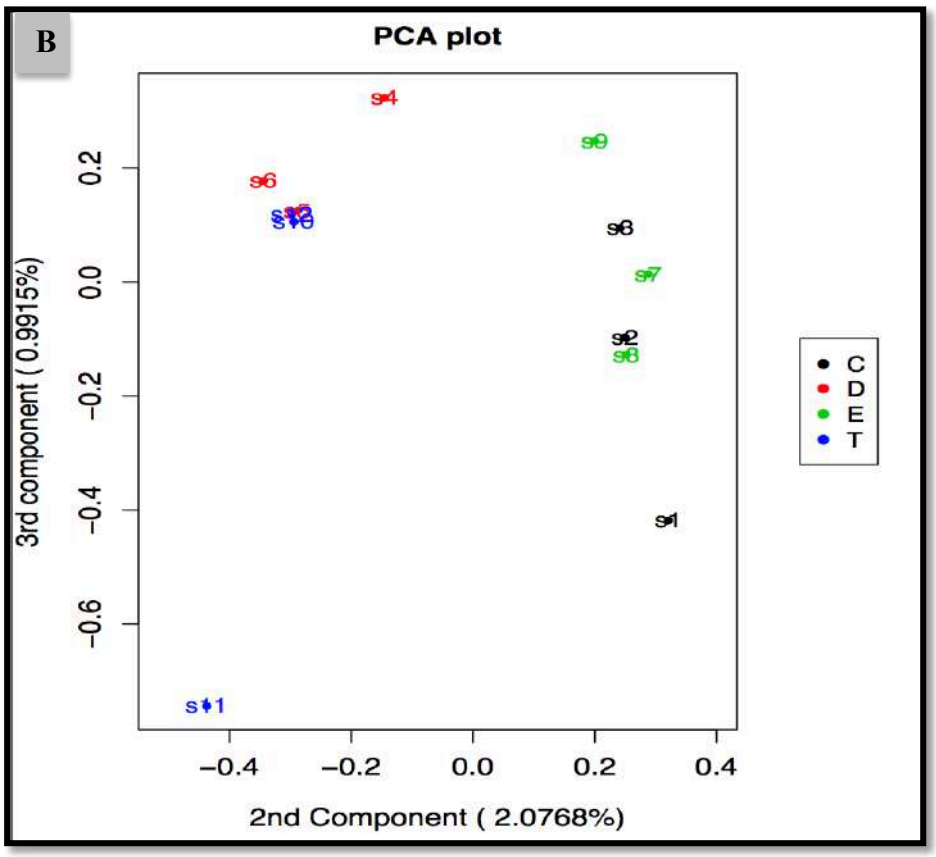

Figure 6.4 Principle Component Plot (PCP) shows the relationship between samples. (A) PC1 versus PC2 identifies clearly separated groups (wild type, C) and (Evolved strain, E) from (*desK* mutant, D) and (*SAOUHSC_01312* mutant, T). (B) PC2 versus PC3 shows that sample one from (01312 mutant strain T) is an outlier.

6.3.4.2 Differential expression genes detection

In comparison with wild type, a total of 308 DE genes were identified with the *desR* mutant (D, Table 6.3). Of these, 199 (64.61%) genes were up-regulated while 109 (35.38%) genes were down-regulated. In contrast, there were only 5 genes detected to be down-regulated in the wild type group (C) compared with the evolved *desR* (SHG01) strain group. Additionally, a total of 523 genes were found to be differential expressed between the wild type (C) group and *SAOUHSC_01312* mutant (T) meaning the latter had the higher number of expressed genes compared with the two other groups, *desK* mutant and evolved *desR* (SHG01) strain. Among these identified DE genes of the *SAOUHSC_01312* mutant, there were 298 (56.97%) up-regulated genes while 225 (43.02%) genes were down-regulated. Additionally, the *desK* mutant group (D) was compared with the evolved *des*R (SHG01) strain group (E) and 252 genes was detected. 99 (39.28%) of these were upregulated while 153 (60.71%) were down-regulated (Table 6.3). Notably, of the 308 genes that were differentially expressed in the *desK* mutant, 229 genes were similarly regulated as the *SAOUHSC_01312* mutant (Fig. 6.5).

Table 6.3. Numbers of differently expressed genes detected all contrasts. Wild type compared with *desK* mutant (D), evolved desR strain (E) and *SAOUHSC_01312* mutant (T). Further comparison is made with *desK* mutant (D) with evolved *desR* (SHG01) strain (E).

Sample ID	Total number DE	Number up-regulated	Number down-regulated
WT (C) Vs Δ desK (D)	308	199	109
WT (C) Vs Evolved (E)	5	0	5
WT (C) Vs Δ 01312 (T)	523	298	225
Δ desK (D) Vs Evolved (E)	252	99	153

A visualisation of up and down DE genes for all comparisons was performed (Fig 6.6) where Log_2FC was plotted against log2CPM (counts per million mapped reads). The DE genes were coloured as red dots on the plot while those are not significantly different were indicated by black dots. Significantly differentially expressed genes between the two groups were defined as those with FDR-adjusted P-value < 5%. Up-regulated transcripts were visualised as positive values while down-regulated transcripts were displayed as negative values symmetrically about the x-axis (Fig 6.6).

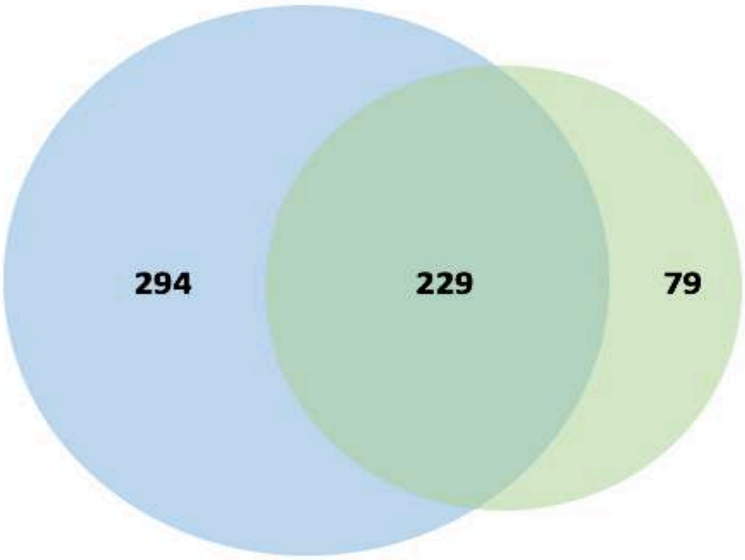

Figure 6.5 Venn diagram of the number of genes whose expression in the *desK* mutant have overlapping DE expression with the *SAOUHSC_01312* mutant, with values relative to wild type control. There were 229 genes similarly regulated in both mutant strains, 79 genes were DE expressed in the *desK* mutant (light green) and not DE in *SAOUHSC_01312* mutant (blue). Plus 294 genes were DE expressed in the *SAOUHSC_01312* mutant (blue) not DE expressed in the *desK* mutant (light green).

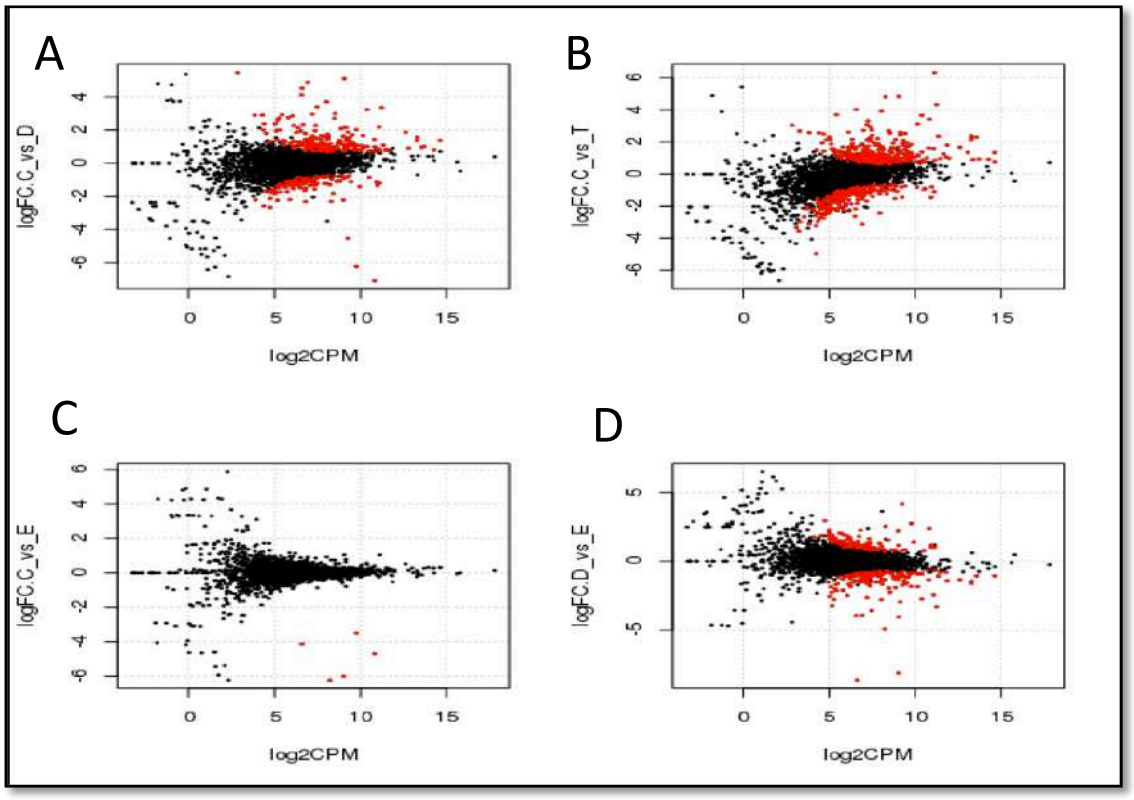

Figure 6.6 Differential gene expression plot. Each plot shows the log2FC against log2CPM values for all comparisons. (A) Wild type vs *desR* mutant (B) wild type vs *SAOUHSC_01312* mutant (C) wild type vs evolved *S. aureus* (D) *desK* mutant vs evolved *desR* (SHG01) strain. Significant DE genes display as red dots while non-significant DE genes display as black dots.

6.3.4.3 Functional classification of differentially expressed genes

Gene Ontology is an international standardised system used for functional classification of predicted genes. There are three main GO categories: cellular component, biological process and molecular function. The DE genes between wild type and the *desK* mutant and between wild type and the *SAOUHSC_01312* mutant were subjected to a GO enrichment analysis (Fig 6.7 and 6.8). These analyses showed a total of 50 significant terms in the cellular component, biological process, and molecular function categories. The proportion of those DE genes relative to each functional category and sub-category were determined to compare the mutants.

In the *desK* mutant dataset, 80% of the genes assigned to nitrate reductase complex were DE indicating a prominent pathway expression change.

Additionally, 41.18% assigned to cell wall and 8.31% with plasma membrane were DE (Fig 6.7A). Within the biological process categories of glycolysis and gluconeogenesis (75%) and (50%) of the genes were DE, respectively (Fig 6.7B), whereas among the molecular function category, electron transfer functions (53.33%) followed by haem binding (35.71%) were DE (Fig 6.7C).

In comparison, the *SAOUHSC_01312* mutant dataset revealed the top three cellular component GO terms represented by their proportion of DE genes were cell wall (52.95%), nitrate reductase complex (40%) and extracellular region (30.53%) (Fig 6.8A). Within the biological process GO terms, candidate DE genes were associated with glycolytic process (83%), glucose metabolic process (50%) and cytolysis (41.7%) (Fig 6.8B). Lipid binding (50%) and electron transfer activity (46.67%) were the main molucular functions (6.8C).

To determine the biological pathways activated in both the *desK* and *SAOUHSC_01312* mutants, pathways enriched with DE genes were identified using tools of the KEGG database. In the *desK* mutant, the enriched KEGG pathways were identified as oxidative phosphorylation (100%) and glycolysis/gluconeogenesis (71.80%) (Fig 6.8D). The same pathways were enriched in the *SAOUHSC_01312* ABC transporter mutant, plus ribosome synthesis (96.30%) that was not enriched in the *desK* mutant (Fig 6.7D).

A schematic diagram was drawn using KEGG to identify the DE genes in central pathways due to deletion of the *desK* gene. Linked genes found to be repressed included those involved in glycolysis/gluconeogenesis and tricarboxylic acid (TCA) cycle (Fig 6.9).

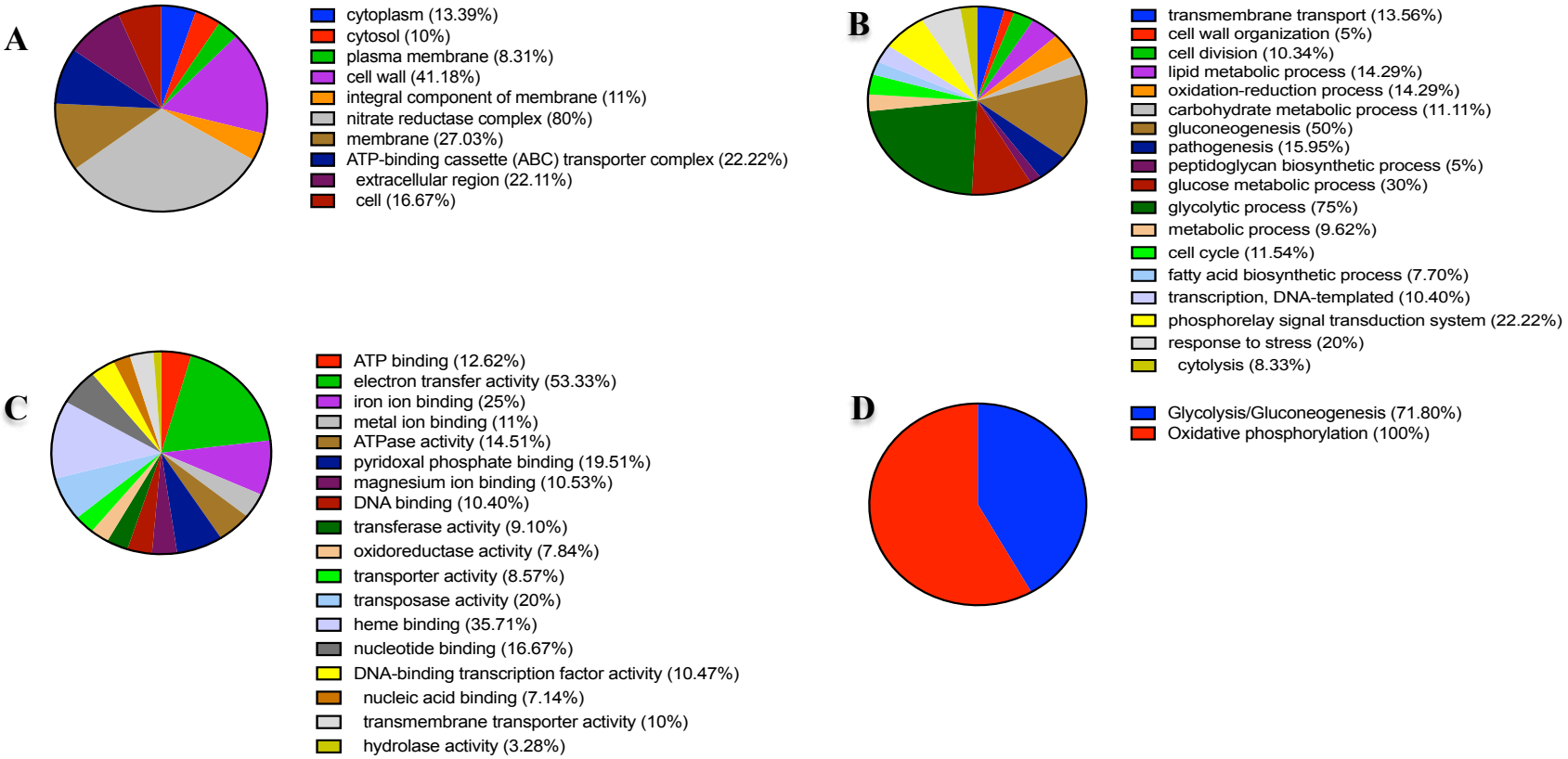

Figure 6.7 Gene ontology (GO) classification of the TOP 50 GO terms in a *desK* mutant and KEGG pathways of DE genes. Results are summarised in three main GO categories: (A) cellular component, (B) biological process, and (C) molecular function and according to KEGG mapper (D) KEGG pathways. The numbers in brackets represent the proportion of genes within each GO term.

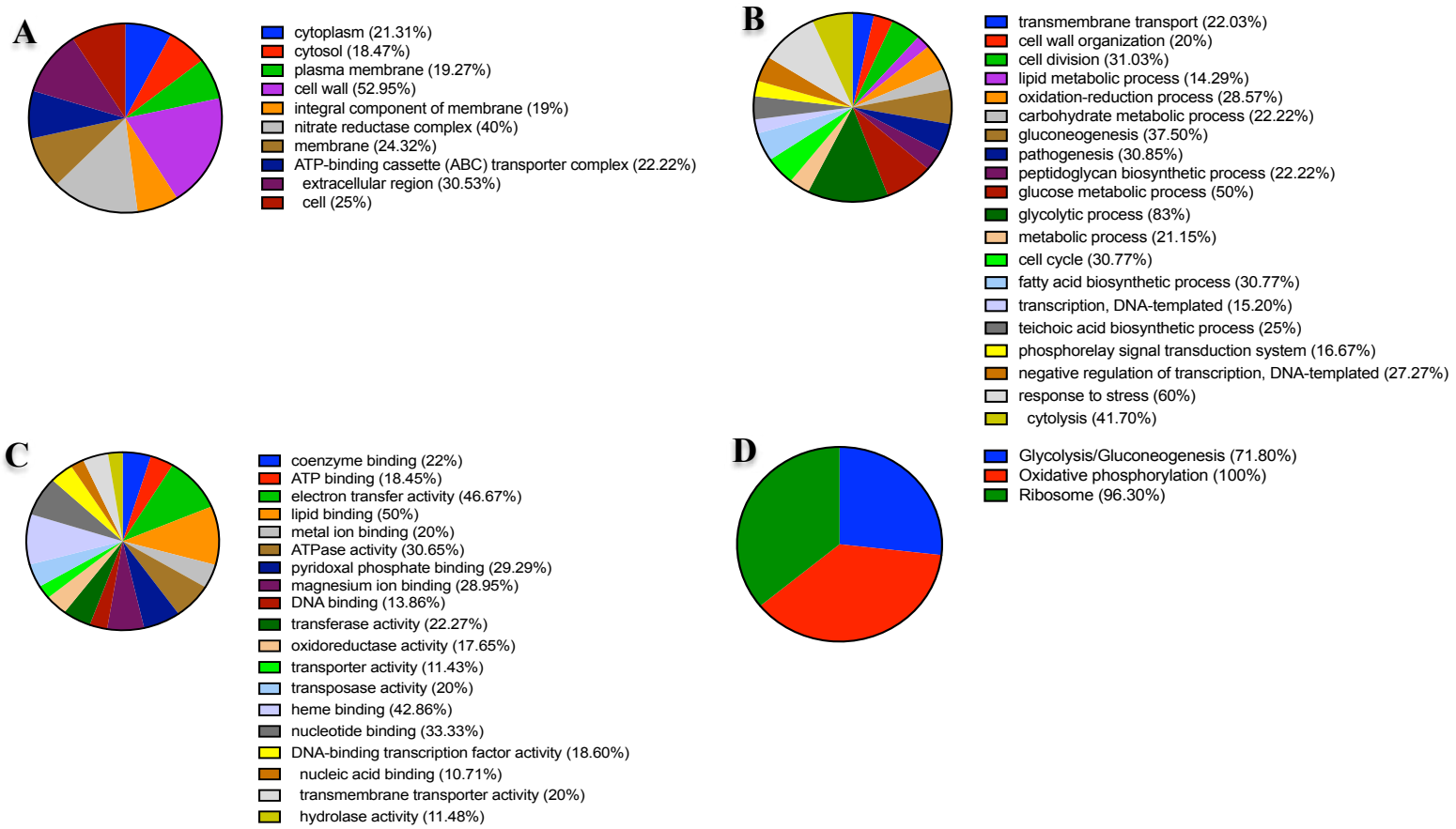

Figure 6.8 Gene ontology (GO) classification of the TOP 50 GO terms in 01312 putative transporter mutant and KEGG pathways of DE genes. Results are summarised in three main GO categories: (A) cellular component, (B) biological process, and (C) molecular function and according to KEGG mapper (D) KEGG pathways. The numbers in brackets represent the proportion of genes within each GO term.

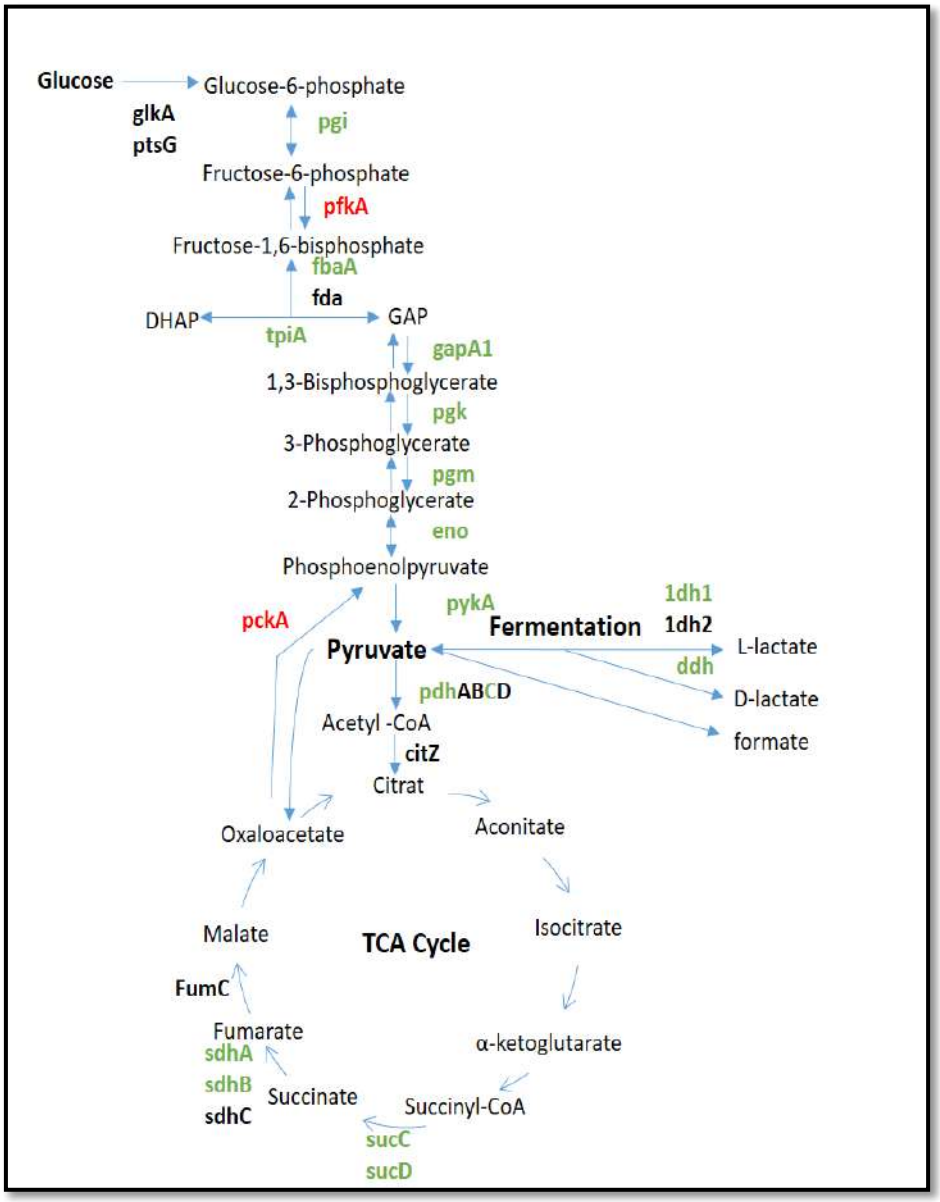

Figure 6.9 Effect of *desK* deletion on the expression of central metabolic pathways. DE genes affected in carbohydrate metabolism and the TCA cycle are shown after using KEGG mapper. Upregulated genes are shown in red, downregulated genes are shown in green and genes not changed shown in black.

6.3.4.4 The DesKR TCS regulon

As described above, five genes were DE regulated between the wild type strain (C) and the evolved *desR* (SHG01) strain (E). The contrast with the *desR* mutant strain is striking, even more so when those five genes significantly overexpressed in the evolved *desR* SNP strain include the four *desKR* operon genes: ABC transporter genes *SAOUHSC_01311* (11.24-fold) and *SAOUHSC_01312* (26.17-fold), the histidine kinase gene *desK* (17.39-fold), and response regulator *desR* (74.54-fold). In addition, the second transcriptional unit was that encoding the hypothetical protein *SAOUHSC_01315* (64-fold) (Fig. 6.10). This DE levels for the DesKR regulon independent of receiving the stimulus and these genes may be strongly induced by the antimicrobial (NRBS/PKs) produced by *S. epidermidis* B155.

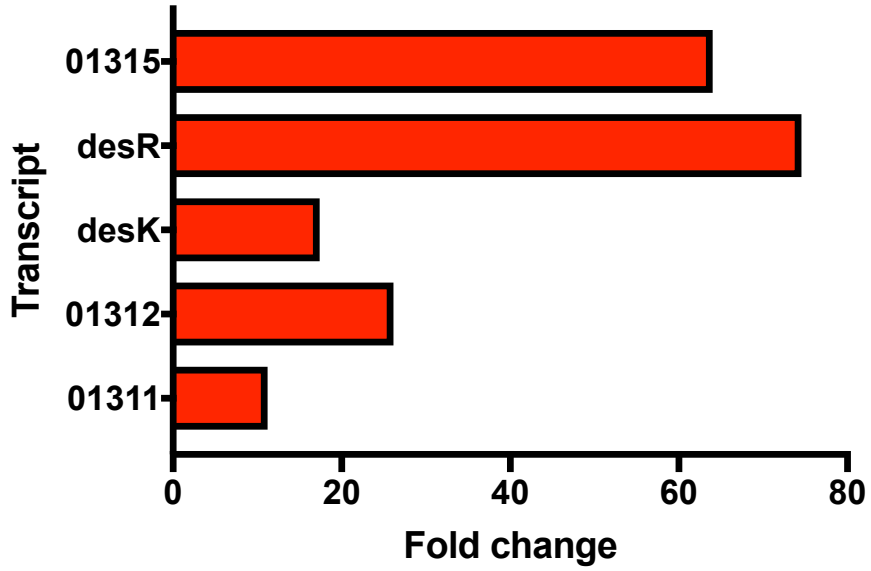

Figure 6.10 Fold change expression of the DesKR regulon in evolved *desR S. aureus* (SHG01) compared with wild type *S. aureus* SH1000. Genes were up regulated in evolved *S. aureus* compared with wild type including the *desKR* operon: *SAOUHSC_01311, SAOUHSC_01312*, *desK*, *desR*; and additionally the downstream, opposite strand-encoded *SAOUHSC_01315*.

Deletion of *desK* or *SAOUHSC_01312* genes dramatically altered expression with hundreds of DE genes identified. Gene lists were annotated and grouped for function using Database for Annotation, Visualisation and Integrated Discovery (DAVID) (Table 6.4). From the analysis, it was observed that genes associated with glycolysis and pyruvate metabolism were DE. Glycolytic genes that direct the conversion of phosphorylated sugar to pyruvate, including *pgm, gapA* and *pgk* exhibited lower

expression in both mutants compared with the wild type strain. Additionally, *ldh1* that encodes L-lactate dehydrogenase was downregulated in both the *desK* and *SAOUHSC_01312* mutant strains (10.13 and 20.25-fold, respectively).

Transcription of genes involved in TCA energy production were also affected by mutation of *desK* and *SAOUHSC_01312* genes. Two genes associated with succinate metabolism, *sdhA* and *sdhB*, were downregulated in both *S. aureus* mutant strains. Both *sucC and sucD,* which encode succinyl-CoA synthetase subunits beta and alpha, respectively, were downregulated in the *desK* mutant, while only *sucD* was downregulated in the *SAOUHSC_01312* mutant. All four genes *sdhA, sdhB, sucC* and *sucD* are critical in TCA cycle function. Genes encoding subunits of ATP synthase were downregulated in both mutants compared with their parent strain; these genes include the F_0F_1 type ATP synthase *atpABDCH* operon. ATP synthesis from ADP and P_i is catalysed by the ATP synthase complex (F_oF_1 ATPase) and is driven by the proton gradient generated by respiration (Vestergaard *et al.*, 2017).

The *desK* mutant showed significant downregulation of genes encoding proteins involved in nitrogen metabolism, including nitrate reductase (*narG/narH/narI*) (7.94, 5.03, 6.54-fold, respectively) and nitrite reductase (*nasD/nasE)* (29.04 and 44.32, respectively*)* while *ureC* encoding urease subunit C *and ureD/ureF* genes encoding the urease accessory protein were upregulated*.* The *SAOUHSC_01312* transporter mutant was observed to have lower expression of *nasE* encoding nitrate reductase (8.22-fold) but no DE of urease genes.

The expression of a subset of virulence genes implicated in host colonisation by *S. aureus* were observed to have different expression patterns between the two mutants. Many virulence factors were upregulated in both strains. For example, the genes encoding several cell wall-associated proteins: including Sdr proteins (*sdrC* and *sdrD*) *sdrD* only DE in *SAOUHSC_01312* mutant; fibronectin binding proteins (*fnbA* and *fnbB*) were upregulated in the *desR* mutant but *fnbA* was not significantly DE in the *SAOUHSC_01312* mutant. *IsdA* was upregulated in both mutants and is a broad specificity adhesin that increases cell hydrophobicity independent of its role in haem-iron acquisition (Clarke *et al.*, 2007); and clumping factor A (*clfA*) was

down-regulated in both mutants. The secreted alpha toxin (*hla*) was upregulated in the *desK* mutant while (*hld*) encoding δ-hemolysin was strongly downregulated (28.25-fold) in the *SAOUHSC_01312* transporter mutant. The expression of the serine protease genes (*splACED)* was increased in both mutants.

Inactivation of *desK or SAOUHSC_01312* genes led to altered expression of key regulatory loci including *agrA* (downregulated in the *desK* mutant) and *agrC* (downregulated in *SAOUHSC_01312* mutant). Transcription of the regulator gene *sarS,* was up regulated (2.94-fold) in *SAOUHSC_01312* mutant. *SarS* belongs to the SarA protein family of global regulators of virulence gene expression in *S. aureus* (Cheung *et al.*, 2004). Furthermore, both *desK* and *SAOUHSC_01312* mutants showed downregulated DE of *sarZ* (13.08-fold and 15.24-fold, respectively). SarZ is involved in the regulation of several virulence genes, particularly exoproteins, such as hemolysins and proteases (Ballal *et al.*, 2009). Transcription of *rot* was upregulated in both mutants; rot positively regulates *sarS* expression and genes encoding cell surface adhesins (*sdrC*, *clfB* and *spa*).

Genes involved in the stress response showed lower expression in both mutants compared with wild type. Methionine sulfoxide reductase A *msrA1* which provides protection against oxidative stress was downregulated in the *SAOUHSC_01312* transporter mutant. Genes encoding proteins conferring thermotolerance in bacteria, such as chaperone protein hchA and *clpP* were downregulated in both mutants while *clpX* was downregulated in only the transporter mutant. Expression of the *SAOUHSC_02670* gene encoding small heat shock protein HSP20 was significantly lower in the *desK* and *SAOUHSC_01312* mutant (34.05-fold and 29.04-fold, respectively). General stress protein 20U (*dps*) was also downregulated in both mutants. In addition, expression of *cspB* gene encoding for cold shock protein and the general stress protein genes *uspA1* and *uspA2* showed decreased in both mutants.

Associated with an implicated role in membrane function for the DesKR TCS, several genes associated with lipid metabolism were differentially expressed. Of note, the *cls1* gene involved in cardiolipin production was upregulated in the *desK* mutant

(22.94-fold). It was also expressed positively in the *SAOUHSC_01312* mutant but did not reach the threshold for DE significance. However, the expression of genes predicated to play a role in fatty acid metabolism were downregulated in the *SAOUHSC_01312* mutant compared with wild type, including (*fabG, fabH, fabF* and *acpP).* The *SAOUHSC_01312* mutant also showed increased expression of genes required for the transport, activation, and β-oxidation of long-chain fatty acids including *fadB* and *fadE.* The expression of *glpD* that encodes aerobic glycerol 3-phosphate dehydrogenase associated with glycerophospholipid metabolism was lower in both mutants. Transcription of *crtN*, which encodes squalene synthase in carotenoid biosynthesis was down regulated in the *desK* mutant.

Capsular biosynthesis polysaccharides genes *cap1A, 5B, 8C, 5E, 5J, 8F* showed increased DE in the *SAOUHSC_01312* mutant compared with wild type while only the *cap5J* gene was upregulated in the *desK* mutant. The *tagAB* operon for teichoic acid biosynthesis showed increased DE in the transporter mutant while only *tagA* was increased in the *desK* mutant. In contrast, cell divsion protein genes were downregulated in *SAOUHSC_01312* mutant including *divIB, ftsZ and mraZ*.

Several genes encoding proteins of amino acid production: leucine (*leuD)* and threonine *(thrC and ilvA2)* were upregulated in both mutants compared with wild type, while those for arginine biosynthesis (*argH* and *argG*) were downregulated. With respect to histidine biosynthesis, the *hisD* gene encoding histidinol dehydrogenase was upregulated in the *desK* mutant, while *hisA* encoding 1-(5-phosphoribosyl)-5-[(5-phosphoribosylamino) methylideneamino] imidazole-4-carboxamide isomerase was downregulated in the *SAOUHSC_01312* mutant.

Transcripts encoding iron and haem uptake functions were upregulated in both mutants, including *isdA,* while other downregulated genes include *hmp* and *fdhA.* The *sbnACEFG* genes encoding siderophore biosynthesis proteins were upregulated around 4-fold, only in the *SAOUHSC_01312* mutant.

Transcription of a broad range of functions were differentially regulated from mutation of the genes encoding the DesKR TCS and associated ABC transport system

of *S. aureus*. The wide range of genes with altered expression in the mutants is likely to be a consequence of multiple transcription activators with altered expression includin, SrrA and Agr TCS; repressors SarA, SarS, SarZ, MgrA, accessory sigma factor B, and SpoVG, CodY, SpxA.

Table 6.4. Genes differentially expressed in the *desK* and *01312* mutant strains relative to wild type *S. aureus* SH1000 (p <0.05, FDR corrected). Genes absent from one mutant strain are indicated with an (X) in fold change column.

	Gene name	Function	Fold change (log_2)	
Carbohydrate metabolism			**Δ desK**	**Δ 01312**
	fbaA	fructose-bisphosphate aldolase	-1.07	-1.31
	pykA	pyruvate kinase	-1.00	-1.33
	ldh1	L-lactate dehydrogenase	-3.34	-4.34
	eno	phosphopyruvate hydratase	-0.99	-1.38
	gapA	glyceraldehyde-3-phosphate dehydrogenase	-1.70	-1.96
	tpiA	triosephosphate isomerase	-1.75	-1.67
	pfkA	6-phosphofructokinase	-0.84	-1.00
	pgi	glucose-6-phosphate isomerase	-0.87	-0.66
	acsA	acetate--CoA ligase	X	+2.31
	pgm	2,3-bisphosphoglycerate-independent phosphoglycerate mutase	-1.70	-1.22
	pgk	phosphoglycerate kinase	-1.54	-1.75
	fdhD	formate dehydrogenase accessory protein	+1.05	X
	glkA	glucokinase	X	-1.08
	SAOUHSC_02267	fructokinase	+0.87	-1.28
Energy production and conversion	*mpsA*	NADH dehydrogenase subunit 5	-1.51	X
	sdhA	succinate dehydrogenase flavoprotein subunit	-0.85	-1.38
	sdhB	succinate dehydrogenase iron-sulfur subunit	-1.17	-1.52
	sucC	succinyl-CoA synthetase subunit beta	-1.16	-1.16
	sucD	succinyl-CoA synthetase subunit alpha	X	-0.98
	cydB	cytochrome d ubiquinol oxidase subunit II	-1.28	-1.28
	Ddh	D-lactate dehydrogenase	-1.60	-1.50
	pflB	Formate acetyltrasferase	-0.81	-1.33
	ald1	alanine dehydrogenase	X	+2.32
	qoxC	*cytochrome c oxidase subunit III*	-0.73	X
	atpA	*F0F1 ATP synthase subunit alpha*	-0.64	-0.96
	atpB	*F0F1 ATP synthase subunit B*	X	-1.08
	atpD	*F0F1 ATP synthase subunit beta*	X	-1.01
	atpC	*F0F1 ATP synthase subunit C*	X	-1.24
	atpH	*F0F1 ATP synthase subunit delta*	-0.91	X
	pflA	pyruvate formate-lyase 1 activating enzyme	-4.12	-4.04
Virulence associated	*lukD*	leukotoxin LukD	+1.63	X
	fnbB	fibronectin binding protein B	+1.32	+1.03
	fnbA	fibronectin-binding protein A	+0.96	X
	isdA	iron-regulated surface determinant protein A	+1.31	+1.33
	sdrC	fibrinogen-binding protein SdrC	+1.29	+1.97

	sdrD	fibrinogen-binding protein SdrD	X	+0.83
	fmtA	methicillin resistance protein	+1.28	+0.83
	spa	Immunoglobulin G binding protein A	X	+2.43
	clfA	clumping factor	-0.89	-1.62
	hld	delta-hemolysin	X	-4.82
	hla	alpha-hemolysin	+1.19	X
	eta	exfoliative toxin A	X	+0.91
	splA	serine protease	+2.66	+2.45
	splC	serine protease	+1.53	+1.14
	splD	serine protease	+1.70	+1.72
	splE	serine protease	+1.19	+1.20
Stress response	*msrA1*	methionine sulfoxide reductase A	X	-1.19
	hchA	chaperone protein HchA	-0.85	-0.97
	cidC	pyruvate oxidase	-0.47	X
	cspB	cold shock protein	-1.04	-1.40
	SAOUHSC_02670	small heat shock protein Hsp20	-5.09	-4.86
	clpP	ATP-dependent Clp protease proteolytic subunit	-0.79	-1.07
	clpX	ATP-dependent protease ATP-binding subunit ClpX	-0.75	X
	dps	general stress protein 20U	-0.81	-0.93
	asp23	alkaline shock protein 23	-1.25	-2.53
	uspA1	universal stress protein family protein	-0.73	-1.88
	uspA2	universal stress protein family protein	-1.19	-1.96
Lipid metabolism	*glpD*	aerobic glycerol-3-phosphate dehydrogenase	-1.42	-1.85
	fabG	3-oxoacyl-(acyl-carrier-protein) reductase	X	-0.76
	fabH	3-oxoacyl-ACP synthase III	X	-0.83
	fabF	3-oxoacyl- synthase	X	-0.81
	acpP	acyl carrier protein	X	-0.91
	Cls1	cardiolipin synthetase	+4.52	
	SAOUHSC_02772	short chain dehydrogenase	-1.99	-1.57
	fadB	3-hydroxyacyl-CoA dehydrogenase	X	+1.47
	fadD	acyl-CoA dehydrogenase FadD-like protein	X	+1.77
	fadE	long-chain acyl-CoA synthetase	X	+1.34
	fadX	Acyl CoA:acetate/3-ketoacid CoA transferase	X	+1.09
	crtN	squalene synthase	-1.24	X
	SAOUHSC_01830	glycerophosphoryl diester phosphodiesterase	X	+0.95
	SAOUHSC_01596	short-chain oxidoreductase family protein	+1.21	X
	plc	1-phosphatidylinositol phosphodiesterase	+2.56	+2.95
ABC transporter proteins	*glcB*	PTS system glucose-specific transporter subunit II ABC	-1.20	-0.85
	pmtA	ABC transporter ATP-binding protein	+1.23	+0.85
	cntB	peptide ABC transporter permease	+1.07	+1.30
	mntC	ABC transporter substrate-binding protein	-1.02	-1.15
	mntB	manganese ABC transporter permease	-1.49	-1.37
	SAOUHSC_03019	ABC transporter ATP-binding protein	+1.68	+1.13

Cell wall, cell division and cell envelope	*opp-2D*	peptide ABC transporter ATP-binding protein	X	+2.14
	glnQ	amino acid ABC transporter ATP-binding protein	-3.41	-2.74
	SAOUHSC_00169	peptide ABC transporter permease	X	+2.32
	cap1A	capsular polysaccharide biosynthesis protein	X	+2.24
	cap5B	capsular polysaccharide biosynthesis protein	X	+2.78
	cap8C	capsular polysaccharide biosynthesis protein	X	+1.48
	cap5E	capsular polysaccharide biosynthesis protein	X	+1.59
	cap5J	capsular polysaccharide biosynthesis protein	+1.11	+1.20
	cap8F	capsular polysaccharide biosynthesis protein	X	+1.52
	divIB	cell division protein	X	-0.68
	ftsA	cell division protein FtsA	X	-0.92
	ftsZ	cell division protein FtsZ	X	-0.79
	mraZ	cell division protein MraZ	X	-1.11
	tagA	teichoic acid biosynthesis protein	+0.82	+1.29
	tagB	teichoic acid biosynthesis protein	X	+1.34
	murG	undecaprenyldiphospho-muramoylpentapeptide beta-N-acetylglucosaminyltransferase	X	-1.07
	murF	UDP-N-acetylmuramoylalanyl-D-glutamyl-2, 6-diaminopimelate--D-alanyl-D-alanyl ligase	-0.90	-0.71
Amino acid production	*leuD*	3-isopropylmalate dehydratase small subunit	+1.63	+2.19
	ald1	alanine dehydrogenase	X	+2.31
	ilvA2	threonine dehydratase	+1.29	+1.62
	thrC	threonine synthase	+1.76	X
	argH	argininosuccinate lyase	-1.26	-1.53
	argG	argininosuccinate synthase	-2.27	-2.61
	hisA	1-(5-phosphoribosyl)-5-[(5-phosphoribosylamino)methylideneamino] imidazole-4-carboxamide isomerase	-2.90	X
	trpB	tryptophan synthase subunit beta	X	+1.07
	hisD	histidinol dehydrogenase	X	+1.87
	pyrB	aspartate carbamoyltransferase catalytic subunit	-2.01	-1.44
	pyrC	dihydroorotase	-0.74	-0.96
	metB	trans-sulfuration enzyme family protein	X	+1.08
Nitrogen metabolism	*narG*	nitrate reductase subunit alpha	-2.99	-2.56
	narH	nitrate reductase subunit beta	-2.33	X
	narI	respiratory nitrate reductase subunit gamma	-2.71	X

	nasD	Assimilatory nitrite reductase [NAD(P)H] large subunit	-4.86	X
	nasE	assimilatory nitrite reductase [NAD(P)H] small subunit	-5.47	-3.04
	nirR	nitrite reductase transcriptional regulator	-2.15	-1.65
	glnA	glutamine synthetase	X	-1.21
	arcC	carbamate kinase	+1.08	+0.93
	ureD	urease accessory protein	+0.82	X
	ureC	urease subunit alpha	+1.05	X
	ureF	urease accessory protein	+1.36	X
	hutH	Histidine ammonia-lyase	X	+1.87
Gene regulators	*sigB*	RNA polymerase sigma factor	X	-1.20
	sarS	accessory regulator-like protein sarS	X	+1.56
	sarZ	transcriptional regulator	-3.71	-3.93
	agrA	accessory gene regulator protein A	-0.74	X
	agrC	accessory gene regulator protein C	X	-1.02
	sarA	accessory regulator A	X	+1.02
	SpoVG	regulatory protein SpoVG	-1.49	-2.25
	rot	virulence factor regulator protein	+1.26	+1.28
	mgrA	MarR family regulatory protein mgrA	-1.06	-1.11
	codY	transcriptional repressor	X	-1.19
	srrA	DNA-binding response regulator	-1.29	-1.24
	spxA	transcriptional regulator Spx	X	-1.08
DNA replication, recombination, and repair	*pdhB*	pyruvate dehydrogenase complex, E1 component subunit beta	X	-1.03
	SAOUHSC_00699	deoxyribodipyrimidine photolyase	X	+1.02
	SbcD	exonuclease SbcD	X	+1.46
	SAOUHSC_01720	Holliday junction resolvase-like protein	-0.93	-1.05
	dinP	DNA polymerase IV	X	+1.00
	SAOUHSC_01734	recombination factor protein RarA	+0.87	+0.99
Transcription and translation	*rpsA*	30S ribosomal protein S1	-1.49	-1.54
	rplN	50S ribosomal protein L14	X	-0.83
	rplO	50S ribosomal protein L15	X	-0.91
	rpmB	50S ribosomal protein L28	X	-0.86
	rplL	50S ribosomal protein L9	X	-0.70
	glyS	glycyl-tRNA synthetase	-0.72	-1.03
	serS	seryl-tRNA synthetase	-0.84	-0.83
	tyrS	tyrosyl-tRNA synthetase	-0.77	-0.84
	fusA	elongation factor G	X	-0.89
	efp	elongation factor P	X	-0.71
Iron acquisition	*hemQ*	haem peroxidase	-0.66	-1.14
	feoB	ferrous iron transport protein B	-1.94	-1.66
	isdA	iron-regulated surface determinant protein A	+1.31	+1.33
	hmp	globin domain-containing protein	X	-0.84
	fdhA	formate dehydrogenase subunit alpha	-1.13	-1.17
	sbnA	2,3-diaminopropionate biosynthesis protein SbnA	X	+2.75
	sbnC	siderophore biosynthesis IucC family protein	X	+1.81

	sbnE	siderophore biosynthesis IucA family protein	X	+2.33
	sbnF	siderophore biosynthesis IucC family protein	X	+2.27
	sbnG	2-dehydro-3-deoxyglucarate aldolase	X	+2.16
Unknown function	*SAOUHSC_02426*		-1.20	-1.05
	SAOUHSC_00941		X	+3.34
	SAOUHSC_01503		+1.18	+1.11
	SAOUHSC_00270		+1.83	+0.79
	SAOUHSC_01834		-1.64	-1.06
	SAOUHSC_A02856		-2.70	-2.69
	SAOUHSC_02780		-3.23	-3.67

6.3.5 Confirmation of gene expression using qPCR

Validation of the RNA-seq data was performed by transcript quantification using qPCR for selected DE genes in the *desK* and *SAOUHSC_01312* mutants. For each selected gene, the fold changes in relative transcript abundance between wild type and mutant strains were determined and then compared with RNA-seq data. At least three biological and technical qPCR replicates were used for each gene**.** RNA integrity was assessed by gel electrophoresis prior to conversion to cDNA for qPCR.

The *isdA*, *sarZ* and *cls1* transcript levels and *isdA*, *sarZ* and *ldh1* transcript levels were assessed for *desK* mutant and *SAOUHSC_01312* mutant strains respectively. Relative expression was normalised against *rpoB*. All primers that were selected had efficiency values > 90% generating products of approximately 150 bp in length. The primers and their efficiency values are shown in Table 6.5.

Table 6.5 List of primers used for. qPCR.

Gene name	Primer sequences	Efficiency (%)	References
rpoB	F-GCGAACATGCAACGTCAAG R-GACCTCTGTGCTTAGCTGTAATAGC	97.0	(Moran *et al.*, 2017)
cls1	F-CGTATCAGTGGGCACAGCAA R-CAGACAGCGGTCTATTGGCA	96.35	This study
isdA	F-CAATCAAGCTGTAAGTG R-CCTAAAAGGGCAAGTGTTGCG	94.6	(Zhao, 2017)
sarZ	F-ATTCTGGAACACTGACACCAT R-CAGAAATTTCAGCAAGAGGGC	93.67	This study
ldh1	F-CGAAGCGTTCGATGTTGCG R-CAATTTGCGCTTTGCCCTCA	91.77	This study

The qPCR data obtained were in good agreement with RNA-Seq results for both *desK* and *SAOUHSC_01312* mutants showing very similar trends, which confirmed the reliability of sequencing data (Fig. 6.11 A&B). In the *desK* mutant, the fold level change in expression of *cls1* was lower in qPCR assays compared with RNA-seq, while *isdA* was slightly higher in qPCR (Fig. 6.11A). In contrast, *sarZ* showed greater downregulation in qPCR in both mutants (Fig. 6.11 A&B). Overall, the results from qPCR are consistent with RNA-seq data with respect to similarity of fold changes and direction of regulation.

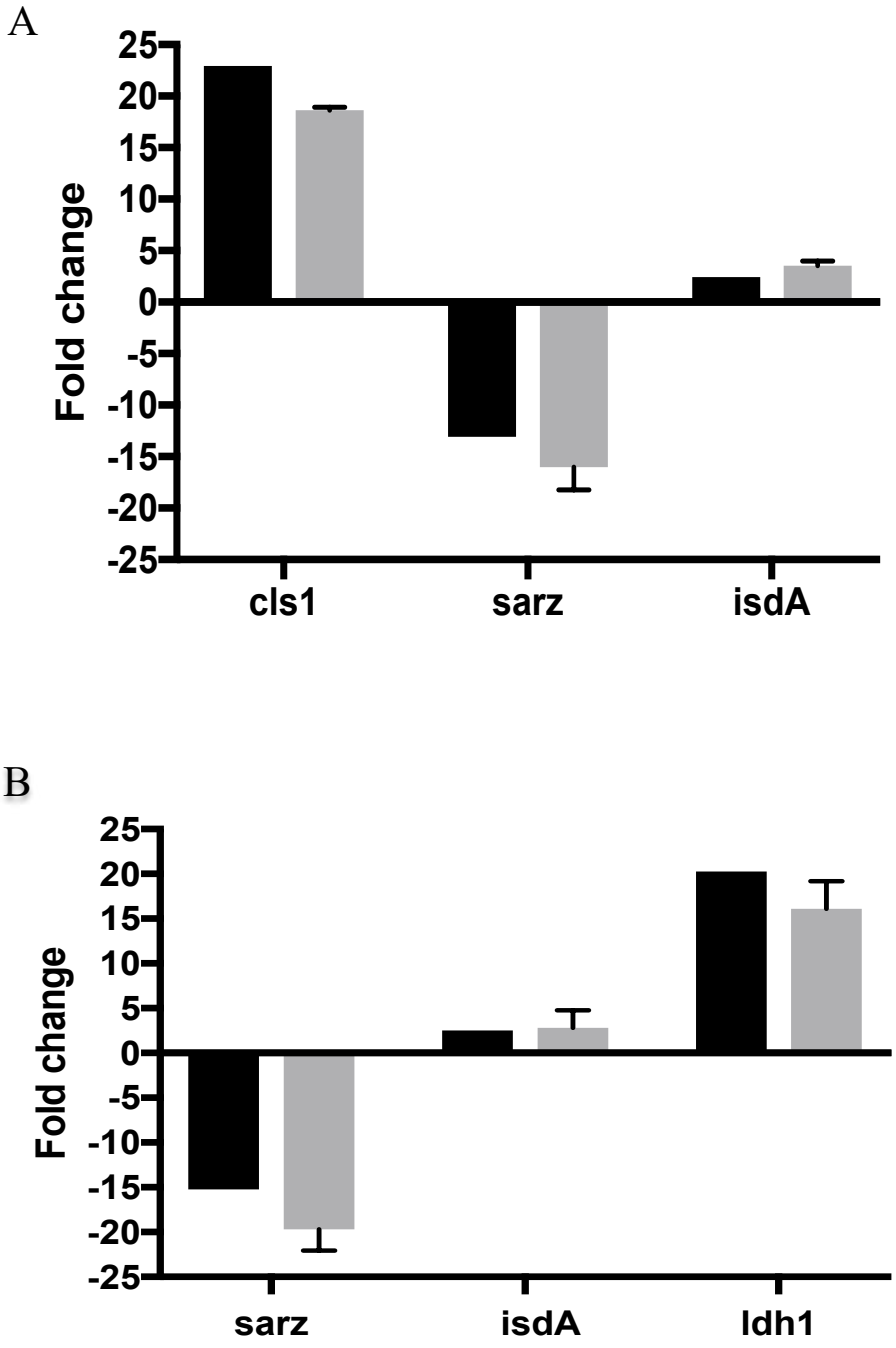

Figure 6.11 Differential expression of *cls1*, *sarZ* and *isdA* in the *desK* mutant (A) and *sarZ*, *isdA* and *ldh1* in the *SAOUHSC_01312* mutant (B) by qPCR. Black bars indicate the fold-level changes in gene expression from RNA-Seq data while grey bars indicates fold-level changes in gene expression from qPCR. Error bars represent the range of relative expression calculated using $2^{-(\Delta\Delta CT \pm SD)}$.

6.4 Discussion

Having established the importance of the DesKR TCS in *S. aureus* resistance to antimicrobial secreted by *S. epidermidis* B155, it was considered important to characterise the transcriptome profile of operon mutants compared with parental wild-type. For this analysis of *S. aureus*, the evolved resistance *desR* SNP strain (SHG01), a *desK* allelic replacement mutant and a deletion mutant of ABC transporter *SAOUHSC_01312* gene were compared with their isogenic parent.

Several RNA-Seq studies have revealed increased information content by depletion of ribosomal RNA to improve the quantitation of mRNA by RNA-Seq technology (Westermann *et al.*, 2012). Earlier bacterial transcriptome studies suggested accurate coverage requires a minimum of 2-5 million reads from an rRNA-depleted library (Westermann *et al.*, 2012). Furthermore, paired end sequencing is a powerful strategy that has enabled the characterisation and quantitation of bacterial transcriptomes with or without annotated genomes (Fang and Cui, 2011). There are many causes of variability within sequence replicates that may affect quality, such as variation between the individual lanes within a flow cell, variation from one flow cell to another (Fang and Cui, 2011) and library preparation effects (Bullard *et al.*, 2010).

Biological replicates of the *S. aureus* samples in this study revealed a lower correlation value within *SAOUHSC_01312* mutant group samples, which could be because biological variation from the library preparation process and the sequencing runs and usually biological variation are greater than technical variation (McIntyre *et al.*, 2011). However, biological replicates cannot be avoided because it is the only way to provide statistical power in the analysis of differential expression of genes.

RNA-Seq analysis of the evolved *desR* (SHG01) strain of *S. aureus* revealed that the expression of five genes was massively upregulated compared with wild type. No other significantly DE gene expression was identified. Notably, these five highly upregulated genes represent the four genes of the *desKR* operon; encoding

histidine kinase DesK, the response regulator DesR, the ABC transporter subunit genes *SAOUHSC_01311* and *SAOUHSC_ 01312*. In addition, the downstream monocistronic operon encoding the hypothetical protein SAOUHSC_01315. These data demonstrate that the *cls1* gene (SAOUHSC_01310) encoding cardiolipin synthesis was not significantly DE and would therefore not appear to be part of the DesKR operon or regulon.

The importance of ABC transporters in conferring resistance to antimicrobial drugs has been demonstrated in multiple studies. For example, the ABC transporter YxdLM was greatly induced by the presence of human cathelicidin LL-37 in *B. subtilis* controlled by the YxdJK TCS system (Pietiäinen *et al.*, 2005). Additionally, expression of the ABC transporter *VraDE* was the most strongly induced response of cells after treatment with α-helical CAMPs such as dermaseptin K4-S4 and ovispirin-1 (Pietiäinen *et al.*, 2009). These outcomes revealed that antimicrobial peptides can be very specific at activating stress sensors and their activation mechanisms are based on charge or structural properties of the peptides and their mechanism of action. Massively increased expression of the *SAOUHSC_01311-01312-desK-desR* operon in the *desR* (SHG01) strain supports that the sensing mechanism is co-expressed with the ABC transport genes in a stimulus-independent scenario. Whether this coexpression is always dependent on the transport functions of *SAOUHSC_01311-01312* requires further experiments but provides a TCS-linked mechanism of efflux for toxic compounds or accumulated host molecules. These results provide further support to genome sequencing identified SNPs in chapter 4 that indicated the *desKR* locus has a role in countering the antimicrobial products of *S. epidermidis* B155.

Transcriptome analysis identified 308 DE genes in the *desK* mutant and 523 DE genes in the *SAOUHSC_01312* mutant. Subsequent GO analysis was used because of its benefits in genome-wide expression studies to reduce complexity and highlight important biological processes (Young *et al.*, 2010). KEGG enrichment analyses were also performed to obtain further insights of the biological function of specific DE genes. TOP 50 enriched terms were identified according to GO

analysis of the DE genes between the *desK* mutant and *SAOUHSC_01312* mutant compared to wild type. Overall, there were many broad similarities in the key pathways with modulated expression with different numbers of genes DE in prominent categories of function. There were also clear differences indicating that abrogation of the activity via TCS or transporter was not evidently equivalent. For both mutants, nitrate reductase activity and cell wall function were the major classes of cellular components that were DE. For moleculer functions, electron transfer activity represented an enriched class of DE genes in the *desK* mutant while lipid binding was the most enriched pathway in the *SAOUHSC_01312* mutant. The main biological processes/KEGG pathways that showed consistency in term of major classes assigned belonged to the glycolysis/gluconeogenesis and energy production (oxidative phosphorylation pathway).

Inactivation of the *desK* or *SAOUHSC_01312* genes in *S. aureus* to different extents decreased expression of genes within major central metabolic pathways of oxidative energy production, including glycolysis, gluconeogenesis and TCA cycle. The downregulation of genes associated with carbohydrate metabolism, most likely glucose, and energy production. This decreased *S. aureus* oxidative metabolism includes gluconeogenesis genes (*gabA*, *pgi*, *pgk*) and the tricarboxylic acid cycle TCA genes (*sucCD*, *sdhAB*). Altered TCA cycle activity has been reported to affect the expression of staphylococcal virulence factors (Zhu *et al.*, 2011), antibiotic resistance (Nelson *et al.*, 2007) and the production of the main biofilm carbohydrate, polysaccharide intercellular adhesin (PIA) (Gaupp *et al.*, 2010). TCA cycle inactivation delays cutaneous ulcer resolution in soft tissue-infected mice (Somerville *et al.*, 2002). These results corroborated the results of Kim et al. who reported that lower expression of genes involved in energy-providing pathways in a *desR* mutant of *S. aureus* Mu50, supporting a reduced oxidative energy efficient generating strain compared with its parent (Kim *et al.*, 2016). In addition to oxidative metabolism gene repression, genes encoding proteins of anaerobic energy production and fermentation, including lactate dehydrogenase *ldh1,* were found to be highly downregulated. Lactate dehydrogenase catalyses the conversion of pyruvate to lactate. The L-lactate

produced by this process allows *S. aureus* to maintain redox homeostasis , which is important during nitrosative stress caused by activated phagocytes and is essential for virulence (Richardson *et al.*, 2008). The earlier study of Mu50 showed that the lactate dehydrogenase protein level was lower in a *desR* mutant relative to parent strain. This decreased activity may explain why the *desR* mutant has reduced virulence, owing to reduced survival from the radical nitric oxide (Kim *et al.*, 2016). The concomitant downregulation of anaerobic metabolism might indicate a general stress management problem for the cell or a redirection of metabolism through alternative pathways such as substrate level phosphorylation.

The likelihood of alternative pathways for energy production is supported further. *S. aureus* senses the availability of oxygen and can adapt to a dynamic host environment with oxygen limitations by employing nitrate respiration with nitrate as the terminal electron acceptor (Burke and Lascelles, 1975). The *nasDE/narGHI* genes, encoding the nitrite/nitrate assimilation system and *nirR* encoding nitrite reductase transcriptional regulator were markedly downregulated in both mutants, particularly the *desK* mutant. Genes encoding urease (*ureDCF*) and carbamate kinase (*arcC*) were up regulated in the *desK* mutant, which may assist production of energy and ammonia to counteract reduced pH. Nitrate is an important nitrogen source for many bacteria. During aerobic growth, bacteria can use nitrate and nitrite as the sole nitrogen source. Nitrate is converted through nitrite to ammonium by assimilatory nitrate and nitrite reductases. The resulting ammonium is then incorporated into amino acids via the glutamine synthetase-glutamate synthase action (Lin and Stewart, 1996). Previous study has demonstrated that the YhcSR TCS may sense nitrate and thereby contribute to the modulation of the nitrate respiratory pathway (Yan *et al.*, 2011). The reduced expression of nitrate respiratory pathway genes by deletion of *desK* may indicate the DesKR TCS regulates a core function that when disrupted alters metabolism in a general manner.

S. aureus TCS and SarA family proteins are widely described for their control of virulence factor expression (Chaves-Moreno *et al.*, 2016). The *SAOUHSC_01312*

mutant has increased expression of the *sarA* locus that might be responsible for the higher expression of *fnbB,* encoding fibronectin binding protein and *sdrC* encoding fibrinogen-binding protein (Chien *et al.*, 1999; Dunman *et al.*, 2001). SarZ activates *mgrA* (SarA family protein) transcription and the *agr* RNAIII molecule and deletion of *sarZ in S. aureus* increases transcription of *spa,* encoding surface protein A (Tamber and Cheung, 2009). In the study here, *sarZ* and *mgrA* transcription was significantly downregulated in both the *desK* and SAOUHSC_01312 mutants, which may have produced increased transcription of *spa*, in the *SAOUHSC_01312* mutant. SarS is a 250-residue SarA-family protein that activates *spa* transcription and was upregulated in the *SAOUHSC_01312* mutant. The complexity of identifying a single gene with multiple regulators is not simply unraveled, whereby inactivation of *desK* and *SAOUHSC_01312* genes reduced *agr* transcription, *agrA* was lower in the *desK* mutant while *agrC* and *hld* was decreased in the *SAOUHSC_01312* mutant where *hld* is encoded within the *agr* locus and is derived from translation of RNAIII, the effector molecule of *agr* (Sakoulas *et al.*, 2002). Furthermore, expression of *agrA* is also altered in a *sarZ* mutant in comparison with the wild-type (Tamber and Cheung, 2009). This may mean there is a link between the central functional role of the DesKR TCS and SarZ. The SarA-family protein Rot is another virulence regulator and was upregulated in both mutants. Rot negatively regulates genes encoding secreted proteins such as hemolysins (Said-Salim *et al.*, 2003).

Of particular interest, the *desK* mutant exhibited a very high expression level of *cls1* gene transcription that encodes a cardiolipin synthase. In *S. aureus*, there are two cardiolipin synthases, *Cls1* and *Cls2* (Koprivnjak *et al.*, 2011; Tsai *et al.*, 2011). An earlier study showed that *cls2* encodes the major cardiolipin synthase and contributes to membrane accumulation of cardiolipin lipid under normal and high salt conditions. However, *cls1* had an essential role under stress conditions (Tsai *et al.*, 2011). A separate study proposed that *cls1* was generated from *cls2* by gene duplication after the divergence of the genus *Staphylococcus* and that the alternative cardiolipin synthase encoded by this gene confers improved survival in response to acid stress (Ohniwa *et al.*, 2013). While there is no known reason for increased expression of cardiolipin in the *desK* mutant, it could be that

disruption of *desK* gene indirectly affected cardiolipin synthase expression in response to stress from disrupted metabolism, where temperature was previously reported as a stimulus (Bernal *et al.*, 2007). The *SAOUHSC_01312* mutant did not reveal a significant change in the expression of cardiolipin but it showed downregulation of *fabG*, *fabH* and *fabF* genes. These genes are involved in the type II fatty acid synthesis (FAS) pathway and they encode for enzymes involved in the assembly of important cellular components in the bacteria including lipopolysaccharides, lipoproteins, phospholipids, mycolic acids and the cell envelope (Park *et al.*, 2007). The reduced gene transcription of these enzymes might be required to modify permeability of the lipid bilayer and increase its stabilisation, which supports a potential role of the *SAOUHSC_01311-01312-desk-desR* operon in some unknown aspect of membrane function. One or many key processes could be affected in the *desK* mutant, such as active transport of solutes, passive transport of hydrophobic molecules and protein-protein interactions (Chung *et al.*, 2013). If this disruption occurred in the *SAOUHSC_01312* mutant, then any antimicrobial such as that produced by *S. epidermidis* B155 might more easily enter the cells via passive transport. In chapter 5, it was revealed there was a SNP within the *fabI* gene in the *S. aureus* evolved strain (SHG02), supporting a role of fatty acid synthesis together with DesKR TCS activity in resistance of *S. aureus*. Genes of the fatty acid degradation *fad* operon (*fadB*, *fadD*, *fadE* and *fadX*) were upregulated in the *SAOUHSC_01312* mutant. The *glpD* gene encoding glycerophospholipid biosynthesis was lower in both mutants compared with wild type. *S. aureus* can change its membrane lipids to counteract the effects of skin fatty acids. A recent transcriptional study of *S. aureus* in response to sapienic acid revealed that cell membrane glycerophospholipid biosynthesis genes were down regulated while fatty acid degradation genes were upregulated which they combined together supporting that the sapienic acid is detoxified and incorporated into membrane lipids and lipoproteins in staphylococci (Moran *et al.*, 2017).

Cold shock protein gene *cspB* was downregulated in both mutant strains compared with wild type and may contribute to the loss of pigmentation. Production of carotenoid pigment in *S. aureus* is associated with the cold shock

proteins of *S. aureus.* The loss of cold shock protein CspA can decrease gene expression of *crtN* encoding 4,4′-diaponeurosporene in pigment biosynthesis and the alternative sigma factor SigB (Katzif *et al.*, 2005). Notably, expression of the *crtN* gene was lower in the *desK* mutant while *sigB* expression was decreased in the *SAOUHSC_01312* mutant, which supported that lower expression of cold shock protein related to pigment synthesis rather than temperature. Small heat shock protein Hsp20 was strongly downregulated in both mutants compared with wild type. This gene is dirctly located downstream of *sarZ* which was downregulated and may thereby affect the Hsp20 gene. Methionine sulfoxide reductases are enzymes modifying oxidised methionine residues. A mutant lacking MsrA2 was more sensitive to oxidative stress with decreased survival in mice (Michalik *et al.*, 2017). MsrA1 also exhibited decreased expression level in the *SAOUHSC_01312* mutant. The transcriptional regulator Spx is proposed to be required for the MSRA1/MSRB upregulation in *S. aureus* (Singh *et al.*, 2018) and was downregulated in the *SAOUHSC_01312* mutant. Downregulation of Dps and MsrA proteins were previously shown for the *desR* mutant (*SAV1322*) of Mu50 compared with wild type. However, their study revealed there was a lack of correlation between transcriptome and proteome data (Kim *et al.*, 2016). Several stress genes showed down regulation, such as *hchA* encoding chaperone protein and *clpP* encoding ATP-dependent Clp protease proteolytic subunit. Clp proteases play a key role in bacterial adaptation to multiple stresses by their degradation of accumulated misfolded proteins (Jenkins *et al.*, 2013). ClpL, which is involved in temperature tolerance is downregulated in a SarA mutant (Dunman *et al.*, 2001). Downregulation of these genes may refer to stress response genes being upregulated in stationary phase, while in log phase many ribosomal proteins are abundantly expressed (Thompson *et al.*, 2003). In *E. coli, hchA* mutants showed a reduced ability to survive in deep stationary phase relative to wild type (Mujacic and Baneyx, 2006).

The presented results confirm involvement of the DesRK operon in the resistance of *S. aureus* to the novel antimicrobial produced by *S. epidermidis* B155 and suggest the role of the regulon in a key cellular process executed via the ABC transporters with potential involvement of SAOUHSC_01315. This key function

is evident in the operon mutants which have defects in energy production, lipid methoblism and regulation of virulence factors.

Chapter 7: General discussion and future directions

7.1 Key findings and recommended future work

Competition between microorganisms is often mediated through bioactive metabolites synthesised by bacteria. These secondary metabolites may be essential under competitive stress and for bacteria to persist stably in these environments. Staphylococci are known to produce a wide range of antimicrobials to interfere with each other and impede growth of other bacteria. The interactions between different staphylococci is of particular interest as these molecules appear to be important colonisation factors (Otto, 2010). The starting point for this study was the screening of antimicrobial activity among coagulase-negative staphylococcal (CoNS) isolates, particularly *S. epidermidis* and their ability to restrict *S. aureus* growth. The screening assay described here allowed for rapid detection of secreted antimicrobials by these bacteria that may be important for competitive interactions. In ***Chapter three***, it was identified that many CoNS strains were able to inhibit the growth of *S. aureus* strains demonstrating potentially important roles of a broad range of staphylococcal species interactions in driving *S. aureus* distribution in human body. This supported previous studies that reported the interactions between bacteria colonising the anterior nares based on culture dependent studies (Wos-Oxley *et al.*, 2010). Libberton *et al.,* reported that among nasal bacteria, *S. epidermidis* and *S. hominis* were the species found to be most negatively associated with *S. aureus* (Libberton *et al.*, 2014). The results here showed that *S. epidermidis* and *S. capitis* were the most strongly inhibitory towards all *S. aureus* tested strains, including SH1000, Newman, USA300 and B32. Also, trait variation was evident, whereby not all strains of a given species could produce or induce antibiotic production to affect all of the tested *S. aureus* strains. This can be due to absence of genes for inhibitor biosyntheis or the lack of strong effects of interacting bacteria related to specific signals known as competitor sensing (Cornforth and Foster, 2013). From the results here further research may make it possible to exploit the inhibitory mechanisms of these staphylococcal species, either alone or in synergistic combinations with each other or other antimicrobial compounds.

The primary aim of the research study was to experimentally test whether *Staphylococcus* species can evolve during their interaction with respect to either antimicrobial production or resistance and what range of molecular changes occur. Due to the frequent cooccurrence of *S. aureus* and *S. epidermidis* colonising the same human niches, these species may exhibit extensive inter-species interactions. The strain *S. epidermidis* B155 that produces an unidentified inhibitor and *S. aureus* SH1000 strain were chosen to identify the possible species interactions. Both species were cocultured in *vitro* using either planktonic liquid batch culture or sessile culture on agar plates. Both methods showed that at beginning of the growth experiments, *S. aureus* had a reduction in its population size relative to *S. epidermidis* B155 producer strain which showed a greater fitness suggesting benefits of toxin production. This could support the idea that induction of antibiotic activity is occurring as is reported among bacterial species during interspecific interactions. Further experiments are required to investigate if this occurs in this scenario. It was demonstrated previously that the abundance of *S. aureus* causes an increase in *S. epidermidis* population on the skin through activation of the immune system and antimicrobial peptide production(Cogen *et al.*, 2010). A prior study showed that simultaneous prevalence of both *S. epidermidis* and *S. aureus* during AD disease flares indicated a correlation between these staphylococci and it was suggested that increased *S. epidermidis* might reflect an antagonistic mechanism to control *S. aureus* (Kong *et al.*, 2012). It was hypothesised that competition between producer strain and sensitive strain would subject the sensitive strain to strong selection pressure for resistant clones to emerge. By transferring the community every day to fresh growth medium, it was found that *S. aureus* successfully evolved resistance to *S. epidermidis* B155 with an increased yield of *S. aureus* after several days. Emergence of resistance in *S. aureus*, led to the experiments being stopped at day 15 in the case of planktonic culture and day 8 for sessile agar culture.

Within communities, *S. aureus* resistance emerges to several antibiotics by acquisition of determinants via HGT of MGEs (Jensen and Lyon, 2009). Development of resistance can also be accrued in single cells by mutations that alter drug binding sites or by increasing expression of endogenous efflux pumps.

Single mutations confer resistance of *S. aureus* to different antimicrobials, such as fluoroquinolones and rifampin (Friedman *et al.*, 2006). Multiple mutations, such as changes in *walKR, vraSR, rpoC* and *dlt* genes are required to achieve a higher level of resistance to vancomycin and daptomycin resistance (Foster, 2017). To capture the genetic changes accrued in both *S. aureus* SH1000 and *S. epidermidis* B155, whole genome sequencing was performed for both species selected from different days of the coculture (described in ***Chapter four***). Importantly, *S. aureus* resistance clones showed single nucleotide changes in either the sensor histidine kinase *desK* or response regulator *desR* comprising the DesKR TCS system where both genes are located downstream of ABC transporter genes which may be controlled by the DesKR TCS. Several resistance mechanisms in *S. aureus* were identified by mutations in TCS genes. In both *S. aureus* and *S. epidermidis,* the glycopeptide resistance-associated TCR (GraSR) has been considered a good model to regulate resistance to multiple cationic antimicrobial peptides (CAMPs) and it is associated with bacterial survival within neutrophils (Gaupp *et al.*, 2012). So far, DesKR locus has not been extensively studied for its physiological role in *S. aureus,* whereas it is well characterised in *B. subtilis.* To my knowledge, this locus has not been previously described as drug target in staphylococci.

The *S. aureus* TCS identified in this study and proposed to be DesKR by Kim et al., (2016) appears to shares similar levels of sequence similarity with the YvfTU TCS of *B. subtilis*. There are two conserved ABC-transporter genes *yvfR* and *yvfS* located adjacent of *yvfTU.* The function of *B. subtilis* YvfTU TCS is not well characterised, with one study showing that expression of *plcR,* which encodes a transcriptional regulator was affected by the *yvfTU* mutation in *B. cereus* taking into account the close locations of these genes (Brillard *et al.*, 2008). *B. subtilis* DesKR was also found to be involved in the regulation of the YvfTU TCS (Kobayashi *et al.*, 2001). The analysis of YvfTU should therefore be extended in future to determine whether there is functional overlap and a relationship with the TCS proposed as DesKR TCS in *S. aureus.* The potential for both functions of DesKR and YvfTU of *B. subtilis* to be recruited to the TCS of *S. aureus* called DesKR remain possible.

The exact mechanism by which the DesKR system mediates *S. aureus* resistance is still unknown and additional research is needed to elucidate underlying mechanisms. One possibility is that it might be associated with alteration of membrane lipid composition or its membrane homeostasis since DeskR system is involved in controlling membrane fluidity in response to changes in environmental temperature in *B. subtilis* (Bredeston *et al.*, 2011) and the membrane, together with peptidoglycan are important antimicrobial targets. Supporting this, a SNP was identified upstream of the essential *fabI* gene that encodes the enzyme enoyl-acyl carrier protein reductase, which is involved in synthesis of fatty acid. Metabolism of type II fatty acids and in particular FabI, are among the most highly investigated targets for development of new antimicrobial compounds (Furi *et al.*, 2016). Previous studies identified that the resistance mechanism to triclosan involves overexpression of *fabI* through increased expression of a native gene or acquisition of an additional copy on a mobile genetic element (Fan *et al.*, 2002; Furi *et al.*, 2016). Another mechanism of triclosan resistance including mutations in *fabI* gene inhibits the formation of the ENR-NAD^+-triclosan ternary complex in *E. coli, S. aureus* and *Mycobacterium tuberculosis* (Heath *et al.,* 2000; Parikh *et al.,* 2000).

The sequencing and assembly of the *S. epidermidis* B155 genome into 6 contigs was helpfully enabled by the long read PacBio sequencing technology. The first large contig is proposed to comprise the whole bacterial chromosome, and the other five are proposed to be plasmids. Plasmid contig 2 appeared to encode a novel NRPS/PKS molecule. The gene cluster was annotated using AntiSMASH and it was revealed that the cluster has around 75% to 81% similarity with gene clusters found in *Streptococcus mutans*. One possibility is that this plasmid or the NRPS/PKS biosynthetic gene cluster was horizontally acquired directly or indirectly from S. *mutans*. This *Streptococcus* is mostly isolated from the human oral cavity (Krzyściak *et al.,* 2014), and the *mitis* group of streptococci are frequently isolated from skin (Gao *et al*., 2007). Consequently, it can be hypothesised that *S. aureus* DesKR TCS could have some roles in resistance to *S. mutans* producing polyketide, which increases survival. The efflux ABC transporter comprising *SAOUHSC*_01311-01312 subunits might have a primary

role in export of classes of molecule such as the NRPS/PKS antimicrobial or it could be a secondary role of the transporter that has an undetermined primary substrate.

Metagenomics studies of different human body surfaces revealed that there are diverse biosynthetic gene clusters involved in secondary metabolites production. Bioinformatic genome analysis of *Propionibacterium propionicum* isolated from oral cavity identified a gene cluster that may be responsible for mediating the synthesis of an antimicrobial marinomycin-related macrolide, which is classified as a type of polyketide (PKs)(Donia *et al.*, 2014). This highlights that antimicrobial peptides help to increase bacterial fitness in the human microbiota (Krismer *et al.*, 2017).

To investigate the diversity of antimicrobials that might be sensed/effluxed by the DesKR TCS, up to 200 *S. epidermidis* isolates, plus multiple other CoNS and species isolated from skin or the anterior nares were tested with *S. aureus* evolved strain (SHG01) to identify any with antimicrobials that cannot inhibit the evolved *desR* SNP strain (SHG01) but inhibited the parent strain SH1000. SHG01 strain was found to be resistant to one *Bacillus* isolate. Consequently, its 16S rDNA sequence and then the whole genome of the isolate was sequenced identifying *Bacillus flexus.* After assembly, bioinformatic analysis revealed the genome of *B. flexus* included a polyketide type III cluster and linear azol(in)e-containing peptides (LAP). Although the two molecular products of the respective gene clusters of *B. flexus* and *S. epidermidis* B155 are not identical, their inhibitory action was the same and they are within a functionally similar class of toxins. Further investigations are needed to identify how similar the two mechanisms are. Also the structure determination of these two antimicrobial will need to be obtained by nuclear magnetic resonance (NMR) spectroscopy.

Several roles of the DesKR TCS were described in ***Chapter five***. It was of particular interest to confirm the operon contributed to resistance of *S. aureus* to the NRPS/PKS molecule produced by *S. epidermidis* B155. This was achieved by generating the SNP in SH1000 but which resulted in additional SNPs that were

proposed to have arisen by subsequent selection. DesKR TCS operon as a resistance module is part of a spectrum of activities in *S. aureus*. Multiple regulatory elements modulate resistance of *S. aureus* to antibiotics. For example, MgrA has a role in regulation of multidrug transporters, and has also been shown to influence resistance to methicillin (Chen *et al.*, 2006). In addition, the essential TCS of *S. aureus,* WalKR was revealed to contribute to high level glycopeptide and methicillin resistance in different *S. aureus* strains (Martin *et al.*, 2002; Dubrac *et al.*, 2007).

S. aureus efflux pumps contributed to the extrusion of one or several classes of antimicrobial and contribute to multidrug resistance. To date, up to ten multidrug transporters have been characterised in *S. aureus*, encoded either in the chromosome such as LmrS, NorA, NorB, NorC, SdrM, MdeA MepA, Sav1866 and Tet38 or encoded on plasmids, including TetA(K), TetA(L), QacA, QacB, QacC, QacJ, and QacG (Costa *et al.*, 2013; Sapula and Brown, 2016). NorA and NorB are the most studied multidrug transporter in *S. aureus* (Ubukata *et al.*, 1989; Yoshida *et al.*, 1990). Both belong to the major facilitator transporter family MFS and they confer resistance to a wide range of chemically diverse compounds (Costa *et al.*, 2013; Sapula and Brown, 2016). NorA was found to be mostly expressed on the membrane of the bacterial cell and shows efflux pump activity of hydrophilic compounds, such as quinolones and dyes including ethidium bromide (Andersen *et al.*, 2015). Furthermore, efflux pump FarE of the fatty acid resistance system, which belongs to the resistance-nodulation-division (RND) family showed over expression in response to arachidonic and linoleic acids, supporting its implication in innate immunity in humans (Alnaseri *et al.*, 2015). Tet38 promotes resistance to fatty acids, in addition to tetracycline and also has a contribution in *S. aureus* colonisation of mouse skin and increases its ability to survive in the environment of an abscess (Truong-Bolduc *et al.*, 2015). Studies suggested that the increased efflux of antibiotics from the bacterial cell can allow bacteria to survive antimicrobial pressures longer than estimated. This outcome means bacteria may gain spontaneous mutations on target proteins and become drug resistant due to the increased evolutionary window (Jang, 2016).

Both the *desK* and the *SAOUHSC_01312* transporter mutants had increased sensitivity to *S. epidermidis* B155 antimicrobial compared with *S. aureus* wild-type. This finding supported the hypothesis that the DesKR locus is responsible for resistance to antimicrobial with DesK functioning as sensor histidine kinases and DesR as the transcriptional regulator. While the *SAOUHSC_01312* transporter could have a key role in efflux of the antimicrobial, it may also act to recognise the target-peptide within the cell membrane as the stimulus for the DesKR TCS to provides protection of *S. aureus* from polyketides. Since the *SAOUHSC_*0*1312* mutant was found to be more sensitive to the PKs/NRBS molecule compared with wild type, it might be functionally equivalent to the ABC transporters that is important for bacitracin sensing and signalling by BceSR (Ohki *et al.*, 2003). To support these results, competition experiments between SH1000 wild type and *SAOUHSC_01312* or mutants with *S. epidermidis* B155 could also be performed to confirm that mutant strains cannot evolve resistance. Also complementation of *desK* and *SAOUHSC_01312* should be conducted to determine whether complemented strains would be able to restore the phenotype to the parent strain.

It was notable that the transcription of *desR* was found to be upregulated in response to cell exposure with sapienic acid in *S. aureus* Newman (Moran *et al.*, 2017). Sapienic acid (C16:1Δ6) is the most ubiquitous and abundant fatty acid present on human skin and is a major antimicrobial lipid against staphylococci (Takigawa *et al.*, 2005). Sapienic acid acts by causing depolarisation of the plasma membrane of *S. aureus* (Moran *et al.*, 2017). Potentially *desKR* regulation could be required for resistance to sapienic acid, facilitating the bacteria to evade host defence systems, however, first it should be tested that sapienic acid stimulates *SAOUHSC_*01311-01312 ABC transporter expression. Toxic fatty acids present a problem for the cell to incorporate into their metabolism due to their specific unsatutration or chain length and the DesKR TCS could act as a membrane sentinel for lipids and other membrane-integrating molecules that alter specific properties such as fluidity, thickness or polarity.

S. aureus pathogenicity and persistence are associated with mechanisms of survival that involve structural, metabolic, proteomic and genomic changes in response to temperature variation (Alreshidi and Dunstan, 2013). Given the homology of the putative DesKR TCS with the archetypal DesKR of *B. subtilis*, the growth of the *desK* mutant and *SAOUHSC_01312* mutant was tested at different temperatures. The *desK* mutant showed defective growth at all temperatures compared with WT meaning the *desK* mutant might affect a key cell membrane property such as fluidity, which could explain the decrease in survival. However, the *SAOUHSC_01312* mutant displayed similar growth in comparison with the wild type at each temperature. While the reason of this observation is currently unknown, it will be necessary to integrate the function of *SAOUHSC_01315*, where the function of this short integral membrane protein is unknown. The gene *SAOUHSC_01315* is convergently transcribed immediately adjacent and appears to be the fifth of 5 genes in the DesKR regulon. The in-frame deletion mutant of *SAOUHSC_01312* has the potential to retain expression of DesKR and SAOUHSC_01315 but not functional activity of the ABC transporter *SAOUHSC_01311-01312*. The transporter might serve DesKR TCS to detect signals from temperature changes or may serve to transport a key membrane component, be that a normal or damaged component that needs to be removed. Due to the adjacent location of the cardiolipin synthase gene *cls1* to the *desKR* locus and its very high induction in the *desK* mutant cardiolipin might be implicated directly or indirectly in the central role of the TCS or might reflect its central activity. Cardiolipin is important for some cellular functions under high temperature and it facilitates oxidative phosphorylation, which results in bacterial resistance to environmental factors, including high temperatures (Schlame *et al.*, 2000). Though ultimately this should be investigated in several others strains and species to confirm the hypothesis plus further study by lipidomics, proteomics and metabolomics are required to determine the nature of changes in the evolved *desR* SNP mutant, SHG01.

Further experiments revealed that the inactivation of *desK* and *SAOUHSC_01312* genes reduced pigment production. Pigmentation has benefits to bacteria for survival in certain environments and antioxidant properties are frequently cited

(Liu *et al.*, 2005; Liu *et al.*, 2008). The staphyloxanthin pigment has properties that modulate the rigidity of *S. aureus* membrane whilst afford protection against host defences, such as cationic peptides (Gaupp *et al.*, 2012). Reductions in pigmentation in both mutants correspond with changes to the ability to regulate function in membrane properties or signalling transduction pathways, involved in metabolism of membrane. Nevertheless, how the DesKR can interact with other systems that contribute to regulation of cell membrane remains elusive.

To understand genes regulated by the DesKR TCS, in ***chapter six*** transcriptome analysis was performed. The evolved strain (SHG01) showed the genes most probably directly regulated by the DesKR TCS. Resistance to PKS/NRBS produced by *S. epidermidis* B155 would appear to be solely due to five genes, comprising the *SAOUHSC*_01311-01312-desK-desR operon due to their highly upregulated transcript levels. In addition, the convergent *SAOUHSC_01315* monocistronic operon is equally highly expressed supporting it being involved in resistance to the antimicrobial, but this must first be tested experimentally. In contrast the transcriptome analysis for *desK* mutant and *SAOUHSC_01312* mutant, although relatively similar to each other, revealed hundreds of DE genes compared with wild-type. The major pathways with differential expression common to both mutants related to carbohydrate and energy metabolism, transcription regulators, virulence genes and ribosomal proteins. Clear differences between *desK* and *SAOUHSC_01312* mutants was evident and the *cls1* gene was highly upregulated in *desK* mutant, which may indicate the desKR locus contributes to cardiolipin transportation and its regulation or that cardiolipin provides a solution to the defect caused by inactivity of the DesKR TCS. Many transcriptional regulators are affected by deletion of *desK* and *SAOUHSC_01312* genes such as the SarA-family regulator genes *sarA*, *sarS*, *sarZ*, *rot* and *mgrA.* Additionally, quorum sensing TCS genes *agrAC* were DE. Falord *et al.,* reported the first linking between GraSR TCS and the AgrCA which is the major virulence regulatory system in *S. aureus* (Falord *et al.*, 2011). The overlap between TCS, including DesKR, will be important to determine, since many of the DE genes are members of the Agr, SrrAB, SaeRS, GraSR, VraSR and WalKR regulons. Proteomic analysis could be conducted for both mutants to determine how much the results

correlated with transcriptomic data and to identify common features between both approaches. Potentially, major advances could be made with lipidomic and metabolomic studies to attempt to reveal the activity of the DesKR TCS and the SNP variant SHG01 could prove invaluable for this being successful.

In closing, *S. aureus* mutations were identified in the two component system DesKR indicating that this bacterium has an additional mechanism to cope with interspecific competition. Also it appears that an important genetic determinant of resistance to *S. epidermidis* B155 antimicrobial was identified here that provides resistance to a novel type of polyketide previously undescribed in staphylococci. Because of increases in skin diseases and taking into account the resistance of skin pathogens, such as MRSA to conventional therapies, the primary goal from this and subsequent studies should be to search for new classes of compounds with novel targets and new mechanisms of action. The identification of a novel antimicrobial in staphylococci and resistance mechanism in *S. aureus* was truly unexpected. A framework for discovery can subsequently be applied and expanded to study various bacterial interactions either cooperative or competitive, which will help to understand the composition and the dynamics of human skin microbial communities. The ecological implications of the findings warrant further study.

7.2 Study limitations

This study contributes to better understanding of microbial interactions particularly between staphylococci that colonise human skin. The design made it relatively easy to test the interactions between two or more bacteria *in vitro* and such studies might be good indicators of interactions *in vivo* (Iwase *et al.*, 2010). In this study, the competition experiments were performed *in vitro* thus, it is not known how the data would differ *in vivo.* Furthermore, the interactions between microorganisms in natural environments are much more complex and can be different depending on the variable environmental conditions. Therefore, experiments conducted in the laboratory is likely a snapshot of the actual situation and will not give a whole, complex picture of the interactions happening in nature. However, testing the inhibitory effect of such antibiotics in laboratory

experiments show they were always found to be effective (Turpin *et al.*, 1992; Wiener, 2000). However, some antibiotics may simply be signalling molecules in their natural environment, and may never reach growth inhibitory concentrations (Linares *et al.*, 2006). Competition methods used in this work depend on CFU, which can easily reveal a difference between species, thus it is required that populations can be discriminated depending on observation of bacterial colony morphology (Moutinho Jr *et al.*, 2017). However, this method only cannot be used to study cocultures of morphologically dissimilar individuals and different tests should be used for those not easily distinguished.

Secondly, just four *S. aureus* strains were used as indicator isolates and it is clear that here is no single strain that will be representative of the entire diverse species. However, this was necessary to make the screening of a large number of natural isolates possible. Despite the study focus on the naturally antagonistic interactions between species, the lab strain SH1000 was used for consistency in competition experiments. Although SH1000 is genetically well-defined (Horsburgh *et al.*, 2002), more work will certainly be needed to assess whether *S. aureus* skin isolates have properties similar to SH1000 strain, due to the high genotypic diversity of natural *S. aureus* isolates (Moore and Lindsay, 2001; Sakwinska *et al.*, 2009).

Referances

Abbas, S., R. Senthilkumar and S. Arjunan, 2014. Isolation and molecular characterization of microorganisms producing novel antibiotics from soil sample. European Journal of Experimental Biology, 4(5): 149-155.

Abdelnour, A., S. Arvidson, T. Bremell, C. Ryden and A. Tarkowski, 1993. The accessory gene regulator (*agr*) controls *Staphylococcus aureus* virulence in a murine arthritis model. Infection and immunity, 61(9): 3879-3885.

Abdulkadir, M., & S., Waliyu, 2012. Screening and isolation of the soil bacteria for ability to produce antibiotics. *European Journal of applied sciences*, *4*(5), 211-215.

Aguilar, P.S., J.E. Cronan and D. De Mendoza, 1998. A *Bacillus subtilis* gene induced by cold shock encodes a membrane phospholipid desaturase. Journal of bacteriology, 180(8): 2194-2200.

Aguilar, P.S., A.M. Hernandez-Arriaga, L.E. Cybulski, A.C. Erazo and D. de Mendoza, 2001. Molecular basis of thermosensing: A two-component signal transduction thermometer in *Bacillus subtilis*. The EMBO journal, 20(7): 1681-1691.

Al-Dayel, M., 2015. *Staphylococcus aureus* survival mechanisms from skin antimicrobials (Doctoral dissertation, University of Liverpool).

Aleti, G., A. Sessitsch and G. Brader, 2015. Genome mining: Prediction of lipopeptides and polyketides from *Bacillus* and related firmicutes. Computational and structural biotechnology journal, 13: 192-203.

Alibayov, B., L. Baba-Moussa, H. Sina, K. Zdeňková and K. Demnerová, 2014. *Staphylococcus aureus* mobile genetic elements. Molecular biology reports, 41(8): 5005-5018.

Allen, H.K., J. Trachsel, T. Looft and T.A. Casey, 2014. Finding alternatives to antibiotics. Annals of the New York Academy of Sciences, 1323(1): 91-100.

Alnaseri, H., B. Arsic, J.E. Schneider, J.C. Kaiser, Z.C. Scinocca, D.E. Heinrichs and M.J. McGavin, 2015. Inducible expression of a resistance-nodulation-division-type efflux pump in *Staphylococcus aureus* provides resistance to linoleic and arachidonic acids. Journal of bacteriology, 197(11): 1893-1905.

Alreshidi, M. and H. Dunstan, 2013. Staphylococcal phenomics: Metabolomic and proteomic responses to environmental stressors.

Amissah, N.A., M.A. Chlebowicz, A. Ablordey, C.S. Tetteh, I. Prah, A.W. Friedrich, J.M. van Dijl, Y. Stienstra and J.W. Rossen, 2017. Virulence potential of *Staphylococcus aureus* isolates from buruli ulcer patients. International Journal of Medical Microbiology.

Anders, S. and W. Huber, 2010. Differential expression analysis for sequence count data. Genome biology, 11(10): R106.

Anders, S., P.T. Pyl and W. Huber, 2015. Htseq—a python framework to work with high-throughput sequencing data. Bioinformatics, 31(2): 166-169.

Andersen, J., G.-X. He, P. Kakarla, R. KC, S. Kumar, W. Lakra, M. Mukherjee, I. Ranaweera, U. Shrestha and T. Tran, 2015. Multidrug efflux pumps from enterobacteriaceae, *Vibrio cholerae* and *Staphylococcus aureus* bacterial food pathogens. International journal of environmental research and public health, 12(2): 1487-1547.

Andersson, D.I., D. Hughes and J.Z. Kubicek-Sutherland, 2016. Mechanisms and consequences of bacterial resistance to antimicrobial peptides. Drug Resistance Updates, 26: 43-57.

Andrey, D.O., A. Renzoni, A. Monod, D.P. Lew, A.L. Cheung and W.L. Kelley, 2010. Control of the *Staphylococcus aureus* toxic shock *tst* promoter by the global regulator sara. Journal of bacteriology, 192(22): 6077-6085.

Anton, A., C. Große, J. Reißmann, T. Pribyl and D.H. Nies, 1999. CzcD is a heavy metal ion transporter involved in regulation of heavy metal resistance in *Ralstonia sp.* Strain ch34. Journal of bacteriology, 181(22): 6876-6881.

Argemi, X., V. Martin, V. Loux, S. Dahyot, J. Lebeurre, A. Guffroy, M. Martin, A. Velay, D. Keller and P. Riegel, 2017. Whole-genome sequencing of seven strains of *Staphylococcus lugdunensis* allows identification of mobile genetic elements. Genome biology and evolution, 9(5).

Arias, C.A., D. Panesso, D.M. McGrath, X. Qin, M.F. Mojica, C. Miller, L. Diaz, T.T. Tran, S. Rincon and E.M. Barbu, 2011. Genetic basis for in vivo daptomycin resistance in enterococci. New England Journal of Medicine, 365(10): 892-900.

Arteaga, R.D.C., S. Ichiwaki, K. Massini, L.M. Garrido, E.M.B. Rosero and G. Padilla, 2017. Screening of polyketide genes from brazilian atlantic forest soil. Universitas Scientiarum, 22(1): 87-96.

Arvidson, S., 2006. Extracellular enzymes. In: Gram-positive pathogens, second edition. American Society of Microbiology: pp: 478-485.

Asaduzzaman, S.M., J.-i. Nagao, H. Iida, T. Zendo, J. Nakayama and K. Sonomoto, 2009. Nukacin isk-1, a bacteriostatic lantibiotic. Antimicrobial agents and chemotherapy, 53(8): 3595-3598.

Ashburner, M., C.A. Ball, J.A. Blake, D. Botstein, H. Butler, J.M. Cherry, A.P. Davis, K. Dolinski, S.S. Dwight and J.T. Eppig, 2000. Gene ontology: Tool for the unification of biology. Nature genetics, 25(1): 25.

Aso, Y., J.-I. Nagao, H. Koga, K.-I. Okuda, Y. Kanemasa, T. Sashihara, J. Nakayama and K. Sonomoto, 2004. Heterologous expression and functional analysis of the gene cluster for the biosynthesis of and immunity to the lantibiotic, nukacin isk-1. Journal of bioscience and bioengineering, 98(6): 429-436.

Aswani, V., D. M. Tremblay, S. Moineau, S. K. Shukla., 2011. S*taphylococcus epidermidis* bacteriophages from the anterior nares of humans. Appl. Environ. Microbiol., 77(21), 7853-7855.

Auer, P.L. and R.W. Doerge, A two-stage poisson model for testing rna-seq data. Statistical applications in genetics and molecular biology, 10(1).

Ballal, A., B. Ray and A.C. Manna, 2009. *sarZ*, a *sarA* family gene, is transcriptionally activated by MgrA and is involved in the regulation of genes encoding exoproteins in *Staphylococcus aureus*. Journal of bacteriology, 191(5): 1656-1665.

Balouiri, M., M. Sadiki and S.K. Ibnsouda, 2016. Methods for in vitro evaluating antimicrobial activity: A review. Journal of pharmaceutical analysis, 6(2): 71-79.

Barakat, M., P. Ortet and D.E. Whitworth, 2010. P2cs: A database of prokaryotic two-component systems. Nucleic acids research, 39(suppl_1): D771-D776.

Barger, S.R., B.C. Hoefler, A. Cubillos-Ruiz, W.K. Russell, D.H. Russell and P.D. Straight, 2012. Imaging secondary metabolism of *Streptomyces sp*. Mg1

during cellular lysis and colony degradation of competing *Bacillus subtilis*. Antonie Van Leeuwenhoek, 102(3): 435-445.

Bastos, M., H. Ceotto, M. Coelho and J. Nascimento, 2009. Staphylococcal antimicrobial peptides: Relevant properties and potential biotechnological applications. Current pharmaceutical biotechnology, 10(1): 38-61.

Baur, S., M. Rautenberg, M. Faulstich, T. Grau, Y. Severin, C. Unger, W.H. Hoffmann, T. Rudel, I.B. Autenrieth and C. Weidenmaier, 2014. A nasal epithelial receptor for *Staphylococcus aureus* WTA governs adhesion to epithelial cells and modulates nasal colonization. Plos pathogens, 10(5): e1004089.

Bayer, M.G., J.H. Heinrichs and A.L. Cheung, 1996. The molecular architecture of the *sar* locus in *Staphylococcus aureus*. Journal of bacteriology, 178(15): 4563-4570.

Beaume, M., D. Hernandez, L. Farinelli, C. Deluen, P. Linder, C. Gaspin, P. Romby, J. Schrenzel and P. Francois, 2010. Cartography of methicillin-resistant *S. aureus* transcripts: Detection, orientation and temporal expression during growth phase and stress conditions. PLoS One, 5(5): e10725.

Beier, D. and R. Gross, 2006. Regulation of bacterial virulence by two-component systems. Current opinion in microbiology, 9(2): 143-152.

Benjak, A., C. Sala and R.C. Hartkoorn, 2015. Whole-genome sequencing for comparative genomics and de novo genome assembly. *Mycobacteria* Protocols: 1-16.

Benjamini, Y. and Y. Hochberg, 1995. Controlling the false discovery rate: A practical and powerful approach to multiple testing. Journal of the royal statistical society. Series B (Methodological): 289-300.

Bernal, P., J. Muñoz-Rojas, A. Hurtado, J.L. Ramos and A. Segura, 2007. A *pseudomonas putida* cardiolipin synthesis mutant exhibits increased sensitivity to drugs related to transport functionality. Environmental microbiology, 9(5): 1135-1145.

Bertrand, S., N. Bohni, S. Schnee, O. Schumpp, K. Gindro and J.-L. Wolfender, 2014. Metabolite induction via microorganism co-culture: A potential way to enhance chemical diversity for drug discovery. Biotechnology advances, 32(6): 1180-1204.

Bessesen, M.T., C.V. Kotter, B.D. Wagner, J.C. Adams, S. Kingery, J.B. Benoit, C.E. Robertson, E.N. Janoff and D.N. Frank, 2015. MRSA colonization and the nasal microbiome in adults at high risk of colonization and infection. Journal of Infection, 71(6): 649-657.

Bierbaum, G. and H.-G. Sahl, 1991. Induction of autolysis of *Staphylococcus simulans* 22 by pep5 and misin and influence of the cationic peptides on the activity of the autolytic enzymes. Nisin and novel lantibiotics: 386.

Bischoff, M., P. Dunman, J. Kormanec, D. Macapagal, E. Murphy, W. Mounts, B. Berger-Bächi and S. Projan, 2004. Microarray-based analysis of the *Staphylococcus aureus* σb regulon. Journal of bacteriology, 186(13): 4085-4099.

Bischoff, M., J. Entenza and P. Giachino, 2001. Influence of a functional σB operon on the global regulators *sar* and *agr* in *Staphylococcus aureus*. Journal of bacteriology, 183(17): 5171-5179.

Blevins, J.S., A.F. Gillaspy, T.M. Rechtin, B.K. Hurlburt and M.S. Smeltzer, 1999. The staphylococcal accessory regulator (sar) represses transcription of the

staphylococcus aureus collagen adhesin gene (cna) in an agr-independent manner. Molecular microbiology, 33(2): 317-326.
Blin, K., M.H. Medema, D. Kazempour, M.A. Fischbach, R. Breitling, E. Takano and T. Weber, 2013. Antismash 2.0—a versatile platform for genome mining of secondary metabolite producers. Nucleic acids research, 41(W1): W204-W212.
Bloudoff, K. and T.M. Schmeing, 2017. Structural and functional aspects of the nonribosomal peptide synthetase condensation domain superfamily: Discovery, dissection and diversity. Biochimica et Biophysica Acta (BBA)-Proteins and Proteomics, 1865(11): 1587-1604.
Bonelli, R.R., T. Schneider, H.-G. Sahl and I. Wiedemann, 2006. Insights into in vivo activities of lantibiotics from gallidermin and epidermin mode-of-action studies. Antimicrobial agents and chemotherapy, 50(4): 1449-1457.
Botella, E., S.K. Devine, S. Hubner, L.I. Salzberg, R.T. Gale, E.D. Brown, H. Link, U. Sauer, J.D. Codée and D. Noone, 2014. Phor autokinase activity is controlled by an intermediate in wall teichoic acid metabolism that is sensed by the intracellular pas domain during the phopr-mediated phosphate limitation response of *Bacillus subtilis*. Molecular microbiology, 94(6): 1242-1259.
Bottomly, D., N.A. Walter, J.E. Hunter, P. Darakjian, S. Kawane, K.J. Buck, R.P. Searles, M. Mooney, S.K. McWeeney and R. Hitzemann, 2011. Evaluating gene expression in CS7BL/6J and DBA/2J mouse striatum using RNA-seq and microarrays. PloS one, 6(3): e17820.
Braff, M.H., M. Zaiou, J. Fierer, V. Nizet and R.L. Gallo, 2005. Keratinocyte production of cathelicidin provides direct activity against bacterial skin pathogens. Infection and immunity, 73(10): 6771-6781.
Bredeston, L., D. Marciano, D. Albanesi, D. De Mendoza and J. Delfino, 2011. Thermal regulation of membrane lipid fluidity by a two-component system in *Bacillus subtilis*. Biochemistry and Molecular Biology Education, 39(5): 362-366.
Brillard, J., K. Susanna, C. Michaud, C. Dargaignaratz, M. Gohar, C. Nielsen-Leroux, N. Ramarao, A.-B. Kolstø, D. Lereclus and V. Broussolle, 2008. The yvfTU two-component system is involved in *plcR* expression in *Bacillus cereus*. BMC microbiology, 8(1): 183.
Brouwer, S., T.C. Barnett, T. Rivera-Hernandez, M. Rohde and M.J. Walker, 2016. *Streptococcus pyogenes* adhesion and colonization. FEBS letters, 590(21): 3739-3757.
Brown, A.F., J.M. Leech, T.R. Rogers and R.M. McLoughlin, 2013. S*taphylococcus aureus* colonization: Modulation of host immune response and impact on human vaccine design. Frontiers in immunology, 4.
Brown, J., D.L. Shriner, R.A. Schwartz and C.K. Janniger, 2003. Impetigo: An update. International journal of dermatology, 42(4): 251-255.
Brunskill, E.W. and K.W. Bayles, 1996. Identification and molecular characterization of a putative regulatory locus that affects autolysis in *Staphylococcus aureus*. Journal of bacteriology, 178(3): 611-618.
Brunskill, E.W. and K.W. Bayles, 1996. Identification of lytSR-regulated genes from *Staphylococcus aureus*. Journal of bacteriology, 178(19): 5810-5812.

Bullard, J.H., E. Purdom, K.D. Hansen and S. Dudoit, 2010. Evaluation of statistical methods for normalization and differential expression in mRNA-seq experiments. BMC bioinformatics, 11(1): 94.

Burke, K.A. and J. Lascelles, 1975. Nitrate reductase system in *Staphylococcus aureus* wild type and mutants. Journal of Bacteriology, 123(1): 308-316.

Campbell, J., A.K. Singh, J.G. Swoboda, M.S. Gilmore, B.J. Wilkinson and S. Walker, 2012. An antibiotic that inhibits a late step in wall teichoic acid biosynthesis induces the cell wall stress stimulon in *Staphylococcus aureus*. Antimicrobial agents and chemotherapy: AAC. 05938-05911.

Cavaco, L., H. Hasman, M. Stegger, P.S. Andersen, R. Skov, A.C. Fluit, T. Ito and F.M. Aarestrup, 2010. Cloning and occurrence of *czrC*, a gene conferring cadmium and zinc resistance in methicillin-resistant *Staphylococcus aureus* CC398 isolates. Antimicrobial agents and chemotherapy, 54(9): 3605-3608.

Celiker, H. and J. Gore, 2012. Competition between species can stabilize public-goods cooperation within a species. Molecular Systems Biology, 8(1): 621.

Ceotto, H., J. dos Santos Nascimento, M.A.V. de Paiva Brito and M.d.C. de Freire Bastos, 2009. Bacteriocin production by *Staphylococcus aureus* involved in bovine mastitis in brazil. Research in microbiology, 160(8): 592-599.

Challis, G.L., J. Ravel and C.A. Townsend, 2000. Predictive, structure-based model of amino acid recognition by nonribosomal peptide synthetase adenylation domains. Chemistry & biology, 7(3): 211-224.

Chamberlain, N. and B. Imanoel, 1996. Genetic regulation of fatty acid modifying enzyme from *Staphylococcus aureus*. Journal of medical microbiology, 44(2): 125-129.

Chambers, H.F. and F.R. DeLeo, 2009. Waves of resistance: *Staphylococcus aureus* in the antibiotic era. Nature Reviews Microbiology, 7(9): 629-641.

Chan, W.C., B.J. Coyle and P. Williams, 2004. Virulence regulation and quorum sensing in staphylococcal infections: Competitive AgrC antagonists as quorum sensing inhibitors. Journal of medicinal chemistry, 47(19): 4633-4641.

Chao, L. and B.R. Levin, 1981. Structured habitats and the evolution of anticompetitor toxins in bacteria. Proceedings of the National Academy of Sciences, 78(10): 6324-6328.

Chaves-Moreno, D., M.L. Wos-Oxley, R. Jáuregui, E. Medina, A.P. Oxley and D.H. Pieper, 2016. Exploring the transcriptome of *Staphylococcus aureus* in its natural niche. Scientific reports, 6: 33174.

Chen, P.R., T. Bae, W.A. Williams, E.M. Duguid, P.A. Rice, O. Schneewind and C. He, 2006. An oxidation-sensing mechanism is used by the global regulator MgrA in *Staphylococcus aureus.* Nature chemical biology, 2(11): 591.

Chen, X.-H., J. Vater, J. Piel, P. Franke, R. Scholz, K. Schneider, A. Koumoutsi, G. Hitzeroth, N. Grammel and A.W. Strittmatter, 2006. Structural and functional characterization of three polyketide synthase gene clusters in *Bacillus amyloliquefaciens* FZB 42. Journal of bacteriology, 188(11): 4024-4036.

Cheung, A.L., A.S. Bayer, G. Zhang, H. Gresham and Y.-Q. Xiong, 2004. Regulation of virulence determinants in vitro and in vivo in *Staphylococcus aureus*. FEMS Immunology & Medical Microbiology, 40(1): 1-9.

Cheung, A.L., M.G. Bayer and J.H. Heinrichs, 1997. Sar genetic determinants necessary for transcription of RNAII and RNAIII in the agr locus of *Staphylococcus aureus*. Journal of bacteriology, 179(12): 3963-3971.

Cheung, A.L., K.J. Eberhardt, E. Chung, M.R. Yeaman, P.M. Sullam, M. Ramos and A.S. Bayer, 1994. Diminished virulence of a sar-/agr-mutant of *Staphylococcus aureu*s in the rabbit model of endocarditis. The Journal of clinical investigation, 94(5): 1815-1822.

Cheung, A.L., K.A. Nishina, M.P. Trotonda and S. Tamber, 2008. The sarA protein family of *Staphylococcus aureus*. The international journal of biochemistry & cell biology, 40(3): 355-361.

Cheung, A.L., K. Schmidt, B. Bateman and A.C. Manna, 2001. SarS, a sarA homolog repressible by *agr*, is an activator of protein a synthesis in S*taphylococcus aureus*. Infection and immunity, 69(4): 2448-2455.

Cheung, G.Y., R. Wang, B.A. Khan, D.E. Sturdevant and M. Otto, 2011. Role of the accessory gene regulator *agr* in community-associated MRSA pathogenesis. Infection and immunity.

Chien, Y.-t., A.C. Manna, S.J. Projan and A.L. Cheung, 1999. SarA, a global regulator of virulence determinants in *Staphylococcus aureus*, binds to a conserved motif essential for *sar*-dependent gene regulation. Journal of Biological Chemistry, 274(52): 37169-37176.

Chin, C.-S., D.H. Alexander, P. Marks, A.A. Klammer, J. Drake, C. Heiner, A. Clum, A. Copeland, J. Huddleston and E.E. Eichler, 2013. Nonhybrid, finished microbial genome assemblies from long-read SMRT sequencing data. Nature methods, 10(6): 563.

Christensen, G.J., C.F. Scholz, J. Enghild, H. Rohde, M. Kilian, A. Thürmer, E. Brzuszkiewicz, H.B. Lomholt and H. Brüggemann, 2016. Antagonism between *Staphylococcus epidermidis* and *propionibacterium acnes* and its genomic basis. BMC genomics, 17(1): 152.

Chung, P.Y., L.Y. Chung and P. Navaratnam, 2013. Transcriptional profiles of the response of methicillin-resistant *Staphylococcus aureus* to pentacyclic triterpenoids. PLoS One, 8(2): e56687.

Cingolani, P., A. Platts, L.L. Wang, M. Coon, T. Nguyen, L. Wang, S.J. Land, X. Lu and D.M. Ruden, 2012. A program for annotating and predicting the effects of single nucleotide polymorphisms, snpEff: SNPs in the genome of *drosophila melanogaster* strain W1118; iso-2; iso-3. Fly, 6(2): 80-92.

Clarke, S.R., R. Mohamed, L. Bian, A.F. Routh, J.F. Kokai-Kun, J.J. Mond, A. Tarkowski and S.J. Foster, 2007. The *Staphylococcus aureus* surface protein isdA mediates resistance to innate defenses of human skin. Cell Host & Microbe, 1(3): 199-212.

Clauditz, A., A. Resch, K.-P. Wieland, A. Peschel and F. Götz, 2006. Staphyloxanthin plays a role in the fitness of *Staphylococcus aureus* and its ability to cope with oxidative stress. Infection and immunity, 74(8): 4950-4953.

Coates-Brown, R., J.C. Moran, P. Pongchaikul, A.C. Darby and M.J. Horsburgh, 2018. Comparative genomics of *Staphylococcus* reveals determinants of speciation and diversification of antimicrobial defense. Frontiers in Microbiology, 9(2753). Available from https://www.frontiersin.org/article/10.3389/fmicb.2018.02753.DOI 10.3389/fmicb.2018.02753.

Coates, R., J. Moran and M.J. Horsburgh, 2014. Staphylococci: Colonizers and pathogens of human skin. Future microbiology, 9(1): 75-91.

Coelho, M.L.V., J. dos Santos Nascimento, P.C. Fagundes, D.J. Madureira, S.S. de Oliveira, M.A.V. de Paiva Brito and M.d.C. de Freire Bastos, 2007. Activity of staphylococcal bacteriocins against *Staphylococcus aureus* and *Streptococcus agalactiae* involved in bovine mastitis. Research in microbiology, 158(7): 625-630.

Cogen, A., V. Nizet and R. Gallo, 2008. Skin microbiota: A source of disease or defence? British Journal of Dermatology, 158(3): 442-455.

Cogen, A.L., K. Yamasaki, K.M. Sanchez, R.A. Dorschner, Y. Lai, D.T. MacLeod, J.W. Torpey, M. Otto, V. Nizet and J.E. Kim, 2010. Selective antimicrobial action is provided by phenol-soluble modulins derived from *Staphylococcus epidermidis*, a normal resident of the skin. Journal of Investigative Dermatology, 130(1): 192-200.

Cornforth, D.M. and K.R. Foster, 2013. Competition sensing: The social side of bacterial stress responses. Nature Reviews Microbiology, 11(4): 285.

Costa, S.S., M. Viveiros, L. Amaral and I. Couto, 2013. Multidrug efflux pumps in *Staphylococcus aureus*: An update. The open microbiology journal, 7: 59.

Costello, E.K., C.L. Lauber, M. Hamady, N. Fierer, J.I. Gordon and R. Knight, 2009. Bacterial community variation in human body habitats across space and time. Science, 326(5960): 1694-1697.

Crandall, A.D. and T.J. Montville, 1998. Nisin resistance in *Listeria monocytogenes* ATCC 700302 is a complex phenotype. Applied and Environmental Microbiology, 64(1): 231-237.

Cuaron, J.A., S. Dulal, Y. Song, A.K. Singh, C.E. Montelongo, W. Yu, V. Nagarajan, R.K. Jayaswal, B.J. Wilkinson and J.E. Gustafson, 2013. Tea tree oil-induced transcriptional alterations in *Staphylococcus aureus*. Phytotherapy research, 27(3): 390-396.

Cui, L., X. Ma, K. Sato, K. Okuma, F.C. Tenover, E.M. Mamizuka, C.G. Gemmell, M.-N. Kim, M.-C. Ploy and N. El Solh, 2003. Cell wall thickening is a common feature of vancomycin resistance in *Staphylococcus aureus*. Journal of clinical microbiology, 41(1): 5-14.

Cybulski, L.E., D. Albanesi, M.C. Mansilla, S. Altabe, P.S. Aguilar and D. De Mendoza, 2002. Mechanism of membrane fluidity optimization: Isothermal control of the *Bacillus subtilis* acyl-lipid desaturase. Molecular microbiology, 45(5): 1379-1388.

Cybulski, L.E., J. Ballering, A. Moussatova, M.E. Inda, D.B. Vazquez, T.A. Wassenaar, D. de Mendoza, D.P. Tieleman and J.A. Killian, 2015. Activation of the bacterial thermosensor DesK involves a serine zipper dimerization motif that is modulated by bilayer thickness. Proceedings of the National Academy of Sciences: 201422446.

Cybulski, L.E., G. Del Solar, P.O. Craig, M. Espinosa and D. De Mendoza, 2004. *Bacillus subtilis* DesR functions as a phosphorylation-activated switch to control membrane lipid fluidity. Journal of Biological Chemistry, 279(38): 39340-39347.

Davidson, A.L., E. Dassa, C. Orelle and J. Chen, 2008. Structure, function, and evolution of bacterial ATP-binding cassette systems. Microbiology and Molecular Biology Reviews, 72(2): 317-364.

Davies, J., 2006. Are antibiotics naturally antibiotics? Journal of Industrial Microbiology and Biotechnology, 33(7): 496-499.
De Leo, V., L. Catucci, A. Ventrella, F. Milano, A. Agostiano and A. Corcelli, 2009. Cardiolipin increases in chromatophores isolated from *Rhodobacter sphaeroides* after osmotic stress: Structural and functional roles. Journal of lipid research, 50(2): 256-264.
De Maayer, P., W.-Y. Chan, J. Blom, S.N. Venter, B. Duffy, T.H. Smits and T.A. Coutinho, 2012. The large universal pantoea plasmid LPP-1 plays a major role in biological and ecological diversification. BMC genomics, 13(1): 625.
De Souza, T.K., S.S. Soares, L.B. Benitez and M.B. Rott, 2017. Interaction between methicillin-resistant *Staphylococcus aureus* (MRSA) and acanthamoeba polyphaga. Current microbiology, 74(5): 541-549.
Dekio, I., H. Hayashi, M. Sakamoto, M. Kitahara, T. Nishikawa, M. Suematsu and Y. Benno, 2005. Detection of potentially novel bacterial components of the human skin microbiota using culture-independent molecular profiling. Journal of medical microbiology, 54(12): 1231-1238.
Delaune, A., O. Poupel, A. Mallet, Y.-M. Coic, T. Msadek and S. Dubrac, 2011. Peptidoglycan crosslinking relaxation plays an important role in *Staphylococcus aureus* walKR-dependent cell viability. PloS one, 6(2): e17054.
de Lima Procópio, R. E., da Silva, I. R., Martins, M. K., de Azevedo, J. L., & de Araújo, J. M. (2012). Antibiotics produced by Streptomyces. The Brazilian Journal of infectious diseases, 16(5), 466-471.
Demain, A.L. and A. Fang, 2000. The natural functions of secondary metabolites. In: History of modern biotechnology i. Springer: pp: 1-39.
Deora, R., T. Tseng and T.K. Misra, 1997. Alternative transcription factor sigmaSB of *Staphylococcus aureus*: Characterization and role in transcription of the global regulatory locus sar. Journal of bacteriology, 179(20): 6355-6359.
Dhople, V.M. and R. Nagaraj, 2005. Conformation and activity of δ-lysin and its analogs. Peptides, 26(2): 217-225.
Dischinger, J., M. Josten, C. Szekat, H.-G. Sahl and G. Bierbaum, 2009. Production of the novel two-peptide lantibiotic lichenicidin by *Bacillus licheniformis* DSM 13. PLoS One, 4(8): e6788.
Donadio, S., M.J. Staver, J.B. McAlpine, S.J. Swanson and L. Katz, 1991. Modular organization of genes required for complex polyketide biosynthesis. Science, 252(5006): 675-679.
Dong, Y.-H., A.R. Gusti, Q. Zhang, J.-L. Xu and L.-H. Zhang, 2002. Identification of quorum-quenching N-acyl homoserine lactonases from Bacillus species. Applied and environmental microbiology, 68(4): 1754-1759.
Dong, Z. and Y. Chen, 2013. Transcriptomics: Advances and approaches. Science China Life Sciences, 56(10): 960-967.
Donia, M.S., P. Cimermancic, C.J. Schulze, L.C.W. Brown, J. Martin, M. Mitreva, J. Clardy, R.G. Linington and M.A. Fischbach, 2014. A systematic analysis of biosynthetic gene clusters in the human microbiome reveals a common family of antibiotics. Cell, 158(6): 1402-1414.
dos Santos Nascimento, J., M.L.V. Coelho, H. Ceotto, A. Potter, L.R. Fleming, Z. Salehian, I.F. Nes and M.d.C. de Freire Bastos, 2012. Genes involved in immunity to and secretion of aureocin A53, an atypical class II bacteriocin

produced by *Staphylococcus aureus* A53. Journal of bacteriology, 194(4): 875-883.
dos Santos Nascimento, J., P.C. Fagundes, M.A.V. de Paiva Brito, K.R.N. Dos Santos and M.d.C. de Freire Bastos, 2005. Production of bacteriocins by coagulase-negative staphylococci involved in bovine mastitis. Veterinary microbiology, 106(1-2): 61-71.
Drake, D.R., K.A. Brogden, D.V. Dawson and P.W. Wertz, 2008. Thematic review series: Skin lipids. Antimicrobial lipids at the skin surface. Journal of lipid research, 49(1): 4-11.
Draper, L.A., K. Grainger, L.H. Deegan, P.D. Cotter, C. Hill and R.P. Ross, 2009. Cross-immunity and immune mimicry as mechanisms of resistance to the lantibiotic lacticin 3147. Molecular microbiology, 71(4): 1043-1054.
Dubrac, S., I.G. Boneca, O. Poupel and T. Msadek, 2007. New insights into the walK/walR (yycG/yycF) essential signal transduction pathway reveal a major role in controlling cell wall metabolism and biofilm formation in *Staphylococcus aureus*. Journal of bacteriology, 189(22): 8257-8269.
Dubrac, S. and T. Msadek, 2004. Identification of genes controlled by the essential yycG/yycF two-component system of *Staphylococcus aureus*. Journal of bacteriology, 186(4): 1175-1181.
Dunlap, C.A., S.-J. Kim, S.-W. Kwon and A.P. Rooney, 2015. Phylogenomic analysis shows that *Bacillus amyloliquefaciens* subsp. Plantarum is a later heterotypic synonym of *Bacillus methylotrophicus*. International journal of systematic and evolutionary microbiology, 65(7): 2104-2109.
Dunman, P.á., E. Murphy, S. Haney, D. Palacios, G. Tucker-Kellogg, S. Wu, E. Brown, R. Zagursky, D. Shlaes and S. Projan, 2001. Transcription profiling-based identification of *Staphylococcus aureus* genes regulated by the agr and/or sarA loci. Journal of bacteriology, 183(24): 7341-7353.
Duthie, E. and L.L. Lorenz, 1952. Staphylococcal coagulase: Mode of action and antigenicity. Microbiology, 6(1-2): 95-107.
Eberhard, W.G., 1990. Evolution in bacterial plasmids and levels of selection. The Quarterly review of biology, 65(1): 3-22.
Edwards, M.L., P.K. Fagan, B.J. Currie and K.S. Sriprakash, 2004. The fibronectin-binding capacity and host cell adherence of *Streptococcus pyogenes* strains are discordant with each other. Microbes and infection, 6(13): 1156-1162.
Eguchi, Y. and R. Utsumi, 2008. Introduction to bacterial signal transduction networks. In: Bacterial signal transduction: Networks and drug targets. Springer: pp: 1-6.
Elias, P.M. and K. Feingold, 1992. Lipids and the epidermal water barrier: Metabolism, regulation, and pathophysiology. In: Seminars in dermatology. pp: 176-182.
Ernst, C.M. and A. Peschel, 2011. Broad-spectrum antimicrobial peptide resistance by mpr-mediated aminoacylation and flipping of phospholipids. Molecular microbiology, 80(2): 290-299.
Ernst, C.M., P. Staubitz, N.N. Mishra, S.-J. Yang, G. Hornig, H. Kalbacher, A.S. Bayer, D. Kraus and A. Peschel, 2009. The bacterial defensin resistance protein MprF consists of separable domains for lipid lysinylation and antimicrobial peptide repulsion. PLoS pathogens, 5(11): e1000660.

Esquenazi, E., Y.-L. Yang, J. Watrous, W.H. Gerwick and P.C. Dorrestein, 2009. Imaging mass spectrometry of natural products. Natural product reports, 26(12): 1521-1534.

Fabret, C. and J.A. Hoch, 1998. A two-component signal transduction system essential for growth of *Bacillus subtilis*: Implications for anti-infective therapy. Journal of bacteriology, 180(23): 6375-6383.

Fair, R.J. and Y. Tor, 2014. Antibiotics and bacterial resistance in the 21st century. Perspectives in medicinal chemistry, 6: PMC. S14459.

Falkinham, J. O., Wall, T. E., Tanner, J. R., Tawaha, K., Alali, F. Q., Li, C., & Oberlies, N. H., 2009. Proliferation of antibiotic-producing bacteria and concomitant antibiotic production as the basis for the antibiotic activity of Jordan's red soils. *Appl. Environ. Microbiol.*, *75*(9), 2735-2741.

Falord, M., G. Karimova, A. Hiron and T. Msadek, 2012. GraxSR proteins interact with the VraFG ABC transporter to form a five-component system required for cationic antimicrobial peptide sensing and resistance in *Staphylococcus aureus*. Antimicrobial agents and chemotherapy, 56(2): 1047-1058.

Falord, M., U. Mäder, A. Hiron, M. Debarbouille and T. Msadek, 2011. Investigation of the staphylococcus aureus GraSR regulon reveals novel links to virulence, stress response and cell wall signal transduction pathways. PloS one, 6(7): e21323.

Fan, F., K. Yan, N.G. Wallis, S. Reed, T.D. Moore, S.F. Rittenhouse, W.E. DeWolf, J. Huang, D. McDevitt and W.H. Miller, 2002. Defining and combating the mechanisms of triclosan resistance in clinical isolates of *Staphylococcus aureus*. Antimicrobial agents and chemotherapy, 46(11): 3343-3347.

Fang, Z. and X. Cui, 2011. Design and validation issues in RNA-seq experiments. Briefings in bioinformatics, 12(3): 280-287.

Faruque, S.M. and J.J. Mekalanos, 2012. Phage-bacterial interactions in the evolution of toxigenic *Vibrio cholerae*. Virulence, 3(7): 556-565.

Ferrarini, M., M. Moretto, J.A. Ward, N. Šurbanovski, V. Stevanović, L. Giongo, R. Viola, D. Cavalieri, R. Velasco and A. Cestaro, 2013. An evaluation of the PacBio RS platform for sequencing and de novo assembly of a chloroplast genome. BMC genomics, 14(1): 670.

Ferreira, A.M., K.B. Martins, V.R.d. Silva, A.L. Mondelli and M.d.L.R.d. Cunha, 2017. Correlation of phenotypic tests with the presence of the *blaZ* gene for detection of beta-lactamase. brazilian journal of microbiology, 48(1): 159-166.

Fey, P.D. and M.E. Olson, 2010. Current concepts in biofilm formation of *Staphylococcus epidermidis*. Future microbiology, 5(6): 917-933.

Finotello, F. and B. Di Camillo, 2015. Measuring differential gene expression with RNA-seq: Challenges and strategies for data analysis. Briefings in functional genomics, 14(2): 130-142.

Fischbach, M.A. and C.T. Walsh, 2006. Assembly-line enzymology for polyketide and nonribosomal peptide antibiotics: Logic, machinery, and mechanisms. Chemical reviews, 106(8): 3468-3496.

Fleming, V., E. Feil, A.K. Sewell, N. Day, A. Buckling and R.C. Massey, 2006. Agr interference between clinical *Staphylococcus aureus* strains in an insect model of virulence. Journal of bacteriology, 188(21): 7686-7688.

Fontana, M.B.C., M.d.C.F. de Bastos and A. Brandelli, 2006. Bacteriocins pep5 and epidermin inhibit *Staphylococcus epidermidis* adhesion to catheters. Current Microbiology, 52(5): 350-353.

Foster, T.J., 2005. Immune evasion by staphylococci. Nature Reviews Microbiology, 3(12): 948-958.

Foster, T.J., 2017. Antibiotic resistance in *Staphylococcus aureus*. Current status and future prospects. Fems microbiology reviews, 41(3): 430-449.

Foster, T. J., Geoghegan, J. A., Ganesh, V. K., & Höök, M., 2014. Adhesion, invasion and evasion: the many functions of the surface proteins of *Staphylococcus aureus*. Nature Reviews Microbiology, 12(1), 49.

Foster, T.J. and M. Höök, 1998. Surface protein adhesins of *Staphylococcus aureus* Trends in microbiology, 6(12): 484-488..

Fournier, B. and D.C. Hooper, 2000. A new two-component regulatory system involved in adhesion, autolysis, and extracellular proteolytic activity of *Staphylococcus aureus*. Journal of bacteriology, 182(14): 3955-3964.

Fournier, B., A. Klier and G. Rapoport, 2001. The two-component system ArlS–ArlR is a regulator of virulence gene expression in *Staphylococcus aureus*. Molecular microbiology, 41(1): 247-261.

Frank, D.N., L.M. Feazel, M.T. Bessesen, C.S. Price, E.N. Janoff and N.R. Pace, 2010. The human nasal microbiota and *Staphylococcus aureus* carriage. PLoS One, 5(5): e10598.

Freeman, Z.N., S. Dorus and N.R. Waterfield, 2013. The kdpD/kdpE two-component system: Integrating k+ homeostasis and virulence. PLoS pathogens, 9(3): e1003201.

Friedman, L., J.D. Alder and J.A. Silverman, 2006. Genetic changes that correlate with reduced susceptibility to daptomycin in *Staphylococcus aureus*. Antimicrobial agents and chemotherapy, 50(6): 2137-2145.

Frost, L.S., R. Leplae, A.O. Summers and A. Toussaint, 2005. Mobile genetic elements: The agents of open source evolution. Nature Reviews Microbiology, 3(9): 722-732.

Fuchs, S., H. Mehlan, J. Bernhardt, A. Hennig, S. Michalik, K. Surmann, J. Pané-Farré, A. Giese, S. Weiss and L. Backert, 2018. Aureowiki- the repository of the *Staphylococcus aureus* research and annotation community. International Journal of Medical Microbiology, 308(6): 558-568.

Funa, N., Y. Ohnishi, I. Fujii, M. Shibuya, Y. Ebizuka and S. Horinouchi, 1999. A new pathway for polyketide synthesis in microorganisms. Nature, 400(6747): 897.

Furi, L., R. Haigh, Z.J. Al Jabri, I. Morrissey, H.-Y. Ou, R. León-Sampedro, J.L. Martinez, T.M. Coque and M.R. Oggioni, 2016. Dissemination of novel antimicrobial resistance mechanisms through the insertion sequence mediated spread of metabolic genes. Frontiers in microbiology, 7: 1008.

Gagliano, V.J. and R. Hinsdill, 1970. Characterization of a *Staphylococcus aureus* bacteriocin. Journal of bacteriology, 104(1): 117-125.

Gal-Mor, O. and B.B. Finlay, 2006. Pathogenicity islands: A molecular toolbox for bacterial virulence. Cellular microbiology, 8(11): 1707-1719.

Gao, Z., C.-h. Tseng, Z. Pei and M.J. Blaser, 2007. Molecular analysis of human forearm superficial skin bacterial biota. Proceedings of the National Academy of Sciences, 104(8): 2927-2932.

Gardete, S., S. Wu, S. Gill and A. Tomasz, 2006. Role of VraSR in antibiotic resistance and antibiotic-induced stress response in *Staphylococcus aureus*. Antimicrobial agents and chemotherapy, 50(10): 3424-3434.

Gardner, A., S.A. West and A. Buckling, 2004. Bacteriocins, spite and virulence. Proceedings of the Royal Society of London B: Biological Sciences, 271(1547): 1529-1535.

Gaupp, R., N. Ledala and G.A. Somerville, 2012. Staphylococcal response to oxidative stress. Frontiers in cellular and infection microbiology, 2: 33.

Gaupp, R., S. Schlag, M. Liebeke, M. Lalk and F. Götz, 2010. Advantage of upregulation of succinate dehydrogenase in *Staphylococcus aureus* biofilms. Journal of bacteriology, 192(9): 2385-2394.

Geisinger, E., R.P. Adhikari, R. Jin, H.F. Ross and R.P. Novick, 2006. Inhibition of rot translation by RNAIII, a key feature of agr function. Molecular microbiology, 61(4): 1038-1048.

Gerke, C., A. Kraft, R. Süßmuth, O. Schweitzer and F. Götz, 1998. Characterization of the N-acetylglucosaminyltransferase activity involved in the biosynthesis of the *Staphylococcus epidermidis* polysaccharide intercellular adhesin. Journal of Biological Chemistry, 273(29): 18586-18593.

Giambiagi-Marval, M., M. Mafra, E. Penido and M. Bastos, 1990. Distinct groups of plasmids correlated with bacteriocin production in *Staphylococcus aureus*. Microbiology, 136(8): 1591-1599.

Gillaspy, A.F., S.G. Hickmon, R.A. Skinner, J.R. Thomas, C.L. Nelson and M.S. Smeltzer, 1995. Role of the accessory gene regulator (agr) in pathogenesis of staphylococcal osteomyelitis. Infection and immunity, 63(9): 3373-3380.

Gillor, O., A. Etzion and M. Riley, 2008. The dual role of bacteriocins as anti-and probiotics. Applied microbiology and biotechnology, 81(4): 591-606.

Goerke, C., S. Campana, M.G. Bayer, G. Döring, K. Botzenhart and C. Wolz, 2000. Direct quantitative transcript analysis of the agr regulon of *Staphylococcus aureus* during human infection in comparison to the expression profile in vitro. Infection and immunity, 68(3): 1304-1311.

Gonzalez, D.J., N.M. Haste, A. Hollands, T.C. Fleming, M. Hamby, K. Pogliano, V. Nizet and P.C. Dorrestein, 2011. Microbial competition between *Bacillus subtilis* and *Staphylococcus aureus* monitored by imaging mass spectrometry. Microbiology, 157(9): 2485-2492.

Gordon, D.M. and M.A. Riley, 1999. A theoretical and empirical investigation of the invasion dynamics of colicinogeny. Microbiology, 145(3): 655-661.

Götz, F., S. Perconti, P. Popella, R. Werner and M. Schlag, 2014. Epidermin and gallidermin: Staphylococcal lantibiotics. International Journal of Medical Microbiology, 304(1): 63-71.

Grandgirard, D., L. Furi, M.L. Ciusa, L. Baldassarri, D.R. Knight, I. Morrissey, C.R. Largiadèr, S.L. Leib and M.R. Oggioni, 2015. Mutations upstream of fabI in triclosan resistant *Staphylococcus aureus* strains are associated with elevated fabi gene expression. BMC genomics, 16(1): 1.

Grebe, T.W. and J.B. Stock, 1999. The histidine protein kinase superfamily. In: Advances in microbial physiology. Elsevier: pp: 139-227.

Grice, E.A., H.H. Kong, S. Conlan, C.B. Deming, J. Davis, A.C. Young, G.G. Bouffard, R.W. Blakesley, P.R. Murray and E.D. Green, 2009. Topographical and

temporal diversity of the human skin microbiome. science, 324(5931): 1190-1192.
Grice, E.A., H.H. Kong, G. Renaud, A.C. Young, G.G. Bouffard, R.W. Blakesley, T.G. Wolfsberg, M.L. Turner and J.A. Segre, 2008. A diversity profile of the human skin microbiota. Genome research, 18(7): 1043-1050.
Grice, E.A. and J.A. Segre, 2011. The skin microbiome. Nature Reviews Microbiology, 9(4): 244-253.
Groicher, K.H., B.A. Firek, D.F. Fujimoto and K.W. Bayles, 2000. The *Staphylococcus aureus* lrgAB operon modulates murein hydrolase activity and penicillin tolerance. Journal of bacteriology, 182(7): 1794-1801.
Grüner, B., S.-R. Han, H.-G. Meyer, U. Wulf, S. Bhakdi and E. Siegel, 2007. Characterization of a catalase-negative methicillin-resistant *Staphylococcus aureus* strain. Journal of clinical microbiology, 45(8): 2684-2685.
Guder, A., I. Wiedemann and H.G. Sahl, 2000. Posttranslationally modified bacteriocins—the lantibiotics. Peptide Science, 55(1): 62-73.
Gustafsson, E. and J. Oscarsson, 2008. Maximal transcription of *aur* (aureolysin) and *sspA* (serine protease) in *Staphylococcus aureus* requires staphylococcal accessory regulator R (*sarR*) activity. FEMS microbiology letters, 284(2): 158-164.
Haag, A.F. and F. Bagnoli, 2015. The role of two-component signal transduction systems in *Staphylococcus aureus* virulence regulation.
Habets, M.G., T. Czaran, R.F. Hoekstra and J.A.G. de Visser, 2007. Spatial structure inhibits the rate of invasion of beneficial mutations in asexual populations. Proceedings of the Royal Society of London B: Biological Sciences, 274(1622): 2139-2143.
Hadjithomas, M., I.-M.A. Chen, K. Chu, A. Ratner, K. Palaniappan, E. Szeto, J. Huang, T. Reddy, P. Cimermančič and M.A. Fischbach, 2015. Img-abc: A knowledge base to fuel discovery of biosynthetic gene clusters and novel secondary metabolites. MBio, 6(4): e00932-00915.
Hafkin, B., N. Kaplan and B. Murphy, 2015. Efficacy and safety of AFN-1252, the first *Staphylococcus*-specific antibacterial agent, in the treatment of ABSSSI, including patients with significant co-morbidities. Antimicrobial agents and chemotherapy: AAC. 01741-01715.
Hahn, M. and T. Stachelhaus, 2004. Selective interaction between nonribosomal peptide synthetases is facilitated by short communication-mediating domains. Proceedings of the National Academy of Sciences, 101(44): 15585-15590.
Hall, J.W., J. Yang, H. Guo and Y. Ji, 2016. The *Staphylococcus aureus* AirSR two-component system mediates reactive oxygen species resistance via transcriptional regulation of staphyloxanthin production. Infection and immunity: IAI. 00838-00816.
Hanahan, D., Jessee, J., and Bloom, F.R., 1991. Plasmid transformation of *Escherichia coli* and other bacteria. Methods in Enzymology 204, 63-113
Han, L., K.C. Vickers, D.C. Samuels and Y. Guo, 2014. Alternative applications for distinct RNA sequencing strategies. Briefings in bioinformatics, 16(4): 629-639.

Hancock, R.E.W. and H.-G. Sahl, 2006. Antimicrobial and host-defense peptides as new anti-infective therapeutic strategies. Nature biotechnology, 24(12): 1551-1557.

Hanzelmann, D., H.-S. Joo, M. Franz-Wachtel, T. Hertlein, S. Stevanovic, B. Macek, C. Wolz, F. Götz, M. Otto and D. Kretschmer, 2016. Toll-like receptor 2 activation depends on lipopeptide shedding by bacterial surfactants. Nature communications, 7: 12304.

Harrington, N. 2017. A genomic approach to the functional characterisation of the *Staphylococcus aureus* SH1000 genes *SAOUHSC_01312* and *SAOUHSC_01314*.

Harrison, F., J. Paul, R.C. Massey and A. Buckling, 2008. Interspecific competition and siderophore-mediated cooperation in *Pseudomonas aeruginosa*. The ISME journal, 2(1): 49.

Hasper, H.E., N.E. Kramer, J.L. Smith, J. Hillman, C. Zachariah, O.P. Kuipers, B. De Kruijff and E. Breukink, 2006. An alternative bactericidal mechanism of action for lantibiotic peptides that target lipid II. Science, 313(5793): 1636-1637.

Heath, R.J., J. Li, G.E. Roland and C.O. Rock, 2000. Inhibition of the *Staphylococcus aureus* NADPH-dependent enoyl-acyl carrier protein reductase by triclosan and hexachlorophene. Journal of Biological Chemistry, 275(7): 4654-4659.

Heath, R.J. and C.O. Rock, 1995. Enoyl-acyl carrier protein reductase (FabI) plays a determinant role in completing cycles of fatty acid elongation in *Escherichia coli*. Journal of Biological Chemistry, 270(44): 26538-26542.

Heather, J.M. and B. Chain, 2016. The sequence of sequencers: The history of sequencing DNA. Genomics, 107(1): 1-8.

Héchard, Y. and H.-G. Sahl, 2002. Mode of action of modified and unmodified bacteriocins from Gram-positive bacteria. Biochimie, 84(5-6): 545-557.

Heidrich, C., U. Pag, M. Josten, J. Metzger, R.W. Jack, G. Bierbaum, G. Jung and H.-G. Sahl, 1998. Isolation, characterization, and heterologous expression of the novel lantibiotic epicidin 280 and analysis of its biosynthetic gene cluster. Applied and environmental microbiology, 64(9): 3140-3146.

Heilmann, C., J. Hartleib, M.S. Hussain and G. Peters, 2005. The multifunctional *Staphylococcus aureus* autolysin aaa mediates adherence to immobilized fibrinogen and fibronectin. Infection and immunity, 73(8): 4793-4802.

Heilmann, C., O. Schweitzer, C. Gerke, N. Vanittanakom, D. Mack and F. Götz, 1996. Molecular basis of intercellular adhesion in the biofilm-forming *Staphylococcus epidermidis*. Molecular microbiology, 20(5): 1083-1091.

Hell, W., H.G.W. Meyer and S.G. Gatermann, 1998. Cloning of aas, a gene encoding a *Staphylococcus saprophyticus* surface protein with adhesive and autolytic properties. Molecular microbiology, 29(3): 871-881.

Herbert, S., A. Bera, C. Nerz, D. Kraus, A. Peschel, C. Goerke, M. Meehl, A. Cheung and F. Götz, 2007. Molecular basis of resistance to muramidase and cationic antimicrobial peptide activity of lysozyme in staphylococci. PLoS pathogens, 3(7): e102.

Hibbing, M.E., C. Fuqua, M.R. Parsek and S.B. Peterson, 2010. Bacterial competition: Surviving and thriving in the microbial jungle. Nature Reviews Microbiology, 8(1): 15-25.

Hildebrand, M., L.E. Waggoner, H. Liu, S. Sudek, S. Allen, C. Anderson, D.H. Sherman and M. Haygood, 2004. bryA: An unusual modular polyketide synthase gene from the uncultivated bacterial symbiont of the marine bryozoan *Bugula neritina*. Chemistry & biology, 11(11): 1543-1552.

Hiradate, S., S. Yoshida, H. Sugie, H. Yada and Y. Fujii, 2002. Mulberry anthracnose antagonists (iturins) produced by *Bacillus amyloliquefaciens* rc-2. Phytochemistry, 61(6): 693-698.

Hiraoka, S., H. Matsuzaki and I. Shibuya, 1993. Active increase in cardiolipin synthesis in the stationary growth phase and its physiological significance in *Escherichia coli*. FEBS letters, 336(2): 221-224.

Hiron, A., M. Falord, J. Valle, M. Débarbouillé and T. Msadek, 2011. Bacitracin and nisin resistance in *Staphylococcus aureus*: A novel pathway involving the bras/brar two-component system (SA2417/SA2418) and both the BraD/BraE and VraD/VraE ABC transporters. Molecular microbiology, 81(3): 602-622.

Hoffmann, A., T. Schneider, U. Pag and H.-G. Sahl, 2004. Localization and functional analysis of PepI, the immunity peptide of Pep5-producing *Staphylococcus epidermidis* strain 5. Applied and environmental microbiology, 70(6): 3263-3271.

Holland, K.T. and R.A. Bojar, 2002. Cosmetics. American journal of clinical dermatology, 3(7): 445-449.

Hopwood, D.A. and D.H. Sherman, 1990. Molecular genetics of polyketides and its comparison to fatty acid biosynthesis. Annual review of genetics, 24(1): 37-62.

Horsburgh, M.J., J.L. Aish, I.J. White, L. Shaw, J.K. Lithgow and S.J. Foster, 2002. SigmaB modulates virulence determinant expression and stress resistance: Characterization of a functional rsbU strain derived from *Staphylococcus aureus* 8325-4. Journal of bacteriology, 184(19): 5457-5467.

Howden, B.P., J.K. Davies, P.D. Johnson, T.P. Stinear and M.L. Grayson, 2010. Reduced vancomycin susceptibility in *Staphylococcus aureus*, including vancomycin-intermediate and heterogeneous vancomycin-intermediate strains: Resistance mechanisms, laboratory detection, and clinical implications. Clinical microbiology reviews, 23(1): 99-139.

Howden, B.P., C.R. McEvoy, D.L. Allen, K. Chua, W. Gao, P.F. Harrison, J. Bell, G. Coombs, V. Bennett-Wood and J.L. Porter, 2011. Evolution of multidrug resistance during *Staphylococcus aureus* infection involves mutation of the essential two component regulator walKR. PLoS pathogens, 7(11): e1002359.

Huang, Y.-C., Y.-M. Lin, T.-W. Chang, S.-J. Wu, Y.-S. Lee, M.D.-T. Chang, C. Chen, S.-H. Wu and Y.-D. Liao, 2007. The flexible and clustered lysine residues of human ribonuclease 7 are critical for membrane permeability and antimicrobial activity. Journal of Biological Chemistry, 282(7): 4626-4633.

Hyatt, D., G.-L. Chen, P.F. LoCascio, M.L. Land, F.W. Larimer and L.J. Hauser, 2010. Prodigal: Prokaryotic gene recognition and translation initiation site identification. BMC bioinformatics, 11(1): 119.

Ingavale, S., W. van Wamel, T.T. Luong, C.Y. Lee and A.L. Cheung, 2005. Rat/MgrA, a regulator of autolysis, is a regulator of virulence genes in *Staphylococcus aureus*. Infection and immunity, 73(3): 1423-1431.

Inglis, R.F., A. Gardner, P. Cornelis and A. Buckling, 2009. Spite and virulence in the bacterium *Pseudomonas aeruginosa*. Proceedings of the National Academy of Sciences, 106(14): 5703-5707.

Iwase, T., Y. Uehara, H. Shinji, A. Tajima, H. Seo, K. Takada, T. Agata and Y. Mizunoe, 2010. *Staphylococcus epidermidis* Esp inhibits *Staphylococcus aureus* biofilm formation and nasal colonization. Nature, 465(7296): 346-349.

Iwatsuki, K., O. Yamasaki, S. Morizane and T. Oono, 2006. Staphylococcal cutaneous infections: Invasion, evasion and aggression. Journal of dermatological science, 42(3): 203-214.

Jack, R.W., J.R. Tagg and B. Ray, 1995. Bacteriocins of Gram-positive bacteria. Microbiological reviews, 59(2): 171-200.

Jamrozy, D., F. Coll, A.E. Mather, S.R. Harris, E.M. Harrison, A. MacGowan, A. Karas, T. Elston, M.E. Török and J. Parkhill, 2017. Evolution of mobile genetic element composition in an epidemic methicillin-resistant *Staphylococcus aureus*: Temporal changes correlated with frequent loss and gain events. BMC genomics, 18(1): 684.

Janek, D., A. Zipperer, A. Kulik, B. Krismer and A. Peschel, 2016. High frequency and diversity of antimicrobial activities produced by nasal staphylococcus strains against bacterial competitors. PLoS Pathog, 12(8): e1005812.

Jang, S., 2016. Multidrug efflux pumps in *Staphylococcus aureus* and their clinical implications. Journal of Microbiology, 54(1): 1-8.

Janzon, L. and S. Arvidson, 1990. The role of the delta-lysin gene (*hld*) in the regulation of virulence genes by the accessory gene regulator (*agr*) in *Staphylococcus aureus*. The EMBO journal, 9(5): 1391-1399.

Jenke-Kodama, H. and E. Dittmann, 2009. Bioinformatic perspectives on NRPs/PKs megasynthases: Advances and challenges. Natural product reports, 26(7): 874-883.

Jenke-Kodama, H., A. Sandmann, R. Müller and E. Dittmann, 2005. Evolutionary implications of bacterial polyketide synthases. Molecular biology and evolution, 22(10): 2027-2039.

Jenkins, R., N. Burton and R. Cooper, 2013. Proteomic and genomic analysis of methicillin-resistant *Staphylococcus aureus* (MRSA) exposed to manuka honey in vitro demonstrated down-regulation of virulence markers. Journal of Antimicrobial Chemotherapy, 69(3): 603-615.

Jensen, S.O. and B.R. Lyon, 2009. Genetics of antimicrobial resistance in *Staphylococcus aureus*. Future microbiology, 4(5): 565-582.

Ji, Q., L. Zhang, F. Sun, X. Deng, H. Liang, T. Bae and C. He, 2012. *Staphylococcus aureus* CymR is a new thiol-based oxidation-sensing regulator of stress resistance and oxidative response. Journal of Biological Chemistry, 287(25): 21102-21109.

Joh, D., E.R. Wann, B. Kreikemeyer, P. Speziale and M. Höök, 1999. Role of fibronectin-binding MSCRAMMS in bacterial adherence and entry into mammalian cells. Matrix Biology, 18(3): 211-223.

Joo, H.-S. and M. Otto, 2015. Mechanisms of resistance to antimicrobial peptides in staphylococci. Biochimica et Biophysica Acta (BBA)-Biomembranes, 1848(11): 3055-3061.

Jorge, A.M., J. Schneider, S. Unsleber, N. Göhring, C. Mayer and A. Peschel, 2017. Utilization of glycerophosphodiesters by *Staphylococcus aureus*. Molecular microbiology, 103(2): 229-241.

Kahl, B.C., K. Becker and B. Löffler, 2016. Clinical significance and pathogenesis of staphylococcal small colony variants in persistent infections. Clinical microbiology reviews, 29(2): 401-427.

Kaletta, C., K.-D. Entian, R. Kellner, G. Jung, M. Reis and H.-G. Sahl, 1989. Pep5, a new lantibiotic: Structural gene isolation and prepeptide sequence. Archives of Microbiology, 152(1): 16-19.

Kanehisa, M., S. Goto, Y. Sato, M. Kawashima, M. Furumichi and M. Tanabe, 2013. Data, information, knowledge and principle: Back to metabolism in KEGG. Nucleic acids research, 42(D1): D199-D205.

Karlowsky, J.A., N. Kaplan, B. Hafkin, D.J. Hoban and G.G. Zhanel, 2009. AFN-1252, a *fabI* inhibitor, demonstrates a Staphylococcus-specific spectrum of activity. Antimicrobial agents and chemotherapy, 53(8): 3544-3548.

Katzif, S., E.-H. Lee, A.B. Law, Y.-L. Tzeng and W.M. Shafer, 2005. CspA regulates pigment production in *Staphylococcus aureus* through a sigB-dependent mechanism. Journal of bacteriology, 187(23): 8181-8184.

Kawada-Matsuo, M., Y. Yoshida, N. Nakamura and H. Komatsuzawa, 2011. Role of two-component systems in the resistance of *Staphylococcus aureus* to antibacterial agents. Virulence, 2(5): 427-430.

Kawada-Matsuo, M., Y. Yoshida, T. Zendo, J. Nagao, Y. Oogai, Y. Nakamura, K. Sonomoto, N. Nakamura and H. Komatsuzawa, 2013. Three distinct two-component systems are involved in resistance to the class I bacteriocins, nukacin isk-1 and nisin a, in *Staphylococcus aureus*. PloS one, 8(7): e69455.

Kawada-Matsuo, M., F. Shammi, Y. Oogai, N. Nakamura, M. Sugai and H. Komatsuzawa, 2016. C55 bacteriocin produced by ETB-plasmid positive *Staphylococcus aureus* strains is a key factor for competition with *S. aureus* strains. Microbiology and immunology, 60(3): 139-147.

Kędzierska, B. and F. Hayes, 2016. Emerging roles of toxin-antitoxin modules in bacterial pathogenesis. Molecules, 21(6): 790.

KELLNER, R., G. JUNG, T. HÖRNER, H. ZÄHNER, N. SCHNELL, K.D. ENTIAN and F. GÖTZ, 1988. Gallidermin: A new lanthionine-containing polypeptide antibiotic. European Journal of Biochemistry, 177(1): 53-59.

Kenny, J.G., D. Ward, E. Josefsson, M. Jonsson, J. Hinds, H.H. Rees, J.A. Lindsay, A. Tarkowski and M.J. Horsburgh, 2009. The *Staphylococcus aureus* response to unsaturated long chain free fatty acids: Survival mechanisms and virulence implications. PloS one, 4(2): e4344.

Khan, S.T., J. Musarrat, A.A. Alkhedhairy and S. Kazuo, 2014. Diversity of bacteria and polyketide synthase associated with marine sponge haliclona sp. Annals of microbiology, 64(1): 199-207.

Khare, A. and S. Tavazoie, 2015. Multifactorial competition and resistance in a two-species bacterial system. PLoS genetics, 11(12): e1005715.

Kies, S., C. Vuong, M. Hille, A. Peschel, C. Meyer, F. Götz and M. Otto, 2003. Control of antimicrobial peptide synthesis by the *agr* quorum sensing system in

Staphylococcus epidermidis: Activity of the lantibiotic epidermin is regulated at the level of precursor peptide processing. Peptides, 24(3): 329-338.

Kim, J.W., H.-K. Kim, G.S. Kang, I.-H. Kim, H.S. Kim, Y.S. Lee and J.I. Yoo, 2016. The SAV1322 gene from *Staphylococcus aureus*: Genomic and proteomic approaches to identification and characterization of gene function. BMC microbiology, 16(1): 206.

Kim, P.I., J.K. Sohng, C. Sung, H.-S. Joo, E.-M. Kim, T. Yamaguchi, D. Park and B.-G. Kim, 2010. Characterization and structure identification of an antimicrobial peptide, hominicin, produced by *Staphylococcus hominis* MBBL 2–9. Biochemical and biophysical research communications, 399(2): 133-138.

Kim, Y., X. Wang, Q. Ma, X.-S. Zhang and T.K. Wood, 2009. Toxin-antitoxin systems in *Escherichia coli* influence biofilm formation through Yjgk (TabA) and fimbriae. Journal of bacteriology, 191(4): 1258-1267.

Kimura, H., H. Matsusaki, T. Sashihara, K. Sonomoto and A. Ishizaki, 1998. Purification and partial identification of bacteriocin Isk-1, a new lantibiotic produced by *pediococcus sp.* Isk-1. Bioscience, biotechnology, and biochemistry, 62(12): 2341-2345.

King, M.D., B.J. Humphrey, Y.F. Wang, E.V. Kourbatova, S.M. Ray and H.M. Blumberg, 2006. Emergence of community-acquired methicillin-resistant *Staphylococcus aureus* USA300 clone as the predominant cause of skin and soft-tissue infections. Annals of internal medicine, 144(5): 309-317.

King, N.P., S.A. Beatson, M. Totsika, G.C. Ulett, R.A. Alm, P.A. Manning and M.A. Schembri, 2011. UafB is a serine-rich repeat adhesin of *Staphylococcus saprophyticus* that mediates binding to fibronectin, fibrinogen and human uroepithelial cells. Microbiology, 157(4): 1161-1175.

Klaenhammer, T.R., 1993. Genetics of bacteriocins produced by *lactic acid* bacteria. FEMS microbiology reviews, 12(1-3): 39-85.

Kloos, W.E. and K.H. Schleifer, 1975. Isolation and characterization of staphylococci from human skin II. Descriptions of four new species: *Staphylococcus warneri*, *Staphylococcus capitis*, *Staphylococcus hominis*, and *Staphylococcus simulans*. International Journal of Systematic Bacteriology, 25(1): 62-79.

Kobayashi, K., M. Ogura, H. Yamaguchi, K.-I. Yoshida, N. Ogasawara, T. Tanaka and Y. Fujita, 2001. Comprehensive DNA microarray analysis of *Bacillus subtilis* two-component regulatory systems. Journal of bacteriology, 183(24): 7365-7370.

Kocianova, S., C. Vuong, Y. Yao, J.M. Voyich, E.R. Fischer, F.R. DeLeo and M. Otto, 2005. Key role of poly-γ-dl-glutamic acid in immune evasion and virulence of *Staphylococcus epidermidis*. The Journal of clinical investigation, 115(3): 688-694.

Kohler, T., C. Weidenmaier and A. Peschel, 2009. Wall teichoic acid protects *Staphylococcus aureus* against antimicrobial fatty acids from human skin. Journal of bacteriology, 191(13): 4482-4484.

Kolar, S.L., V. Nagarajan, A. Oszmiana, F.E. Rivera, H.K. Miller, J.E. Davenport, J.T. Riordan, J. Potempa, D.S. Barber and J. Koziel, 2011. NsaRS is a cell-envelope-stress-sensing two-component system of *Staphylococcus aureus*. Microbiology, 157(8): 2206-2219.

Kolbe, D.L. and S.R. Eddy, 2011. Fast filtering for RNA homology search. Bioinformatics, 27(22): 3102-3109.

Kommineni, S., D.J. Bretl, V. Lam, R. Chakraborty, M. Hayward, P. Simpson, Y. Cao, P. Bousounis, C.J. Kristich and N.H. Salzman, 2015. Bacteriocin production augments niche competition by enterococci in the mammalian gastrointestinal tract. Nature, 526(7575): 719.

Kong, H.H., J. Oh, C. Deming, S. Conlan, E.A. Grice, M.A. Beatson, E. Nomicos, E.C. Polley, H.D. Komarow and P.R. Murray, 2012. Temporal shifts in the skin microbiome associated with disease flares and treatment in children with atopic dermatitis. Genome research.

Koprivnjak, T., D. Zhang, C. Ernst, A. Peschel, W. Nauseef and J. Weiss, 2011. Characterization of *Staphylococcus aureus* cardiolipin synthases 1 and 2 and their contribution to accumulation of cardiolipin in stationary phase and within phagocytes. Journal of bacteriology: JB. 00288-00211.

Kordel, M., R. Benz and H. Sahl, 1988. Mode of action of the staphylococcin like peptide Pep 5: Voltage-dependent depolarization of bacterial and artificial membranes. Journal of bacteriology, 170(1): 84-88.

Koren, S., M.C. Schatz, B.P. Walenz, J. Martin, J.T. Howard, G. Ganapathy, Z. Wang, D.A. Rasko, W.R. McCombie and E.D. Jarvis, 2012. Hybrid error correction and de novo assembly of single-molecule sequencing reads. Nature biotechnology, 30(7): 693.

Krismer, B., M. Liebeke, D. Janek, M. Nega, M. Rautenberg, G. Hornig, C. Unger, C. Weidenmaier, M. Lalk and A. Peschel, 2014. Nutrient limitation governs *Staphylococcus aureus* metabolism and niche adaptation in the human nose. PLoS pathogens, 10(1): e1003862.

Krismer, B., C. Weidenmaier, A. Zipperer and A. Peschel, 2017. The commensal lifestyle of *Staphylococcus aureus* and its interactions with the nasal microbiota. Nature reviews microbiology, 15(11): 675.

Krzyściak, W., A. Jurczak, D. Kościelniak, B. Bystrowska and A. Skalniak, 2014. The virulence of *Streptococcus mutans* and the ability to form biofilms. European Journal of Clinical Microbiology & Infectious Diseases, 33(4): 499-515.

Kullik, I., P. Giachino and T. Fuchs, 1998. Deletion of the alternative sigma factor σb in *Staphylococcus aureus* reveals its function as a global regulator of virulence genes. Journal of bacteriology, 180(18): 4814-4820.

Kuroda, M., H. Hayashi and T. Ohta, 1999. Chromosome-determined zinc-responsible operon *czr* in *Staphylococcus aureus* strain 912. Microbiology and immunology, 43(2): 115-125.

Kuroda, M., H. Kuroda, T. Oshima, F. Takeuchi, H. Mori and K. Hiramatsu, 2003. Two-component system vraSR positively modulates the regulation of cell-wall biosynthesis pathway in *Staphylococcus aureus*. Molecular microbiology, 49(3): 807-821.

Kuroda, M., K. Kuwahara-Arai and K. Hiramatsu, 2000. Identification of the up- and down-regulated genes in vancomycin-resistant *Staphylococcus aureus* strains Mu3 and Mu50 by cDNA differential hybridization method. Biochemical and biophysical research communications, 269(2): 485-490.

Kuroda, M., Y. Tanaka, R. Aoki, D. Shu, K. Tsumoto and T. Ohta, 2008. *Staphylococcus aureus* giant protein Ebh is involved in tolerance to

transient hyperosmotic pressure. Biochemical and biophysical research communications, 374(2): 237-241.

Kusuma, C., A. Jadanova, T. Chanturiya and J.F. Kokai-Kun, 2007. Lysostaphin-resistant variants of *Staphylococcus aureus* demonstrate reduced fitness in vitro and in vivo. Antimicrobial agents and chemotherapy, 51(2): 475-482.

Lagesen, K., P. Hallin, E.A. Rødland, H.-H. Stærfeldt, T. Rognes and D.W. Ussery, 2007. Rnammer: Consistent and rapid annotation of ribosomal RNA genes. Nucleic acids research, 35(9): 3100-3108.

Lai, Y., A.L. Cogen, K.A. Radek, H.J. Park, D.T. MacLeod, A. Leichtle, A.F. Ryan, A. Di Nardo and R.L. Gallo, 2010. Activation of TLR2 by a small molecule produced by *Staphylococcus epidermidis* increases antimicrobial defense against bacterial skin infections. Journal of Investigative Dermatology, 130(9): 2211-2221.

Langmead, B. and S.L. Salzberg, 2012. Fast gapped-read alignment with Bowtie 2. Nature methods, 9(4): 357.

Lasa, I., A. Toledo-Arana, A. Dobin, M. Villanueva, I.R. de los Mozos, M. Vergara-Irigaray, V. Segura, D. Fagegaltier, J.R. Penadés and J. Valle, 2011. Genome-wide antisense transcription drives mRNA processing in bacteria. Proceedings of the National Academy of Sciences, 108(50): 20172-20177.

Laslett, D. and B. Canback, 2004. Aragorn, a program to detect tRNA genes and tmRNA genes in nucleotide sequences. Nucleic acids research, 32(1): 11-16.

Lather, P., A. Mohanty, P. Jha, A.K. Garsa and S. Sood, 2015. Changes associated with cell membrane composition of *Staphylococcus aureus* on acquisition of resistance against class II a bacteriocin and its in vitro substantiation. European Food Research and Technology, 240(1): 101-107.

Lee, D.-Y., K. Yamasaki, J. Rudsil, C.C. Zouboulis, G.T. Park, J.-M. Yang and R.L. Gallo, 2008. Sebocytes express functional cathelicidin antimicrobial peptides and can act to kill *Propionibacterium acnes*. The Journal of investigative dermatology, 128(7): 1863.

Lertcanawanichakul, M. and S. Sawangnop, 2011. A comparison of two methods used for measuring the antagonistic activity of *Bacillus* species. Walailak Journal of Science and Technology (WJST), 5(2): 161-171.

Levinger, O., T. Bikels-Goshen, E. Landau, M. Fichman and R. Shapira, 2012. Epigallocatechin gallate (EGCG) induces upregulation of the two-component VraSR system by evoking a cell wall stress response in *Staphylococcus aureus*. Applied and environmental microbiology: AEM. 02253-02212.

Lewis, K., 2013. Platforms for antibiotic discovery. Nature reviews Drug discovery, 12(5): 371.

Li, H. and R. Durbin, 2009. Fast and accurate short read alignment with burrows–wheeler transform. bioinformatics, 25(14): 1754-1760.

Li, H., B. Handsaker, A. Wysoker, T. Fennell, J. Ruan, N. Homer, G. Marth, G. Abecasis and R. Durbin, 2009. The sequence alignment/map format and samtools. Bioinformatics, 25(16): 2078-2079.

Li, M., D.J. Cha, Y. Lai, A.E. Villaruz, D.E. Sturdevant and M. Otto, 2007. The antimicrobial peptide-sensing system aps of *Staphylococcus aureus*. Molecular microbiology, 66(5): 1136-1147.

Li, M.H., P.M. Ung, J. Zajkowski, S. Garneau-Tsodikova and D.H. Sherman, 2009. Automated genome mining for natural products. BMC bioinformatics, 10(1): 185.

Li, R., C.-L. Hsieh, A. Young, Z. Zhang, X. Ren and Z. Zhao, 2015. Illumina synthetic long read sequencing allows recovery of missing sequences even in the "finished" c. Elegans genome. Scientific reports, 5: 10814.

Li, S., H. Huang, X. Rao, W. Chen, Z. Wang and X. Hu, 2014. Phenol-soluble modulins: Novel virulence-associated peptides of staphylococci. Future microbiology, 9(2): 203-216.

Libberton, B., R.E. Coates, M.A. Brockhurst and M.J. Horsburgh, 2014. Evidence that intraspecific trait variation among nasal bacteria shapes the distribution of *Staphylococcus aureus*. Infection and immunity, 82(9): 3811-3815.

Libberton, B., M.J. Horsburgh and M.A. Brockhurst, 2015. The effects of spatial structure, frequency dependence and resistance evolution on the dynamics of toxin-mediated microbial invasions. Evolutionary applications, 8(7): 738-750.

Lin, J.T. and V. Stewart, 1996. Nitrate and nitrite-mediated transcription antitermination control of *nasF* (nitrate assimilation) operon expression in *klebsiella pneumoniae* M5al. Journal of molecular biology, 256(3): 423-435.

Linares, J.F., I. Gustafsson, F. Baquero and J. Martinez, 2006. Antibiotics as intermicrobial signaling agents instead of weapons. Proceedings of the National Academy of Sciences, 103(51): 19484-19489.

Liou, G.F. and C. Khosla, 2003. Building-block selectivity of polyketide synthases. Current opinion in chemical biology, 7(2): 279-284.

Little, A.E., C.J. Robinson, S.B. Peterson, K.F. Raffa and J. Handelsman, 2008. Rules of engagement: Interspecies interactions that regulate microbial communities. Annu. Rev. Microbiol., 62: 375-401.

Liu, C.-I., G.Y. Liu, Y. Song, F. Yin, M.E. Hensler, W.-Y. Jeng, V. Nizet, A.H.-J. Wang and E. Oldfield, 2008. A cholesterol biosynthesis inhibitor blocks *Staphylococcus aureus* virulence. Science, 319(5868): 1391-1394.

Liu, G.Y., 2009. Molecular pathogenesis of *Staphylococcus aureus* infection. Pediatric research, 65(5): 71R.

Liu, G.Y., A. Essex, J.T. Buchanan, V. Datta, H.M. Hoffman, J.F. Bastian, J. Fierer and V. Nizet, 2005. *Staphylococcus aureus* golden pigment impairs neutrophil killing and promotes virulence through its antioxidant activity. The Journal of experimental medicine, 202(2): 209-215.

Liu, G.Y., A. Essex, J.T. Buchanan, V. Datta, H.M. Hoffman, J.F. Bastian, J. Fierer and V. Nizet, 2005. *Staphylococcus aureus* golden pigment impairs neutrophil killing and promotes virulence through its antioxidant activity. Journal of Experimental Medicine, 202(2): 209-215.

Liu, L., T. Hao, Z. Xie, G.P. Horsman and Y. Chen, 2016. Genome mining unveils widespread natural product biosynthetic capacity in human oral microbe *Streptococcus mutans*. Scientific reports, 6: 37479.

Lopez, C.S., A.F. Alice, H. Heras, E.A. Rivas and C. Sanchez-Rivas, 2006. Role of anionic phospholipids in the adaptation of *Bacillus subtilis* to high salinity. Microbiology, 152(3): 605-616.

Love, M.I., W. Huber and S. Anders, 2014. Moderated estimation of fold change and dispersion for RNA-seq data with DESeq2. Genome biology, 15(12): 550.

Lowy, F.D., 1998. *Staphylococcus aureus* infections. New England Journal of Medicine, 339(8): 520-532.

Lu, Z.H. and M. Solioz, 2001. Copper induced proteolysis of the CopZ copper chaperone of *Enterococcus hirae*. Journal of Biological Chemistry.

Luong, T.T., P.M. Dunman, E. Murphy, S.J. Projan and C.Y. Lee, 2006. Transcription profiling of the *mgrA* regulon in *Staphylococcus aureus*. Journal of bacteriology, 188(5): 1899-1910.

Lyon, B.R., J.W. May and R.A. Skurray, 1984. Tn4001: A gentamicin and kanamycin resistance transposon in *Staphylococcus aureus*. Molecular and General Genetics MGG, 193(3): 554-556.

MacLea, K.S. and A.M. Trachtenberg, 2017. Complete genome sequence of *Staphylococcus epidermidis* ATCC 12228 chromosome and plasmids, generated by long-read sequencing. Genome announcements, 5(36): e00954-00917.

MacLean, R.C., A.R. Hall, G.G. Perron and A. Buckling, 2010. The population genetics of antibiotic resistance: Integrating molecular mechanisms and treatment contexts. Nature Reviews Genetics, 11(6): 405.

Madhusoodanan, J., K.S. Seo, B. Remortel, J.Y. Park, S.Y. Hwang, L.K. Fox, Y.H. Park, C.F. Deobald, D. Wang and S. Liu, 2011. An enterotoxin-bearing pathogenicity island in *Staphylococcus epidermidis*. Journal of bacteriology, 193(8): 1854-1862.

Majeed, H., O. Gillor, B. Kerr and M.A. Riley, 2011. Competitive interactions in *Escherichia coli* populations: The role of bacteriocins. The ISME journal, 5(1): 71.

Malachowa, N. and F.R. DeLeo, 2010. Mobile genetic elements of *Staphylococcus aureus*. Cellular and molecular life sciences, 67(18): 3057-3071.

Malanovic, N. and K. Lohner, 2016. Antimicrobial peptides targeting Gram-positive bacteria. Pharmaceuticals, 9(3): 59.

Manna, A. and A.L. Cheung, 2001. Characterization of *sarR*, a modulator of sar expression in *Staphylococcus aureus*. Infection and immunity, 69(2): 885-896.

Manna, A.C. and A.L. Cheung, 2003. *sarU*, a *sarA* homolog, is repressed by *sarT* and regulates virulence genes in *Staphylococcus aureus*. Infection and immunity, 71(1): 343-353.

Manna, A.C., S.S. Ingavale, M. Maloney, W. Van Wamel and A.L. Cheung, 2004. Identification of *sarV* (SA2062), a new transcriptional regulator, is repressed by *sarA* and *mgrA* (SA0641) and involved in the regulation of autolysis in *Staphylococcus aureus*. Journal of bacteriology, 186(16): 5267-5280.

Mantione, K.J., R.M. Kream, H. Kuzelova, R. Ptacek, J. Raboch, J.M. Samuel and G.B. Stefano, 2014. Comparing bioinformatic gene expression profiling methods: Microarray and RNA-seq. Medical science monitor basic research, 20: 138.

Margolis, E., 2009. Hydrogen peroxide-mediated interference competition by *Streptococcus pneumoniae* has no significant effect on *Staphylococcus*

aureus nasal colonization of neonatal rats. Journal of bacteriology, 191(2): 571-575.
Margolles, A., A.B. Florez, J.A. Moreno, D. Van Sinderen and G. Clara, 2006. Two membrane proteins from *Bifidobacterium breve* UCC2003 constitute an ABC-type multidrug transporter. Microbiology, 152(12): 3497-3505.
Maria-Neto, S., K.C. de Almeida, M.L.R. Macedo and O.L. Franco, 2015. Understanding bacterial resistance to antimicrobial peptides: From the surface to deep inside. Biochimica et Biophysica Acta (BBA)-Biomembranes, 1848(11): 3078-3088.
Marioni, J.C., C.E. Mason, S.M. Mane, M. Stephens and Y. Gilad, 2008. RNA-seq: An assessment of technical reproducibility and comparison with gene expression arrays. Genome research.
Marmann, A., A.H. Aly, W. Lin, B. Wang and P. Proksch, 2014. Co-cultivation—a powerful emerging tool for enhancing the chemical diversity of microorganisms. Marine drugs, 12(2): 1043-1065.
Martín, M. and D. de Mendoza, 2013. Regulation of *Bacillus subtilis* DesK thermosensor by lipids. Biochemical Journal, 451(2): 269-275.
Martin, P., Y. Bao, E. Boyer, K. Winterberg, L. McDowell, M. Schmid and J. Buysse, 2002. Novel locus required for expression of high-level macrolide-lincosamide-streptogramin B resistance in *Staphylococcus aureus*. Journal of bacteriology, 184(20): 5810-5813.
McAuliffe, O., R.P. Ross and C. Hill, 2001. Lantibiotics: Structure, biosynthesis and mode of action. FEMS microbiology reviews, 25(3): 285-308.
McIntyre, L.M., K.K. Lopiano, A.M. Morse, V. Amin, A.L. Oberg, L.J. Young and S.V. Nuzhdin, 2011. RNA-seq: Technical variability and sampling. BMC genomics, 12(1): 293.
McKenney, D., J. Hübner, E. Muller, Y. Wang, D.A. Goldmann and G.B. Pier, 1998. The ica locus of *Staphylococcus epidermidis* encodes production of the capsular polysaccharide/adhesin. Infection and immunity, 66(10): 4711-4720.
Medema, M.H., K. Blin, P. Cimermancic, V. de Jager, P. Zakrzewski, M.A. Fischbach, T. Weber, E. Takano and R. Breitling, 2011. Antismash: Rapid identification, annotation and analysis of secondary metabolite biosynthesis gene clusters in bacterial and fungal genome sequences. Nucleic acids research, 39(suppl_2): W339-W346.
Meehl, M., S. Herbert, F. Götz and A. Cheung, 2007. Interaction of the GraRS two-component system with the VraFG ABC transporter to support vancomycin-intermediate resistance in *Staphylococcus aureus*. Antimicrobial agents and chemotherapy, 51(8): 2679-2689.
Meyer, C., G. Bierbaum, C. Heidrich, M. Reis, J. Süling, M.I. Iglesias-Wind, C. Kempter, E. Molitor and H.G. Sahl, 1995. Nucleotide sequence of the lantibiotic Pep5 biosynthetic gene cluster and functional analysis of PepP and PepC. European Journal of Biochemistry, 232(2): 478-489.
Michalik, S., M. Depke, A. Murr, M.G. Salazar, U. Kusebauch, Z. Sun, T.C. Meyer, K. Surmann, H. Pförtner and P. Hildebrandt, 2017. A global *Staphylococcus aureus* proteome resource applied to the in vivo characterization of host-pathogen interactions. Scientific reports, 7(1): 9718.
Michel-Briand, Y. and C. Baysse, 2002. The pyocins of *Pseudomonas aeruginosa*. Biochimie, 84(5-6): 499-510.

Mishra, N.N., G.Y. Liu, M.R. Yeaman, C.C. Nast, R.A. Proctor, J. McKinnell and A.S. Bayer, 2011. Carotenoid-related alteration of cell membrane fluidity impacts *Staphylococcus aureus* susceptibility to host defense peptides. Antimicrobial agents and chemotherapy, 55(2): 526-531.

Mitrophanov, A.Y. and E.A. Groisman, 2008. Signal integration in bacterial two-component regulatory systems. Genes & Development, 22(19): 2601-2611.

Molohon, K.J., P.M. Blair, S. Park, J.R. Doroghazi, T. Maxson, J.R. Hershfield, K.M. Flatt, N.E. Schroeder, T. Ha and D.A. Mitchell, 2016. Plantazolicin is an ultranarrow-spectrum antibiotic that targets the *Bacillus anthracis* membrane. ACS infectious diseases, 2(3): 207-220.

Montgomery, C.P., S. Boyle-Vavra and R.S. Daum, 2009. The arginine catabolic mobile element is not associated with enhanced virulence in experimental invasive disease caused by the community-associated methicillin-resistant *Staphylococcus aureus* USA300 genetic background. Infection and immunity, 77(7): 2650-2656.

Moore, P. and J. Lindsay, 2001. Genetic variation among hospital isolates of methicillin-sensitive *Staphylococcus aureus*: Evidence for horizontal transfer of virulence genes. Journal of clinical microbiology, 39(8): 2760-2767.

Moran, J.C., J.A. Alorabi and M.J. Horsburgh, 2017. Comparative transcriptomics reveals discrete survival responses of *S. aureus* and *S. epidermidis* to sapienic acid. Frontiers in microbiology, 8: 33.

Moran, J.C., E.L. Crank, H.A. Ghabban and M.J. Horsburgh, 2016. Deferred growth inhibition assay to quantify the effect of bacteria-derived antimicrobials on competition. Journal of visualized experiments: JoVE(115).

Morfeldt, E., D.v. Taylor, A. Von Gabain and S. Arvidson, 1995. Activation of alpha-toxin translation in *Staphylococcus aureus* by the trans-encoded antisense RNA, RNAIII. The EMBO journal, 14(18): 4569-4577.

Morfeldt, E., K. Tegmark and S. Arvidson, 1996. Transcriptional control of the *agr*-dependent virulence gene regulator, RNAIII, in *Staphylococcus aureus*. Molecular microbiology, 21(6): 1227-1237.

Morin, P.J., 1999. Community ecology.

Morris, R.P., J.A. Leeds, H.U. Naegeli, L. Oberer, K. Memmert, E. Weber, M.J. LaMarche, C.N. Parker, N. Burrer and S. Esterow, 2009. Ribosomally synthesized thiopeptide antibiotics targeting elongation factor Tu. Journal of the American Chemical Society, 131(16): 5946-5955.

Moutinho Jr, T.J., J.C. Panagides, M.B. Biggs, G.L. Medlock, G.L. Kolling and J.A. Papin, 2017. Novel co-culture plate enables growth dynamic-based assessment of contact-independent microbial interactions. PloS one, 12(8): e0182163.

Mujacic, M. and F. Baneyx, 2006. Regulation of *Escherichia coli hchA*, a stress-inducible gene encoding molecular chaperone Hsp31. Molecular microbiology, 60(6): 1576-1589.

Mulcahy, M.E., J.A. Geoghegan, I.R. Monk, K.M. O'Keeffe, E.J. Walsh, T.J. Foster and R.M. McLoughlin, 2012. Nasal colonisation by *Staphylococcus aureus* depends upon clumping factor B binding to the squamous epithelial cell envelope protein loricrin. PLoS pathogens, 8(12): e1003092.

Müller, A., H. Ulm, K. Reder-Christ, H.-G. Sahl and T. Schneider, 2012. Interaction of type a lantibiotics with undecaprenol-bound cell envelope precursors. Microbial Drug Resistance, 18(3): 261-270.

Munita, J.M. and C.A. Arias, 2016. Mechanisms of antibiotic resistance. Microbiology spectrum, 4(2).

Muthaiyan, A., E.M. Martin, S. Natesan, P.G. Crandall, B.J. Wilkinson and S.C. Ricke, 2012. Antimicrobial effect and mode of action of terpeneless cold-pressed valencia orange essential oil on methicillin-resistant *Staphylococcus aureus*. Journal of applied microbiology, 112(5): 1020-1033.

Muthaiyan, A., J.A. Silverman, R.K. Jayaswal and B.J. Wilkinson, 2008. Transcriptional profiling reveals that daptomycin induces the *Staphylococcus aureus* cell wall stress stimulon and genes responsive to membrane depolarization. Antimicrobial agents and chemotherapy, 52(3): 980-990.

Mwangi, M.M., S.W. Wu, Y. Zhou, K. Sieradzki, H. de Lencastre, P. Richardson, D. Bruce, E. Rubin, E. Myers and E.D. Siggia, 2007. Tracking the in vivo evolution of multidrug resistance in *Staphylococcus aureus* by whole-genome sequencing. Proceedings of the National Academy of Sciences, 104(22): 9451-9456.

Nagao, J.-i., S.M. Asaduzzaman, Y. Aso, K.-i. Okuda, J. Nakayama and K. Sonomoto, 2006. Lantibiotics: Insight and foresight for new paradigm. Journal of bioscience and bioengineering, 102(3): 139-149.

Nagase, N., A. Sasaki, K. Yamashita, A. Shimizu, Y. Wakita, S. Kitai and J. Kawano, 2002. Isolation and species distribution of staphylococci from animal and human skin. Journal of Veterinary Medical Science, 64(3): 245-250.

Nair, S.P., M. Bischoff, M.M. Senn and B. Berger-Bächi, 2003. The σB regulon influences internalization of *Staphylococcus aureus* by osteoblasts. Infection and immunity, 71(7): 4167-4170.

Nakatsuji, T., T.H. Chen, S. Narala, K.A. Chun, T. Yun, F. Shafiq, P.F. Kotol, A. Bouslimani, A.V. Melnik and H. Latif, 2017. Antimicrobials from human skin commensal bacteria protect against *Staphylococcus aureus* and are deficient in atopic dermatitis. Science translational medicine, 9(378): eaah4680.

Nanoukon, C., X. Argemi, F. Sogbo, J. Orekan, D. Keller, D. Affolabi, F. Schramm, P. Riegel, L. Baba-Moussa and G. Prévost, 2017. Pathogenic features of clinically significant coagulase-negative staphylococci in hospital and community infections in Benin. International Journal of Medical Microbiology, 307(1): 75-82.

Nascimento, J., H. Ceotto, S. Nascimento, M. Giambiagi-deMarval, K. Santos and M. Bastos, 2006. Bacteriocins as alternative agents for control of multiresistant staphylococcal strains. Letters in applied microbiology, 42(3): 215-221.

Nelson, J.L., K.C. Rice, S.R. Slater, P.M. Fox, G.L. Archer, K.W. Bayles, P.D. Fey, B.N. Kreiswirth and G.A. Somerville, 2007. Vancomycin-intermediate *Staphylococcus aureus* strains have impaired acetate catabolism: Implications for polysaccharide intercellular adhesin synthesis and autolysis. Antimicrobial agents and chemotherapy, 51(2): 616-622.

Nies, D.H., 1992. Czcr and czcd, gene products affecting regulation of resistance to cobalt, zinc, and cadmium (czc system) in alcaligenes eutrophus. Journal of bacteriology, 174(24): 8102-8110.

Nieto, C., I. Cherny, S.K. Khoo, M.G. de Lacoba, W.T. Chan, C.C. Yeo, E. Gazit and M. Espinosa, 2007. The *yefM-yoeB* toxin-antitoxin systems of *Escherichia coli* and *Streptococcus pneumoniae*: Functional and structural correlation. Journal of bacteriology, 189(4): 1266-1278.

Nishijima, S., Y. Asami, N. Uetake, S. Yamagoe, A. Ohta and I. Shibuya, 1988. Disruption of the *Escherichia coli cls* gene responsible for cardiolipin synthesis. Journal of bacteriology, 170(2): 775-780.

Nolan, T., R.E. Hands and S.A. Bustin, 2006. Quantification of mRNA using real-time RT-PCR. Nature protocols, 1(3): 1559.

Nolle, N., C.F. Schuster and R. Bertram, 2013. Two paralogous *yefM-yoeB* loci from *Staphylococcus* equorum encode functional toxin–antitoxin systems. Microbiology, 159(8): 1575-1585.

Novick, R., 2006. Staphylococcal pathogenesis and pathogenicity factors: Genetics and regulation. Gram-positive pathogens, 2: 496.

Novick, R., S. Projan, J. Kornblum, H. Ross, G. Ji, B. Kreiswirth, F. Vandenesch and S. Moghazeh, 1995. The *agr* P2 operon: An autocatalytic sensory transduction system in *Staphylococcus aureus*. Molecular and General Genetics MGG, 248(4): 446-458.

Novick, R.P., 1991. [27] Genetic systems in staphylococci. Methods in enzymology, 204: 587-636.

Novick, R.P. and E. Geisinger, 2008. Quorum sensing in staphylococci. Annual review of genetics, 42: 541-564.

Novick, R.P. and D. Jiang, 2003. The staphylococcal *SaeRS* system coordinates environmental signals with *agr* quorum sensing. Microbiology, 149(10): 2709-2717.

Novick, R.P., H. Ross, S. Projan, J. Kornblum, B. Kreiswirth and S. Moghazeh, 1993. Synthesis of staphylococcal virulence factors is controlled by a regulatory RNA molecule. The EMBO journal, 12(10): 3967-3975.

Nurjadi, D., Herrmann, E., Hinderberger, I., & Zanger, P., 2012. Impaired β-defensin expression in human skin links DEFB1 promoter polymorphisms with persistent *Staphylococcus aureus* nasal carriage. The Journal of infectious diseases, 207(4), 666-674.

Ohki, R., K. Tateno, W. Masuyama, S. Moriya, K. Kobayashi and N. Ogasawara, 2003. The BceRS two-component regulatory system induces expression of the bacitracin transporter, BceAB, in *Bacillus subtilis*. Molecular microbiology, 49(4): 1135-1144.

Ohniwa, R.L., K. Kitabayashi and K. Morikawa, 2013. Alternative cardiolipin synthase Cls1 compensates for stalled Cls2 function in *Staphylococcus aureus* under conditions of acute acid stress. FEMS microbiology letters, 338(2): 141-146.

Okoniewski, M.J. and C.J. Miller, 2006. Hybridization interactions between probesets in short oligo microarrays lead to spurious correlations. BMC bioinformatics, 7(1): 276.

Ongena, M., E. Jourdan, A. Adam, M. Paquot, A. Brans, B. Joris, J.L. Arpigny and P. Thonart, 2007. Surfactin and fengycin lipopeptides of *Bacillus subtilis* as

elicitors of induced systemic resistance in plants. Environmental microbiology, 9(4): 1084-1090.
Otto, M., 2008. Staphylococcal biofilms. In: Bacterial biofilms. Springer: pp: 207-228.
Otto, M., 2009. *Staphylococcus epidermidis*—the ''accidental'' pathogen. Nature Reviews Microbiology, 7(8): 555-567.
Otto, M., 2010. *Staphylococcus* colonization of the skin and antimicrobial peptides. Expert review of dermatology, 5(2): 183-195.
Otto, M., 2013. Community-associated MRSA: What makes them special? International Journal of Medical Microbiology, 303(6): 324-330.
Otto, M., 2014. *Staphylococcus aureus* toxins. Current opinion in microbiology, 17: 32-37.
Otto, M., H. Echner, W. Voelter and F. Götz, 2001. Pheromone cross-inhibition between *Staphylococcus aureus* and *Staphylococcus epidermidis*. Infection and immunity, 69(3): 1957-1960.
Paharik, A.E., C.P. Parlet, N. Chung, D.A. Todd, E.I. Rodriguez, M.J. Van Dyke, N.B. Cech and A.R. Horswill, 2017. Coagulase-negative staphylococcal strain prevents *Staphylococcus aureus* colonization and skin infection by blocking quorum sensing. Cell host & microbe, 22(6): 746-756. e745.
Pal, C., K. Asiani, S. Arya, C. Rensing, D.J. Stekel, D.J. Larsson and J.L. Hobman, 2017. Metal resistance and its association with antibiotic resistance. In: Advances in microbial physiology. Elsevier: pp: 261-313.
Pappas, A., 2009. Epidermal surface lipids. Dermato-endocrinology, 1(2): 72-76.
Parikh, S.L., G. Xiao and P.J. Tonge, 2000. Inhibition of InhA, the enoyl reductase from *mycobacterium tuberculosis*, by triclosan and isoniazid. Biochemistry, 39(26): 7645-7650.
Park, B., V. Nizet and G.Y. Liu, 2008. Role of *Staphylococcus aureus* catalase in niche competition against *Streptococcus pneumoniae*. Journal of bacteriology, 190(7): 2275-2278.
Park, H.S., Y.M. Yoon, S.J. Jung, I.N.R. Yun, C.M. Kim, J.M. Kim and J.-H. Kwak, 2007. Cg400462, a new bacterial enoyl–acyl carrier protein reductase (FabI) inhibitor. International journal of antimicrobial agents, 30(5): 446-451.
Patel, R.K. and M. Jain, 2012. NGS QQ toolkit: A toolkit for quality control of next generation sequencing data. PloS one, 7(2): e30619.
Patti, J.M., B.L. Allen, M.J. McGavin and M. Hook, 1994. MSCRAMM-mediated adherence of microorganisms to host tissues. Annual Reviews in Microbiology, 48(1): 585-617.
Payne, D.J., W.H. Miller, V. Berry, J. Brosky, W.J. Burgess, E. Chen, W.E. DeWolf, A.P. Fosberry, R. Greenwood and M.S. Head, 2002. Discovery of a novel and potent class of FabI-directed antibacterial agents. Antimicrobial agents and chemotherapy, 46(10): 3118-3124.
Payne, D.J., P.V. Warren, D.J. Holmes, Y. Ji and J.T. Lonsdale, 2001. Bacterial fatty-acid biosynthesis: A genomics-driven target for antibacterial drug discovery. Drug discovery today, 6(10): 537-544.
Pekkonen, M., T. Ketola and J.T. Laakso, 2013. Resource availability and competition shape the evolution of survival and growth ability in a bacterial community. PLoS One, 8(9): e76471.

Pelz, A., K.-P. Wieland, K. Putzbach, P. Hentschel, K. Albert and F. Götz, 2005. Structure and biosynthesis of staphyloxanthin from *Staphylococcus aureus*. Journal of Biological Chemistry.

Peschel, A., 2002. How do bacteria resist human antimicrobial peptides?. Trends in microbiology, 10(4): 179-186.

Peschel, A., M. Otto, R.W. Jack, H. Kalbacher, G. Jung and F. Götz, 1999. Inactivation of the dlt operon in *Staphylococcus aureus* confers sensitivity to defensins, protegrins, and other antimicrobial peptides. Journal of Biological Chemistry, 274(13): 8405-8410.

Peschel, A. and H.-G. Sahl, 2006. The co-evolution of host cationic antimicrobial peptides and microbial resistance. Nature Reviews Microbiology, 4(7): 529.

Petersen, T.N., S. Brunak, G. von Heijne and H. Nielsen, 2011. Signalp 4.0: Discriminating signal peptides from transmembrane regions. Nature methods, 8(10): 785.

Pietiäinen, M., P. François, H.-L. Hyyryläinen, M. Tangomo, V. Sass, H.-G. Sahl, J. Schrenzel and V.P. Kontinen, 2009. Transcriptome analysis of the responses of *Staphylococcus aureus* to antimicrobial peptides and characterization of the roles of *vraDE* and *vraSR* in antimicrobial resistance. BMC genomics, 10(1): 429.

Pietiäinen, M., M. Gardemeister, M. Mecklin, S. Leskelä, M. Sarvas and V.P. Kontinen, 2005. Cationic antimicrobial peptides elicit a complex stress response in *Bacillus subtilis* that involves ECF-type sigma factors and two-component signal transduction systems. Microbiology, 151(5): 1577-1592.

Planson, A.G., P. Carbonell, I. Grigoras and J.L. Faulon, 2011. Engineering antibiotic production and overcoming bacterial resistance. Biotechnology journal, 6(7): 812-825.

Polak-Berecka, M., A. Waśko and D. Koston, 2009. Comparison of different methods for detection of antimicrobial activity of probiotic strains of *Lactobacillus rhamnosus* against some food spoilage microorganisms. Annales UMCS, Biologia, 64(1): 15-24.

Popella, P., S. Krauss, P. Ebner, M. Nega, J. Deibert and F. Götz, 2016. VraH is a third component of the *Staphylococcus aureus* vraDEH system involved in gallidermin and daptomycin resistance and pathogenicity. Antimicrobial agents and chemotherapy: AAC. 02865-02815.

Poston, S. and F.L.S. Hee, 1991. Genetic characterisation of resistance to metal ions in methicillin-resistant *Staphylococcus aureus*: Elimination of resistance to cadmium, mercury and tetracycline with loss of methicillin resistance. Journal of medical microbiology, 34(4): 193-201.

Pragman, A.A. and P.M. Schlievert, 2004. Virulence regulation in *Staphylococcus aureus*: the need for in *vivo* analysis of virulence factor regulation. FEMS Immunology & Medical Microbiology, 42(2): 147-154.

Pragman, A.A., J.M. Yarwood, T.J. Tripp and P.M. Schlievert, 2004. Characterization of virulence factor regulation by SrrAB, a two-component system in *Staphylococcus aureus*. Journal of bacteriology, 186(8): 2430-2438.

Priyadarshi, A., E.E. Kim and K.Y. Hwang, 2010. Structural insights into *Staphylococcus aureus* enoyl-acp reductase (FabI), in complex with NADP

and triclosan. Proteins: Structure, Function, and Bioinformatics, 78(2): 480-486.

Qiu, R., W. Pei, L. Zhang, J. Lin and G. Ji, 2005. Identification of the putative Staphylococcal AgrB catalytic residues involving in the proteolytic cleavage of AgrD to generate autoinducing peptide. Journal of Biological Chemistry.

Rajkumar, A.P., P. Qvist, R. Lazarus, F. Lescai, J. Ju, M. Nyegaard, O. Mors, A.D. Børglum, Q. Li and J.H. Christensen, 2015. Experimental validation of methods for differential gene expression analysis and sample pooling in RNA-seq. BMC genomics, 16(1): 548.

Ramsey, M.M., M.O. Freire, R.A. Gabrilska, K.P. Rumbaugh and K.P. Lemon, 2016. *Staphylococcus aureus* shifts toward commensalism in response to *Corynebacterium* species. Frontiers in microbiology, 7: 1230.

Rankin, D.J., E.P. Rocha and S.P. Brown, 2011. What traits are carried on mobile genetic elements, and why?. Heredity, 106(1): 1-10.

Rasch, M. and S. Knöchel, 1998. Variations in tolerance of *Listeria monocytogenes* to nisin, pediocin PA-1 and bavaricin A. Letters in Applied Microbiology, 27(5): 275-278.

Regev-Yochay, G., K. Trzciński, C.M. Thompson, R. Malley and M. Lipsitch, 2006. Interference between *Streptococcus pneumoniae* and *Staphylococcus aureus*: in *vitro* hydrogen peroxide-mediated killing by *Streptococcus pneumoniae*. Journal of bacteriology, 188(13): 4996-5001.

Reinholz, M., T. Ruzicka and J. Schauber, 2012. Cathelicidin LL-37: an antimicrobial peptide with a role in inflammatory skin disease. Annals of Dermatology, 24(2): 126-135.

Renzoni, A., D.O. Andrey, A. Jousselin, C. Barras, A. Monod, P. Vaudaux, D. Lew and W.L. Kelley, 2011. Whole genome sequencing and complete genetic analysis reveals novel pathways to glycopeptide resistance in *Staphylococcus aureus*. PLoS One, 6(6): e21577.

Reyes, D., D.O. Andrey, A. Monod, W.L. Kelley, G. Zhang and A.L. Cheung, 2011. Coordinated regulation by AgrA, SarA and SarR to control *agr* expression in *Staphylococcus aureus*. Journal of bacteriology: JB. 05436-05411.

Rice, L.B., 2006. Antimicrobial resistance in gram-positive bacteria. American journal of infection control, 34(5): S11-S19.

Richardson, A.R., S.J. Libby and F.C. Fang, 2008. A nitric oxide–inducible lactate dehydrogenase enables *Staphylococcus aureus* to resist innate immunity. Science, 319(5870): 1672-1676.

Riley, M.A. and J.E. Wertz, 2002. Bacteriocins: Evolution, ecology, and application. Annual Reviews in Microbiology, 56(1): 117-137.

Robinson, M.D., D.J. McCarthy and G.K. Smyth, 2010. Edger: A bioconductor package for differential expression analysis of digital gene expression data. Bioinformatics, 26(1): 139-140.

Rogasch, K., V. Rühmling, J. Pané-Farré, D. Höper, C. Weinberg, S. Fuchs, M. Schmudde, B.M. Bröker, C. Wolz and M. Hecker, 2006. Influence of the two-component system SaeRS on global gene expression in two different *Staphylococcus aureus* strains. Journal of bacteriology, 188(22): 7742-7758.

Rogers, K.L., M.E. Rupp and P.D. Fey, 2008. The presence of *icaADBC* is detrimental to the colonization of human skin by *Staphylococcus*

epidermidis. Applied and environmental microbiology, 74(19): 6155-6157.

Romantsov, T., S. Helbig, D.E. Culham, C. Gill, L. Stalker and J.M. Wood, 2007. Cardiolipin promotes polar localization of osmosensory transporter ProP in *Escherichia coli.* Molecular microbiology, 64(6): 1455-1465.

Roongsawang, N., S.P. Lim, K. Washio, K. Takano, S. Kanaya and M. Morikawa, 2005. Phylogenetic analysis of condensation domains in the nonribosomal peptide synthetases. FEMS microbiology letters, 252(1): 143-151.

Roth, R.R. and W.D. James, 1988. Microbial ecology of the skin. Annual Reviews in Microbiology, 42(1): 441-464.

Roy, U., M.R. Islam, J.-i. Nagao, H. Iida, A.-A. Mahin, M. Li, T. Zendo, J. Nakayama and K. Sonomoto, 2014. Bactericidal activity of nukacin ISK-1: An alternative mode of action. Bioscience, biotechnology, and biochemistry, 78(7): 1270-1273.

Royce, T.E., J.S. Rozowsky and M.B. Gerstein, 2007. Toward a universal microarray: Prediction of gene expression through nearest-neighbor probe sequence identification. Nucleic acids research, 35(15): e99.

Rutherford, S.T. and B.L. Bassler, 2012. Bacterial quorum sensing: Its role in virulence and possibilities for its control. Cold Spring Harbor perspectives in medicine, 2(11): a012427.

Ryu, S., P.I. Song, C.H. Seo, H. Cheong and Y. Park, 2014. Colonization and infection of the skin by *S. aureus*: immune system evasion and the response to cationic antimicrobial peptides. International journal of molecular sciences, 15(5): 8753-8772.

Sabala, I., E. Jagielska, P.T. Bardelang, H. Czapinska, S.O. Dahms, J.A. Sharpe, R. James, M.E. Than, N.R. Thomas and M. Bochtler, 2014. Crystal structure of the antimicrobial peptidase lysostaphin from *Staphylococcus simulans*. The FEBS journal, 281(18): 4112-4122.

Sahl, H.-G. and G. Bierbaum, 1998. Lantibiotics: Biosynthesis and biological activities of uniquely modified peptides from gram-positive bacteria. Annual Reviews in Microbiology, 52(1): 41-79.

Said-Salim, B., P. Dunman, F. McAleese, D. Macapagal, E. Murphy, P. McNamara, S. Arvidson, T. Foster, S. Projan and B. Kreiswirth, 2003. Global regulation of *Staphylococcus aureus* genes by Rot. Journal of bacteriology, 185(2): 610-619.

Saising, J., L. Dube, A.-K. Ziebandt, S.P. Voravuthikunchai, M. Nega and F. Götz, 2012. Activity of gallidermin on *Staphylococcus aureus* and *Staphylococcus epidermidis* biofilms. Antimicrobial agents and chemotherapy: AAC. 01296-01212.

Saita, E., D. Albanesi and D. de Mendoza, 2016. Sensing membrane thickness: lessons learned from cold stress. Biochimica et Biophysica Acta (BBA)-Molecular and Cell Biology of Lipids, 1861(8): 837-846.

Sakoulas, G., G.M. Eliopoulos, R.C. Moellering, C. Wennersten, L. Venkataraman, R.P. Novick and H.S. Gold, 2002. Accessory gene regulator (*agr*) locus in geographically diverse *Staphylococcus aureus* isolates with reduced susceptibility to vancomycin. Antimicrobial Agents and Chemotherapy, 46(5): 1492-1502.

Sakwinska, O., G. Kuhn, C. Balmelli, P. Francioli, M. Giddey, V. Perreten, A. Riesen, F. Zysset, D.S. Blanc and P. Moreillon, 2009. Genetic diversity and

ecological success of *Staphylococcus aureus* strains colonizing humans. Applied and environmental microbiology, 75(1): 175-183.
Sakınç, T., B. Kleine, N. Michalski, M. Kaase and S.G. Gatermann, 2009. SdrI of *Staphylococcus saprophyticus* is a multifunctional protein: localization of the fibronectin-binding site. FEMS microbiology letters, 301(1): 28-34.
Sánchez, C.J., K. Mende, M.L. Beckius, K.S. Akers, D.R. Romano, J.C. Wenke and C.K. Murray, 2013. Biofilm formation by clinical isolates and the implications in chronic infections. BMC infectious diseases, 13(1): 47.
Sapula, S.A. and M.H. Brown, 2016. Antimicrobial drug efflux pumps in *Staphylococcus aureus*. In efflux-mediated antimicrobial resistance in bacteria: Mechanisms, regulation and clinical implications, X.-Z. LiC. A. Elkins and H. I. Zgurskaya, (Eds.). Springer International Publishing, Cham: pp: 165-195.
Saroj, S.D., L. Maudsdotter, R. Tavares and A.-B. Jonsson, 2016. Lactobacilli interfere with *Streptococcus pyogenes* hemolytic activity and adherence to host epithelial cells. Frontiers in microbiology, 7: 1176.
Scherlach, K. and C. Hertweck, 2009. Triggering cryptic natural product biosynthesis in microorganisms. Organic & biomolecular chemistry, 7(9): 1753-1760.
Schillinger, U. and F.K. Lücke, 1989. Antibacterial activity of *Lactobacillus* sake isolated from meat. Applied and environmental microbiology, 55(8): 1901-1906.
Schlag, S., S. Fuchs, C. Nerz, R. Gaupp, S. Engelmann, M. Liebeke, M. Lalk, M. Hecker and F. Götz, 2008. Characterization of the oxygen-responsive NreaBC regulon of *Staphylococcus aureus*. Journal of bacteriology, 190(23): 7847-7858.
Schlame, M., D. Rua and M.L. Greenberg, 2000. The biosynthesis and functional role of cardiolipin. Progress in lipid research, 39(3): 257-288.
Schmidt, K.A., A.C. Manna, S. Gill and A.L. Cheung, 2001. SarT, a repressor of α-hemolysin in *Staphylococcus aureus*. Infection and immunity, 69(8): 4749-4758.
Schnell, N., K.-D. Entian, U. Schneider, F. Götz, H. Zähner, R. Kellner and G. Jung, 1988. Prepeptide sequence of epidermin, a ribosomally synthesized antibiotic with four sulphide-rings. Nature, 333(6170): 276.
Schoenfelder, S.M., C. Lange, M. Eckart, S. Hennig, S. Kozytska and W. Ziebuhr, 2010. Success through diversity–how *Staphylococcus epidermidis* establishes as a nosocomial pathogen. International Journal of medical microbiology, 300(6): 380-386.
Scholz, R., K.J. Molohon, J. Nachtigall, J. Vater, A.L. Markley, R.D. Süssmuth, D.A. Mitchell and R. Borriss, 2011. Plantazolicin, a novel microcin B17/streptolysin S-like natural product from *Bacillus amyloliquefaciens* FZB42. Journal of bacteriology, 193(1): 215-224.
Schwamborn, K. and R.M. Caprioli, 2010. Molecular imaging by mass spectrometry—looking beyond classical histology. Nature Reviews Cancer, 10(9): 639.
Seemann, T., 2014. Prokka: Rapid prokaryotic genome annotation. Bioinformatics, 30(14): 2068-2069.
Sharma-Kuinkel, B.K., E.E. Mann, J.-S. Ahn, L.J. Kuechenmeister, P.M. Dunman and K.W. Bayles, 2009. The *Staphylococcus aureus* lytSR two-component

regulatory system affects biofilm formation. Journal of bacteriology, 191(15): 4767-4775.
Shintani, M., Z.K. Sanchez and K. Kimbara, 2015. Genomics of microbial plasmids: Classification and identification based on replication and transfer systems and host taxonomy. Frontiers in microbiology, 6: 242.
Shoji, M., L. Cui, R. Iizuka, A. Komoto, H.-m. Neoh, Y. Watanabe, T. Hishinuma and K. Hiramatsu, 2011. The *walK* and *clpP* mutations confer reduced vancomycin susceptibility on *Staphylococcus aureus*. Antimicrobial agents and chemotherapy: AAC. 01563-01510.
Shu, M., Y. Wang, J. Yu, S. Kuo, A. Coda, Y. Jiang, R.L. Gallo and C.-M. Huang, 2013. Fermentation of *Propionibacterium acnes*, a commensal bacterium in the human skin microbiome, as skin probiotics against methicillin-resistant S*taphylococcus aureus*. PLoS One, 8(2): e55380.
Simões, L.C., M. Simoes and M.J. Vieira, 2007. Biofilm interactions between distinct bacterial genera isolated from drinking water. Applied and Environmental Microbiology, 73(19): 6192-6200.
Singh, M., S. Chaudhary and D. Sareen, 2017. Non-ribosomal peptide synthetases: Identifying the cryptic gene clusters and decoding the natural product. Journal of biosciences, 42(1): 175-187.
Singh, V., K. Singh and K. Baum, 2018. The role of methionine sulfoxide reductases in oxidative stress tolerance and virulence of *Staphylococcus aureus* and other bacteria. Antioxidants, 7(10): 128.
Singh, V.K., M. Syring, A. Singh, K. Singhal, A. Dalecki and T. Johansson, 2012. An insight into the significance of the DnaK heat shock system in *Staphylococcus aureus*. International Journal of Medical Microbiology, 302(6): 242-252.
Sîrbu, A., G. Kerr, M. Crane and H.J. Ruskin, 2012. RNA-seq vs dual-and single-channel microarray data: Sensitivity analysis for differential expression and clustering. PloS one, 7(12): e50986.
Sitthisak, S., L. Knutsson, J.W. Webb and R.K. Jayaswal, 2007. Molecular characterization of the copper transport system in *Staphylococcus aureus*. Microbiology, 153(12): 4274-4283.
Slattery, M., I. Rajbhandari and K. Wesson, 2001. Competition-mediated antibiotic induction in the marine bacterium *Streptomyces tenjimariensis*. Microbial Ecology, 41(2): 90-96.
Somerville, G.A., C.I. Morgan, J.R. Fitzgerald, D.W. Dorward, L.J. Reitzer and J.M. Musser, 2002. *Staphylococcus aureus* aconitase inactivation unexpectedly inhibits post-exponential-phase growth and enhances stationary-phase survival. Infection and immunity, 70(11): 6373-6382.
Song, Y., A. Rubio, R.K. Jayaswal, J.A. Silverman and B.J. Wilkinson, 2013. Additional routes to *Staphylococcus aureus* daptomycin resistance as revealed by comparative genome sequencing, transcriptional profiling, and phenotypic studies. PLoS One, 8(3): e58469.
Soutourina, O., S. Dubrac, O. Poupel, T. Msadek and I. Martin-Verstraete, 2010. The pleiotropic CymR regulator of *Staphylococcus aureus* plays an important role in virulence and stress response. PLoS Pathogens, 6(5): e1000894.
Starcevic, A., J. Zucko, J. Simunkovic, P.F. Long, J. Cullum and D. Hranueli, 2008. Clustscan: An integrated program package for the semi-automatic

annotation of modular biosynthetic gene clusters and in silico prediction of novel chemical structures. Nucleic acids research, 36(21): 6882-6892.
Staubitz, P., H. Neumann, T. Schneider, I. Wiedemann and A. Peschel, 2004. Mprf-mediated biosynthesis of lysylphosphatidylglycerol, an important determinant in staphylococcal defensin resistance. FEMS microbiology letters, 231(1): 67-71.
Stefaniak, A.B. and C.J. Harvey, 2006. Dissolution of materials in artificial skin surface film liquids. Toxicology in Vitro, 20(8): 1265-1283.
Stein, T., S. Heinzmann, I. Solovieva and K.-D. Entian, 2003. Function of *Lactococcus lactis* nisin immunity genes *nisI* and *nisFEG* after coordinated expression in the surrogate host *Bacillus subtilis*. Journal of Biological Chemistry, 278(1): 89-94.
Strieker, M., A. Tanović and M.A. Marahiel, 2010. Nonribosomal peptide synthetases: Structures and dynamics. Current opinion in structural biology, 20(2): 234-240.
Stubbendieck, R.M. and P.D. Straight, 2016. Multifaceted interfaces of bacterial competition. Journal of bacteriology, 198(16): 2145-2155.
Su, J., M. Iehara, J. Yasukawa, Y. Matsumoto, H. Hamamoto and K. Sekimizu, 2015. A novel mutation in the *vraS* gene of *Staphylococcus aureus* contributes to reduce susceptibility against daptomycin. The Journal of antibiotics, 68(10): 646.
Sugimoto, S., T. Iwamoto, K. Takada, K.-i. Okuda, A. Tajima, T. Iwase and Y. Mizunoe, 2013. *Staphylococcus epidermidis* ESP degrades specific proteins associated with *Staphylococcus aureus* biofilm formation and host-pathogen interaction. Journal of bacteriology, 195(8): 1645-1655.
Sun, F., Q. Ji, M.B. Jones, X. Deng, H. Liang, B. Frank, J. Telser, S.N. Peterson, T. Bae and C. He, 2011. AirSR, a [2FE-2S] cluster-containing two-component system, mediates global oxygen sensing and redox signaling in *Staphylococcus aureus*. Journal of the American Chemical Society, 134(1): 305-314.
Tait, K. and I. Sutherland, 2002. Antagonistic interactions amongst bacteriocin-producing enteric bacteria in dual species biofilms. Journal of applied microbiology, 93(2): 345-352.
Takala, T.M. and P.E. Saris, 2006. C terminus of nisI provides specificity to nisin. Microbiology, 152(12): 3543-3549.
Takigawa, H., H. Nakagawa, M. Kuzukawa, H. Mori and G. Imokawa, 2005. Deficient production of hexadecenoic acid in the skin is associated in part with the vulnerability of atopic dermatitis patients to colonization by *Staphylococcus aureus*. Dermatology, 211(3): 240-248.
Tamber, S. and A.L. Cheung, 2009. SarZ promotes the expression of virulence factors and represses biofilm formation by modulating *sarA* and *agr* in *Staphylococcus aureus*. Infection and immunity, 77(1): 419-428.
Tannock, G.W., 1994. Normal microflora: An introduction to microbes inhabiting the human body. Springer.
Tanous, C., O. Soutourina, B. Raynal, M.-F. Hullo, P. Mervelet, A.-M. Gilles, P. Noirot, A. Danchin, P. England and I. Martin-Verstraete, 2008. The *cymR* regulator in complex with the enzyme CysK controls cysteine metabolism in *Bacillus subtilis*. Journal of Biological Chemistry, 283(51): 35551-35560.

Tao, L., X. Wu and B. Sun, 2010. Alternative sigma factor σH modulates prophage integration and excision in *Staphylococcus aureus*. PLoS pathogens, 6(5): e1000888.

Tasara, T., N. Cernela and R. Stephan, 2013. Function impairing mutations in *blaZ* and *blaR* genes of penicillin susceptible *Staphylococcus aureus* strains isolated from bovine mastitis. Schweiz. Arch. Tierheilkd, 155, 359-363.

Tegmark, K., A. Karlsson and S. Arvidson, 2000. Identification and characterization of sarH1, a new global regulator of virulence gene expression in S*taphylococcus aureus*. Molecular microbiology, 37(2): 398-409.

Thoendel, M. and A.R. Horswill, 2010. Biosynthesis of peptide signals in gram-positive bacteria. In: Advances in applied microbiology. Elsevier: pp: 91-112.

Thompson, L.J., D.S. Merrell, B.A. Neilan, H. Mitchell, A. Lee and S. Falkow, 2003. Gene expression profiling of *Helicobacter pylori* reveals a growth-phase-dependent switch in virulence gene expression. Infection and immunity, 71(5): 2643-2655.

Torres, V.J., D.L. Stauff, G. Pishchany, J.S. Bezbradica, L.E. Gordy, J. Iturregui, K.L. Anderson, P.M. Dunman, S. Joyce and E.P. Skaar, 2007. A *Staphylococcus aureus* regulatory system that responds to host heme and modulates virulence. Cell host & microbe, 1(2): 109-119.

Trapnell, C., D.G. Hendrickson, M. Sauvageau, L. Goff, J.L. Rinn and L. Pachter, 2013. Differential analysis of gene regulation at transcript resolution with RNA-seq. Nature biotechnology, 31(1): 46.

Traxler, M.F., J.D. Watrous, T. Alexandrov, P.C. Dorrestein and R. Kolter, 2013. Interspecies interactions stimulate diversification of the *Streptomyces coelicolor* secreted metabolome. MBio, 4(4): e00459-00413.

Truong-Bolduc, Q., G. Bolduc, H. Medeiros, J. Vyas, Y. Wang and D. Hooper, 2015. Role of the Tet38 efflux pump in *Staphylococcus aureus* internalization and survival in epithelial cells. Infection and immunity, 83(11): 4362-4372.

Truong-Bolduc, Q., P. Dunman, T. Eidem and D. Hooper, 2011. Transcriptional profiling analysis of the global regulator NorG, a GntR-like protein of *Staphylococcus aureus*. Journal of bacteriology: JB. 05847-05811.

Tsai, M., R.L. Ohniwa, Y. Kato, S.L. Takeshita, T. Ohta, S. Saito, H. Hayashi and K. Morikawa, 2011. *Staphylococcus aureus* requires cardiolipin for survival under conditions of high salinity. BMC microbiology, 11(1): 13.

Tuchscherr, L., M. Bischoff, S.M. Lattar, M.N. Llana, H. Pförtner, S. Niemann, J. Geraci, H. Van de Vyver, M.J. Fraunholz and A.L. Cheung, 2015. Sigma factor sigB is crucial to mediate *Staphylococcus aureus* adaptation during chronic infections. PLoS pathogens, 11(4): e1004870.

Turpin, P.E., V.K. Dhir, K.A. Maycroft, C. Rowlands and E.M. Wellington, 1992. The effect of *Streptomyces* species on the survival of *Salmonella* in soil. FEMS Microbiology Letters, 101(4): 271-280.

Tyc, O., M. van den Berg, S. Gerards, J.A. van Veen, J.M. Raaijmakers, W. De Boer and P. Garbeva, 2014. Impact of interspecific interactions on antimicrobial activity among soil bacteria. Frontiers in microbiology, 5: 567.

Ubukata, K., N. Itoh-Yamashita and M. Konno, 1989. Cloning and expression of the *norA* gene for fluoroquinolone resistance in *Staphylococcus aureus*. Antimicrobial agents and chemotherapy, 33(9): 1535-1539.

Unsay, J.D., K. Cosentino, Y. Subburaj and A.J. García-Sáez, 2013. Cardiolipin effects on membrane structure and dynamics. Langmuir, 29(51): 15878-15887.

Utaida, S., P. Dunman, D. Macapagal, E. Murphy, S. Projan, V. Singh, R. Jayaswal and B. Wilkinson, 2003. Genome-wide transcriptional profiling of the response of *Staphylococcus aureus* to cell-wall-active antibiotics reveals a cell-wall-stress stimulon. Microbiology, 149(10): 2719-2732.

Utsumi, R., 2008. Bacterial signal transduction: Networks and drug targets. Springer New York.

Vagner, V., E. Dervyn and S.D. Ehrlich, 1998. A vector for systematic gene inactivation in *Bacillus subtilis*. Microbiology, 144(11): 3097-3104.

Van Melderen, L., 2010. Toxin–antitoxin systems: Why so many, what for? Current opinion in microbiology, 13(6): 781-785.

Van Melderen, L. and M.S. De Bast, 2009. Bacterial toxin–antitoxin systems: More than selfish entities? PLoS genetics, 5(3): e1000437.

Van Vliet, A.H., 2009. Next generation sequencing of microbial transcriptomes: Challenges and opportunities. FEMS microbiology letters, 302(1): 1-7.

Velho-Pereira, S. and N. Kamat, 2011. Antimicrobial screening of *Actinobacteria* using a modified cross-streak method. Indian journal of pharmaceutical sciences, 73(2): 223.

Vestergaard, M., K. Nøhr-Meldgaard, M.S. Bojer, C.K. Nielsen, R.L. Meyer, C. Slavetinsky, A. Peschel and H. Ingmer, 2017. Inhibition of the ATP synthase eliminates the intrinsic resistance of *Staphylococcus aureus* towards polymyxins. Mbio, 8(5): e01114-01117.

von Bronk, B., S.A. Schaffer, A. Götz and M. Opitz, 2017. Effects of stochasticity and division of labor in toxin production on two-strain bacterial competition in *Escherichia coli*. PLoS biology, 15(5): e2001457.

Wandersman, C. and P. Delepelaire, 2004. Bacterial iron sources: From siderophores to hemophores. Annu. Rev. Microbiol., 58: 611-647.

Wang, H., D.P. Fewer, L. Holm, L. Rouhiainen and K. Sivonen, 2014. Atlas of nonribosomal peptide and polyketide biosynthetic pathways reveals common occurrence of nonmodular enzymes. Proceedings of the National Academy of Sciences, 111(25): 9259-9264.

Wang, R., N. Kalchayanand, J.W. Schmidt and D.M. Harhay, 2013. Mixed biofilm formation by shiga toxin–producing *Escherichia coli* and *Salmonella enterica serovar typhimurium* enhanced bacterial resistance to sanitization due to extracellular polymeric substances. Journal of Food Protection®, 76(9): 1513-1522.

Wang, W., Q. Guo, X. Xu, Z.-k. Sheng, X. Ye and M. Wang, 2014. High-level tetracycline resistance mediated by efflux pumps tet (a) and tet (a)-1 with two start codons. Journal of medical microbiology, 63(11): 1454-1459.

Wang, Y., S. Kuo, M. Shu, J. Yu, S. Huang, A. Dai, R.L. Gallo and C.-M. Huang, 2014. *Staphylococcus epidermidis* in the human skin microbiome mediates fermentation to inhibit the growth of *propionibacterium acnes*: Implications of probiotics in acne vulgaris. Applied microbiology and biotechnology, 98(1): 411-424.

Wang, Z., M. Gerstein and M. Snyder, 2009. RNA-seq: A revolutionary tool for transcriptomics. Nature reviews genetics, 10(1): 57.

Weidenmaier, C., J.F. Kokai-Kun, S.A. Kristian, T. Chanturiya, H. Kalbacher, M. Gross, G. Nicholson, B. Neumeister, J.J. Mond and A. Peschel, 2004. Role of teichoic acids in *Staphylococcus aureus* nasal colonization, a major risk factor in nosocomial infections. Nature medicine, 10(3): 243-245.

Weidenmaier, C., A. Peschel, V.A. Kempf, N. Lucindo, M.R. Yeaman and A.S. Bayer, 2005. DltABCD-and MprF-mediated cell envelope modifications of *Staphylococcus aureus* confer resistance to platelet microbicidal proteins and contribute to virulence in a rabbit endocarditis model. Infection and immunity, 73(12): 8033-8038.

Wellington, E.M., A.B. Boxall, P. Cross, E.J. Feil, W.H. Gaze, P.M. Hawkey, A.S. Johnson-Rollings, D.L. Jones, N.M. Lee and W. Otten, 2013. The role of the natural environment in the emergence of antibiotic resistance in gram-negative bacteria. The Lancet infectious diseases, 13(2): 155-165.

Westermann, A.J., S.A. Gorski and J. Vogel, 2012. Dual RNA-seq of pathogen and host. Nature Reviews Microbiology, 10(9): 618.

Wiener, P., 1996. Experimental studies on the ecological role of antibiotic production in bacteria. Evolutionary Ecology, 10(4): 405-421.

Wiener, P., 2000. Antibiotic production in a spatially structured environment. Ecology Letters, 3(2): 122-130.

Wilaipun, P., T. Zendo, K.-i. Okuda, J. Nakayama and K. Sonomoto, 2008. Identification of the nukacin KQU-131, a new type-a (II) lantibiotic produced by *Staphylococcus hominis* KQU-131 isolated from Thai fermented fish product (Pla-ra). Bioscience, biotechnology, and biochemistry, 72(8): 2232-2235.

Wilkens, S., 2015. Structure and mechanism of ABC transporters. F1000prime reports, 7.

Wilks, S.S., 1938. The large-sample distribution of the likelihood ratio for testing composite hypotheses. The Annals of Mathematical Statistics, 9(1): 60-62.

Williams, M.R. and R.L. Gallo, 2015. The role of the skin microbiome in atopic dermatitis. Current allergy and asthma reports, 15(11): 65.

Williston, E.H., P. Zia-Walrath and G.P. Youmans, 1947. Plate methods for testing antibiotic activity of *Actinomycetes* against virulent human type tubercle Bacilli. Journal of bacteriology, 54(5): 563.

Wloch-Salamon, D.M., D. Gerla, R.F. Hoekstra and J.A.G. de Visser, 2008. Effect of dispersal and nutrient availability on the competitive ability of toxin-producing yeast. Proceedings of the Royal Society of London B: Biological Sciences, 275(1634): 535-541.

Woappi, Y., P. Gabani and O.V. Singh, 2013. Emergence of antibiotic-producing microorganisms in residential versus recreational microenvironments. British microbiology research journal, 3(3): 280.

Wolz, C., P. Pöhlmann-Dietze, A. Steinhuber, Y.T. Chien, A. Manna, W. Van Wamel and A. Cheung, 2000. Agr-independent regulation of fibronectin-binding protein (s) by the regulatory locus sar in *Staphylococcus aureus*. Molecular microbiology, 36(1): 230-243.

Worthington, R.J., M.S. Blackledge and C. Melander, 2013. Small-molecule inhibition of bacterial two-component systems to combat antibiotic resistance and virulence. Future medicinal chemistry, 5(11): 1265-1284.

Wos-Oxley, M.L., I. Plumeier, C. Von Eiff, S. Taudien, M. Platzer, R. Vilchez-Vargas, K. Becker and D.H. Pieper, 2010. A poke into the diversity and associations within human anterior nare microbial communities. The ISME journal, 4(7): 839-851.

Wu, S., H. de Lencastre and A. Tomasz, 1996. Sigma-B, a putative operon encoding alternate sigma factor of *Staphylococcus aureus* RNA polymerase: Molecular cloning and DNA sequencing. Journal of bacteriology, 178(20): 6036-6042.

Wu, Y., J. Wang, T. Xu, J. Liu, W. Yu, Q. Lou, T. Zhu, N. He, H. Ben and J. Hu, 2012. The two-component signal transduction system ArlRS regulates *Staphylococcus epidermidis* biofilm formation in an ica-dependent manner. PloS one, 7(7): e40041.

Xavier, B.M. and J.B. Russell, 2006. Bacterial competition between a bacteriocin-producing and a bacteriocin-negative strain of *Streptococcus bovis* in batch and continuous culture. FEMS microbiology ecology, 58(3): 317-322.

Xia, G., L. Maier, P. Sanchez-Carballo, M. Li, M. Otto, O. Holst and A. Peschel, 2010. Glycosylation of wall teichoic acid in *Staphylococcus aureus* by tarM. Journal of Biological Chemistry, 285(18): 13405-13415.

Xiong, Y.-Q., W. Van Wamel, C.C. Nast, M.R. Yeaman, A.L. Cheung and A.S. Bayer, 2002. Activation and transcriptional interaction between agr RNAII and RNAIII in *Staphylococcus aureus* in vitro and in an experimental endocarditis model. The Journal of infectious diseases, 186(5): 668-677.

Xu, H., T.J. Sullivan, J.-i. Sekiguchi, T. Kirikae, I. Ojima, C.F. Stratton, W. Mao, F.L. Rock, M. Alley and F. Johnson, 2008. Mechanism and inhibition of saFabI, the enoyl reductase from *Staphylococcus aureus*. Biochemistry, 47(14): 4228-4236.

Xu, T., Y. Wu, Z. Lin, R. Bertram, F. Götz, Y. Zhang and D. Qu, 2017. Identification of genes controlled by the essential YycFG two-component system reveals a role for biofilm modulation in *Staphylococcus epidermidis*. Frontiers in microbiology, 8: 724.

Yan, M., C. Yu, J. Yang and Y. Ji, 2011. The essential two-component system, YhcSR, is involved in the regulation of the nitrate respiratory pathway of *Staphylococcus aureus*. Journal of bacteriology.

Yang, S.-J., A.S. Bayer, N.N. Mishra, M. Meehl, N. Ledala, M.R. Yeaman, Y.Q. Xiong and A.L. Cheung, 2012. The *Staphylococcus aureus* two-component regulatory system, GraRS, senses and confers resistance to selected cationic antimicrobial peptides. Infection and immunity, 80(1): 74-81.

Yao, J., J.B. Maxwell and C.O. Rock, 2013. Resistance to AFN-1252 arises from missense mutations in *Staphylococcus aureus* enoyl-acyl carrier protein reductase (FabI). Journal of Biological Chemistry: JBC. M113. 512905.

Ye, J., G. Coulouris, I. Zaretskaya, I. Cutcutache, S. Rozen and T.L. Madden, 2012. Primer-BLAST: A tool to design target-specific primers for polymerase chain reaction. BMC bioinformatics, 13(1): 134.

Ye, J., A. Kandegedara, P. Martin and B.P. Rosen, 2005. Crystal structure of the *Staphylococcus aureus* pI258 cadC Cd (II)/Pb (II)/Zn (II)-responsive repressor. Journal of bacteriology, 187(12): 4214-4221.

Yeaman, M.R. and N.Y. Yount, 2003. Mechanisms of antimicrobial peptide action and resistance. Pharmacological reviews, 55(1): 27-55.

Yim, G., H.H. Wang and J. Davies, 2006. The truth about antibiotics. International Journal of Medical Microbiology, 296(2-3): 163-170.

Yoshida, H., M. Bogaki, S. Nakamura, K. Ubukata and M. Konno, 1990. Nucleotide sequence and characterization of the *Staphylococcus aureus norA* gene, which confers resistance to quinolones. Journal of bacteriology, 172(12): 6942-6949.

Young, M.D., M.J. Wakefield, G.K. Smyth and A. Oshlack, 2010. Gene ontology analysis for RNA-seq: Accounting for selection bias. Genome biology, 11(2): R14.

Yu, D., F. Xu, J. Zeng and J. Zhan, 2012. Type III polyketide synthases in natural product biosynthesis. IUBMB life, 64(4): 285-295.

Zanger, P., J. Holzer, R. Schleucher, H. Scherbaum, B. Schittek and S. Gabrysch, 2010. Severity of *Staphylococcus aureus* infection of the skin is associated with inducibility of human β-defensin 3 but not human β-defensin 2. Infection and immunity, 78(7): 3112-3117.

Zanger, P., J. Holzer, R. Schleucher, H. Steffen, B. Schittek and S. Gabrysch, 2009. Constitutive expression of the antimicrobial peptide RNase 7 is associated with *Staphylococcus aureus* infection of the skin. The Journal of infectious diseases, 200(12): 1907-1915.

Zanger, P., D. Nurjadi, B. Vath and P.G. Kremsner, 2011. Persistent nasal carriage of *Staphylococcus aureus* is associated with deficient induction of human β-defensin 3 after sterile wounding of healthy skin in vivo. Infection and immunity.

Zhang, T., J.K. Muraih, N. Tishbi, J. Herskovitz, R.L. Victor, J. Silverman, S. Uwumarenogie, S.D. Taylor, M. Palmer and E. Mintzer, 2014. Cardiolipin prevents membrane translocation and permeabilization by daptomycin. Journal of Biological Chemistry: jbc. M114. 554444.

Zhang, Y.Q., S.X. Ren, H.L. Li, Y.X. Wang, G. Fu, J. Yang, Z.Q. Qin, Y.G. Miao, W.Y. Wang and R.S. Chen, 2003. Genome-based analysis of virulence genes in a non-biofilm-forming *Staphylococcus epidermidis* strain (ATCC12228). Molecular microbiology, 49(6): 1577-1593.

Zhao, S., Fung-Leung, W. P., Bittner, A., Ngo, K., & Liu, X. (2014). Comparison of RNA-Seq and microarray in transcriptome profiling of activated T cells. *PloS one*, *9*(1), e78644.

Zhong, Q., V.M. Gohil, L. Ma and M.L. Greenberg, 2004. Absence of cardiolipin results in temperature sensitivity, respiratory defects, and mitochondrial DNA instability independent of Pet56. Journal of Biological Chemistry.

Zhu, L., K. Inoue, S. Yoshizumi, H. Kobayashi, Y. Zhang, M. Ouyang, F. Kato, M. Sugai and M. Inouye, 2009. *Staphylococcus aureus* MazF specifically cleaves a pentad sequence, UACAU, which is unusually abundant in the mRNA for pathogenic adhesive factor SraP. Journal of bacteriology, 191(10): 3248-3255.

Zhu, Y., R. Nandakumar, M.R. Sadykov, N. Madayiputhiya, T.T. Luong, R. Gaupp, C.Y. Lee and G.A. Somerville, 2011. RpiR homologues may link *Staphylococcus aureus* RNAIII synthesis and pentose phosphate pathway regulation. Journal of bacteriology: JB. 05930-05911.

Ziemert, N., S. Podell, K. Penn, J.H. Badger, E. Allen and P.R. Jensen, 2012. The natural product domain seeker NaPDoS: A phylogeny based bioinformatic

tool to classify secondary metabolite gene diversity. PloS one, 7(3): e34064.
Zipperer, A., M.C. Konnerth, C. Laux, A. Berscheid, D. Janek, C. Weidenmaier, M. Burian, N.A. Schilling, C. Slavetinsky and M. Marschal, 2016. Human commensals producing a novel antibiotic impair pathogen colonization. Nature, 535(7613): 511-516.

Appendix

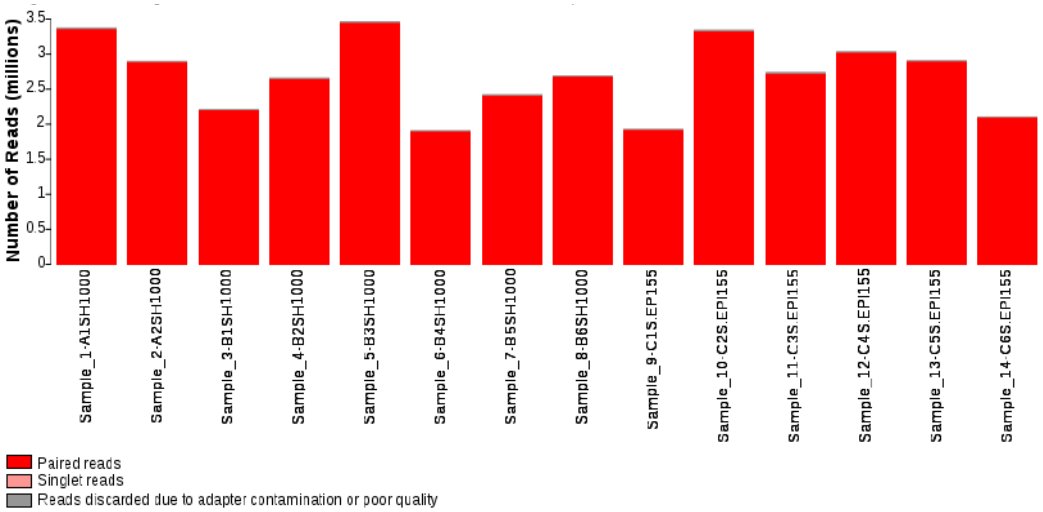

Figure A1 Total number of reads obtained from *S. aureus* SH1000 and *S. epidermidis* B155 isolated from different days in competition experiment. (A1 and A2) *S. aureus* WT day 1 and day15, (B1, B2, B3, B4, B5 and B6) *S. aureus* from mixed culture day 1, 3, 9, 12,13 and 15, (C1, C2, C3, C4, C5 and C6) S. epidermidis from mixed culture day 1, 3, 9, 12, 13 and 15.

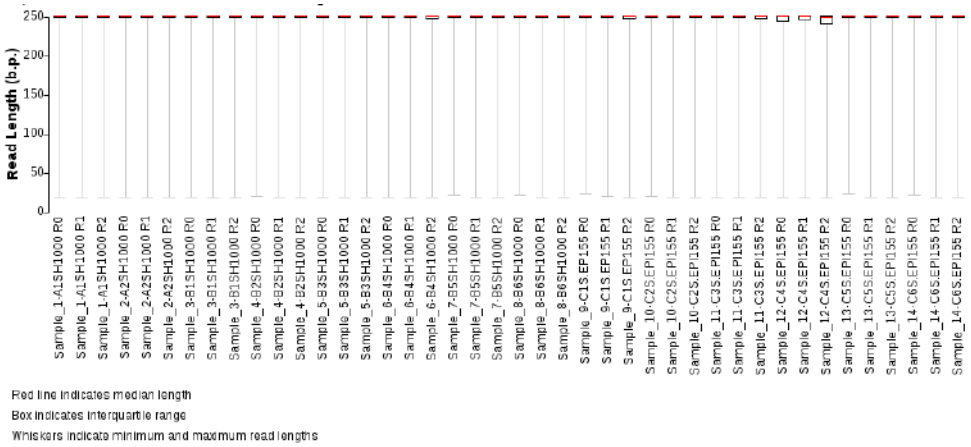

Figure A2 Boxplot showing the distribution of trimmed read lengths: (A1 and A2) *S. aureus* WT day 1 and day 15, (B1, B2, B3, B4, B5 and B6) *S. aureus* from mixed culture day 1, 3, 9, 12,13 and 15, (C1, C2, C3, C4, C5 and C6) *S. epidermidis* from mixed culture day 1, 3, 9, 12, 13 and 15.

Table A1 *S. epidermidis* strains used to test with *S. aureus* (SHG01) to find strain produce the same molucle as *S. epidermidis* B155. Strains obtained courtesy of Llinos Harris, Swansea University.

Species	Strain ID	Relevant characteristics
S. epidermidis	1A	Clinical isolate
S. epidermidis	1B	Clinical isolate
S. epidermidis	7A	Clinical isolate
S. epidermidis	7B	Clinical isolate
S. epidermidis	12A	Clinical isolate
S. epidermidis	12B	Clinical isolate
S. epidermidis	13A	Clinical isolate
S. epidermidis	13B	Clinical isolate
S. epidermidis	14A	Clinical isolate
S. epidermidis	14B	Clinical isolate
S. epidermidis	19A	Clinical isolate
S. epidermidis	19B	Clinical isolate
S. epidermidis	23A	Clinical isolate
S. epidermidis	23B	Clinical isolate
S. epidermidis	25A	Clinical isolate
S. epidermidis	25B	Clinical isolate
S. epidermidis	26A	Clinical isolate
S. epidermidis	26B	Clinical isolate
S. epidermidis	28A	Clinical isolate
S. epidermidis	28B	Clinical isolate
S. epidermidis	33A	Clinical isolate
S. epidermidis	33B	Clinical isolate
S. epidermidis	36A	Clinical isolate
S. epidermidis	36B	Clinical isolate
S. epidermidis	37A	Clinical isolate
S. epidermidis	37B	Clinical isolate
S. epidermidis	38A	Clinical isolate
S. epidermidis	38B	Clinical isolate
S. epidermidis	43A	Clinical isolate
S. epidermidis	43B	Clinical isolate
S. epidermidis	45A	Clinical isolate
S. epidermidis	45B	Clinical isolate
S. epidermidis	46A	Clinical isolate
S. epidermidis	46B	Clinical isolate
S. epidermidis	47A	Clinical isolate
S. epidermidis	47B	Clinical isolate
S. epidermidis	48A	Clinical isolate
S. epidermidis	48B	Clinical isolate
S. epidermidis	51A	Clinical isolate
S. epidermidis	51B	Clinical isolate
S. epidermidis	54A	Clinical isolate
S. epidermidis	54B	Clinical isolate
S. epidermidis	55A	Clinical isolate
S. epidermidis	55B	Clinical isolate
S. epidermidis	56A	Clinical isolate
S. epidermidis	56B	Clinical isolate

S. epidermidis	57A	Clinical isolate
S. epidermidis	57B	Clinical isolate
S. epidermidis	59A	Clinical isolate
S. epidermidis	59B	Clinical isolate
S. epidermidis	60A	Clinical isolate
S. epidermidis	60B	Clinical isolate
S. epidermidis	62A	Clinical isolate
S. epidermidis	62B	Clinical isolate
S. epidermidis	63A	Clinical isolate
S. epidermidis	63B	Clinical isolate
S. epidermidis	68A	Clinical isolate
S. epidermidis	68B	Clinical isolate
S. epidermidis	70A	Clinical isolate
S. epidermidis	70B	Clinical isolate
S. epidermidis	73A	Clinical isolate
S. epidermidis	73B	Clinical isolate
S. epidermidis	74A	Clinical isolate
S. epidermidis	74B	Clinical isolate
S. epidermidis	77A	Clinical isolate
S. epidermidis	77B	Clinical isolate
S. epidermidis	78A	Clinical isolate
S. epidermidis	78B	Clinical isolate
S. epidermidis	79A	Clinical isolate
S. epidermidis	79B	Clinical isolate
S. epidermidis	81A	Clinical isolate
S. epidermidis	81B	Clinical isolate
S. epidermidis	82A	Clinical isolate
S. epidermidis	82B	Clinical isolate
S. epidermidis	83A	Clinical isolate
S. epidermidis	83B	Clinical isolate
S. epidermidis	84A	Clinical isolate
S. epidermidis	84B	Clinical isolate
S. epidermidis	85A	Clinical isolate
S. epidermidis	85B	Clinical isolate
S. epidermidis	88A	Clinical isolate
S. epidermidis	88B	Clinical isolate
S. epidermidis	93A	Clinical isolate
S. epidermidis	93B	Clinical isolate
S. epidermidis	97A	Clinical isolate
S. epidermidis	97B	Clinical isolate
S. epidermidis	99A	Clinical isolate
S. epidermidis	99B	Clinical isolate
S. epidermidis	100A	Clinical isolate
S. epidermidis	100B	Clinical isolate
S. epidermidis	101A	Clinical isolate
S. epidermidis	103A	Clinical isolate
S. epidermidis	103B	Clinical isolate
S. epidermidis	104A	Clinical isolate
S. epidermidis	104B	Clinical isolate
S. epidermidis	105A	Clinical isolate
S. epidermidis	105B	Clinical isolate
S. epidermidis	NA1	Clinical isolate

S. epidermidis	NA5	Clinical isolate
S. epidermidis	NA7	Clinical isolate
S. epidermidis	NA10	Clinical isolate
S. epidermidis	NA14	Clinical isolate
S. epidermidis	NA16	Clinical isolate
S. epidermidis	NA20	Clinical isolate
S. epidermidis	NA21	Clinical isolate
S. epidermidis	NA22	Clinical isolate
S. epidermidis	NA23	Clinical isolate
S. epidermidis	NA24	Clinical isolate
S. epidermidis	NAs1	Clinical isolate
S. epidermidis	NAs2	Clinical isolate
S. epidermidis	NAs3	Clinical isolate
S. epidermidis	NAs4	Clinical isolate
S. epidermidis	NAs5	Clinical isolate
S. epidermidis	NAs6	Clinical isolate
S. epidermidis	NAs7	Clinical isolate
S. epidermidis	NAs8	Clinical isolate
S. epidermidis	NAs12	Clinical isolate
S. epidermidis	NAs14	Clinical isolate
S. epidermidis	NAs16	Clinical isolate
S. epidermidis	NAs17	Clinical isolate
S. epidermidis	NAs19	Clinical isolate
S. epidermidis	NAs22	Clinical isolate
S. epidermidis	8700/01	Clinical isolate
S. epidermidis	8688/01	Clinical isolate
S. epidermidis	9591/01	Clinical isolate
S. epidermidis	9639/01	Clinical isolate
S. epidermidis	9640/01	Clinical isolate
S. epidermidis	5189/99	Clinical isolate
S. epidermidis	5200/99	Clinical isolate
S. epidermidis	6433/99	Clinical isolate
S. epidermidis	6493/99	Clinical isolate
S. epidermidis	6528/99	Clinical isolate
S. epidermidis	9041/01	Clinical isolate
S. epidermidis	3917/99	Clinical isolate
S. epidermidis	3957/99	Clinical isolate
S. epidermidis	1562/00	Clinical isolate
S. epidermidis	1588/00	Clinical isolate
S. epidermidis	4796/00	Clinical isolate
S. epidermidis	4721/00	Clinical isolate
S. epidermidis	4768/00	Clinical isolate
S. epidermidis	5172/02	Clinical isolate
S. epidermidis	5284/02	Clinical isolate
S. epidermidis	3628/99	Clinical isolate
S. epidermidis	3641/99	Clinical isolate
S. epidermidis	1451/02	Clinical isolate
S. epidermidis	2154/02	Clinical isolate
S. epidermidis	2183/02	Clinical isolate
S. epidermidis	9169/01	Clinical isolate
S. epidermidis	9170/01	Clinical isolate
S. epidermidis	5019	Clinical isolate

S. epidermidis	5044	Clinical isolate
S. epidermidis	5060	Clinical isolate
S. epidermidis	5020/98	Clinical isolate
S. epidermidis	5021/98	Clinical isolate
S. epidermidis	5045/98	Clinical isolate
S. epidermidis	4363/02	Clinical isolate
S. epidermidis	4390/02	Clinical isolate
S. epidermidis	5481/01	Clinical isolate
S. epidermidis	5524/01	Clinical isolate
S. epidermidis	5525/01	Clinical isolate
S. epidermidis	5548/02	Clinical isolate

Table A2 Gene ontology (GO) classification of the TOP 50 GO terms in *desK* mutant and *SAOUHSC_01312* putative transporter mutant.

Go ID	Function	Category	Total number of genes in each term	Hit Δ *desK*	Hit Δ *01312*
GO:0005737	cytoplasm	Cellular Component	366	49	78
GO:0005829	cytosol	Cellular Component	157	15	29
GO:0005886	plasma membrane	Cellular Component	301	25	58
GO:0005618	cell wall	Cellular Component	17	7	9
GO:0016021	integral component of membrane	Cellular Component	837	92	159
GO:0009325	nitrate reductase complex	Cellular Component	5	4	2
GO:0016020	membrane	Cellular Component	37	10	9
GO:0043190	ATP-binding cassette (ABC) transporter complex	Cellular Component	18	4	4
GO:0005576	extracellular region	Cellular Component	95	21	29
GO:0005623	cell	Cellular Component	12	2	3
GO:0055085	transmembrane transport	Biological Process	59	8	13
GO:0071555	cell wall organization	Biological Process	40	2	8
GO:0051301	cell division	Biological Process	29	3	9
GO:0006629	lipid metabolic process	Biological Process	14	2	2
GO:0055114	oxidation-reduction process	Biological Process	7	1	2
GO:0005975	carbohydrate metabolic process	Biological Process	27	3	6
GO:0006094	gluconeogenesis	Biological Process	8	4	3
GO:0009405	pathogenesis	Biological Process	94	15	29
GO:0009252	peptidoglycan biosynthetic process	Biological Process	18	1	4
GO:0006006	glucose metabolic process	Biological Process	10	3	5
GO:0006096	glycolytic process	Biological Process	12	9	10
GO:0008152	metabolic process	Biological Process	52	5	11
GO:0007049	cell cycle	Biological Process	26	3	8
GO:0006633	fatty acid biosynthetic process	Biological Process	13	1	4
GO:0006351	transcription, DNA-templated	Biological Process	125	13	19
GO:0019350	teichoic acid biosynthetic process	Biological Process	12	0	3
GO:0000160	phosphorelay signal transduction system	Biological Process	18	4	3
GO:0045892	negative regulation of transcription, DNA-templated	Biological Process	11	0	3
GO:0006950	response to stress	Biological Process	5	1	3

Go ID	Function	Category	Total number of genes in each term	Hit Δ *desK*	Hit Δ *01312*
GO:0019835	cytolysis	Biological Process	12	1	5
GO:0050662	coenzyme binding	Molecular Function	18	0	4
GO:0005524	ATP binding	Molecular Function	309	39	57
GO:0009055	electron transfer activity	Molecular Function	15	8	7
GO:0005506	iron ion binding	Molecular Function	4	1	0
GO:0008289	lipid binding	Molecular Function	2	0	1
GO:0046872	metal ion binding	Molecular Function	192	22	39
GO:0016887	ATPase activity	Molecular Function	62	9	19
GO:0030170	pyridoxal phosphate binding	Molecular Function	41	8	12
GO:0000287	magnesium ion binding	Molecular Function	38	4	11
GO:0003677	DNA binding	Molecular Function	202	21	28
GO:0016740	transferase activity	Molecular Function	22	2	5
GO:0016491	oxidoreductase activity	Molecular Function	51	4	9
GO:0005215	transporter activity	Molecular Function	35	3	4
GO:0004803	transposase activity	Molecular Function	10	2	2
GO:0020037	heme binding	Molecular Function	14	5	6
GO:0000166	nucleotide binding	Molecular Function	18	3	6
GO:0003700	DNA-binding transcription factor activity	Molecular Function	86	9	16
GO:0003676	nucleic acid binding	Molecular Function	28	2	3
GO:0022857	transmembrane transporter activity	Molecular Function	50	5	10
GO:0016787	hydrolase activity	Molecular Function	61	2	7